PROBLEMS CONCERNING THE ELECTRONIC STRUCTURE OF SOLIDS

A Thesis presented in fulfilment of the requirements for the degree of Doctor of Philosophy in the University of Oxford

BODLEIAN LIBRARY OXFORD
DEPOSITED
THESIS
12.xi.69

by

FRANCIS PATRICK LARKINS

Wadham College,
Oxford

Trinity Term
1969

TO MY PARENTS

* * *

ACKNOWLEDGEMENTS

I would like to thank Professor C.A. Coulson for his encouragement and guidance throughout the supervision of this work. I also express by sincere gratitude to Dr. A.B. Lidiard for acting as supervisor during Hilary Term 1969 and for the many helpful discussions throughout my attachment with the Theoretical Physics Division at the Atomic Energy Research Establishment, Harwell. Without the facilities of the Division, so generously provided, much of this work would not have been possible.

It is a great pleasure to express my appreciation to Dr. A.M. Stoneham, A.E.R.E. for his enthusiasm and inspiration throughout the course of this work. I have also benefitted greatly from discussions with various colleagues at the Mathematical Institute, Oxford, and the Theoretical Physics Division, A.E.R.E., Harwell. To these persons I shall always be grateful.

I acknowledge the generosity of the Rhodes Trustees and the Victorian Rhodes Scholarship Committee, Australia, for their financial support from 1966-1969. Also I thank the Warden and Fellows of Wadham College, Oxford, for the award of a Senior Scholarship for the academic year 1968-1969.

Finally, I wish to thank my wife for tolerance, understanding and constant encouragement throughout the whole of this endeavour.

* * *

ABSTRACT

The major emphasis of this thesis relates to the calculation of the electronic structure of the isolated vacancy in the diamond and silicon crystal using the defect molecule approach. The electronic energy levels from an undistorted vacancy calculation are corrected, to a first approximation, for symmetric relaxation and Jahn-Teller distortion effects. The electronic properties of the undistorted neutral divacancy in diamond are also determined. A description of a dynamic relaxation program developed to estimate the displacement of atoms surrounding a point defect in the diamond-type crystal as the result of distortion effects is also reported.

A discussion of the theoretical methods available for the calculation of the electronic structure of point defects in diamond-type crystals and the reasons for choosing the defect molecule approach is presented in section 1.2 of Chapter 1. In the remainder of the chapter the experimental evidence available for the existence of single vacancies, divacancies and the interstitial atom in irradiated diamond and silicon crystals is briefly reviewed. Chapter 2 contains a detailed account of the fundamental aspects of the defect molecule method first proposed by Coulson and Kearsley. The limitations as well as the advantages of this

method are discussed and the modifications made to the model in the present study are outlined. The basic formal relationships required for the calculation of the electronic structure of the undistorted vacancy in its various charge states are developed within this framework.

The results of applying this method to a calculation for the single isolated vacancy in the diamond crystal are presented and discussed in Chapter 3. Four possible charge states of the vacancy; namely, the single positive, the neutral, the single negative and the double negatively charged state are considered. An investigation of the sensitivity of the relative ordering of the energy levels for the various centres to two different choices of basis functions to represent the 2s and 2p orbitals on the atoms in the crystal is undertaken. For the neutral vacancy the ^1E electronic level is predicted to be the ground state of this centre with the $^3T_1$ level the first excited state when simple Slater-type functions are chosen for the 2s and 2p orbitals. However, when the atomic Hartree-Fock functions proposed by Clementi are employed the order of these two levels is inverted. A simple model to examine the influence of delocalizing the electronic wave-function of the defect electrons on the relative ordering of the lowest levels is presented in section 3.5. For the neutral vacancy no change in the ordering of the lowest levels results when a reasonable amount of delocalisation is incorporated. For the negatively charged centre the $^4A_2$ level is reinforced as the lowest electronic level.

The calculation for the electronic structure of the undistorted neutral divacancy in the diamond crystal using a modified antisymmetrized molecular orbital method, based upon the bond method, is reported in Chapter 4. Using simple Slater-type functions for the 2s and 2p orbitals the $^3A_{2g}$ level is predicted to be the ground state of this centre, with spin- and orbitally-allowed transitions to the $^3A_{1u}$ level corresponding to optical absorption in the u-v region of the spectrum.

In Chapter 5 the development of a dynamic relaxation method which enables the displacement of the atoms surrounding a point defect in the diamond-type lattice to be determined free from the constraints of previous models is described. The method relies upon having a valence-force potential function which includes non-central as well as central force terms to describe the interactions between the atoms of the perfect crystal. The interaction between the defect electrons is simulated by applying external forces to the atoms nearest the defect. The method is applicable to a wide range of systems; however, here it has been applied only to the neutral single vacancy in the diamond and silicon crystal which undergoes a tetragonal distortion as a result of the nature of the rebonding forces. Displacements of the atoms in the vicinity of the defect are much greater for the silicon crystal than for the diamond crystal. It has been demonstrated that the displacement of atoms which are fifth neighbour to the defect is greater than that for third or fourth neighbours. As a by-product of the calculation the formation energy of the single vacancy has been evaluated.

The theory of the Jahn-Teller effect, to first order, for the degenerate levels of the vacancy system is developed in Chapter 6 using the rigid atom approximation proposed by Lidiard and Stoneham. The differences between the method used in the present calculation and that developed by Lannoo and co-workers is discussed. The extent of Jahn-Teller splitting for all the lowest levels of the various centres is determined. Contrary to previous suggestions the values obtained for the splittings were found to be insensitive to the choice of basis functions for the valence orbitals. A correction to the lowest energy levels for the symmetry relaxation of the atoms nearest the defect is also made. This latter modification was different for various electronic levels belonging to a particular charge state of the vacancy and consequently is very important in determining the relative ordering of the lowest levels. This is again contrary to what has previously been tacitly assumed. The corrected electronic structure of the neutral vacancy suggests that this centre is not responsible for the GR1 band observed in irradiated diamonds as the $^3T_1$ level is predicted to be the ground state of this centre from all calculations. On the basis of this work it is also unlikely that this band is associated with the negatively charged vacancy; however, this possibility cannot be definitely eliminated.

The electronic structure for the four possible charged states of the single vacancy in the silicon crystal is determined in Chapter 7. The atomic Hartree-Fock functions proposed by Clementi are used to approximate the 3s and 3p orbitals on the silicon atoms in the crystal. Using both an unmodified and a modified antisymmetrized molecular orbital theory it has been demonstrated that electron-electron interaction terms and configuration mixing effects are important in determining the lowest levels of each centre. Again the energy levels resulting from the undistorted calculation are corrected for symmetric relaxation and Jahn-Teller distortion effects. The modified theory predicts ground state levels for the various centres which have the same total spin as those suggested by Watkins from his electron spin resonance experiments.

The most important findings and their implications on further work in this area are reported in a final general discussion.

TABLE OF CONTENTS

Acknowledgements

Abstract i

Chapter 1 FORMULATION OF THE PROBLEM

1.1 Introduction 1
1.2 Theoretical Considerations of the Defect Problem 2
1.3 Experimental Evidence for Point Defects in Irradiated Diamond and Silicon Crystals 7
1.4 Summary and Conclusion 20

Chapter 2 THE DEFECT MOLECULE METHOD

2.1 Introduction 21
2.2 Model for the Isolated Vacancy 22
2.3 Molecular Orbital Wave-functions for the Defect Molecule 25
2.4 The Hamiltonian for the System 31
2.5 Energy Evaluation before Configuration Interaction 34
2.6 Configuration Interaction Effects 39
2.7 Symmetry Considerations Concerning Possible Electronic Transitions 40
2.8 Summary 42

Chapter 3 THE ELECTRONIC STRUCTURE OF THE ISOLATED VACANCY IN DIAMOND

3.1 Introduction 43
3.2 Electronic Structure of the Isolated Vacancy: Slater Functions 45
3.3 Electronic Structure of the Isolated Vacancy: Clementi Functions 49
3.4 Comparison and Discussion of Results 51
3.5 Delocalisation of the Electronic Wave-Function from Vacancy 57
3.6 Summary and Conclusion 65

- - - -

Chapter 4 THE NEUTRAL ISOLATED DIVACANCY IN DIAMOND
4.1 Introduction 67
4.2 Model for the Isolated Divacancy 67
4.3 The Hamiltonian for the System 68
4.4 Molecular Orbital Wave-Functions 69
4.5 Energy Evaluation for the System 75
4.6 Allowed Electronic Transitions 80
4.7 Results 81
4.8 Relation with Experiment 85
4.9 Conclusion 86

Chapter 5 LATTICE DISTORTION AROUND SINGLE VACANCIES IN DIAMOND-TYPE CRYSTALS
5.1 Introduction 88
5.2 Previous Theoretical Models 89
5.3 Dynamic Model for the Defect Lattice 93
5.4 Potential Interaction between atoms in the Diamond-type lattice 96
5.5 Distortion around a single vacancy in the Diamond crystal 104
5.6 Distortion around the single vacancy in the silicon crystal 109
5.7 Discussion of Results and Relation to Experiment 114
5.8 Summary and Conclusion 117

Chapter 6 INVESTIGATION OF THE JAHN-TELLER EFFECTS AND THE SYMMETRIC TERM FOR THE ELECTRONIC LEVELS OF THE SINGLE VACANCY IN DIAMOND
6.1 Introduction 118
6.2 The Static Jahn-Teller Effect for the Vacancy in Diamond 122
6.3 The Effective Frequencies for the Lattice 133
6.4 Magnitude of the Jahn-Teller Effects for the Electronic Levels 137
6.5 Discussion of the Jahn-Teller Calculations 143
6.6 The Symmetric Relaxatin Mode for the Single Vacancy 159
6.7 Discussion of the Results for the Symmetric Relaxation and Comparison of the Calculated Electronic Structure with Experiment 171
6.8 Conclusion 177

- - - -

Chapter 7 ELECTRONIC STRUCTURE OF THE ISOLATED VACANCY IN SILICON

7.1 Introduction 178
7.2 Model for the Isolated Vacancy in Silicon 180
7.3 The Hamiltonian for the System 181
7.4 Determination of Wave-Functions and Energy Level Scheme 183
7.5 Results for the Isolated Vacancy 187
7.6 The Effective Frequencies for the Silicon Lattice 193
7.7 The Symmetric Relaxation Term for the Isolated Vacancy 195
7.8 Jahn-Teller Calculations for the Isolated Vacancy in Silicon 207
7.9 Comments on Results 218
7.10 Conclusion and Summary 220

GENERAL DISCUSSION OF THESIS 221

REFERENCES 228

APPENDIX

- - - -

CHAPTER 1

FORMULATION OF THE PROBLEM

Possible theoretical approaches to the calculation of the electronic structure of point defects in the diamond and silicon crystals are discussed. The reasons for favouring the defect molecule approach are outlined. The experimental evidence for the existence of single vacancies, divacancies and interstitial atoms in irradiated diamond and silicon crystals is also examined.

1.1 Introduction

In this thesis we shall be concerned with the calculation of the electronic structure of primary defects in crystals of the diamond-type structure. The emphasis here is mainly on the electronic properties of the single isolated vacancy and the neutral divacancy in the diamond lattice. However, we have also considered the single isolated vacancy in the silicon crystal. We will be concerned with the influence of such factors as the choice of wave-functions, electron delocalisation phenomenon, Jahn-Teller effects and symmetric relaxation terms on the relative ordering of the lowest electronic levels for some of these systems. Few quantitative theoretical studies have been undertaken to determine the electronic structure of the many-electron point defect systems, vacancies, di-vacancies and interstitial atoms, in valence crystals with the diamond-type structure. Furthermore, the studies undertaken so far have all been based upon one-electron wave-function models. We propose in the remainder of this chapter to review very briefly the

methods available for the determination of the electronic structure of point defects in covalent crystals (section 1.2) and then to discuss some of the experimental results which are relevant to the present thesis (section 1.3).

1.2 Theoretical Considerations of the Defect Problem

The problem of calculating the electronic structure of point defects in valence crystals may be investigated within the framework of the molecular orbital or valence bond method by considering the atoms surrounding the point defect as a 'molecule' in a matrix formed from the rest of the lattice which perturbs its electronic properties [1,2]. Alternatively, band theory methods presently available for the study of shallow and deep traps within the forbidden energy band gap may be used [3,4,5]. The point-ion model, which has been successfully used to calculate the electronic structure of colour centres in alkali halide crystals, has recently been used to determine the lowest electronic states of the neutral vacancy in diamond [6] following a suggestion by Gourary and Fein [7]. It is proposed to briefly consider the relevant studies which have used one or other of these possible methods to assess the advantages and disadvantages of the method before describing the approach used in this thesis. A more detailed discussion of the methods has been presented elsewhere by the author [8].

When using band theory methods a different procedure is necessary depending upon whether one is considering defects which lie deep in the forbidden band gap or near the band edge. In the limit,

for shallow traps where the levels result in highly diffuse states, effective-mass procedures may be used [3]. Such a method is applicable to donor states near the conduction band or acceptor states close to the valence band. In general, the impurity levels should lie within the range 0.01 to 0.1 eV of the relevant band, but in some cases the method has been applied successfully to deeper traps. The 'orbits' or 'spheres of influence' of the shallow states may be as much as 50Å in diameter depending upon the dielectric constant of the crystal. Such a method has been applied successfully to shallow impurity levels which result from doping of the semiconductors silicon and germanium with group V donors (P,As,Sb) [3]. The theory of acceptor states near the valence band is not as well developed because of difficulties associated with obtaining a detailed knowledge of the top of the valence band. Unfortunately, vacancies in the elemental diamond-type crystals are much deeper traps and therefore the effective mass methods are not applicable. At present, little attention has been given to the deep trap problem. Recently, however, there have been two studies based on scattering theory and pseudo-potential methods which have endeavoured to develop a general theory for such centres [4,5].

Bennemann [4] was primarily interested in the calculation of the formation and migration energies of the vacancy and interstitial atom in covalent crystals. However, it is possible that his method may be adaptable to localized energy level calculations. The effective valence and conduction electron wave-functions were

calculated using a tight binding approximation and the crystal potential in the effective Hamiltonian was represented by a self-consistent pseudo-potential. The method was developed within the Green's function formalism, but no actual calculation for point defects was performed. It is a difficult task to incorporate distortion effects for the lattice around the defect into this model. Callaway and Hughes employed a similar approach in an endeavour to calculate the localized electronic energy levels due to the single isolated neutral vacancy [5] and the neutral divacancy [9] in silicon. They considered Bennemann's method unsatisfactory because of the initial assumption of using free-electron wave-functions in zero order. In their study the defect was represented by a pseudo-potential and the wave-functions and the perturbed crystal potential were expanded in terms of Wannier functions for the perfect lattice. Lattice relaxation and distortion effects were neglected in both studies because it was stated that to include such effects in this approach would lead to a prohibitively large computational task.

For the single isolated vacancy in its neutral charge state only the bound state energy for the totally symmetric A_1 level was calculated, while for the isolated divacancy two localized states of different symmetry were found to be possible. Unfortunately, it was necessary to insert rather arbitrarily a parameter, λ, into the determinantal equation for the energies of the bound states to obtain any reasonable agreement with experiment. It is difficult to understand why these workers considered the totally symmetric state

for the vacancy rather than the doubly- or triply-degenerate levels; especially since the work on the diamond vacancy by Coulson and Kearsley [1] would suggest that these levels were more likely to give bound states. While this method represents an important step forward towards obtaining a general method of determining the bound state energies for localized defects there are several difficulties which present themselves. A very large computational effort is involved even using a high speed computer. The inability to feasibly adapt this method to include lattice relaxation and distortion effects is serious. The experimental results of Watkins [10] for the isolated vacancy and divacancy in silicon suggest that Jahn-Teller distortion effects make a major contribution to the localized energies. It is difficult to see how these effects can be incorporated easily within the energy band formalism. Moreover, the difficulty involved in treating the charged defects within the pseudopotential approximation is a serious limitation on the method since these are often the most interesting cases. Lidiard [11] has also pointed out that the method is based upon the one-electron approximation which requires the interelectronic interactions to be independent of the electronic state for its validity. However, this has not been demonstrated for localized states. The energy band approach does have the advantage that it endeavours to locate the defect levels with respect to the valence and conduction band limits. Nevertheless, at this stage the usefulness of the first-principle method is limited.

The qualitative justification for the application of the point-ion model to such defects as the isolated vacancy in covalent crystals has been given in terms of pseudopotential theory by Cohen and Heine [12]. Stoneham [6] used the method for this defect by considering each of the four nearest neighbours to the vacancy in diamond as being replaced by point charges. Then the energies of the valence electrons in their potential field was calculated using smooth variational one-centre wave-functions. The method has the advantage that it is possible to vary the analytical form of the radial functions such that they may have different values, determined self-consistently, for each configuration. This approach is interesting, but not really applicable to a non-polar covalent solid like diamond. It seems a rather drastic assumption to suppose that the atoms surrounding the vacancy may be replaced by point charges. Also the use of one-centre functions expanded around the geometric centre of the defect requires fairly large overlap of orbitals at this point. This conditions is not satisfied for the neutral vacancy in diamond. The neglect of exchange and overlap effects as well as any polarisation effects weakens the value of this model for general application.

The molecular orbital approach to the defect problem first proposed by Coulson and Kearsley [1] does not attempt to locate defect levels within the forbidden band gap or to determine absolute energies. Rather it aims, by an approximate method, to predict the

lowest localized levels and the values of optical transition energies associated with a particular defect. The method has been used for calculations on the various charge states of the vacancy [1,2] the interstitial atom [13] and for quantitative calculations of the Jahn-Teller effect [14] and related electron-lattice coupling effects [15]. It has the advantage of relative simplicity and much of the justification for using such a model must be found in a comparison of the theoretical and experimental results. We have chosen to use this approach and to examine in more detail than previously some of the assumptions underlying the model. In chapter 2 we have discussed the theory of the molecular orbital approach as applied to defect problems in diamond-crystals. A detailed discussion of calculations by other workers has been presented in a dissertation [8] and is not again included here. However, the results of other studies which are relevant to the present work are included at the appropriate places throughout the thesis. In the next section we have examined the most important experimental findings relating to point defects in diamond and silicon crystals.

1.3 Experimental Evidence for Point Defects in Irradiated Diamond and Silicon Crystals

The principal techniques which have been used in the study of point defects in diamond-type crystals are optical absorption and electron paramagnetic resonance spectroscopy. These methods enable information about the ground and excited states and possible

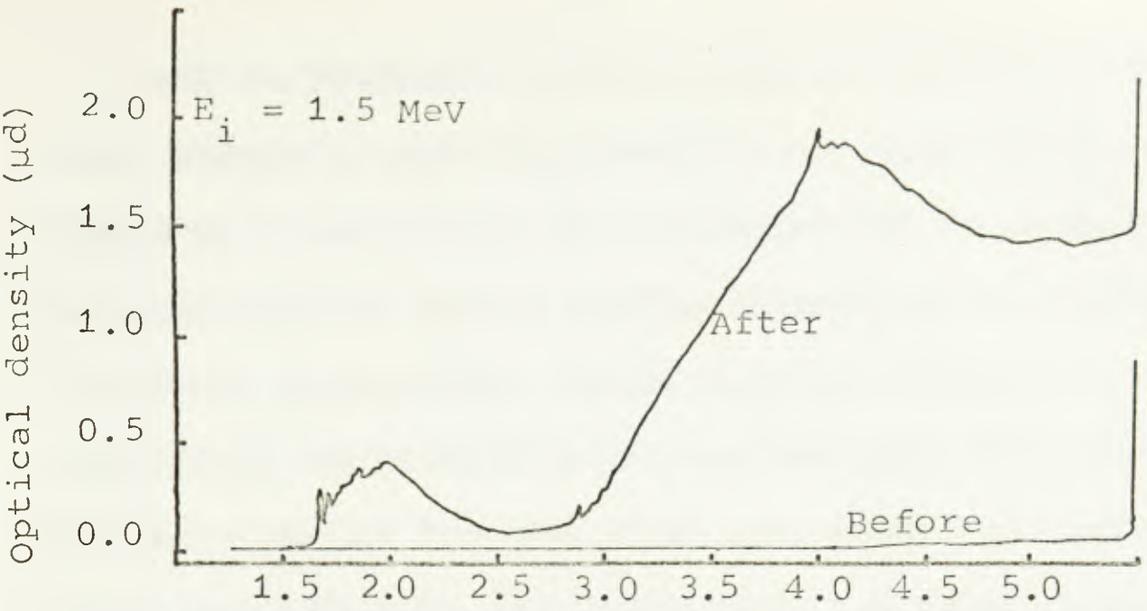
configurations of the defects to be obtained. Further valuable information has also been obtained from transport studies, relaxation and thermodynamic measurements and polarised luminescence work. Our interest in this thesis is focussed on the electronic behaviour of simple point defects in undoped diamond and silicon crystals which are considered to be free from impurity ions. We have reviewed only the most important experimental results here. Several more detailed reviews are available [10,16].

(a) The Diamond Crystal

Naturally occurring diamonds have been classified as type I or type II principally on the basis of their absorption properties in the I.R. visible and u-v regions of the spectrum [17,18]. Type I diamonds show increased absorption below 3,000Å and contain a non-paramagnetic nitrogen impurity [19] believed to be present as platelets oriented in the <100> direction [20]. Some type II diamonds have been shown to be semiconducting [21,22] and to possess acceptor levels about 0.35 eV above the valence band [23]. These are classified type IIb and the non-conducting specimens type IIa. Type I diamonds may also be categorized as Ib or Ia depending upon whether or not paramagnetic substitutional nitrogen in tetrahedral lattice sites is present in the crystal [24]. It is the experimental results on irradiated type IIa crystals that are most relevant to the present investigation. It must be remembered however, that even these diamonds are not spectroscopically pure because of their origin and in some cases have been shown to contain small amount of such

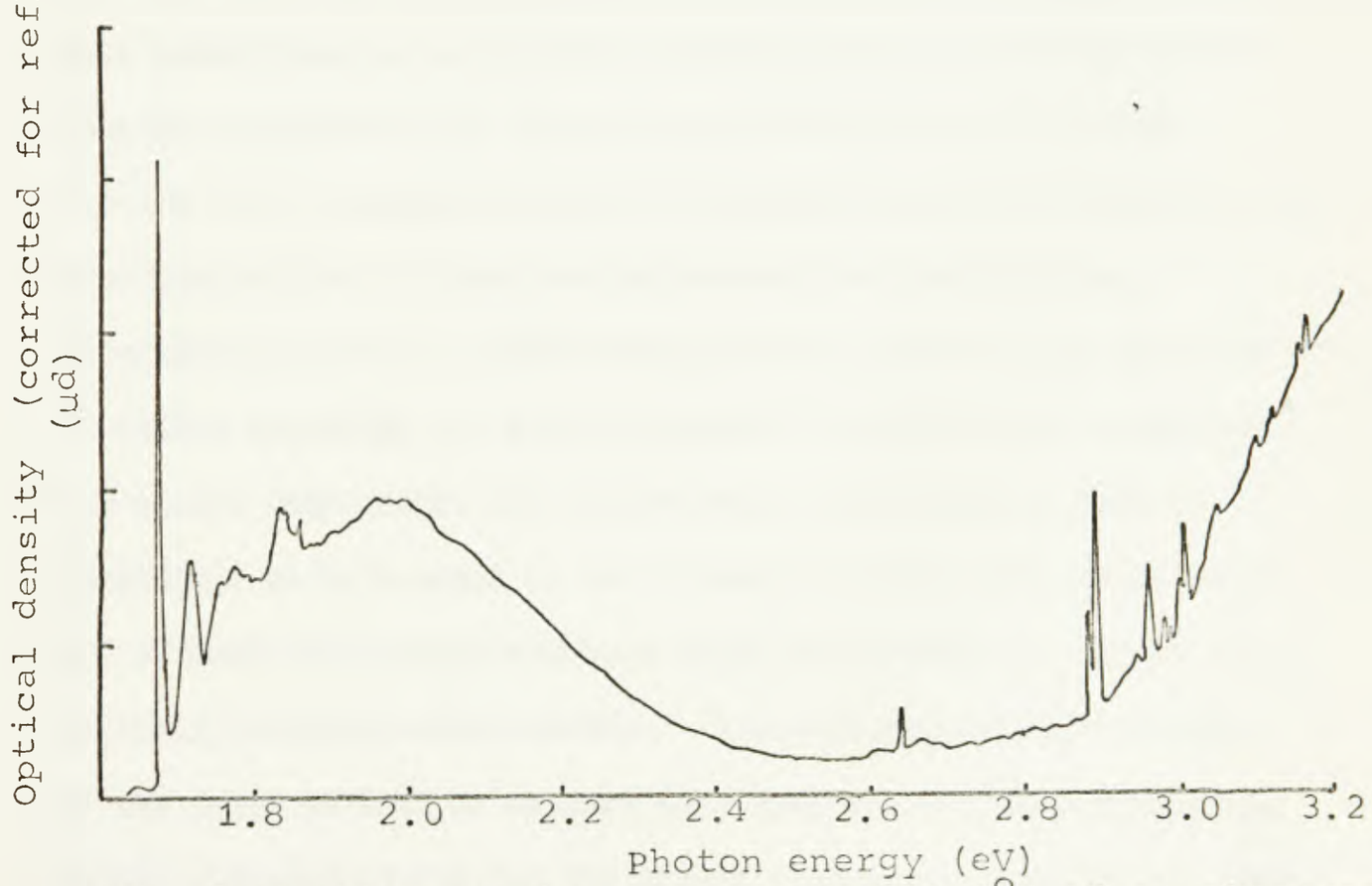
non-gaseous impurities as Si, Ca, Mg, Al, Fe, Ti, B and Cu [25,26]. Therefore, spurious features in isolated spectra may arise. The results that we shall discuss are generally not exclusive to type IIa diamonds.

After irradiation with neutrons, electrons or γ particles type IIa diamonds show optical absorption in a normally transparent region of the spectrum as shown in figure 1.1. The important feature of the absorption spectrum is the appearance of a broad absorption band between 1.65 and 2.4 eV (denoted GR1 by Clark et al [27]). A very intense zero phonon line is resolved at 1.673 eV with a further fine structure superimposed on the broad band. Trifinov [28] has suggested that the form of the GR1 band might be explained in terms of zero, individual and multiple phonon interactions. Clark and Norris [29,30] have shown that the luminescence emission of the GR1 band shows no polarisation at low temperature due to the highly symmetrical state of the centre. Duncan [30] has measured the Huang-Rhys factor, the Stokes Shift and the band width of the band. Irradiation of the crystal also causes optical absorption, commencing at 2.8 eV and increasing to a maximum at 4.0 eV after which it decreases only to be masked by the beginning of the region of continuous absorption. This broad band is known as the u-v band. Sharp absorption lines at 4.133 eV and 3.315 eV in type II diamonds have been used as a measure of the strength of the u-v band [31,32].



ig.1.1a

Liquid nitrogen temperature absorption spectra of electron irradiated type II diamonds. Before and after irradiation with 6.02×10^{17} e-cm^{-2}, 1.5 MeV at 2μA cm^{-2}.



'ig.1.1b

The absorption spectrum recorded at 4.2°K of an electron irradiated type II diamond.

Dyer and Ferdinando [33] have reported that the GR1 and u-v bands produced in type IIa diamonds do not appear in type IIb semi-conducting diamonds until the irradiation dose is sufficient to lead to compensation of all the impurity acceptor centres in the crystal. Irradiation induced donor centres which are optically non-absorbing when ionized are believed to be associated with these bands. It has been suggested that both these bands arise from electronic transitions within the same centre [34]. Optically bleaching experiments [34] on electron irradiated type I diamonds have led to the discovery of a new centre denoted ND1 which is thought to be a defect product of an interstitial and nitrogen in platelet form. This centre acts as an acceptor which is optically inactive when neutral and active when ionized with absorption in the range 3.1-3.8 eV. Electron transfer by thermal excitation results in the bleaching of the GR1 band and enhancement of the ND1 band. Illumination with u-v light causes electron transfer in the reverse direction restoring the band strengths to their former conditions. The centre responsible for the GR1 and u-v absorption band is considered on this model to be a vacancy, with ground state about 2.8 eV below the conduction band edge, which acts as a donor and is optically inactive when ionized. The most significant feature of the study is that it demonstrates that at room temperature the centre responsible for the GR1 band is thermally stable in two states of charge. If this centre is the vacancy then it must be in either the neutral or negatively charged state. Nowadays one of the main

reasons for associating the GR1 band with the vacancy centre seems to arise from the theoretical calculation by Coulson and Kearsley [1] which suggested that there was a correlation between this band and the electronic properties of the neutral charge state of the isolated vacancy.

There have been many studies related to the effect of heat treatment on the absorption spectra of irradiated diamonds. At least three main stages have been observed between 25°C and 1,000°C [35,36]. From 25-275°C no observable change in the absorption spectrum is observed. Between 275-575°C the strength of the GR1 band diminishes and the absorption lines become sharper, but the band does not anneal out. The defect responsible for the GR1 band, sometimes just called the G centre, is considered to be immobile at these temperatures. At higher temperatures the results are conflicting, but some studies suggest that the GR1 band is removed and a new broad band in the region 2.3-2.8 eV appears together with an increased background absorption from 1.2 eV to the beginning of the absorption continuum. This band in type IIa diamonds, denoted TH5 by Clark et al. [37], causes the diamonds to become yellow in appearance and has considerable fine structure at 80°K. Clark (private communication) believes that the TH5 band may arise from an aggregate of vacancies, assuming the origin of the GR1 band to be associated with a vacancy. However, he has also pointed out that nitrogen in diamonds can cause them to have a yellow colour, such that the possibility of an impurity-defect centre should not be discounted.

In recent times there has been much interest in the study of defects in irradiated and naturally occurring diamonds using electron paramagnetic resonance techniques. For the irradiated diamonds many of the spectra are very complicated and the results so far have been generally inconclusive in identifying any centres with certainty. A comprehensive survey of the experimental information to 1964 has been given by Owen [38] and should be consulted for explicit details. We have attempted here to highlight a few of the most important studies which are relevant to this thesis.

Many resonance lines have been observed* but there appears to be two general features for most of the spectra. 1) The signal intensity is roughly proportional to the irradiation dose over a wide range and 2) annealing of the crystal usually leads to removal of, or a considerable reduction in, the intensity of the resonance lines originally observed at room temperature. Perhaps the most interesting study so far is that by Baldwin [40] who found that there was a system of at least three superimposed lines around $g = 2.0025$, using type IIa diamonds irradiated with 0.75 MeV electrons. The principal line, denoted the 'a' system, with $S = \frac{1}{2}$ was anisotropic and enhanced by u-v radiation with energy greater than 2.83 eV and quenched with radiation of around 1.10 eV. Evidence

---

*Unfortunately different nomenclature have developed for referring to the same lines in the resonance spectra depending upon whether electron or neutron irradiated samples are used. We have used the nomenclature of Faulkner and Lomer [39] referring to electron irradiated studies rather than that of Owen [38] as the former is the one in more common use today.

suggested that this centre had a <100> symmetry axis presumably arising from a Jahn-Teller distortion. He also studied the hyperfine interaction effects for the first-and second-nearest neighbour nuclei which suggested that about 10 per cent of the electronic wave function was delocalised. He postulated, partly on the basis of the theoretical study by Coulson and Kearsley [1], that the origin of the 'a' system was the positively charged vacancy and therefore 2.83 eV was the energy required to ionize a neutral lattice vacancy. Unfortunately, little detailed experimental evidence for the above work was ever published and therefore research workers have been rather sceptical of these findings. However, Du Preez [41] reported that preliminary work suggested that the quantitative results of Baldwin were substantially correct, but unfortunately further evidence of this work has also never been published. Therefore, it still remains for this work to be reliably confirmed.

Duncan [42] reported that a single isotropic line was present in his type IIa diamonds before irradiation. He concluded that the centre responsible for this line was identical with that for the 'a' system discussed above and was not therefore solely the product of irradiation. This observation has been confirmed by Dyer and Du Preez [34] but they believed that the 'a' system was just superimposed upon this isotropic line and that different centres were involved. Recently, Lomer et al. [34] reported having observed an intense 'a' line at temperatures as high as 1200°C. The strength of the signal for the 'a' system was found to correlate with the intensity of the background absorption but not with the GR1 band intensity. Samples irradiated with 2 MeV electrons or neutrons show

complicated spectra at room temperature [44,45]. As well as the 'a' system a weak 'b' system of lines with S = 1 which is enhanced by annealing at high temperature is observed. At this stage the origin of the spectrum is unknown, but some workers have attributed its origin to impurity centres while others believe that the resonance lines are associated with pairs of vacancies. A prominent E.S.R. centre called the 'c' system by Faulkner and Lomer [39] and B system by Owen [38] has been observed. Owen's observations suggested that the ground state of this centre was diamagnetic with a paramagnetic state about 300 cm^{-1} (0.037 eV) above this level. Duncan [42] found a correlation between the strength of the 'c' system (S = 1, g = 2.00, D = 0.140 cm^{-1}) with symmetry axis along the <100> direction and the strength of the corresponding optical GR1 band at room temperature. Clark et al. [45] reported that this 'c' system completely annealed out in the region 400–450°C. Since experimental evidence suggest that the G centres are not mobile at such temperatures the conclusion is drawn that the GR1 band and the 'c' lines cannot arise from the same centre. However, they are found in constant proportions in all specimens as direct products of irradiation. It has been very tentatively suggested that the single carbon interstitial atom is responsible for the 'c' system of lines assuming that the G centre is the isolated vacancy. No conclusive evidence is available at present. There are several other complicated systems of E.P.R. lines, denoted d,e,f,g which have been observed by Lomer and colleagues at Reading, but their origin

has not yet been established. The striking thing is that most of these centres have total spin $S \geq 1$, whereas in silicon this is not the case. Watkins (private communication) suggests that this may be due to the long spin-lattice relaxation time for $S = \frac{1}{2}$ centres in the diamond system.

The primary defects such as vacancies and interstitial atoms in the diamond crystal still remain to be positively identified. There are two main reasons for this uncertainty and much can be learned from a comparison with the development of the study of point defects in silicon. Here the work of Watkins [10] is most notable. Firstly, it is almost impossible to obtain diamond crystals free from impurities and very difficult to identify and control the impurity content. For silicon, however, very pure crystals may be grown by a vacuum floating-zone technique and a controlled impurity concentration may be introduced when necessary to aid identification of the charge states of defects. Secondly, most irradiation studies reported have used large doses of high energy irradiation (> 1.5 MeV) and temperatures greater than $0^{o}C$. Again Watkins [10,46] has reported that in silicon such conditions produce complex defects. It is necessary to be careful about extrapolating from one solid to another, but the evidence does suggest that more information about the primary defects could be obtained at lower temperatures.

Because of the experimental difficulties the importance of theoretical calculations as a means of identifying the centres responsible for the observed phenomenon is enhanced. So far the theoretical calculations have been based on very elementary models using simple wave functions and have neglected such effects as possible delocalization of electronic charge from the defect, distortion and relaxation effects and exchange and polarisation terms. Before we can have confidence in the findings of the simplest studies it is necessary to investigate at least some of these effects to see if they do influence the predicted electronic structure of the point defects. This therefore is the essential aim of the present thesis.

(b) The Silicon Crystal

The elegant electron-paramagnetic resonance work by Watkins and Corbett incorporating uniaxial stress techniques, aided by greater purity of samples and controlled doping, have enabled the identification of the primary defects in silicon with reasonable certainty. No attempt has been made here to review the extensive amount of experimental evidence available to demonstrate the existence of the primary defects and defect-impurity atom pairs in silicon as detailed discussions are available elsewhere [10,47]. Rather just the main studies relating to the identification of the vacancy, divacancy and isolated interstitial atom have been mentioned.

Watkins [10,48] has identified two different charge states of the isolated vacancy in p-type silicon by irradiation with 1.5 MeV electrons at $4^{o}K$ and $20^{o}K$. The two spectra denoted G1 and G2 have been identified as originating from the positively ionized vacancy, V^{+},

and the negatively ionized vacancy, V^-, respectively. For both spectra $S = \frac{1}{2}$ such that the ground state of these centres is assumed to be a doublet. The V^+ centre is believed to have a symmetry axis in the <100> direction and the V^- centre a mixed trigonal and tetragonal distortion as a result of a Jahn-Teller distortion of the lattice around the centre due to a degenerate ground state. Analysis of the hyperfine structure suggests that the broken bond orbitals contain about 22 per cent 3s character and 78 per cent 3p character, and that over 60 per cent of the total electronic wave function can be accounted for on the four nearest neighbour atoms to the defect. It has been argued that the neutral vacancy, V^0, does exist, but it is not observed because it has a diamagnetic ground state. Since neither spectrum has been observed in low resistivity n-type silicon, Watkins postulates that an additional charge state, the doubly negatively charged vacancy, $V^=$, may exist. When the Fermi level is locked to a shallow acceptor (B,Al,Ga) neither V^+ nor V^- represent a stable charge state and so it is believed that the neutral vacancy ground state must lie within about 0.05 eV of the valence band edge. The negative vacancy ground state is tentatively considered to be located about 0.25 eV above the valence band.

The magnitude of the Jahn-Teller splittings is estimated experimentally to vary from ~ 0.4 eV for V^+ to ~ 1 eV for the group $\underline{V}$-vacancy pairs to 1-2 eV for the divacancy [49]. The activation energy for reorientation of the V^+ centre is estimated to be only

0.01 to 0.02 eV at 20°K and reorientation is still observable at 2°K. Watkins has had considerable success in explaining his results qualitatively on the basis of a one-electron l.c.a.o. molecular orbital treatment. The migration energy for both V^0 and V^- have been estimated on the basis of annealing studies. The vacancy migration energy in p-type silicon is about 0.33 eV and the signal disappears in a 15 minute anneal at 150-180°K. This value is considered to be for the neutral vacancy. Experiments on n-type silicon suggest that the V^- spectrum disappears at 70-85°K which yields an activation energy for V^- of about 0.18 eV [18]. The self-diffusion energy for a neutral vacancy in silicon is estimated by Watkins to be around 3.5-4.0 eV, although there have been some higher estimates. Since the activation energy is very low most of the diffusion energy arises from a high formation energy.

The interpretation of the results for the divacancy in silicon are more uncertain. However, E.P.R. [46,50] and infra-red absorption measurements [51,52] on irradiated silicon suggest that the defect may exhibit four different charge states; namely, the single positive, neutral, single negative and doubly negatively charged states. The defect is produced as a primary event with 1.1-1.5 MeV electrons at temperatures as low as 20°K. The neutral divacancy in p-type silicon is thought to be about 0.25 eV above the valence band on the basis of doping and optical quenching studies. Through observing the dependence of the E.P.R. spectrum G6, thought to be associated with the negatively charged di-vacancy, on the Fermi level the double-negatively charged state in n-type silicon is estimated to be

about 0.4 eV below the conduction band. Jahn-Teller distortion effects are observed for the lowest levels of the positive and negatively charged divacancy. Radiation-induced infra-red absorption bands in silicon at 1.8-, 3.3- and 3.9μ (i.e. 0.69, 0.38 and 0.32 eV) are all thought to arise from electronic transitions within the divacancy centre from correlations with information available from E.P.R. studies. The nature of the transitions and the electronic structure of the excited states remains to be solved. The activation energy for migration of the divacancy is estimated to be about 1.3 eV and the binding energy 1.5 eV [53]. Again about 60 per cent of the total electronic wavefunction is estimated to be localised on the nearest neighbour atoms.

The interstitial atom has not been observed directly. However, Watkins suggests on the basis on some experiments on aluminium doped p-type silicon that this primary defect may be mobile at temperatures as low as $4^{o}K$.

In chapter 7 of this thesis we propose to investigate the electronic structure of the isolated vacancy in its various charge states in the silicon lattice using the method developed by Coulson and Kearsley [1] as a basis for the calculation. We investigate the importance of the Jahn-Teller and symmetric relaxation terms in predicting the electronic structure of these centres. The formation energy of the neutral vacancy has also been calculated in chapter 5.

1.4 Summary and Conclusion

The possible theoretical approaches to the calculation of the electronic properties of point defects in covalent crystals have been discussed. We have chosen the defect molecule method as the most suitable for our present purposes. The experimental evidence for the existence of single vacancies, divacancies and interstitial atoms in irradiated diamond and silicon crystals has also been examined.

CHAPTER 2

THE DEFECT MOLECULE METHOD

The general theory of the defect molecule method for the isolated single vacancy in its various charge states in the diamond-type lattice is developed.

2.1 Introduction

It is proposed in this chapter to discuss the general theory of the defect molecule approach as it is applied to the isolated vacancy in the diamond-type lattice. We will be considering four possible charge states of the vacancy; namely, the single positive, V^+, the neutral, V^0, the single negative, V^-, and the double negatively charged state, $V^=$. The theory presented here is also relevant to the isolated neutral divacancy problem discussed in chapter 4. The formal expressions for the energy levels of the single vacancy used in subsequent chapters are determined within this framework.

Most of this work has been developed previously. Nevertheless, as it is the fundamental basis on which this thesis is established, and since we have made some important changes, the essential details are again presented here. Most of the discussion is oriented towards the diamond crystal, since that is our primary interest, but it may in general be thought to be equally applicable to the silicon crystal, although there is the need for some slight modifications which are discussed further in the chapter on the silicon vacancy. The chapter commences with a discussion of the model (section 2.2) and then the theory is developed in several subsequent sections.

2.2 Model for the Isolated Vacancy

The carbon atoms of a perfect diamond crystal are considered to be in a tetrahedral sp^3 state, with each atom at the centre of a regular tetrahedron formed by its four neighbours, to which it is covalently bonded. In order to create the vacancy it is necessary to break four bonds. Although there will be some deformation of the lattice around the vacancy there is no quantitative experimental evidence to suggest its extent and therefore in the first approximation we have assumed it to be small. In chapters 5 and 6 we will consider the effect of distortion terms more closely. Nevertheless, the undistorted case is important, because it provides the basis for further electronic calculations. The results obtained from theoretical formation energy studies by Swalin [54] and Seeger et al. [55] suggest that the neglect of distortion effects will be more serious for silicon than for diamond, but their results are too limited to be used as estimates of distortion for electronic calculations. In the model proposed for the electronic calculation each of the four atoms neighbouring the defect will have three of its valence electrons still involved in the formation of localized carbon-carbon bonds to atoms which are second nearest neighbours to the vacancy. There remains a fourth valence electron which in the undisturbed lattice would be bonded with valence electrons on the missing atom.

Following Coulson and Kearsley [1] it is assumed that the electronic properties of the system in the immediate neighbourhood of the defect are dependent on just these four electrons - termed vacancy electrons. The distribution of these vacancy electrons in the electric field of the neighbouring atoms and the much weaker field of the rest of the lattice is therefore to be determined. The contribution to the potential field of the vacancy electron due to atoms which are not nearest neighbours to the defect will be small, because these atoms are fully bonded and appear electrically neutral to a vacancy electron. This model involves two main assumptions.

Firstly, it is assumed that the vacancy electrons occupy orbitals which are localized in the region of the defect. This is certainly a better assumption for the diamond crystal than for silicon. Analysis of the hyperfine constants obtained by Baldwin [40] for what was believed to be the isolated vacancy in diamond suggests that there is about 10 per cent delocalisation of the vacancy wave-function. Whereas Watkins [10] has found that for some silicon vacancy-impurity pairs and possibly also for the silicon vacancy itself delocalisation of the defect electrons may be as much as 40 per cent. We will discuss in the next chapter an attempt which has been made to modify the model to analyse the effect of delocalisation on the electronic levels.

Secondly, it is assumed that the energy levels for the vacancy electrons may be considered without detailed allowance being made for such effects as exchange or polarisation by other electron clouds. Coulson and Kearsley have shown that the transition energies are fairly insensitive to the exchange effects even though the absolute energies are dependent upon them. In the calculation of the silicon vacancy outlined in chapter 7 we have however included some of the exchange effects.

Hence, this model assumes that the electronic character of the defect is dominated by the behaviour of the vacancy electrons. All other electrons of the atoms neighbouring the defect are taken into account only in forming the potential term. The region near the defect is therefore effectively a 'defect molecule' imbedded in the infinite crystal matrix. Because of this molecular character of the problem we are able to use the well-established techniques of molecular-orbital theory to simplify the calculations. Even if the rest of the lattice is not perfect, the present simple model will be applicable provided the other defects are sufficiently well separated from one another such that the interaction between their potential fields is negligible. In the development of the theory the charged vacancies are dealt with in a similar way to the neutral case.

2.3 Molecular Orbital Wave-functions for the Defect Molecule

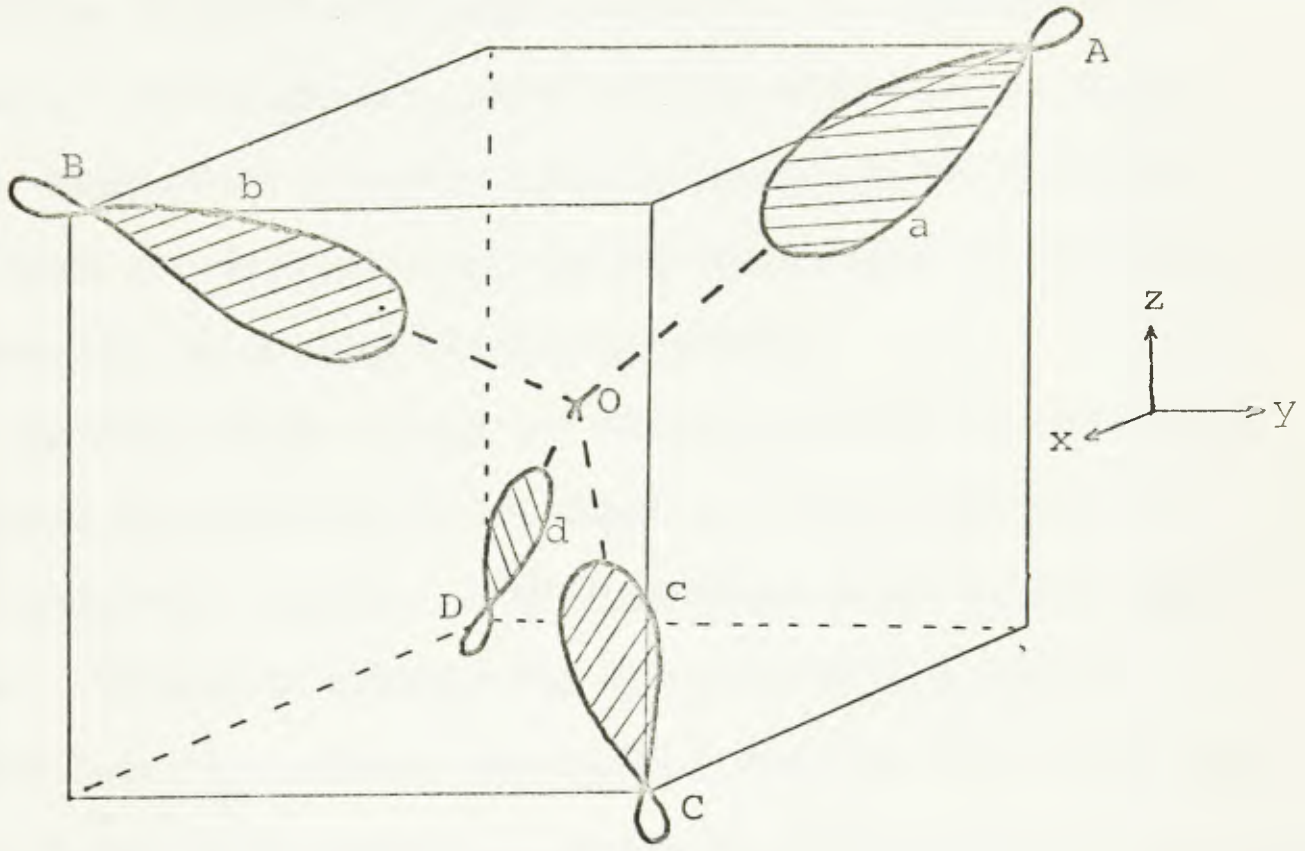
The model for the isolated vacancy is shown in figure 2.1. We shall be primarily interested in the n vacancy electrons which belong to the defect molecule. In the case of the neutral vacancy the four vacancy electrons were in tetrahedral hybrid orbitals, a - d, associated with the atoms A - D before the defect was created. These vacancy electrons originally formed covalent bonds with the valence electrons of a carbon atom at O. For an isolated carbon in a state of sp^3 hybridisation suitable tetrahedral hybrid orbitals are of the form

$$\Psi_i = \tfrac{1}{2}\left[\psi_i(2s) + \sqrt{3}\,\psi_i(2p_\sigma)\right] \qquad (2.1)$$

where the $2p_\sigma$ orbital is along the polar axis of the hybrid. Before atom O was removed the covalent bond between, for example, atoms O and A, may be formed from a hybrid orbital centred at A and directed along $\vec{AO}$ and similar orbital centred at O directed along $\vec{OA}$. These hybrids would have the form given by equation 2.1. A reasonable choice for the localized unbonded orbitals a - d, which are to be combined to build up the complete electronic wave function for the defect molecule within the molecular theory would therefore seem to be

$$x = \tfrac{1}{2}\left[\psi(2s:X) + \sqrt{3}\,\psi(2p_\sigma:X)\right] \qquad (2.2)$$

where x corresponds to orbital a,b,c or d, while X refers to atoms A,B,C and D respectively.



g.2.1 Defect Molecule for Isolated Vacancy:

T_d symmetry

It is possible to use either the molecular orbital (m.o.) or the valence bond (v.b.) method in the solution of the problem. However, because of the non-orthogonality of the tetrahedral hybrid orbitals a,b,c and d the m.o. method is easier to handle. Nevertheless, both methods become identical when ionic structures are included in the v.b. method. Within the m.o. method we have chosen to incorporate the linear combination of atomic orbitals approximation (l.c.a.o. - m.o. - method) and to apply configuration interaction to states of the same symmetry to obtain improved energy values.

For the undistorted vacancy the distance between any two of the atoms nearest the defect is $\sqrt{8}\, a/4$ where a is the cell constant for the diamond-type lattice. For diamond a = 3.56Å and for silicon a = 5.43Å. The defect molecule has the symmetry of a regular tetrahedron i.e. T_d. Hence, the dominant electric field about the vacancy will have this symmetry. It can be shown using standard group theoretical techniques that in a field of T_d symmetry the single-electron molecular orbitals belong to the irreducible representations a_1 and t_2. If we allow the neighbours to the vacancy A,B,C and D to have the co-ordinates $(\bar{1},1,1)$, $(1,\bar{1},1)$, $(1,1,\bar{1})$ and $(\bar{1},\bar{1},\bar{1})$ respectively, in units of a/4 where a is the cell constant, then a suitable set of real non-localized single-electron wave-functions, which are mutually orthogonal and correspond to the symmetry irreducible representations are as follows:

$$
\begin{aligned}
v &\equiv N_1(a + b + c + d) && a_1 \\
t_x &\equiv N_2(-a + b + c - d) && \\
t_y &\equiv N_2(a - b + c - d) && \Big\} \quad t_2 \\
t_z &\equiv N_2(a + b - c - d) &&
\end{aligned}
\tag{2.3}
$$

where $N_1 = 0.5(1 + 3S_{ab})^{-\frac{1}{2}}$, $N_2 = 0.5(1 - S_{ab})^{-\frac{1}{2}}$ and S_{ab} is the overlap integral between two hybrids on neighbouring atoms to the defect. It should be noted that this is not the set chosen by Coulson and Kearsley, but will prove to be more versatile in the calculations to follow.

Each non-degenerate orbital may be occupied by at most two electrons, and each triply degenerate set by at most six electrons in accord with the Pauli Exclusion Principle. Therefore, for a system of n vacancy electrons, where for our purposes n = 3,4,5 or 6, there are only three possible allowed configurations of the form $v^p t_2^{n-p}$ where $0 \leq p \leq 2$. For the neutral vacancy, for example, since there are 8 possible spin orbitals and four vacancy electrons, there are 70 possible four-electron wave-functions for the system. The symmetry states of these four-electron wave-functions corresponding to a particular configuration may be determined using the method of Mulliken [56] of reducing through states of lower symmetry. Since holes transform like particles and the 't shell' is closed at six electrons it follows that t_2^4 transforms as t_2^2, t_2^5 as t_2 and t_2^6 as a_1. For uniqueness it is necessary to choose a sub-group such that each of the irreducible representations from the direct product of that

configuration goes over into a different one-dimensional representation, or a sum of one-dimensional representations of the sub-group. The symmetry and spin multiplicities of the resultant states for each configuration corresponding to the various charges states of the vacancy are given in table 2.1.

In order to represent the symmetry states of each particular configuration we form the n-electron wave-functions that have the correct symmetry and are simultaneous eigenfunctions of S^2 and S_z, where S is the total spin operator and S_z the z component. This is achieved by first choosing a suitable set of Slater determinants as the primitive basis functions belonging to the same eigenvalue of the symmetry states of that particular configuration. For example, we may choose to represent the basis function $\phi_i(R)$ corresponding to the $^2A_1$ symmetry state of the configuration vt_2^4 by the Slater determinant

$$\phi_i(^2A_1) = (v\bar{x}x\bar{y}y\bar{y}) = N \begin{vmatrix} v(1)\ \alpha(1) & x(1)\ \alpha(1) & x(1)\ \beta(1) & y(1)\ \alpha(1) & y(1)\ \beta(1) \\ v(2)\ \alpha(2) & \cdots & \cdots & \cdots & \cdots \\ \cdots & \cdots & \cdots & \cdots & \cdots \\ \cdots & \cdots & \cdots & \cdots & \cdots \\ v(5)\ \alpha(5) & \cdots & \cdots & \cdots & y(5)\ \beta(5) \end{vmatrix}$$

$$N = \frac{1}{(5!)^{\frac{1}{2}}}$$

where the bar over the orbital denotes β spin and its absence α spin. This function is chosen so as to satisfy the eigenvalue equation

TABLE 2.1

Allowed states for the Vacancy

Number of Vacancy electrons, n	Configurations	Symmetry of resultant states
3	v^2t_2	$^2T_2$
	$v\,t_2^2$	$^2A_1 + {}^2E + {}^4T_1 + {}^2T_1 + {}^2T_2$
	t_2^3	$^4A_2 + {}^2E + {}^2T_1 + {}^2T_2$
4	$v^2t_2^2$	$^1A_1 + {}^1E + {}^3T_1 + {}^1T_2$
	$v\,t_2^3$	$^5A_2 + {}^3A_2 + {}^3E + {}^1E + {}^3T_1 + {}^1T_1 + {}^3T_2 + {}^1T_2$
	t_2^4	$^1A_1 + {}^1E + {}^3T_1 + {}^1T_2$
5	$v^2t_2^3$	$^4A_2 + {}^2E + {}^2T_1 + {}^2T_2$
	$v\,t_2^4$	$^2A_1 + {}^2E + {}^4T_1 + {}^2T_1 + {}^2T_2$
	t_2^5	$^2T_2$
6	$v^2t_2^4$	$^1A_1 + {}^1E + {}^3T_1 + {}^1T_2$
	$v\,t_2^5$	$^1T_2 + {}^3T_2$
	t_2^6	$^1A_1$

$$S_z \phi_i(R) = \mathcal{S} \phi_i(R)$$

where

$$\mathcal{S} = \tfrac{1}{2} \hbar(n_\alpha - n_\beta)$$

and n_α and n_β represent the number of columns of α's and β's respectively. In the present work we have chosen S_z = max.spin.

These basis functions are then used to form combinations which have the desired space symmetry. The space transformation properties of these determinants are such that each chosen determinant may either be mapped onto itself or transformed into a linear combination of determinants within the same sub-set under the operations $\mathcal{R}$ of the group, i.e.

$$\mathcal{R} \phi_i(R) = \sum_j a_j \phi_j(R)$$
$$= \psi(R) .$$

Using such group theoretical techniques the transformation properties of each basis function may be determined. Finally, the condition is imposed on the wave-function $\psi(R)$ that it be an eigenfunction of S^2. That is we require that

$$S^2 \Psi(R) = S'(S'+1) \hbar^2 \Psi(R)$$

where S^2 = square of the total spin operator

$$= S_- S_+ + \hbar S_z + S_z^2$$

and

$$\Psi(R) = \sum_k b_k \psi_k(R) \ .$$

This final step may be accomplished either by use of projection operators or, as in the present case, by inspection. The set of un-normalized wave-functions for the various configurations of each of the charge states, V^+, V^0, V^- and $V^=$ are given in Appendix A.1

2.4 The Hamiltonian for the System

The spin-independent Hamiltonian for the defect molecule system (excluding exchange with non-vacancy electrons) may be written, in atomic units, in the following form

$$H = H^0 + H^1 \qquad (2.4)$$

where

$$H^0 = \sum_{i=1}^{n} (T_i + V_i) \qquad (2.5)$$

and

$$H^1 = \sum_{i<j} \frac{1}{r_{ij}} \qquad (2.6)$$

$i,j = 1,2,\ldots n$, where n is the number of vacancy electrons

$$T_i = -\tfrac{1}{2} \nabla_i^2$$

= kinetic energy operator for the i^{th} electron.

V_i represents the potential energy of interaction of the vacancy electron i, with the nuclei, the K-shell electrons surrounding the nuclei of the vacancy atoms and with the bonded valence electrons of

these atoms. The latter electrons may be considered to be in localized tetrahedral hybrids directed along the sets of unbroken bonds at atoms A...D. Therefore

$$V_i = \sum_K V_{Ki} \qquad (2.7)$$

where K = A,B,C,D and, for example, in the case of carbon

$$V_{Ai} = -\frac{6}{r_{Ai}} + \begin{array}{l}\text{repulsion from the two}\\ \text{K-shell electrons around}\\ \text{atom A}\end{array} + \begin{array}{l}\text{repulsion from the}\\ \text{tetrahedral hybrids}\\ \text{around A.}\end{array} \qquad (2.8)$$

These repulsions are just the coulomb repulsions due to the appropriate charge clouds. We may express this term in a convenient form for evaluation by using a method first employed by Goeppert-Mayer and Sklar [57]. In this approximation a term representing the repulsion from a fourth tetrahedral hybrid is added to and subtracted from V_{Ai} such that the potential acting on a defect electron may be written as

$$V_{Ai} = V^o_{Ai} - \int \frac{a(j)^2}{r_{ij}} d\tau_j \quad . \qquad (2.9)$$

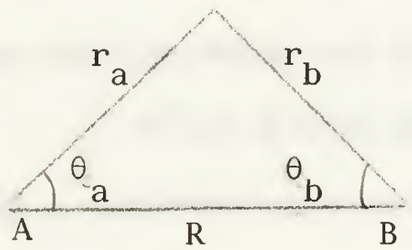
This means that the potential acting on a defect electron due to the positive ion of carbon is equal to the potential due to a neutral carbon in the appropriate valence state (tetrahedrally hybridized in this case) V^o_{Ai}, minus the repulsion from an electron in the fourth tetrahedral hybrid. As previously mentioned the exchange terms are neglected in computing the related part of the energy using the

equation 2.9 for V_{Ai}. The neglect of exchange terms will be more serious in the case of intra-atomic integrals such as $\langle a|V_{Ai}|a\rangle$ than for the inter-atomic integrals. However, previous work by Coulson and Kearsley [1] has shown that the energy level separations for the lowest states are fairly insensitive to the value of this integral so that the above approximation for V_{Ai} was considered to be adequate for the present calculation. As we shall see in chapter 7 we have modified equation 2.8 when considering the silicon vacancy to include exchange terms.

We have used the free atom s and p electron wave-functions for the neutral carbon or silicon atoms in their ground state. For simple analytical forms of the atomic wave-functions, such as those proposed by Slater [58], the terms involving V_{Ai}^{o} may be evaluated by transforming the integrals into elliptical co-ordinates defined by

$$\zeta = \frac{r_a+r_b}{R}, \qquad \eta = \frac{r_a-r_b}{R}, \qquad \phi = \phi_a = \phi_b$$

where r_a, r_b and R are defined in the diagram



The integrals then become separable in terms of incomplete gamma-type functions

$$A_n(\alpha) = \int_0^\infty \zeta^n e^{-\alpha\zeta}\, d\zeta \quad \text{and} \quad B_n(\lambda) = \int_{-1}^{1} \eta^n e^{-\lambda\eta}\, d\eta \,.$$

The values of these integrals may be obtained by a series expansion method or from suitable recurrence relations which may be found in standard works. In the present investigation values of these integrals were obtained using the tables compiled by Flodmark [59]. For complicated functions such as the self-consistent atomic Hartree-Fock functions proposed by Clementi [60] it is more convenient to evaluate the integrals which contribute to the term involving V_{Ai}^{o} independently. A variational calculation for the orbital exponents was not attempted, because of the difficulty involved in evaluating multi-centre integrals and the desire to retain simplicity in the method. Ideally, we should have different s and p wave-functions for each charged state of the vacancy. However, this cannot be accomplished with our simple model.

2.5 Energy Evaluation before Configuration Interaction

In the charge states of the vacancy the energy levels before configuration interaction for the various symmetry states, R, belonging to each configuration are given by

$$E(R) = \frac{\int \Psi^*(R)\, H\, \Psi(R)\, d\tau}{\int \Psi^*(R)\, \Psi(R)\, d\tau} \qquad (2.10)$$

where $\Psi(R)$ is the n-electron wave-function corresponding to a given irreducible representation R of the group T_d, for a particular configuration and given S and S_z as previously defined.

On substitution of the appropriate molecular wave-functions into 2.10 the integration may be reduced to a series of one- and two-electron integrals involving the molecular orbitals v, t_x, t_y and t_z. These primary molecular integrals are given below together with an abbreviated notation for convenience

$$A = \langle v|H^0|v\rangle \,/\, \langle v|v\rangle$$

$$B = \langle t_x|H^0|t_x\rangle \,/\, \langle t_x|t_x\rangle$$

$$C = \langle vv|H^1|vv\rangle \,/\, \langle v|v\rangle^2$$

$$D = \langle t_x t_x|H^1|t_x t_x\rangle \,/\, \langle t_x|t_x\rangle^2$$

$$E = \langle vt_x|H^1|vt_x\rangle \,/\, \langle v|v\rangle \langle t_x|t_x\rangle$$

$$F = \langle t_x t_y|H^1|t_x t_y\rangle \,/\, \langle t_x|t_x\rangle^2$$

$$G = \langle vt_x|H^1|t_x v\rangle \,/\, \langle v|v\rangle \langle t_x|t_x\rangle$$

$$J = \langle t_x t_y|H^1|t_y t_x\rangle \,/\, \langle t_x|t_x\rangle^2$$

$$K = \langle vt_x|H^1|t_y t_z\rangle \,/\, [\langle v|v\rangle \langle t_x|t_x\rangle^3]^{\frac{1}{2}}$$

where $H^0 = T_1 + V_1$ = single particle operator in H

$H^1 = 1/r_{12}$.

The energy expressions E(R) for n=3,4,5 and 6 are given in Appendix A.2, in tabular form in terms of these integrals A...K. These expressions are essentially those obtained by Kearsley [61] and Yamaguchi [2]. However, the form of the expression $E(^2E)$ arising from the $v^2t_2^3$ configuration obtained by Kearsley was incorrect. The corrected expression is given in the Appendix. The integrals containing the molecular orbitals may in turn be expressed in terms of one- and two-electron integrals involving the localized atomic hybrid orbitals a,b,c and d. Finally, all these integrals may be

broken down into one- and two-centre integrals, of Coulomb, hybrid, exchange and ionic type together with some three- and four-centre integrals. The Diatomic Molecular Integral Program adapted with special modifications by Hopgood for the S.R.C. Atlas Computer was used to evaluate all the basic integrals mentioned above. The original version of the program was written by Corbato and Switendick. Details of the numerical methods used and the form of the program are available [62,63]. Three- and four-centre integrals were evaluated by use of the Mulliken approximation [64]. This technique was considered to be adequate for present purposes. Further computation to obtain the molecular integrals was carried out using programs written either in the Algol 60 language for the KDF 9 English Electric Computer at Oxford or in Fortran IV for the IBM 360/65 Computer at A.E.R.E. Harwell.

Coulson and Kearsley showed that if all the intra- and inter-atomic integrals were evaluated non-empirically then, in the case of the diamond vacancy, unsatisfactory results were obtained. It was reasoned that this was not entirely unexpected since previous molecular-orbital calculations for the spectra of some π-electron systems by Moffit [65], Parr and Pariser [66] and others had experienced similar disappointing results with an unmodified theory. The chief cause of the difference between the theoretical and experimental results was shown to be the use of the same analytic functions to calculate both the covalent and ionic terms as they would arise in dealing with neutral and ionized atoms. This discrepancy may be largely corrected by modifications, of a semi-

empirical kind, to the one-centre coulomb integral Q, namely

$$Q = \int \chi_a^*(1)\, \chi_a^*(2)\, \frac{1}{r_{12}}\, \chi_a(1)\, \chi_a(2)\, d\tau_1\, d\tau_2$$

where χ_a is the orbital on atom A under consideration. Pariser [67] argued that a better estimate of Q would be

$$Q = I - A \qquad (2.12)$$

where I is the ionisation potential and A the electron affinity of a neutral carbon atom in its valence state.

In the previous investigation Coulson and Kearsley found that significantly better results were obtained when a modified anti-symmetrical molecular-orbital (a.s.m.o.) method was used. It is necessary, therefore, to modify the intra-atomic coulomb integral, Q, and the self-penetration integral, P. In our problem these integrals are defined as follows

$$\begin{aligned} Q &= \int a^*(1)\, a^*(2)\, \frac{1}{r_{12}}\, a(1)\, a(2)\, d\tau_1\, d\tau_2 \\ P &= \int a^*(1)\, \{T_1 + V_{A1}\}\, a(1)\, d\tau_1 \,. \end{aligned} \qquad (2.13)$$

The approximation Q = I - A still holds in the atomic-orbital approximation where now I and A are respectively the ionisation potential and electron affinity for an isolated carbon or silicon atom in the sp^3 valence state. The quantities cannot be determined directly, but by using the values of I and A for pure s and p orbitals and certain additional experimental data on the term values

of an isolated atom in the sp^3 state they may be estimated. A brief discussion of the method used, based upon the approach of Condon and Shortley [68] and others, is given in Appendix A.3. There is a significant difference between the theoretical and experimentally predicted values obtained for Q. For carbon, using Clementi functions this difference was 4.96 eV, while for silicon it was 3.35 eV.

It follows that the value of the self-penetration integral, P, defined in 2.13 is probably inadequately estimated when using analytical wave-functions. However, it is not easy to obtain even a rough semi-empirical value instead of the analytical one. The integral is sensitive to the specific form of the potential V_{Ai} since the overlap between V_{Ai} and a(i), the orbital under consideration, will be large. The form of V^o_{Ai} will almost certainly be different in the crystal to the isolated atom. Also there will be some deformation of the covalent hybrids which are occupied by the other valence electrons of the atoms nearest the defect. The question of the occupancy of the orbitals and exchange interactions also arises. We assume on average there are three electrons 'belonging' to the atom A from its hybrids which participate in covalent bonding with its nearest neighbours. It is possible, however, to obtain some upper and lower bounds for the value of P. For the lower limit the integral may be considered as the ionisation potential of an electron in the vacancy orbital 'a' in the presence of a carbon atom for which the other three valence electrons are in single occupied orbitals forming covalent bonds tetrahedrally hybridized with random

spin coupling. This is just the negative of the ionisation potential of a tetrahedral hybrid in the sp^3 tetrahedral valence state of the atom. This value may be calculated using the procedure given in Appendix A.3. In practice the value of P will be greater than this lower limit because there will almost certainly be some double occupancy of the tetrahedral hybrid orbitals. For the upper limit we may use the analytical value incorporating the Goeppert-Mayer and Sklar approximation.

For the calculations on the vacancy in the diamond crystal we have considered just the modified case; however, for silicon we have investigated both cases within the a.s.m.o. method. The energy level scheme before configuration interaction may now be determined for the various centres.

2.6 Configuration Interaction Effects

It is well known that configurations of the same symmetry and spin multiplicity (if spin-orbital coupling is neglected) may interact with each other to give an improved value of the energy and the final state wave function. Therefore, the energies calculated before the configurational mixing are of no great value in themselves. If $\Psi_i(R)$ and $\Psi_j(R)$ denote two wave-functions from the same spin-orbital symmetry group R belonging to configurations i and j respectively, then the extent of mixing between the two states depends upon the value of

$$\int \Psi_i^*(R)\ H\ \Psi_j(R)\ d\tau\ .$$

It is easily shown by symmetry arguments that these are the only elements coupling different configurations. The expressions for these integrals connecting the various configurations of a particular symmetry are also given in Appendix A.2. These are as published by Yamaguchi [2] with the exception of the $^1T_2$ symmetry states of V^{2-}, which we believe is in error in the previous work. The final energy values are then the eigenvalues of the matrix whose ij^{th} element is as given above. The improved wave functions may be expressed as

$$\Psi'(R) = \sum_k c_k \Psi_k(R)$$

where k is summed over all the possible configurations belonging to the irreducible representation of the right spin multiplicity R. The c_k's are the coefficients of the components of the final wave function (eigenvectors) corresponding to a particular eigenvalue. These eigenvectors become important when we consider the Jahn-Teller terms in chapter 6.

2.7 Symmetry Considerations Concerning Possible Electronic Transitions

The final energy scheme is thus obtained by applying configuration interaction. There remains the problem of determining the allowed electronic transitions from the ground to the excited state. Selection rules operate to 'allow' or 'forbid' a transition. The intensity or probability of transition depends upon the value of an integral of the form

$$\int \Psi'^{*}(R)\ \underline{\mu}\ \Psi'(R_1)\ d\tau$$

where $\Psi'(R)$ and $\Psi'(R_1)$ are final wave-functions representing the ground and excited states of the defect electrons and $\underline{\mu}$ is an operator corresponding to the vector sum of the three classical components of the electronic dipole moment, i.e.

$$\underline{\mu} = \underline{\mu}_x + \underline{\mu}_y + \underline{\mu}_z$$

where

$$\underline{\mu}_x = e \sum_{i=1}^{n} \underline{x}_i, \quad \underline{\mu}_y = e \sum_{i=1}^{n} \underline{y}_i \quad \text{and} \quad \underline{\mu}_z = e \sum_{i=1}^{n} \underline{z}_i$$

and $\underline{x}_i$, $\underline{y}_i$ and $\underline{z}_i$ are the co-ordinates of the i^{th} electron. Hence, the transition probability will depend upon the values of the quantities I_x, I_y and I_z where

$$I_x \propto \int \Psi'^{*}(R)\ \underline{x}\ \Psi'(R_1)\ d\tau$$

and similarly for I_y and I_z. If the integral is not to vanish then the direct product representation of the product $\Psi'^{*}(R)\ \gamma\ \Psi'(R_1)$, namely $R \otimes \Gamma_\gamma \otimes R_1$, where $\gamma = \underline{x}, \underline{y}$ or $\underline{z}$, must contain the totally symmetric representation A_1. Hence, it is possible to have absorption of light in a preferred direction giving rise to optical dichroism if x,y and z belong to different irreducible representations of the symmetry group.

For the tetrahedral symmetry group, T_d, x,y and z all belong to the T_2 irreducible representation. Therefore, we do not expect to observe dichroism for optical transitions within the undistorted vacancy system. Furthermore, there is also a spin selection rule to be obeyed. This states that the transition between terms with different values of S - the total spin - are forbidden. It is possible, however, under certain conditions to observe so-called forbidden transitions. The allowed electric dipole transitions subject to satisfying the spin selection rule are shown in Table 2.2.

TABLE 2.2

Allowed Transitions with T_d Symmetry

Initial state	A_1	A_2	E	T_1	T_2
Final state	T_2	T_1	T_1,T_2	A_2,E,T_1,T_2	A_1,E,T_1,T_2

2.8 Summary

We have in this chapter developed the general theory of the defect molecule approximation as it is applied to the undistorted isolated vacancy in its various charge states in the diamond-type lattice. The limitations of the model, and the assumptions involved in its use have been discussed. In subsequent chapters we propose to apply this theory to the isolated vacancy and divacancy in diamond and to the isolated vacancy in silicon.

CHAPTER 3

THE ELECTRONIC STRUCTURE OF THE ISOLATED VACANCY IN DIAMOND

The electronic structure of the undistorted vacancy in its various charge states in the diamond crystal is calculated using the method developed in chapter 2. Slater- and Clementi-type functions are used to approximate the 2s and 2p orbitals on the carbon atoms in the crystal. The effect of delocalizing the electronic wave-function from the vacancy on the electronic structure of the defect is also investigated.

3.1 Introduction

In the calculation of the electronic structure of the isolated vacancy within the molecular-orbital treatment, it is necessary to make a choice of suitable functions to represent the s and p orbitals on the atoms nearest the defect in the diamond crystal. Coulson and Kearsley [1] chose to use nodeless simple analytic Slater functions, with screening constant c = 3.19, the free atom value. One difficulty with this choice is that because the 2s function is not orthogonal to the 1s function, the values obtained for the kinetic and potential energy integrals will be in error. It is interesting, therefore, to investigate the sensitivity of the energy levels of the various centres to an alternative choice of functions to represent the 2s and 2p orbitals on the atoms in the crystal. We have considered the self-consistent Hartree-Fock atomic functions proposed by Clementi [60] an adequate alternative for our present purposes. The availability of a fairly efficient integral program enables us to undertake this more detailed treatment without

prohibitive computational difficulties. Our attention has been chiefly confined to the modified theory, which uses the Goeppert-Mayer and Sklar approximation, because these cases would appear to be more physically reasonable.

Because of a numerical error in the estimate of the empirical value for the one-centre coulomb integral, Q, it has been necessary to repeat the calculation of Coulson and Kearsley before comparison could be made. The results of this analysis is given in section 3.2 for the various charge states V^{+},V^{-},V^{o},$V^{=}$. It is by no means certain at this stage that all these centres exist in diamond since none have yet been positively identified. Nevertheless, by analogy with silicon it is possible that they may all exist and so it is interesting to examine their electronic structure. In section 3.3 we present the calculations using the Clementi functions, while in section 3.4 there is a discussion of the results and the possible reason for any differences. Finally, in section 3.5, we have investigated one of the deficiencies of the model proposed in chapter 2. That is, the neglect of any delocalisation of electronic wave-function away from the vacancy, and examined its effect upon the electronic energy levels. In most cases for ease of comparison the results of the two studies are shown on the same diagram or in the same table.

3.2 Electronic Structure of the Isolated Vacancy: Slater Functions

This section discusses the electronic structure of the isolated vacancy in its various charge states only within the modified a.s.m.o. method presented in the previous chapter. We have chosen to represent the 2s and 2p functions on the carbon atoms in the crystal by Slater-type functions with the screening constant c = 3.19 as in the previous study by Coulson and Kearsley. The empirical estimate for the one-centre coulomb integral, Q, evaluated in Appendix A.3 is 12.856 eV (compared with 19.06 eV determined theoretically). This differs from the previous estimate by Coulson and Kearsley of 13.293 eV. We believe that a numerical error occurred in the evaluation of Q by these workers, although the basic formulae were correct. The analytical value of P, the self-penetration integral, is -8.00 eV (case 1), while the estimate of P deduced from the ionisation potential of a tetrahedral hybrid in the sp^3 valence state of the atom is -16.42 eV (case 2).

The values of the one- and two-electron integrals involving the localized hybrid orbitals which are necessary for the present calculation may be found in Appendix A.4. It should be noted that the integrals refer to the notation used in the divacancy calculation such that the integrals involving hybrids a and b are the relevant ones for the vacancy calculation. Using these integrals the necessary one- and two-electron integrals involving the molecular orbitals v, t_x, t_y and t_z, namely A - K, as defined in chapter 2 may be obtained. Table 3.1 shows the values of these integrals. The one-electron integral A and B are given for case 1

and case 2. The resulting energy levels before and after configuration interaction for V^+,V^o,V^- and $V^=$ are shown in fig. 3.1a, 3.2a, 3.3a and 3.4a respectively. Table 3.2 lists the numerical values obtained for the lowest levels after configuration interaction in the two cases. We observe that even though there are fairly large changes in the numerical values of the molecular integrals, A....K, and in the absolute energies (~ 5eV) compared with the previous workers, perhaps surprisingly, there are only small changes in the general features of the energy level calculation. For the neutral vacancy, the ^1E symmetry state is again lowest in energy, but now the $^3T_1$ level is within 0.1 eV of the ground state. This is even closer than had been previously predicted, and moreover, is indeed within the uncertainty of the calculation. It is therefore impossible to say which of these two levels would be lowest. The energy of the spin- and orbitally-allowed $^1E \rightarrow {}^1T_2$ transition is 1.65 to 2.22 eV for the two extreme values of P. This must be compared with the range 1.83 to 2.35 eV predicted earlier. The strong dependence of the energy levels on configuration interaction is again evident.

The electronic structure of the positively ionized vacancy was not examined by the previous workers within the modified theory, because it was considered to be very much less than either V^o or V^-. However, the present calculation suggests that this conclusion may not be valid. An examination of table 3.2 reveals that for case 1 the $^2T_2$ level for V^+ is within 3 eV of the ^1E ground state for V^o and

TABLE 3.1

Values of the Molecular integrals required for the vacancy calculation: modified cases

Integral	Slater Functions	Clementi Functions
A^*	-38.132[+]	-38.315
B^*	-27.972	-26.475
A^x	-43.764	-43.694
B^x	-38.069	-38.726
C	9.820	9.808
D	8.722	8.765
E	9.422	9.487
F	8.332	8.020
G	1.790	1.953
J	0.677	0.474
K	-1.232	-1.217

*Case 1

xCase 2

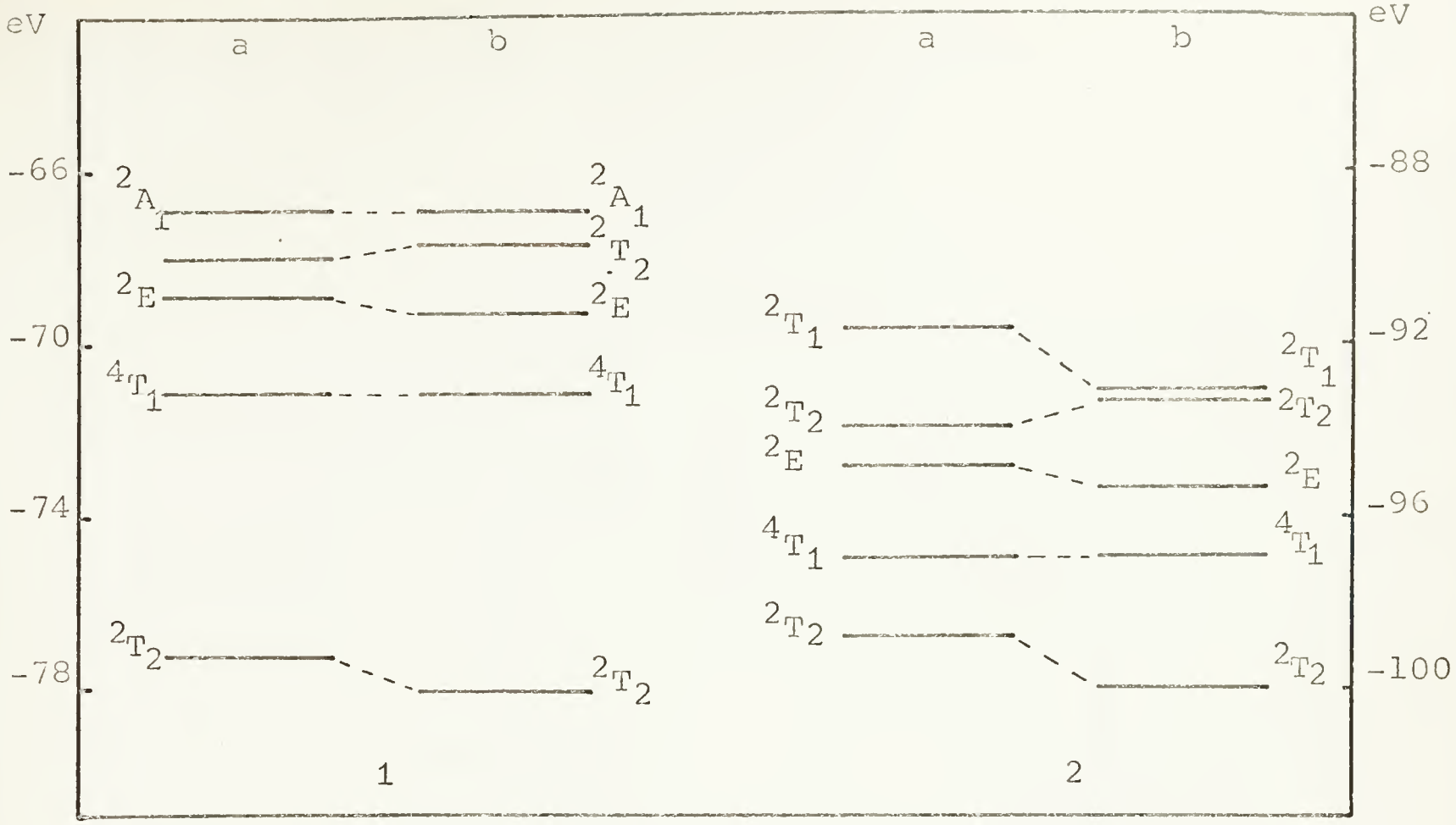
+All energies in electron volts

TABLE 3.2

Energy Levels after Configuration Interaction for Isolated Vacancy

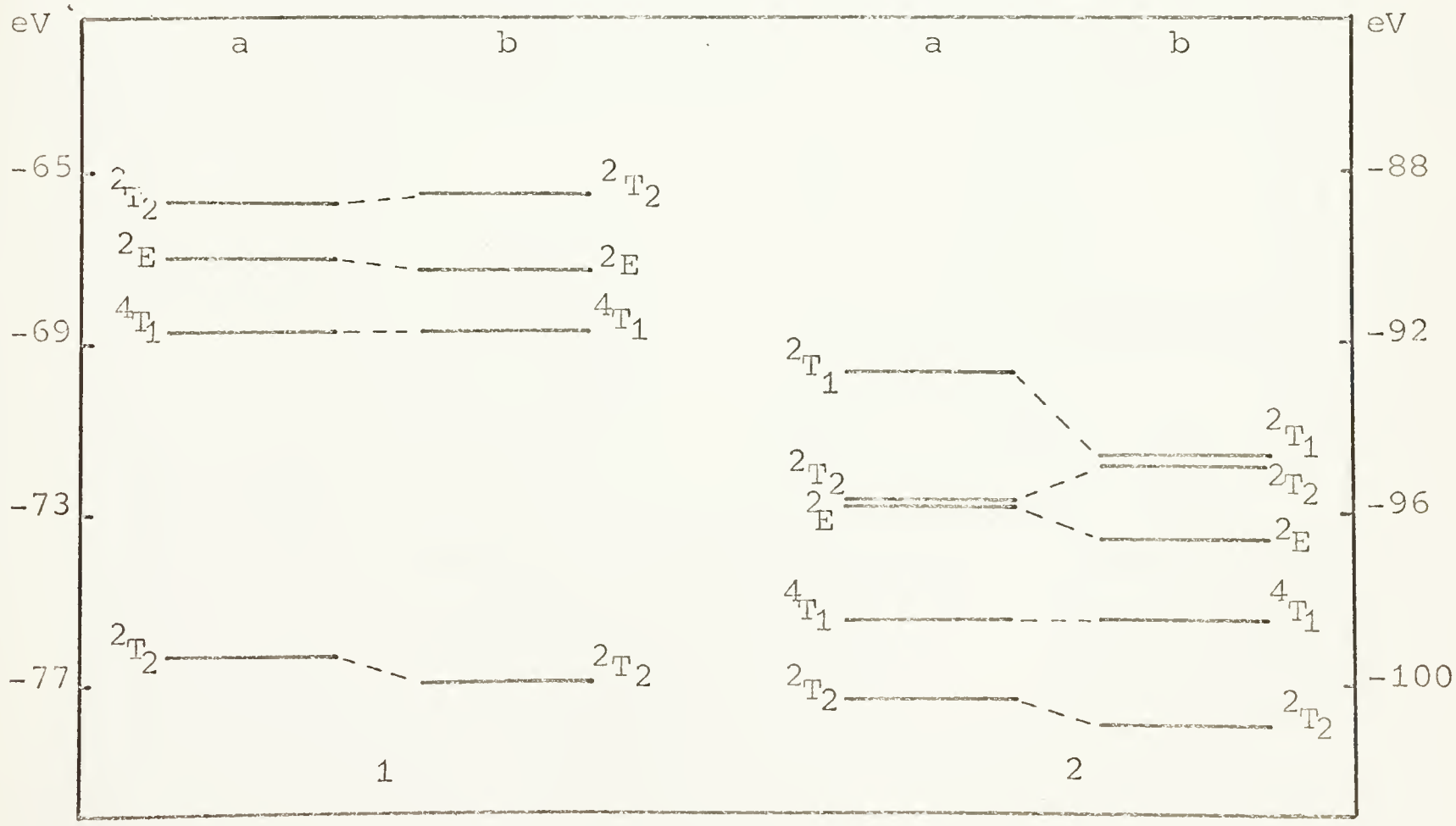
Charge State	Symmetry State	Slater Functions		Clementi Functions	
		case 1	case 2	case 1	case 2
V^+	$^2T_2$	-78.05*	-99.98	-76.93	-100.92
	$^4T_1$	-71.16	-96.98	-68.65	- 98.53
	^2E	-69.30	-95.36	-66.26	- 96.58
	$^2T_1$	-66.48	-93.15	-63.36	- 94.61
V^o	^1E	-81.32	-113.60	-78.45	-115.15
	$^3T_1$	-81.28	-113.51	-78.76	-115.28
	$^5A_2$	-76.18	-112.11	-72.50	-114.64
	$^1T_2$	-79.67	-111.38	-77.61	-113.30
	$^1A_1$	-78.92	-111.01	-76.76	-113.21
V^-	$^4A_2$	-76.23	-117.79	-72.55	-120.06
	^2E	-74.80	-116.96	-71.59	-119.90
	$^2T_1$	-75.56	-117.34	-71.67	-119.54
	$^2T_2$	-74.49	-116.91	-71.03	-120.18
	$^4T_1$	-69.35	-115.37	-64.68	-119.07
$V^=$	^1E	-61.37	-113.03	-56.45	-116.22
	$^3T_1$	-61.76	-113.42	-57.20	-116.96
	$^1T_2$	-61.03	-113.12	-56.77	-117.17
	$^3T_2$	-54.85	-110.98	-49.32	-115.96
	$^1A_1$	-60.01	-112.54	-55.72	-117.28

*All energies are in electron volts.



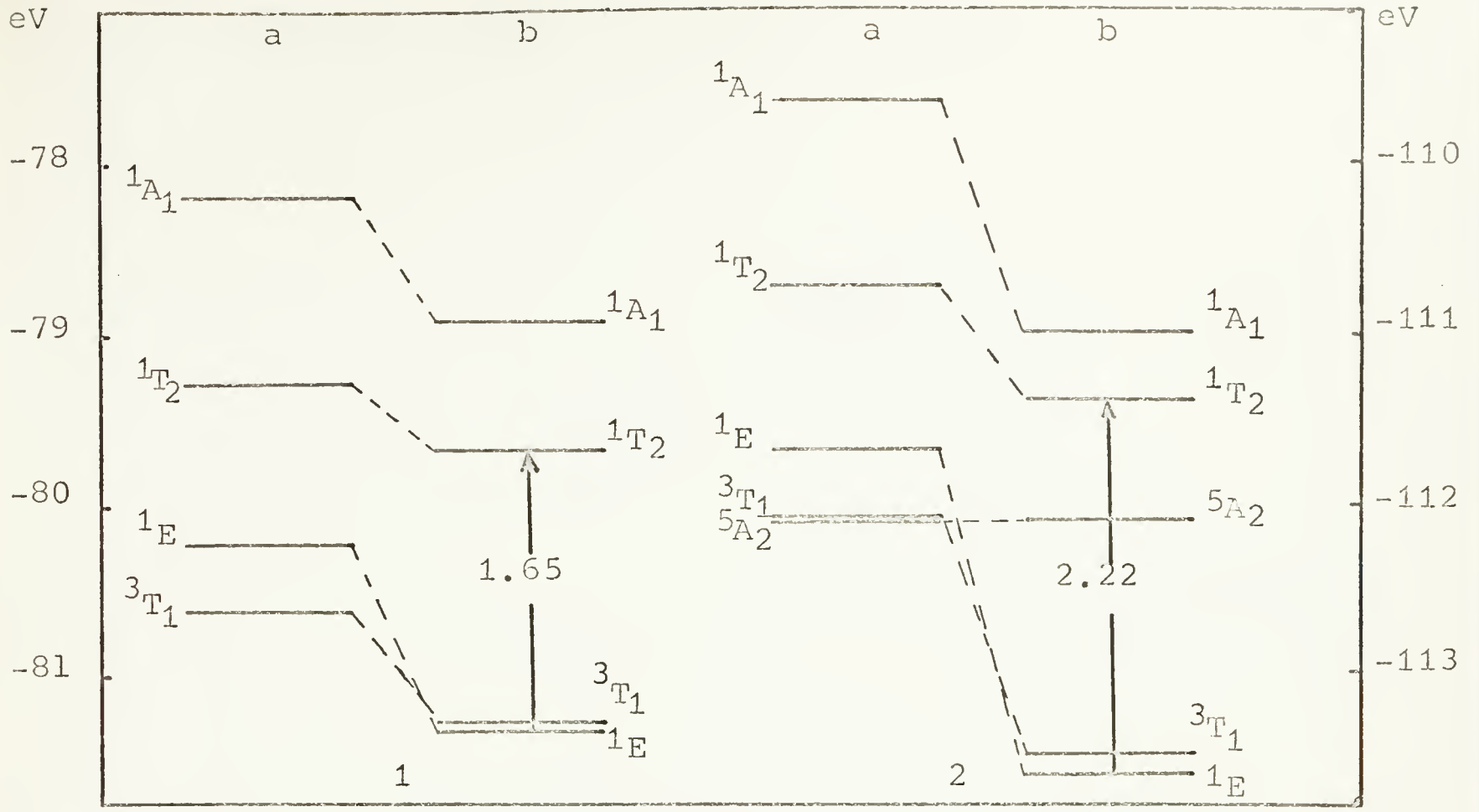
.3.1a Electronic Structure of Positive Vacancy in Diamond: Slater Functions a. before configuration interaction
b. after configuration interaction

1. P = -8.00 eV 2. P = -16.42 eV

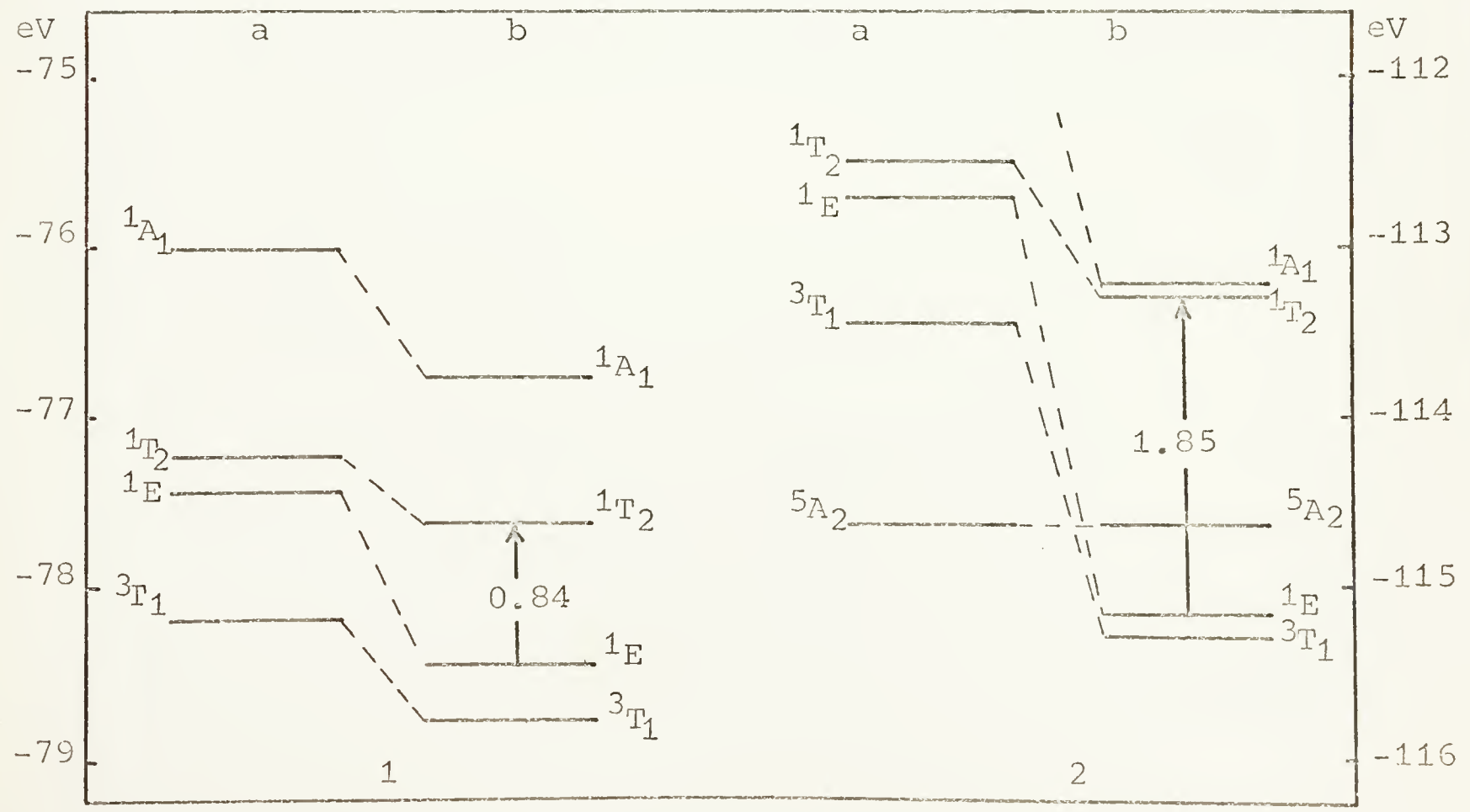


.3.1b Electronic Structure of Positive Vacancy in Diamond: Clementi Functions a. before configuration interaction
b. after configuration interaction

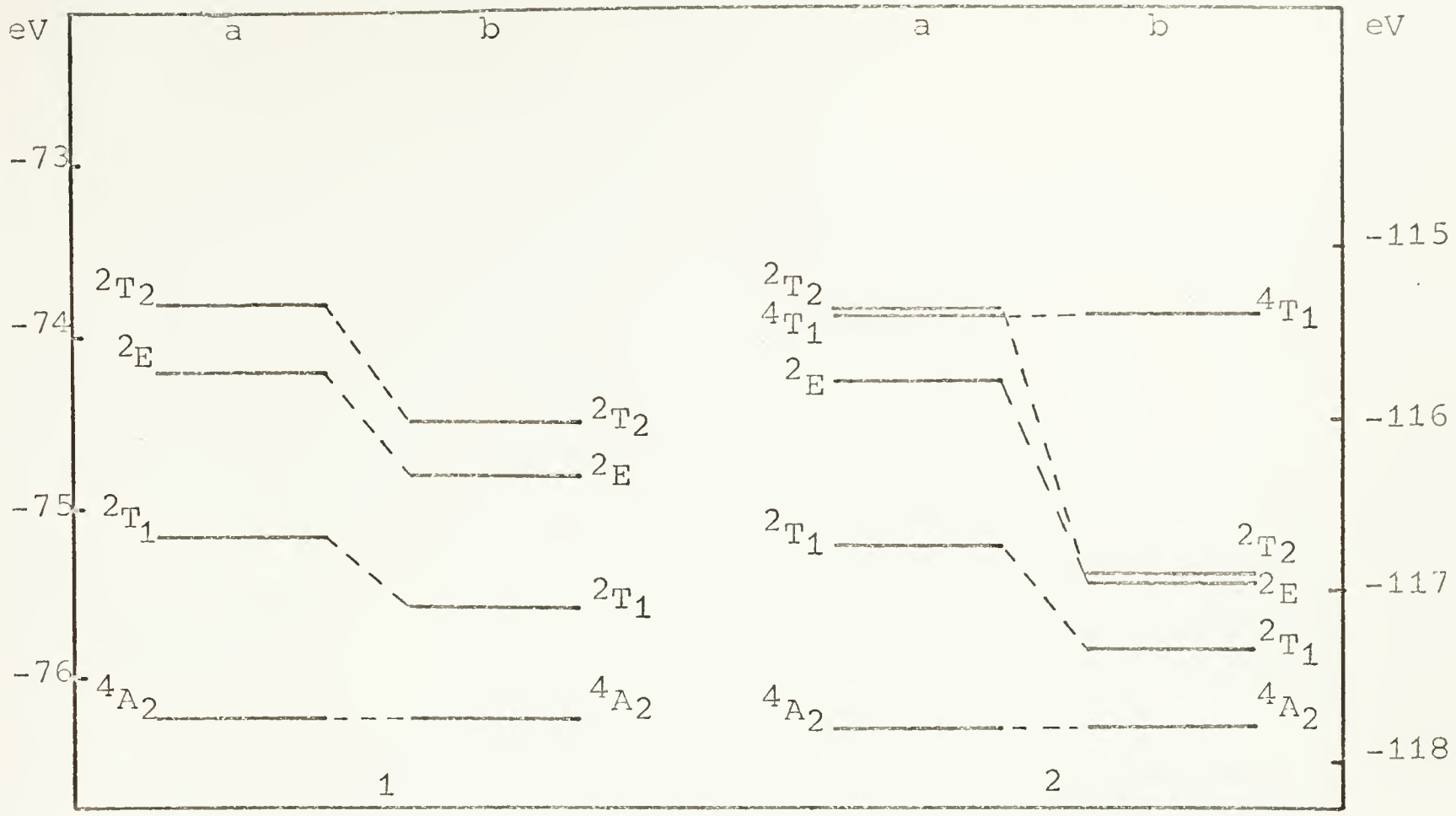
1. P = -7.13 eV, 2. P = -16.42 eV



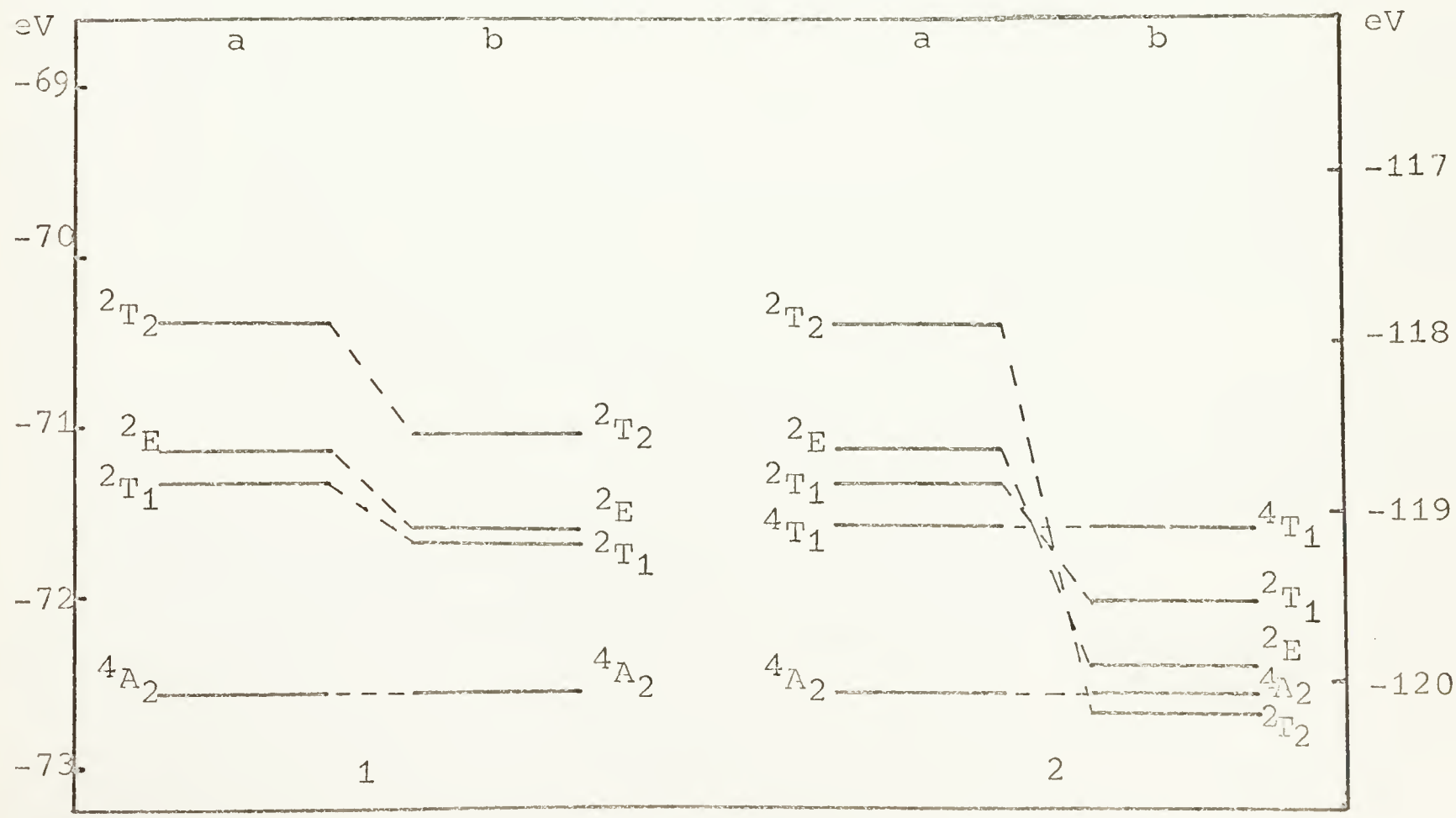
3.2a Electronic Structure of Neutral Vacancy in Diamond: Slater Functions a. before configuration interaction
b. after configuration interaction
1. P = -8.00 eV 2. P = -16.42 eV



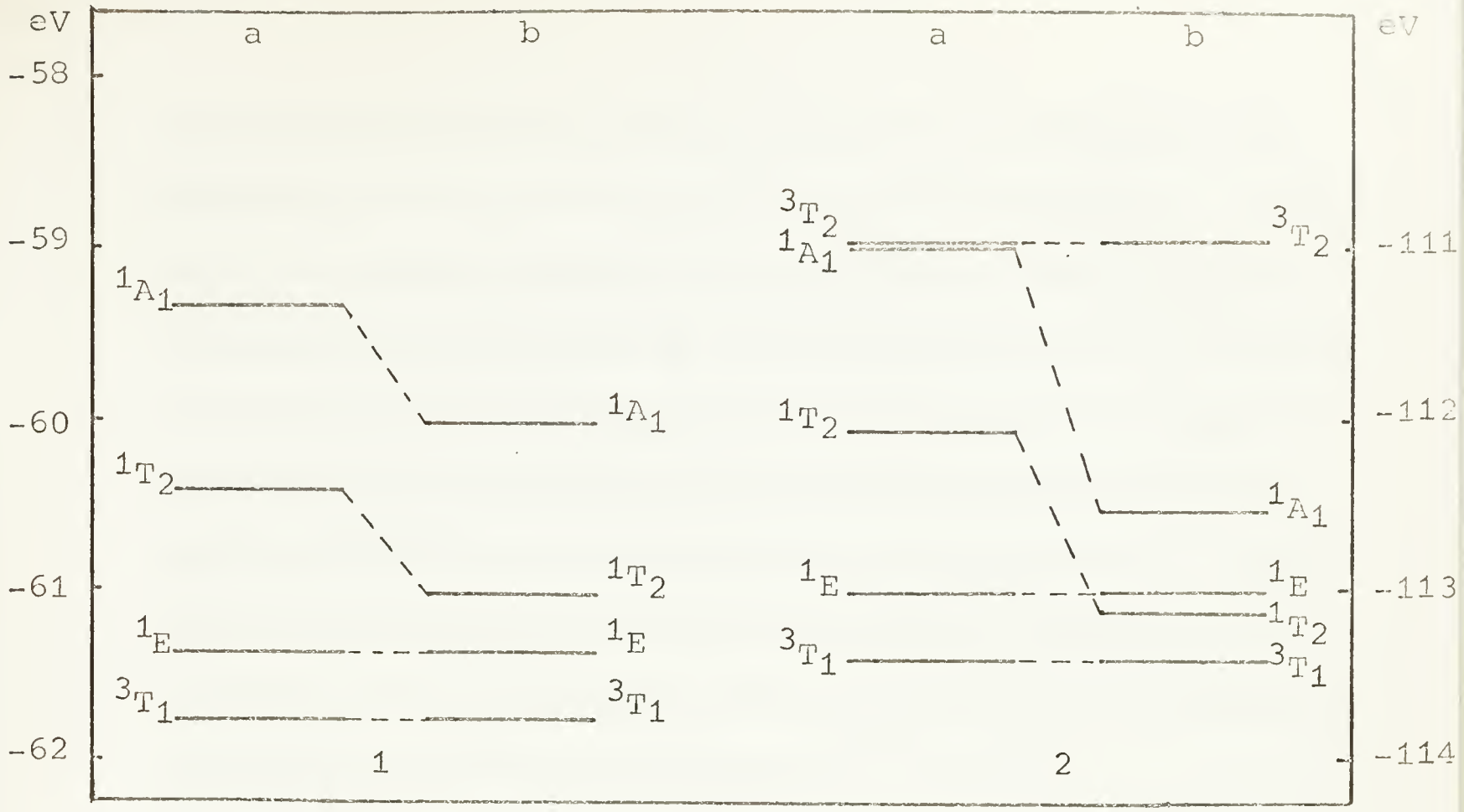
3.2b Electronic Structure of Neutral Vacancy in Diamond: Clementi Functions a. before configuration interaction
b. after configuration interaction
1. P = -7.13 eV 2. P = -16.42 eV



3.3a Electronic Structure of Negative Vacancy in Diamond: Slater Functions a. before configuration interaction
b. after configuration interaction
1. P = -8.00 eV 2. P = -16.42 eV

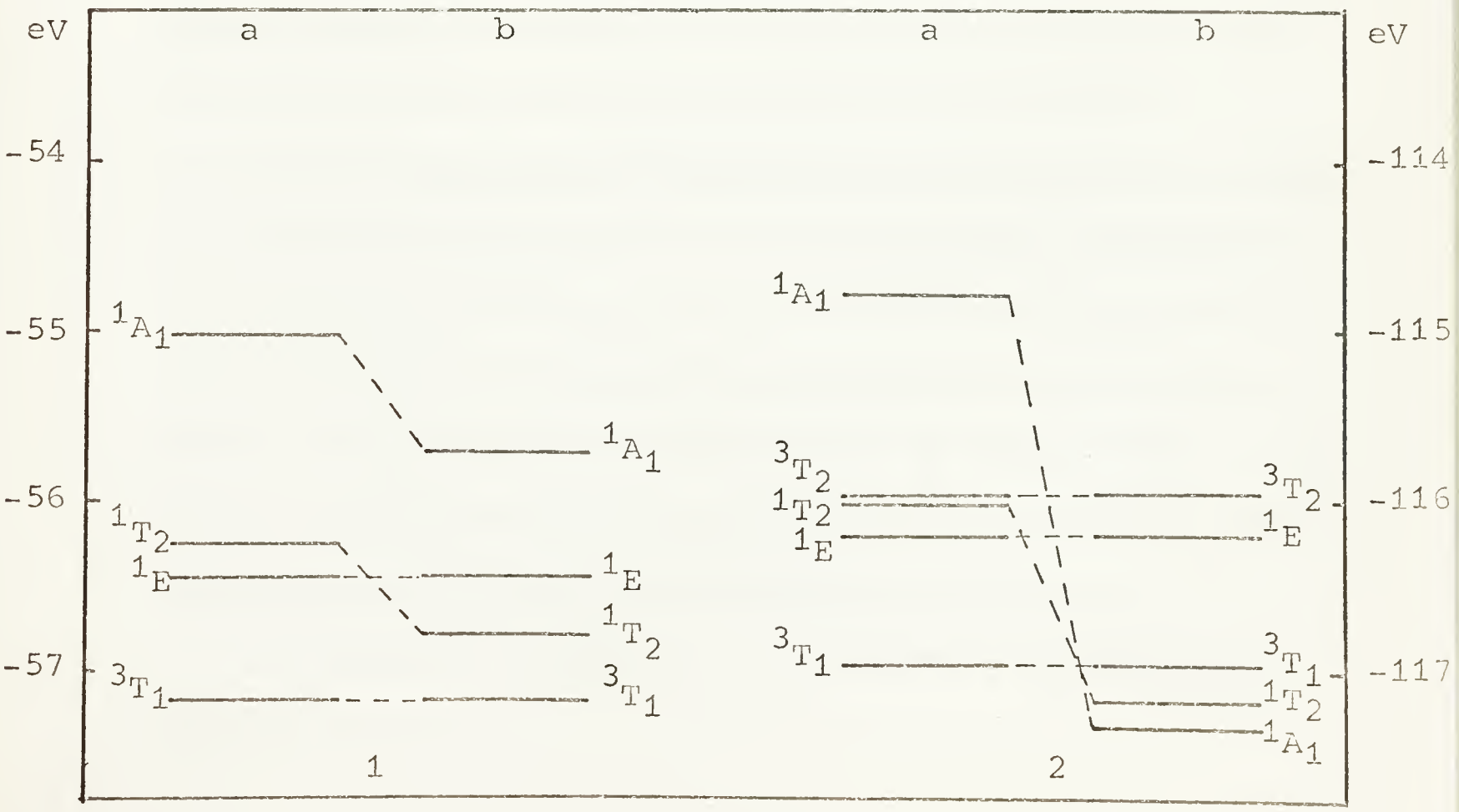


3.3b Electronic Structure of Negative Vacancy in Diamond: Clementi Functions a. before configuration interaction
b. after configuration interaction
1. P = -7.13 eV 2. P = -16.42 eV



.3.4a Electronic Structure of Double Negatively charged Vacancy: Slater Functions
a. before configuration interaction
b. after configuration interaction

1. P = -8.00 eV 2. P = -16.42 eV



.3.4b Electronic Structure of Double Negatively charged Vacancy: Clementi Functions
a. before configuration interaction
b. after configuration interaction

1. P = -7.13 eV 2. P = -16.42 eV

over 2 eV lower than the lowest level for V^-. Admittedly, the situation is much less favourable when case 2 is examined. However, case 1 is usually considered to more closely represent the true situation for reasons outlined in the previous chapter. Of course, we cannot really conclude anything definite about the relative stability of the various defect centres, because of the further inadequacies in the model when applied to charged states. Nevertheless, these calculations do demonstrate that the possible non-existence of V^+ should not be argued on the basis of the unmodified calculation of Coulson and Kearsley.

For V^-, when the correct expression for the lowest ^2E level is used, the results obtained in this study are very similar to the corrected results of the Coulson and Kearsley work. We now postpone further discussion of all these results until after the findings using the Clementi functions have been presented.

3.3 Electronic Structure of the Isolated Vacancy: Clementi Orbitals

For our present purposes, the most convenient alternative set of functions available to examine the sensitivity of the energy levels to the form of the wave-functions for the various charge states of the vacancy, were those obtained by Clementi [60]. Each orbital is conveniently expressed in terms of an analytical basis set of Slater-type functions with appropriate coefficients.

For example, an orbital of s symmetry may be expressed in terms of the basis set

$$\phi_s = \sum_i N_i \, r^{n_i - 1} \, e^{-\zeta_i r}$$

where N_i is the expansion coefficient, ζ_i the orbital exponent and n_i depends upon whether the basis function is 1s, 2s, 3s or 4s. The basis sets of p symmetry for a particular Hartree-Fock orbital may be expressed in a similar manner with the appropriate angular factor. Table 3.3 shows the basis sets used for the 1s, 2s and 2p orbitals of carbon in the present calculation. These are for the ^3P ground state of the isolated atom. In column 1 the notation 1s, 1s, 2s, etc. gives the value of n_i in the basis function. The orbital exponent, ζ_i, is shown in column 2 while in the following two columns the expansion coefficients N_i of the basis set functions for each orbital are shown. These atomic Hartree-Fock functions form an orthogonal set.

TABLE 3.3

Hartree-Fock Functions for Isolated Carbon Atom

Basis	Orbital Exp.	1s	2s	Basis	Orbital Exp.	2p
1s	5.41250	0.92695	-0.20786	2p	0.95540	0.24756
1s	9.28630	0.07665	-0.01175	2p	1.42090	0.57774
2s	1.03110	0.00073	0.06494	2p	2.58730	0.23563
2s	1.50200	-0.00167	0.74109	2p	6.34380	0.01090
2s	2.58975	0.00539	0.34626			
2s	4.25950	0.00210	-0.13208			

In Appendix A.4 may be found the values of the one- and two-electron integrals for the localized atomic hybrid orbitals obtained using these functions in conjunction with the integral program. It is interesting to note that the analytical value for Q is now estimated to be 17.81 eV (compared with 19.06 eV using Slater functions), however this is still 5 eV above the predicted semi-empirical estimate. This suggests that it will again be necessary to use a modified a.s.m.o. theory to predict the electronic structure of the isolated vacancy. The values of the molecular integrals for the modified cases are given in table 3.1. Now, for case 1, P = -7.13 eV while for case 2, P = -16.42 eV. The energy levels before and after configuration interaction for the various charge states of the vacancy, V^{+}, V^{0}, V^{-} and $V^{=}$ are shown in figs. 3.1b, 3.2b, 3.3b and 3.4b respectively. Table 3.2 gives the values for the energies of the lowest symmetry states in each case after configuration interaction. The discussion of these results has been incorporated into the next section for convenience.

3.4 Comparison and Discussion of Results

We commence our discussion by comparing the values obtained for the basic integrals presented in Appendix A.4. Once again we remind the reader that it is the integrals involving the hybrid orbitals 'a' and 'b' that are of interest in the vacancy calculation. While the two-centre Coulomb integrals agree fairly well in both cases the overlap, hybrid and exchange integrals show increased values when the Hartree-Fock functions are used. It is difficult to gauge

just how significant each of these differences is for determining the relative ordering of the energy levels. It is possible to show that the large differences of several electron volts between the one-centre kinetic- and potential-energy integrals for Slater and Clementi-type functions arises because of the non-orthogonality of the 2s Slater function to the 1s function. The overlap integral between the 2s and 1s function on the same centre, $b = \langle 1s|2s\rangle$, is 0.21. If we orthogonalize the 2s function to the 1s using the expression

$$|2s'\rangle = \frac{|2s\rangle - b|1s\rangle}{\sqrt{(1 - b^2)}}$$

then the value obtained for the one-centre kinetic energy integral is ~ 36.5 eV which is in very much better agreement with the Clementi value. However, the integral of primary interest for the calculation is the self-penetration integral, $P = \langle a|T+V_A|a\rangle$ and now we find for case 1, P (Clementi) = -7.13 eV, while P (Slater) = -8.00 eV. For Slater functions at least, the relative ordering of the energy levels is fairly insensitive to the value of P. Therefore, the non-orthogonality of these functions is unlikely to be very significant. We should note that Yamaguchi [2] used orthogonal Slater functions in his unmodified calculations and obtained the same relative ordering of energy levels for V^0 and V^- as Coulson and Kearsley in their unmodified study. The two-centre kinetic energy integral is small, but quite different in the two cases, while the two-centre split nuclear attraction potential integrals differ by over 1 eV. Despite these differences the values of the molecular

integrals shown in Table 3.1 agree rather well. The most significant changes for the two sets of functions are for the B,J and F integrals.

The general feature of all the calculations is the strong dependence of the levels on configuration interaction effects which in some cases are very large and cause the inversion of the energy levels. It is also significant, especially for the Clementi case, that several levels show a marked dependence on the value of P. The most significant are the $^5A_2$ level of V^o, the ^2E and $^2T_2$ levels of V^- and the $^1A_1$ and $^1T_2$ levels of $V^=$. As with the previous study of Coulson and Kearsley the levels are much more compressed in case 2.

The electronic properties predicted for the V^+ centre show good agreement for both sets of functions. The relative ordering of the energy levels is the same for both systems, figure 3.1, and the $^2T_2$ level is clearly lowest at least 2 eV below the $^4T_1$ level. It seems most unlikely that further refinement of the model would cause another level to become the ground state. The calculation predicts that if the V^+ centre exists then it should exhibit paramagnetic resonance with $S = \frac{1}{2}$ and probably be optically inactive. We would expect a Jahn-Teller distortion of this centre because of the degeneracy of the lowest state.

For the neutral vacancy, the calculation using Clementi functions predicts that for both cases the $^3T_1$ level is lowest being 0.31 eV below the ^1E level in case 1 and 0.13 eV below it in case 2. This is in contrast to the Slater calculation where the $^3T_1$ level was 0.04 eV and 0.09 eV above the ^1E level in case 1 and case 2 respectively.

The relative ordering of the other levels of interest is the same in both calculations, as shown in fig. 3.2. It is interesting to note that for the unmodified case, using Clementi functions (Q = 17.81 eV) the ^1E level is lowest 0.48 eV below the $^3T_1$ and with a separation of 7.18 eV between the ^1E and $^1T_2$ level. It is therefore clear that the ordering of the $^3T_1$ and ^1E levels is sensitive to the choice of Q. In the Slater case while there is not actually a change in order with decreasing Q, the energy difference between these two levels does decrease. If one examines the formal expressions for the energy levels of the neutral vacancy before configuration interaction given in Appendix A.2 one observes that the energy difference between the $^3T_1$ and ^1E levels arising from the configuration $v^2t_2^2$ is D - F. Now this difference has increased from 0.39 eV with Slater functions to 0.74 eV with Clementi functions. The interactions with levels from higher configurations is no longer sufficient to invert these two levels in the latter case. The energy difference between the lowest ^1E and $^1T_2$ levels has changed appreciably when we compare the Clementi case with the previous calculation using Slater functions. The separation for these two levels before configuration interaction is formally F - D + 2J. Now, this difference has decreased from +0.96 eV (Slater) to +0.21 eV (Clementi) such that the final energy separations are 0.84 eV (case 1) and 1.85 eV (case 2) using Clementi functions, compared with 1.64 eV (case 1) to 2.21 eV (case 2) using Slater functions.

If the calculation using Clementi functions is correct and the ^1E level is of the order of 0.2 to 0.3 eV above the ground state level then it is extremely unlikely that the GR1 band could be associated with the spin- and orbitally-allowed $^1E \rightarrow {}^1T_2$ transition. However, in view of the assumptions inherent in the model we cannot without further investigation have much confidence in such small differences. On the basis of this model we would predict that the centre would be paramagnetic with S = 1 and undergo Jahn-Teller distortion. In both studies we observe the strong dependence of the position of the $^5A_2$ level on the value of P.

For the V^- centre, both Slater and Clementi functions give similar predictions for case 1; however, the energy levels from the latter study show a significant dependence on the value of P, as can be seen from fig. 3.3. Using Slater functions we predict that the $^4A_2$ level is lowest with the $^2T_1$ level 0.67 eV (case 1) to 0.45 eV (case 2) above the ground state. The changes in the ordering of the energy levels for case 2 using Clementi functions are due largely to the increased configuration interaction with higher states. This arises because the modification in B, the one-electron molecular integral, between case 1 and case 2 is 10.10 eV using Slater functions, whereas it is 12.25 eV in the Clementi study. As a consequence the higher states make a relatively larger contribution to the lowest levels in the latter case. Hence, for example, the $^2T_2$ level is lowered 2.29 eV to become the lowest level, compared with 1.54 eV in the former study. Whereas case 1 of the

Clementi work predicts that the $^4A_2$ level is lowest 0.88 eV below the $^2T_1$ level with the ^2E level 0.08 eV above this level, case 2 predicts that the $^2T_2$ level is lowest 0.12 eV below the $^4A_2$ level and 0.28 eV below the ^2E level. It is clear therefore that it is necessary to examine more closely some of the assumptions involved in the model before we can draw any valid conclusions from this study.

The analysis of the electronic structure of the $V^=$ centre shows similar general features to those discussed for the V^- centre. The $^1A_1$ and $^1T_2$ levels show a strong dependence on P, and hence on the extent of configurational mixing with higher states. This is greatest in the Clementi study when the $^1A_1$ becomes lowest for P = -16.42 eV, 0.11 eV below the $^1T_2$ level and 0.32 eV below the $^3T_1$ level, however it is also a very significant effect using Slater functions. The $^3T_1$ and the ^1E levels have no higher states with which they can interact. If the $^3T_1$ level is lowest for this centre then we would expect it to be paramagnetic and show a Jahn-Teller distortion, however, this would not be so if the $^1A_1$ level was lowest. The varying dependence on the extent of configuration interaction in the two studies can again be related to the changes in the one-electron integral, B. We must remember that the defect molecule approximation as we have presented it will almost certainly be least valid for the $V^=$ centre, because of the neglect of exchange and polarisation terms and the choice of neutral atom wave-functions.

Because of the simplicity of the model and the general uncertainty of these findings one cannot draw any firm conclusions in relation to experiment without a more detailed study of some of the assumptions involved in the calculation. The influence of such factors as possible delocalisation of electrons away from the defect, relaxation of the lattice and possible distortion effects associated with the lowest electronic levels warrant further investigation. It could be that the simplified calculation using Slater functions does in fact give better agreement with experiment than the use of the Hartree-Fock functions. This is not an entirely unknown phenomenon in molecular calculations. In the next section we examine the effect of delocalisation upon the relative ordering of the energy levels for each particular centre, while in chapter 6 it is proposed to take a more critical look at the relaxation and Jahn-Teller problem.

3.5 Delocalisation of the Electronic Wave-Function from Vacancy

One of the chief assumptions of the defect molecule model is that the vacancy electrons are located entirely within the defect and do not diffuse into the rest of the crystal. This is, of course, an approximation to the real situation. In fact, recent electron spin resonance experiments by Baldwin [40] suggest that the delocalisation of the electronic charge from the vacancy in diamond is of the order of 10 per cent. Therefore, a more realistic form for the wave-function of the vacancy electron should represent it as being located most of the time within the defect, but there must be a finite probability of the electron cloud being associated with

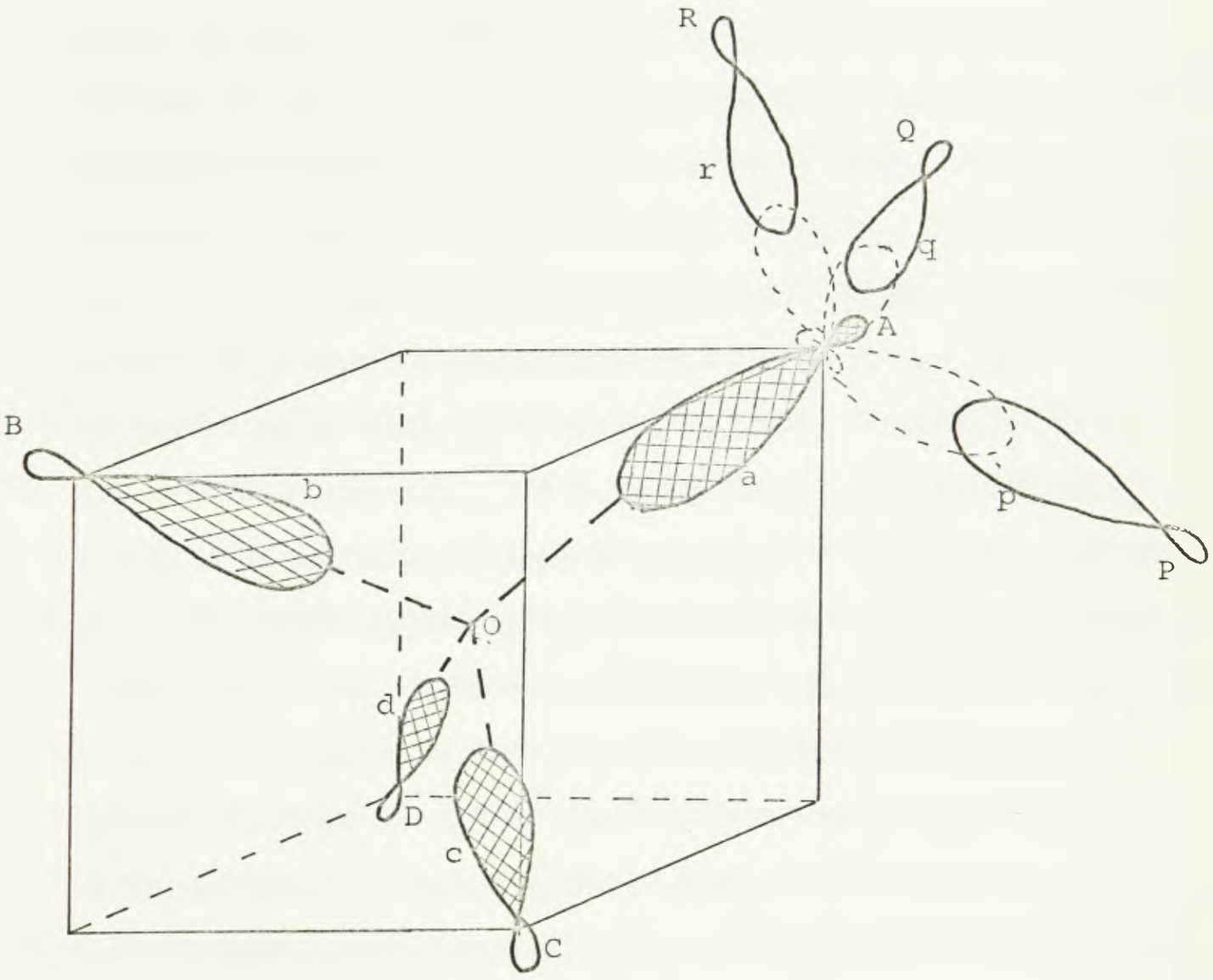
atoms which are not neighbours to the defect. In this preliminary study we have chosen a very simple approach to investigate the effect of delocalisation on the electronic structure of the vacancy in its various charge states.

Consider, as in fig. 3.5, the case of a vacancy electron that was initially in the tetrahedral orbital 'a', associated with atom A, such that $\psi_a = a$. Now, if some of the electronic wave-function of the vacancy electron is to be associated also with the nearest neighbour atoms P,Q,R to atom A, and if we ignore exchange and polarisation effects with other valence electrons in this initial study, then a convenient form for the delocalized electronic wave-function ψ'_a is

$$\psi'_a = \lambda a + \mu(p + q + r) \qquad (3.1)$$

where p,q,r are the tetrahedral hybrid orbitals on atoms P,Q,R directed along $\vec{PA}$, $\vec{QA}$ and $\vec{RA}$ respectively as shown in fig. 3.5. λ and μ are parameters which determine the extent of delocalisation. The relationship between λ and μ is determined by the requirement that ψ'_a is normalized and that $\mu = 0$ when $\lambda = 1$. In a similar way the tetrahedral hybrids, b,c and d may be replaced by ψ'_b, ψ'_c and ψ'_d.

The procedure followed to obtain the new estimates for the energy levels was to replace a,b,c and d in the integrals involved in the energy expressions by ψ'_a, ψ'_b, ψ'_c and ψ'_d, respectively. Expansion of these integrals yields formulae which may be expressed in terms of the atomic hybrid integrals by various powers of λ and μ. For example, the overlap integral between the orbitals ψ'_a and ψ'_b becomes



3.5 Model for isolated vacancy in delocalization study showing first neighbours to Atom A.

$$\langle\psi'_a|\psi'_b\rangle = \langle\lambda a + \mu(p+q+r)|\lambda b + \mu(p'+q'+r')\rangle$$

$$= \lambda^2 \langle a|b\rangle + 2\lambda\,\mu(\langle a|p'\rangle + \langle a|q'\rangle + \langle a|r'\rangle)$$

$$+ \mu^2[\langle(p+q+r)|\ (p'+q'+r')\rangle]$$

where p',q',r' are hybrid orbitals on the nearest neighbour atoms to atom B in the direction of B. Similar expressions may also be obtained for all the other one- and two-electron integrals. With the exception of one-centre kinetic and potential energy integrals we have neglected all terms of $O(\mu^2)$ and above. This is a good approximation because μ is always small in the present calculation and in general so are the integrals multiplied by such powers of μ. This approximation is least valid for the one-centre coulomb integral, but is still reasonable. To evaluate the integrals involving ψ'_a and ψ'_b it is necessary to know the values of all the basic one- and two-centre atomic hybrid integrals at four internuclear distances. Namely, 2.918 a.u., 4.766 a.u., 5.586 a.u. and 7.343 a.u. The first distance corresponds to the nearest-neighbour C - C distances denoted AP, while the latter three distances are all involved in the divacancy calculation, reported in the next chapter. All these integrals have been evaluated using Clementi- and Slater-type functions and are given in Appendix A.4. Once we have evaluated the modified integrals involving ψ'_a and ψ'_b it is a straight forward matter in principle to determine the new energy level schemes for various values of λ.

The normalization condition imposes a constraint on the maximum value of λ, which depends upon the value of the overlap integral between nearest neighbour carbon atoms. For Clementi-type functions, if λ is to be real, $\lambda_{max} = 1.021$, while for Slater-type functions $\lambda_{max} = 1.01$. For $\lambda > 1$, μ is negative, while for $\lambda < 1$, μ is positive. We are mainly interested in the cases where $\lambda < 1$, but it is worth considering the case for $\lambda > 1$. As λ decreases the overlap term $\langle\psi'_a|\psi'_b\rangle$ first increases relative to the value for $\lambda = 1.0$ and reaches a maximum near $\lambda = 0.95$, but for values of $\lambda > 0.80$ it is larger than the initial value. The additional term in the overlap expression arising from the interaction between the orbital 'a' and the hybrids p',q',r' on the nearest neighbour atoms to B is sufficient, for small decreases in λ, to compensate for the diminished overlap contribution from within the vacancy. For $\lambda > 1$ the modified overlap integral is less than S_{ab} because of the negative contribution of the term mentioned above. We have considered the cases $\lambda = 0.95$, $\lambda = 0.90$ and $\lambda = 0.85$. These correspond to approximately 90%, 81% and 72% localisation of the wave-function for the vacancy electron in orbital 'a'. The case where $\lambda = 1.01$ has also been considered. For the lowest value of λ it should be obvious that the approximations of the model will be weakest. However, we consider this approach to be adequate because in the present studies we are primarily interested in the trends which result in the relative ordering of the energy levels with increased delocalisation.

In table 3.4 the values of the one- and two-electron molecular integrals A - K using Slater-type functions for various values of λ are given, while in table 3.5 these integrals using Clementi-type functions

TABLE 3.4

Values of Molecular-Integrals:

Delocalisation study Slater functions

Integral	$\lambda = 1.01$	$\lambda = 1.00$	$\lambda = 0.95$	$\lambda = 0.90$	$\lambda = 0.85$
A^*	-37.739[+]	-37.960[⊕]	-37.278	-35.977	-34.495
B^*	-27.275	-27.678	-27.777	-27.112	-26.174
A^x	-44.286	-43.764	-41.340	-39.088	-36.850
B^x	-38.810	-38.066	-35.167	-32.704	-30.490
C	9.759	9.820	9.101	8.072	7.014
D	8.502	8.722	8.268	7.293	6.236
E	9.301	9.422	8.786	7.759	6.685
F	8.085	8.332	7.924	6.948	5.888
G	1.688	1.790	1.887	1.816	1.682
J	0.471	0.677	0.971	0.961	0.859
K	-1.080	-1.232	-1.417	-1.366	-1.240

*Case 1

xCase 2

+All energies in electron volts

⊕$_p$ = -7.75 eV.

TABLE 3.5

Values of Molecular Integrals:

Delocalisation study Clementi functions

Integral	λ = 1.01	λ = 1.00	λ = 0.95	λ = 0.90	λ = 0.85
A*	-37.695	-38.315	-39.144	-38.776	-37.939
B	-25.699	-26.475	-28.077	-28.380	-28.110
A^x	-43.413	-43.694	-43.610	-42.741	-41.579
B	-38.402	-38.726	-38.678	-37.868	-36.556
C	9.809	9.808	9.120	8.146	7.133
D	8.603	8.765	8.419	7.534	6.523
E	9.435	9.487	8.887	7.911	6.871
F	7.812	8.020	7.775	6.866	5.805
G	1.880	1.953	2.045	1.985	1.863
J	0.284	0.474	0.841	0.865	0.765
K	-1.089	-1.217	-1.425	-1.384	-1.254

*Case 1

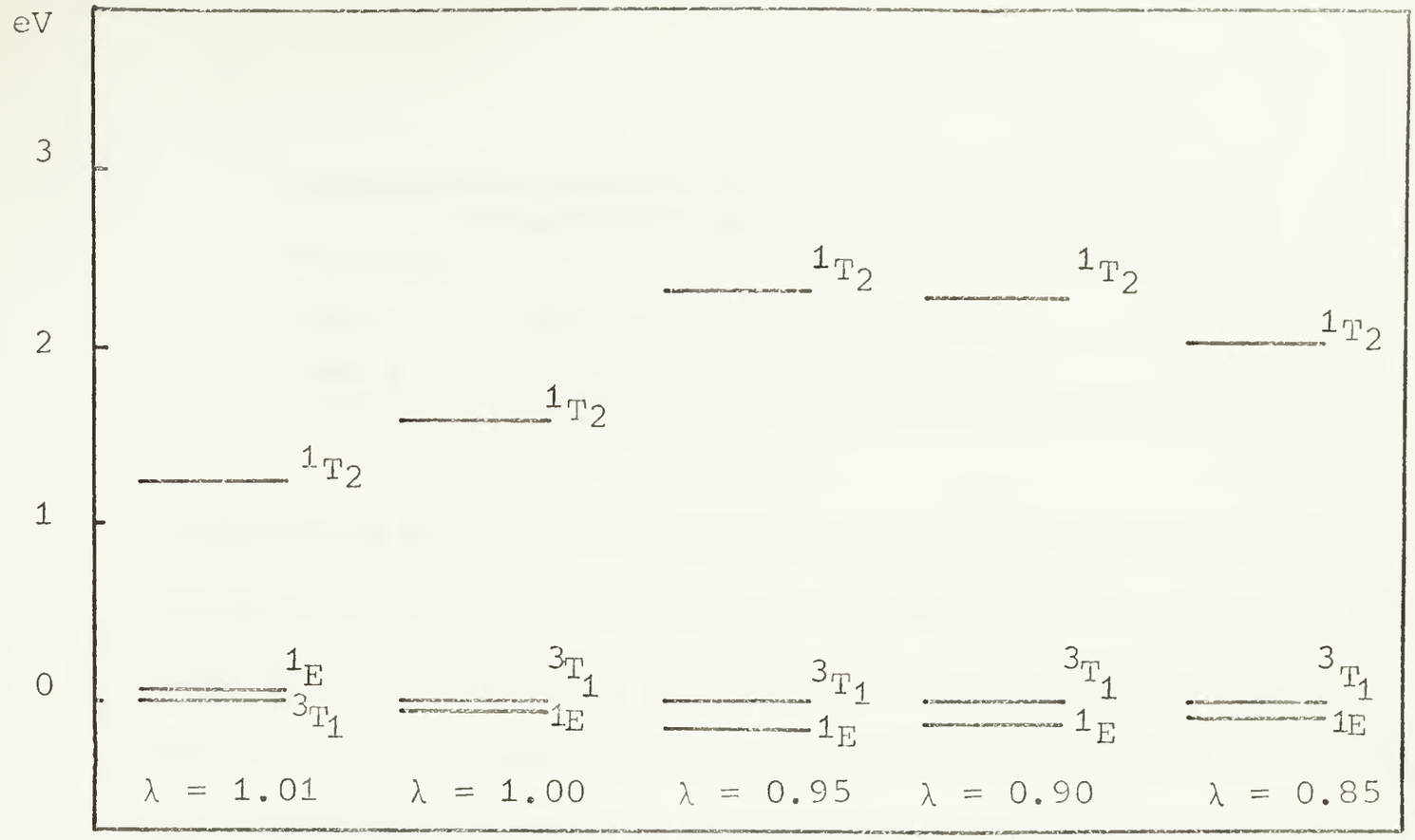
^xCase 2

+All energies in electron volts.

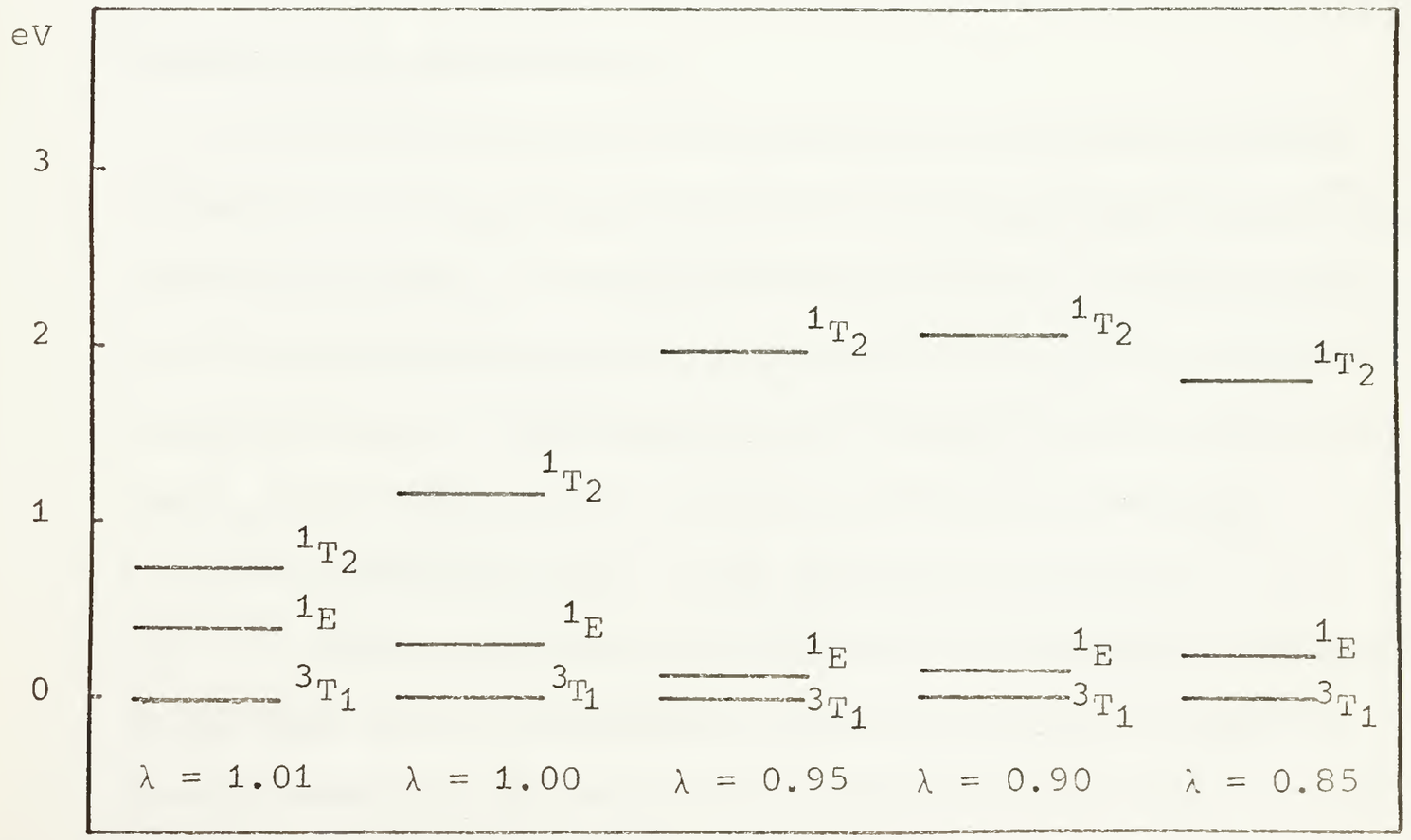
are listed. In the present investigation we have concentrated on the electronic structure of the V^0 and V^- centres mainly to demonstrate the essential features of using such a wave-function. The finding for the V^+ and $V^=$ centres are only briefly discussed.

The lowest levels for the V^0 centre after configuration interaction for various values of λ are given in fig. 3.6. We have presented only the findings for the case 1 approximation because for the alternative value of P similar trends were observed. We have chosen the $^3T_1$ level as our zero of energy for convenience. From figs. 3.6a and 3.6b it is apparent that the general effects associated with delocalisation are independent of the type of function chosen to represent the 2s and 2p orbitals. Two questions are of primary interest to us. a) What happens to the energy separation between the lowest ^1E and $^3T_1$ levels as λ decreases? b) What is the relationship between λ and the $^1E - {}^1T_2$ energy difference?

The important finding is that delocalisation does not cause a change in the ordering of the lowest levels of the neutral vacancy. Using Slater-type functions the ^1E level is always lowest while in the study with Clementi-type functions the $^3T_1$ level is predicted to be the ground state. However, the ^1E state is initially lowered in energy relative to the $^3T_1$ state, but then increases again. As a consequence of this trend, for $\lambda = 0.95$ the ^1E level is 0.16 eV below the $^3T_1$ level (Slater case), while for the Clementi study it is within 0.12 eV of the $^3T_1$ ground state. We also note that the $^1E - {}^1T_2$ energy separation increases to a maximum near $\lambda = 0.95$ then decreases again. For $\lambda = 0.95$ the $^1E - {}^1T_2$ separations are as follows:



g.3.6a Electronic Structure of Neutral Vacancy in Diamond. Delocalisation Study using Slater Functions: Case 1

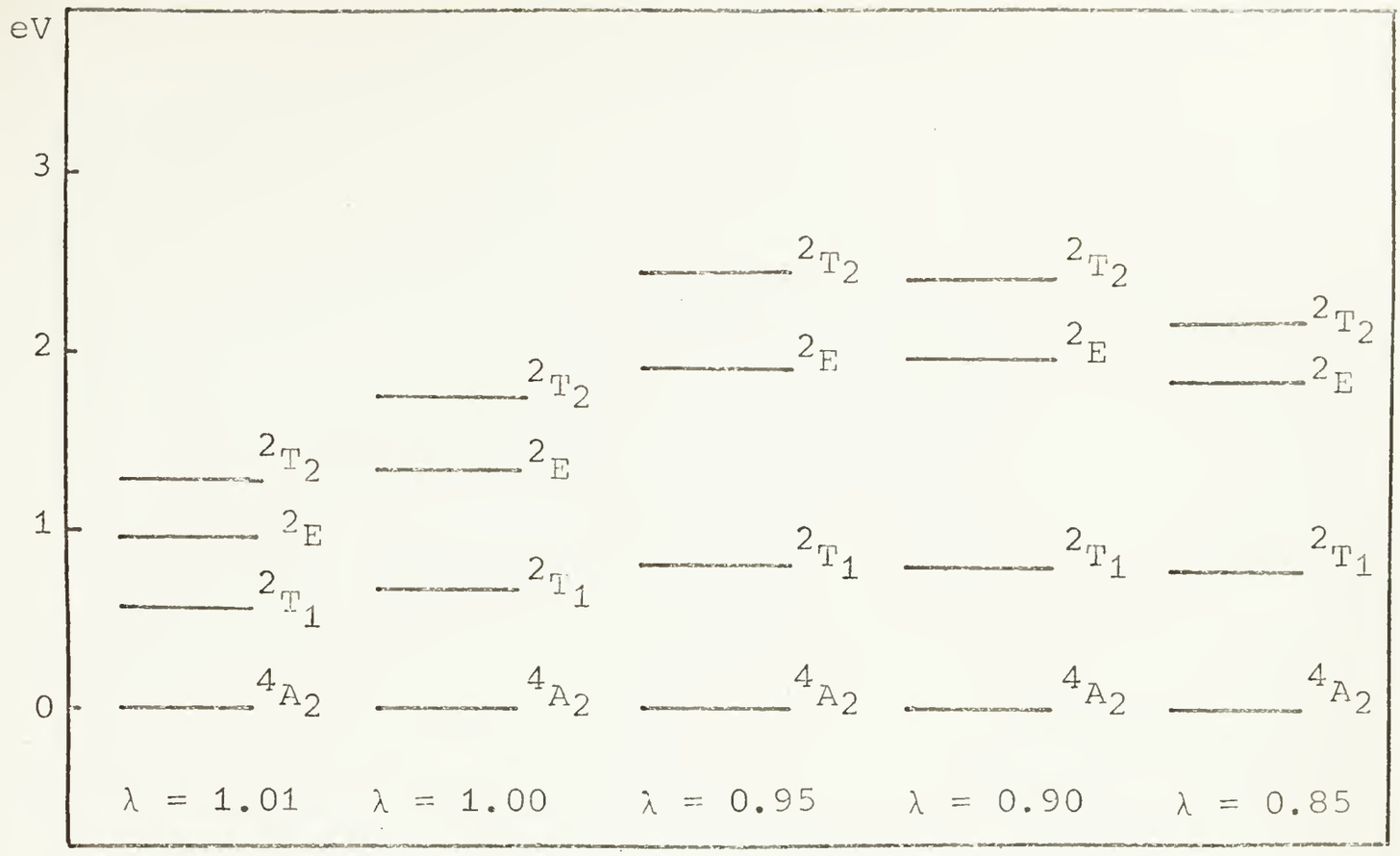


g.3.6b Electronic Structure of Neutral Vacancy in Diamond. Delocalisation Study using Clementi Functions: Case 1

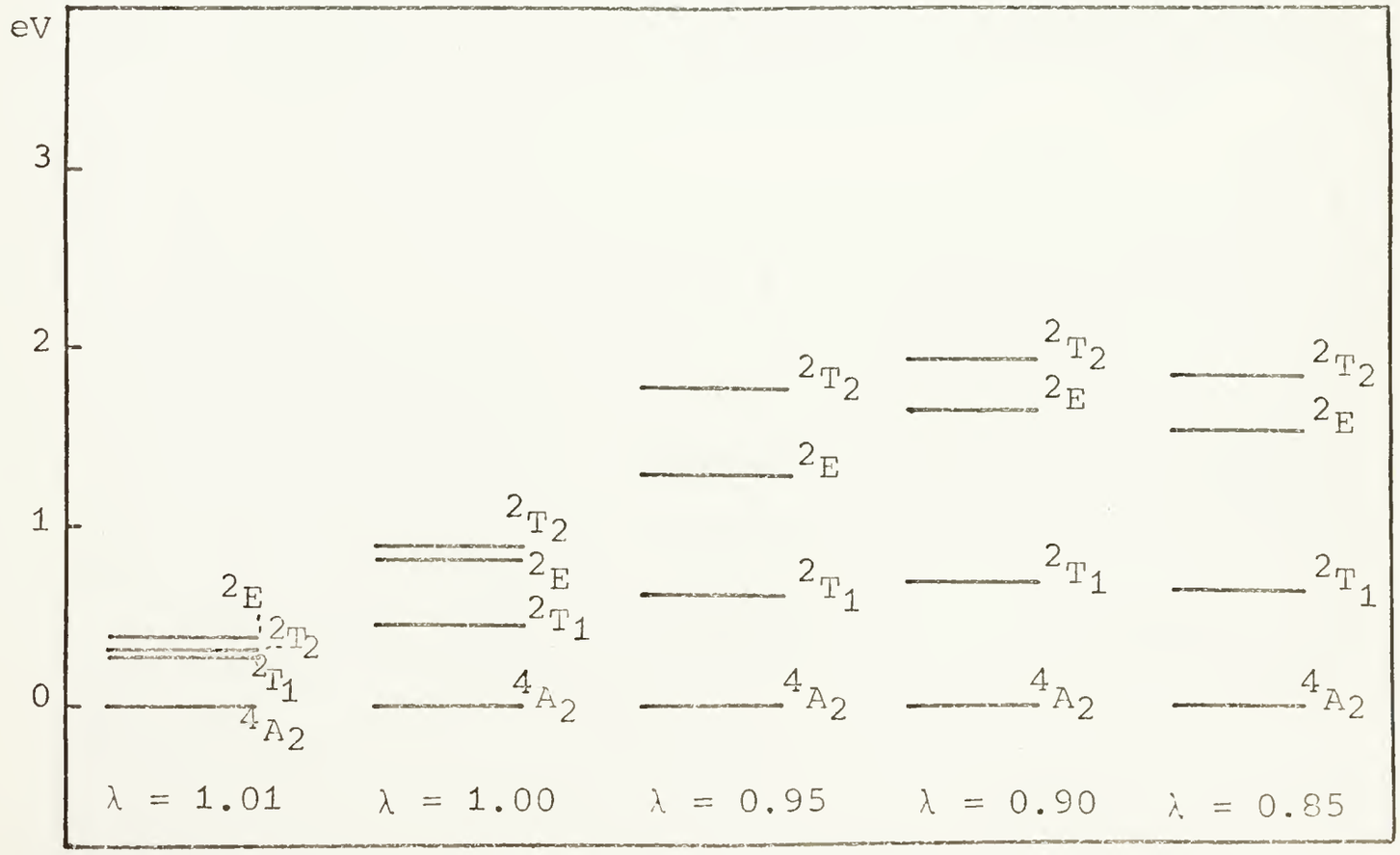
	Slater Functions	Clementi Functions
Case 1	2.41 eV	1.85 eV
Case 2	2.90 eV	2.80 eV

We are able to relate these changes to variations in the D, F and J integrals given in tables 3.4 and 3.5. When $\lambda > 1$ we notice that the trends just continue in the reverse direction and in fact for the Slater calculation (case 1) the $^3T_1$ level does become lowest. The $^5A_2$ level in general increases in energy relative to the $^3T_1$ level as λ decreases. For limited delocalisation the trends in the relative ordering of the energy levels, especially for the Clementi case, adds support to the hypothesis that the neutral vacancy is the primary defect responsible for the GR1 band.

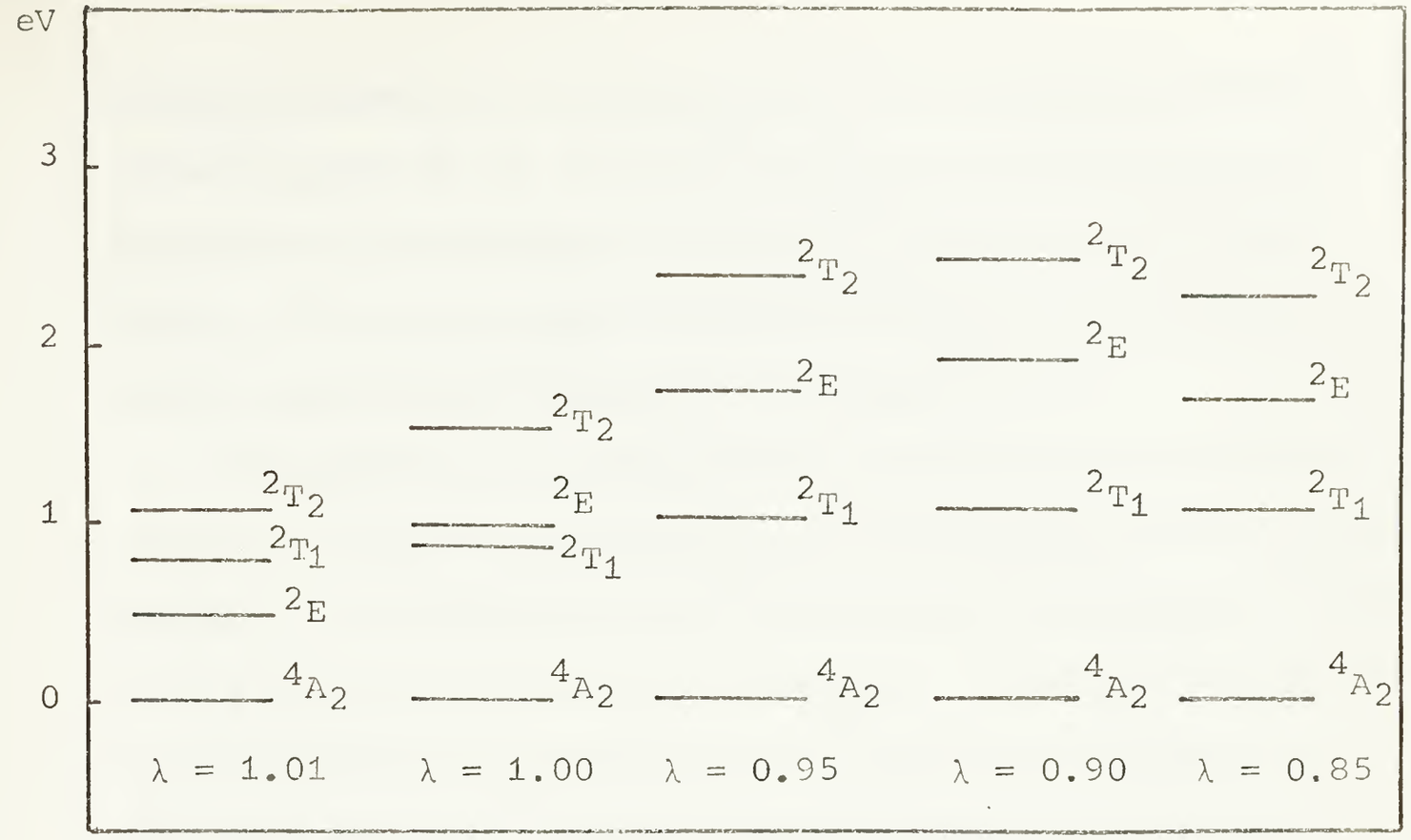
For the V^- centre, we present in fig. 3.7 the results obtained in the Slater study, while in fig. 3.8 the findings using Clementi-type functions are given. The most important finding of these studies is that delocalisation reinforces the conclusion that the $^4A_2$ level is lowest in energy. The energies of the ^2E and $^2T_2$ levels relative to the $^4A_2$ level increases as λ decreases reaching a maximum near $\lambda = 0.90$ approximately 1.0 - 2.0 eV above the ground state. The $^4A_2 - {}^2T_1$ separation is much less sensitive to the extent of delocalisation In all cases where delocalisation is incorporated the $^4A_2$ level is clearly lowest with at least 0.5 eV to the next lowest level. This



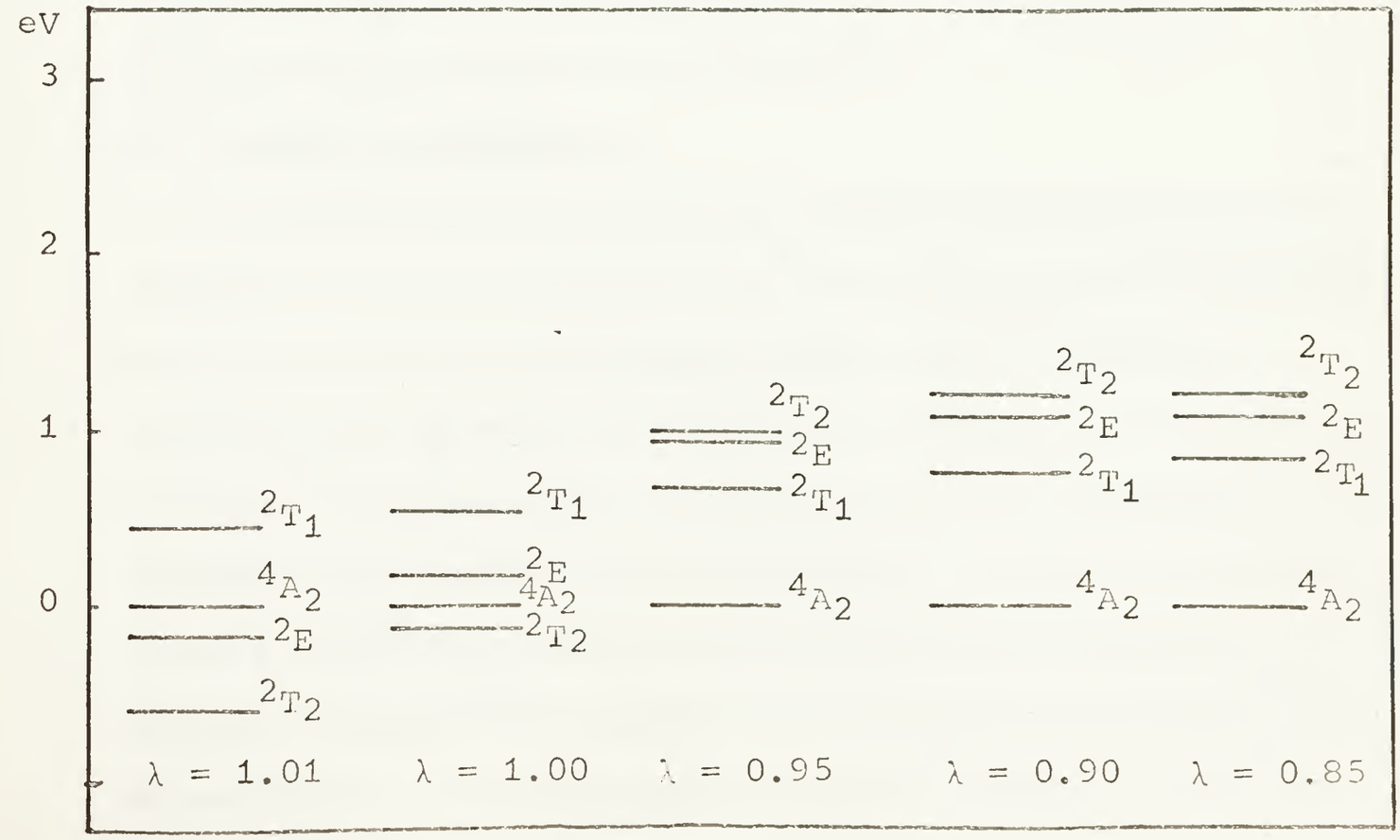
g.3.7a Electronic Structure of Negative Vacancy in Diamond.
Delocalisation Study using Slater Functions: Case 1



.3.7b Electronic Structure of Negative Vacancy in Diamond.
Delocalisation Study using Slater Functions: Case 2



g.3.8a Electronic Structure of Negative Vacancy in Diamond. Delocalisation Study using Clementi Functions: Case 1



g.3.8b Electronic Structure of Negative Vacancy in Diamond. Delocalisation Study using Clementi Functions: Case 2

analysis suggests that if delocalisation is a significant effect and if the $^4A_2$ level is not the lowest level in this centre, then the lowest level is more likely to be the $^2T_1$ rather than the ^2E or $^2T_2$ levels. This is of course a speculative conclusion since there are several other factors to also be considered.

Delocalisation has little effect on the lowest levels of the V^+ centre. The $^2T_2$ level is always at least 2 eV below any of the other levels. It is difficult to see, on the basis of this model, any other level being the ground state of this centre. In the investigation of the sensitivity of the levels of the V^{2-} centre to delocalisation we have found that the $^3T_1$ level is always lowest with the ^1E level 0.35 eV (Slater) and 0.7 eV (Clementi) above this level. The separation between the $^3T_1$ and the lowest $^1A_1$ and $^1T_2$ levels increases as λ decreases, such that they are approximately 1.5 eV (Slater) and 1 eV (Clementi) above the lowest $^3T_1$ level.

3.6 Summary and Conclusion

The electronic structure of the single isolated vacancy in its various charge states has been calculated within a modified molecular orbital theory for two different choices of atomic functions to approximate the 2s and 2p orbitals on the carbon atoms in the diamond crystal. The consequences of neglecting any delocalisation of the electronic wave-function was then examined. While it was necessary to choose a rather crude model the calculation gives some insight into the relative changes in the energies of the various levels with increasing delocalisation. No attempt was made in this chapter to relate the

findings in any detail to the known experimental results. This aspect of the work is discussed in chapter 6, only after the relaxation and distortion studies have been reported.

CHAPTER 4

THE NEUTRAL ISOLATED DIVACANCY IN DIAMOND

The Electronic Structure of the isolated neutral divacancy in an otherwise perfect diamond crystal is calculated using the defect molecule approach. The result suggests that there is a spin- and orbitally-allowed transition of symmetry $^3A_{2g} \rightarrow {}^3A_{1u}$ which contributes to the broad u-v band observed in irradiated diamonds. It is also predicted that this centre should be paramagnetic and show optical dichroism.

4.1 Introduction

In view of the uncertainty which still exists in the interpretation of many of the features of the absorption spectrum of irradiated diamonds, a study of the neutral isolated divacancy in diamond has been undertaken using a similar defect molecule approximation to that proposed for the single vacancy. A preliminary study of this problem was undertaken by Kearsley [61]. For a detailed account of the theory of the bond model the reader is referred to chapter 2. We propose to discuss in this chapter only those features which are specific to the divacancy. Furthermore, we have considered only a modified antisymmetrized molecular orbital theory.

4.2 Model for the Isolated Divacancy

The limitations of the model will be at least as serious as they are for the single vacancy. At present, however, there seems no better alternative way of dealing with the problem. In order to create the divacancy it is necessary to remove two adjacent carbon atoms from their tetrahedral sites. The resulting defect molecule is shown in fig. 4.1. Although there will be some deformation of the lattice around the di-

vacancy at the time of this study there was no quantitative evidence to suggest its extent. Therefore, in the first approximation we have neglected this effect and used the undistorted lattice parameters to specify the model, since this case provides the basis for further electronic calculations. A recent study by Hasiguti [69] using a simplified model and a restricted relaxation procedure suggests that the maximum displacement of any of the nearest neighbour atoms to the divacancy is less than 0.05Å. Again we have assumed that the electronic properties of the system in the immediate neighbourhood of the neutral divacancy are dependent upon just the six vacancy electrons.

4.3 The Hamiltonian for the System

The spin-independent Hamiltonian for the neutral divacancy is similar to that discussed for the single vacancy. However, in the potential term, V_i, we now have to consider the interaction of the i^{th} valence electron with the six atoms which are nearest the defect. Therefore, we have

$$H = \sum_{i=1}^{6} (T_i + V_i) + \sum_{i<j} \frac{1}{r_{ij}}$$

where T_i is the kinetic energy operator for the i^{th} electron and V_i is given by

$$V_i = \sum_{K} V_{Ki}$$

where K = A,B,C,D,E or F and V_{Ki} has the form, and limitations, previously discussed. Terms involving V_{Ki} have been evaluated using

the Goeppert-Mayer and Sklar approximation [57] discussed earlier. The value for the one centre potential term $\langle a| V_A |a\rangle$ used in this study was obtained in a hand calculation using tables of incomplete gamma functions [59] and is slightly different to the computed value used in the single vacancy calculation reported in the previous chapter. This accounts for why the value of P for case 1 is quoted as -7.75 eV here, compared with -8.00 eV previously.

4.4 Molecular Orbital wave-Functions

Before the defect was created, the six vacancy electrons were in the tetrahedral hybrid orbitals, a - f, associated with the atoms A - F, as shown in fig. 4.1. The vacancy electrons originally formed covalent bonds with the valence electrons of a carbon atom at either O or O'. Three different internuclear distances are involved in the present calculation. $AB = \sqrt{3} \times \frac{a}{4}$ Å., $AE = \sqrt{11} \times \frac{a}{4}$ Å., and $AD = \sqrt{19} \times \frac{a}{4}$ Å., where a is the cell constant for the diamond-type lattice.

The symmetry group of the 'molecule' is D_{3d}. Using group theory it is possible to show that in a field of D_{3d} symmetry the single electron molecular orbitals belong to the following irreducible representations

$$a_{1g},\ a_{2u},\ e_u \text{ and } e_g.$$

A suitable set of real non-localized single-electron wave functions, which are mutually orthogonal and correspond to these symmetry irreducible representations are as follows:

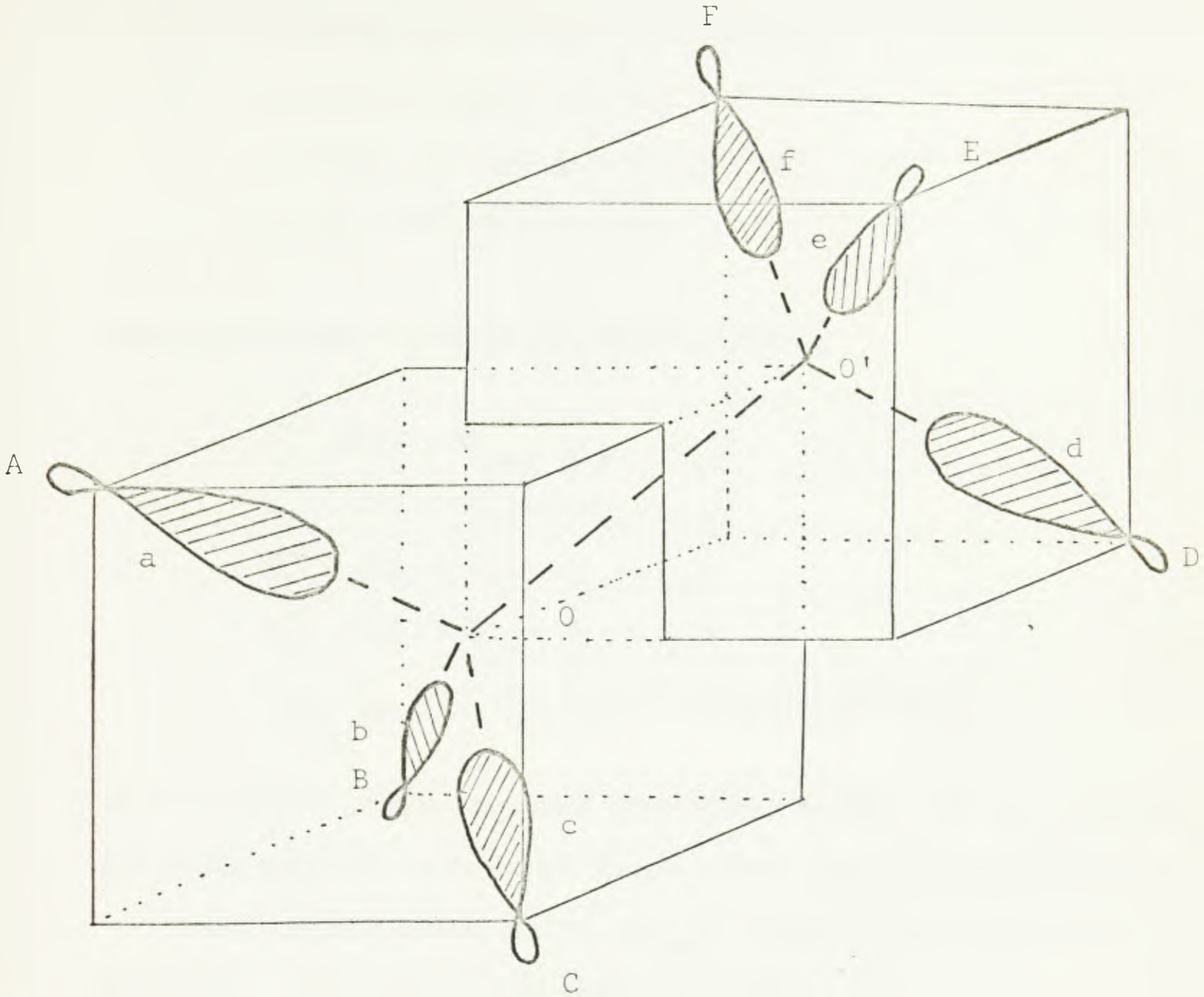


Fig.4.1 Isolated divacancy in diamond - defect molecule

$$v = N_1 (a + b + c + d + e + f) \qquad a_{1g}$$

$$u = N_2 (a + b + c - d - e - f) \qquad a_{2u}$$

$$\left.\begin{aligned} x &= \sqrt{3}N_3 (a + b - 2c + d + e - 2f) \\ y &= N_3 (3a - 3b + 3d - 3e) \end{aligned}\right\} \qquad e_g$$

$$\left.\begin{aligned} z &= \sqrt{3}N_4 (a + b - 2c - d - e + 2f) \\ t &= N_4 (3a - 3b - 3d + 3e) \end{aligned}\right\} \qquad e_u$$

where the normalization constants are given by

$$N_1^{-2} = 6(1 + 2S_{ab} + 2S_{ae} + S_{ad})$$

$$N_2^{-2} = 6(1 + 2S_{ab} - 2S_{ae} - S_{ad})$$

$$N_3^{-2} = 36(1 - S_{ab} - S_{ae} + S_{ad})$$

$$N_4^{-2} = 36(1 - S_{ab} + S_{ae} - S_{ad})$$

S_{ab}, S_{ae} and S_{ad} are the overlap integrals.

It is possible to obtain a more symmetrical complex set of orbitals, but these were less convenient to use in the present calculation.

Each non-degenerate orbital may be occupied by at most two electrons, while each of the doubly-degenerate orbitals by at most four electrons. Since there are 12 possible spin orbitals and six vacancy electrons there are 924 possible six-electron wave functions for the system. For this system of vacancy electrons we have in all 37 possible configurations of the form $a_{1g}^m a_{2u}^n e_g^r e_u^s$. Because of the restriction imposed by the Pauli Principle that the occupation number of any orbital cannot be greater than two the following restrictions are placed on m,n,r and s,

$$0 \leq m, \quad n \leq 2, \quad 0 \leq r, \quad s \leq 4.$$

The symmetry states of the six-electron wave functions corresponding to the particular configurations may be determined using the method of Mulliken [56] of reducing through states of lower symmetry. Since holes transform like particles it follows that e_u^3 will transform like e_u and e_u^4 like a_{1g}, since the 'e_u shell' is filled at four electrons, and similarly for e_g. The symmetry and spin multiplicities of the resultant states of these 37 configurations are shown in table 4.1.

For this divacancy calculation simple analytical forms proposed by Slater [58] for the 2s and 2p wave functions were chosen. As in the previous chapter, the screening constant, c, for these functions is chosen to have the value 3.19, the usual free atom value. Now, in principle, it is a straight forward procedure following the method outlined in chapter 2, to form the six-electron wave-functions to represent all the symmetry states arising from the 37 configurations, and to evaluate the energy levels. However, in practice this is not so easy, even if we make full use of symmetry considerations to factorize the interaction problem.

There are 198 six-electron wave-functions with symmetry ^3E_u, 180 with symmetry ^3E_g, 60 with symmetry ^1E_g and 54 with symmetry ^1E_u. Even if we make maximum use of the double degeneracy of the E-type levels, we shall still have secular determinants of order 30 x 30. In order to reduce this problem to manageable proportions some further simplification is needed.

TABLE 4.1

Allowed States for the Neutral Divacancy

No.	Configuration	Symmetry of the Resultant States
1	$a_{1g}^2 a_{2u}^2 e_g^2$	$^1A_{1g} + {}^3A_{2g} + {}^1E_g$
2	$a_{1g}^2 a_{2u}^2 e_g e_u$	$^3A_{1u} + {}^1A_{1u} + {}^3A_{2u} + {}^1A_{2u} + {}^3E_u + {}^1E_u$
3	$a_{1g}^2 a_{2u}^2 e_u^2$	$^1A_{1g} + {}^3A_{2g} + {}^1E_g$
4	$a_{1g} a_{2u}^2 e_g^3$	$^3E_g + {}^1E_g$
5	$a_{1g} a_{2u}^2 e_g^2 e_u$	$^5E_u + 4{}^3E_u + 3{}^1E_u + {}^3A_{2u} + {}^1A_{2u} + {}^3A_{1i} + {}^1A_{1u}$
6	$a_{1g} a_{2u}^2 e_g e_u^2$	$^5E_g + 4{}^3E_g + 3{}^1E_g + {}^3A_{2g} + {}^1A_{2g} + {}^3A_{1g} + {}^1A_{1g}$
7	$a_{1g} a_{2u}^2 e_u^3$	$^3E_u + {}^1E_u$
8	$a_{1g}^2 a_{2u} e_g^3$	$^3E_u + {}^1E_u$
9	$a_{1g}^2 a_{2u} e_g^2 e_u$	$^5E_g + 4{}^3E_g + 3{}^1E_g + {}^3A_{2g} + {}^1A_{2g} + {}^3A_{1g} + {}^1A_{1g}$
10	$a_{1g}^2 a_{2u} e_g e_u^2$	$^5E_u + 4{}^3E_u + 3{}^1E_u + {}^3A_{2u} + {}^1A_{2u} + {}^3A_{1u} + {}^1A_{1u}$
11	$a_{1g}^2 a_{2u} e_u^3$	$^3E_g + {}^1E_g$
12	$a_{2u}^2 e_g^4$	$^1A_{1g}$
13	$a_{2u}^2 e_g^3 e_u$	$^3A_{1u} + {}^1A_{1u} + {}^3A_{2u} + {}^1A_{2u} + {}^3E_u + {}^1E_u$
14	$a_{2u}^2 e_g^2 e_u^2$	$2{}^3E_g + 3{}^1E_g + {}^5A_{1g} + 3{}^1A_{1g} + {}^3A_{1g} + 2{}^3A_{2g} + {}^1A_{2g}$
15	$a_{2u}^2 e_g e_u^3$	$^3A_{1u} + {}^1A_{1u} + {}^3A_{2u} + {}^1A_{2u} + {}^3E_u + {}^1E_u$
16	$a_{2u}^2 e_u^4$	$^1A_{1g}$
17	$a_{1g}^2 e_g^4$	$^1A_{1g}$
18	$a_{1g}^2 e_g^3 e_u$	$^3A_{1u} + {}^1A_{1u} + {}^3A_{2u} + {}^1A_{2u} + {}^3E_u + {}^1E_u$
19	$a_{1g}^2 e_g^2 e_u^2$	$2{}^3E_g + 3{}^1E_g + {}^5A_{1g} + {}^3A_{1g} + 3{}^1A_{1g} + 2{}^3A_{2g} + {}^1A_{2g}$
20	$a_{1g}^2 e_g e_u^3$	$^3A_{1u} + {}^1A_{1u} + {}^3A_{2u} + {}^1A_{2u} + {}^3E_u + {}^1E_u$

TABLE 4.1 (continued)

21	$a_{1g}^2 e_u^4$	$^1A_{1g}$
22	$a_{1g} a_{2u} e_g^4$	$^3A_{2u} + {}^1A_{2u}$
23	$a_{1g}^1 a_{2u}^1 e_g^3 e_u^1$	$^5A_{2g} + {}^5A_{1g} + {}^5E_g + 3^3A_{2g} + 3^3A_{1g} + 3^3E_g + 2^1A_{2g} + 2^1A_{1g} + 2^1E_g$
24	$a_{1g} a_{2u} e_g^2 e_u^2$	$^7A_{2u} + 3^5A_{2u} + 2^5A_{1u} + 7^3E_u + 6^3A_{2u} + 5^3A_{1u} + 5^1E_u + 4^1A_{2u} + 3^1A_{1u}$
25	$a_{1g} a_{2u} e_g e_u^3$	$^5A_{2g} + {}^5A_{1g} + {}^5E_g + 3^3A_{2g} + 3^3A_{1g} + 3^3E_g + 2^1A_{2g} + 2^1A_{1g} + 2^1E_g$
26	$a_{1g} a_{2u} e_u^4$	$^3A_{2u} + {}^1A_{2u}$
27	$a_{1g} e_g^4 e_u$	$^3E_u + {}^1E_u$
28	$a_{1g} e_g^3 e_u^2$	$^5E_g + 4^3E_g + 3^1E_g + {}^3A_{2g} + {}^1A_{2u} + {}^3A_{1g} + {}^1A_{1g}$
29	$a_{1g} e_g^2 e_u^3$	$^5E_u + 4^3E_u + 3^1E_u + {}^3A_{2u} + {}^1A_{2u} + {}^3A_{1u} + {}^1A_{1u}$
30	$a_{1g} e_g e_u^4$	$^3E_g + {}^1E_g$
31	$a_{2u} e_g^4 e_u$	$^3E_g + {}^1E_g$
32	$a_{2u} e_g^3 e_u^2$	$^5E_u + 4^3E_u + 3^1E_u + {}^3A_{2u} + {}^1A_{2u} + {}^3A_{1u} + {}^1A_{1u}$
33	$a_{2u} e_g^2 e_u^3$	$^5E_g + 4^3E_g + 3^1E_g + {}^3A_{2g} + {}^1A_{2g} + {}^3A_{1g} + {}^1A_{1g}$
34	$a_{2u} e_g e_u^4$	$^3E_u + {}^1E_u$
35	$e_g^4 e_u^2$	$^1A_{1g} + {}^3A_{2g} + {}^1E_g$
36	$e_g^3 e_u^3$	$^3A_{1u} + {}^1A_{1u} + {}^3A_{2u} + {}^1A_{2u} + {}^3E_u + {}^1E_u$
37	$e_g^2 e_u^4$	$^1A_{1g} + {}^3A_{2g} + {}^1E_g$

The aim of the present calculation is to determine the ground state level and the excited levels near this state which result from the presence of a neutral isolated divacancy in the crystal. Therefore, we have argued as follows, on the basis of a one-electron model. If we assume that there is no interaction between the vacancy electrons then it is possible to calculate the relative energies of the single-electron molecular-orbital states. Such a calculation using an empirical value for the one-centre Coulomb integral Q(Q = 12.856 eV) and the calculated 'self penetration integral' P(P = -7.75 eV), results in the following values for the energies

$$A = \frac{\langle v|H^{o}|v\rangle}{\langle v|v\rangle} = -45.650 \text{ eV}$$

$$B = \frac{\langle u|H^{o}|u\rangle}{\langle u|u\rangle} = -43.080 \text{ eV}$$

$$C = \frac{\langle x|H^{o}|x\rangle}{\langle x|x\rangle} = -34.789 \text{ eV}$$

$$D = \frac{\langle z|H^{o}|z\rangle}{\langle z|z\rangle} = -36.741 \text{ eV}$$

where H^{o} is the single-particle operator of the Hamiltonian H.

In the six-electron system, therefore, if there were no interaction between the vacancy electrons, one would expect that the three configurations $a_{1g}^2 a_{2u}^2 e_u^2$, $a_{1g}^2 a_{2u}^2 e_u e_g$ and $a_{1g}^2 a_{2u}^2 e_g^2$ would be lowest in energy. Configurations in which one electron was excited

from an orbital of a_{1g} or a_{2u} symmetry, namely orbital v or u, to an orbital of e_g or e_u symmetry would be expected to constitute the next group of configurations lowest in energy. There are eight such configurations. A further group of 15 configurations results from the promotion of two electrons from the non-degenerate molecular orbitals into the doubly-degenerate ones. Interaction between the electrons will cause the levels from any one configuration to split. It would appear to be a reasonable approximation to assume that a calculation considering the interaction between the first eleven configurations mentioned above would enable the relative ordering of the levels near the ground state to be determined accurately. The present work has been concerned exclusively with the first eleven configurations with the exception that the highest spin symmetry state, $^7A_{2u}$, arising from the configuration $a_{1g}a_{2u}e_g^2e_u^2$ has also been considered. With these approximations the problem, while still being formidable, becomes at least manageable. The un-normalized six-electron wave-functions, $\Psi(R)$, for the first eleven configurations are shown in Appendix B.1.

4.5 Energy Evaluation for the System

The energy of each symmetry state for the various configurations before configuration interaction, $E(R)$, may now be evaluated using the equation

$$E(R) = \frac{\int \Psi^*(R)\, H\, \Psi(R)\, d\tau}{\int \Psi^*(R)\, \Psi(R)\, d\tau}$$

where $\Psi(R)$ is the six-electron determinantal wave-function corresponding to a given irreducible representation R of the group D_{3d}, for a particular configuration of given S and S_z. Again the integration may be reduced to a series of one- and two-electron integrals involving the molecular orbitals v,u,x,y,z and t. In all it is necessary to know the value of 25 two-electron molecular integrals and 4 one-electron molecular integrals. These integrals may in turn be expressed in terms of one- and two-electron integrals involving the localized atomic hybrid orbitals a,b,c,d,e and f. Finally, these integrals may be broken down into basic atomic integrals involving 2s and 2p functions. These integrals must be evaluated at the three internuclear distances AB = 4.766 a.u., AE = 5.586 a.u. and AD = 7.343 a.u.

The Diatomic Molecular Integral Program was again used together with the Mulliken approach for three- and four-centre integrals. The values of the basic integrals may be found in Appendix A.4. Values of the two-electron molecular integrals necessary for the present calculation using Slater orbitals with c = 3.19 are shown in table 4.3. The values of the one-electron integrals for the two cases: 1. Q = 12.856 eV, P = -7.75 eV and 2. Q = 12.856 eV, P = -16.42 eV are shown in table 4.2. The formal expressions for the calculation of the energy E(R) of a given symmetry state belonging to each configuration are listed in Appendix B.2 in terms of the one- and

two-electron molecular integrals previously mentioned. The energy level scheme before configuration interaction for the two cases may now be determined. However, these energies are of no great value in themselves, since we must allow interaction between configurations of the same symmetry. Even with our agreed restriction to the lowest eleven configurations the number of states of a given symmetry in some cases is still considerable. Table 4.4 shows the actual number for each of the fourteen permitted symmetries.

TABLE 4.2

One-Electron Molecular Integrals for the Divacancy

Integral	Case 1	Case 2
$A \equiv \langle v \vert H^{o} \vert v \rangle$	-45.650*	-51.646
$B \equiv \langle u \vert H^{o} \vert u \rangle$	-43.080	-50.211
$C \equiv \langle x \vert H^{o} \vert x \rangle$	-34.789	-45.628
$D \equiv \langle z \vert H^{o} \vert z \rangle$	-36.741	-46.714

*All energies are in electron volts

The symmetry states belonging to the one-dimensional representations and the states of ^5E_u and ^5E_g symmetry present no difficulty and may all be included easily. However, the other E states are more complicated and give rise to larger secular determinants. In order to locate the lowest of these levels accurately perturbation theory can be used, or alternatively, a reasonable number of

TABLE 4.3

Values for the two-electron molecular integrals for the neutral divacancy using Slater orbitals with c = 3.19.

The following abbreviation is used for these integrals to simplify the typing

$$\langle v(1)\ t(2)\left|\frac{1}{r_{12}}\right|\ v(1)\ t(2)\rangle = (v\ v : t\ t)$$

Integral	Designation	Value(eV)	Integral	Designation	Value(eV)
(vv : vv)	E	7.8406	(uu : xx)	T	7.4561
(uu : uu)	F	7.8341	(ux : ux)	U	1.1545
(vv : uu)	G	7.8340	(uu : zz)	V	7.4984
(vu : vu)	J	2.5088	(uz : uz)	W	0.8084
(xx : xx)	K	7.0165	(xx : zz)	X	7.1744
(xx : yy)	L	6.7810	(xx : tt)	x	6.8508
(xy : xy)	l	0.1178	(xz : xz)	Y	2.0212
(zz : zz)	M	7.3445	(xt : xt)	Z	0.3565
(zz : tt)	N	6.9030	(xy : zt)	Γ	0.1618
(zt : zt)	n	0.2212	(xz : yt)	Λ	1.3248
(vv : xx)	p	7.5583	(yz : xt)	r	0.3399
(vx : vx)	Q	0.9028			
(vv : zz)	R	7.5969			
(vz : vz)	S	1.3010			

TABLE 4.4

The Number of Symmetry States from the first 11 configurations of a given symmetry for a Neutral Divacancy

Symmetry	$^1A_{1g}$	$^1A_{1u}$	$^1A_{2u}$	$^1A_{2g}$	^1E_g	^1E_u	$^3A_{1g}$	$^3A_{2g}$	$^3A_{1u}$	$^3A_{2u}$	^3E_g	^3E_u	^5E_u	^5E_g
Number of Symmetry States	4	3	3	2	10	9	2	4	3	3	10	11	2	2

'configurations' of each symmetry may be chosen and this limited amount of configuration interaction applied. In this calculation we have included the interaction between the lowest four states of a particular symmetry in each case. Mixing with higher configurations had negligible effect on the position of the lowest levels, and so this would seem to be a reasonable approximation. In fig.4.2 the lowest energy levels for the neutral isolated divacancy on the modified a.s.m.o. theory for the two extreme values of P, before and after configuration interaction, are shown. In fig. 4.3 an expanded version of the lowest levels is given.

4.6 Allowed Electronic Transitions

For the divacancy system of D_{3d} symmetry the components of the electric dipole operator, which are proportional to x,y and z transform as follows

$$z \subset A_{2u} \qquad x,y \subset E_u \ .$$

Therefore, the allowed electric dipole transitions shown in table 4.5 may occur provided the spin selection rule is satisfied. As discussed previously with such transformations for x,y and z it is possible to get absorption in preferred directions giving rise to optical dichroism.

TABLE 4.5

Allowed Transitions with D_{3d} Symmetry

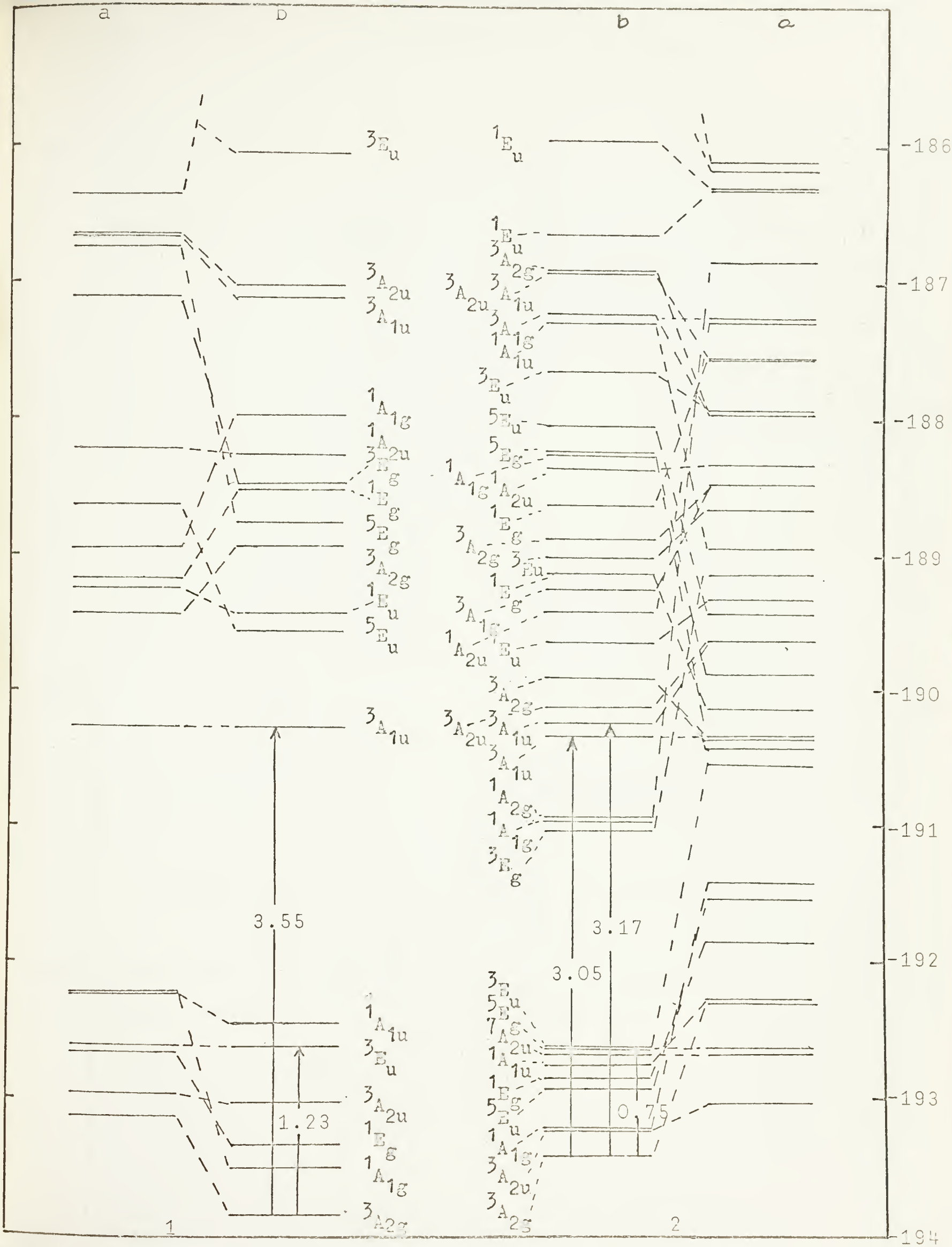
Initial State	A_{2g}	A_{2u}	A_{1g}	A_{1u}	E_g	E_u
Final State z	A_{1u}	A_{1g}	A_{2u}	A_{2g}	E_u	E_g
Final State x,y	E_u	E_g	E_u	E_g	A_{1u}, A_{2u}, E_u	A_{1g}, A_{2g}, E_g

4.7 Results

The characteristics of this system are in many ways similar to those for the Slater case of the neutral vacancy. However, there are some differences.

Configuration interaction has the effect of inverting the ordering of some of the energy levels. In some cases this inversion is accompanied by large energy changes. This effect is most pronounced in case 2. The modified a.s.m.o. theory predicts that in both cases the $^3A_{2g}$ symmetry state is lowest in energy. This state arises principally from the configuration $a_{1g}^2\, a_{2u}^2\, e_u^2$. It is interesting to note that a triplet ground state would be predicted in terms of the one-electron energies for the molecular orbitals given in table 4.2 by application of Hund's rules to the lowest configuration.

If we had considered the wave functions as built out of the six atomic orbitals a.....f, then from Hund's rules the $^7A_{2u}$ state would have been predicted to be lowest in energy before configuration interaction. However, in terms of the one-electron molecular-orbital picture this spin state arises from the configuration $a_{1g}\, a_{2u}\, e_u^2\, e_g^2$



Energy levels of a neutral isolated divacancy on the modified a.s.m.o. theory (1) calculated using Q = 12.856 eV, P = -7.75 eV, (2) calculated using Q = 12.856 eV P = -16.42 eV. (a) before configuration interaction (b) after configuration interaction.

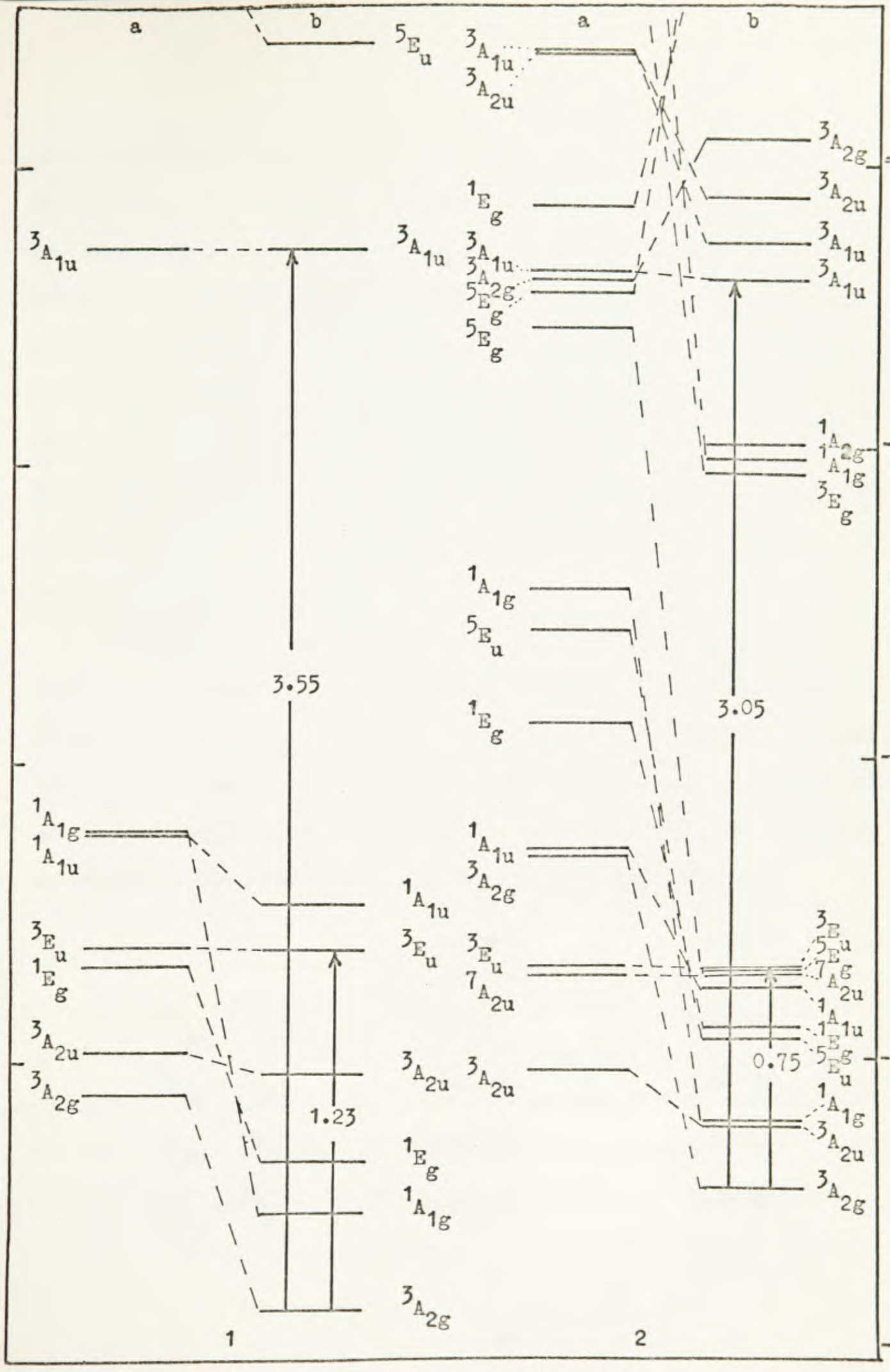


Fig.4.3 Electronic Structure of the Neutral Isolated Divacancy in Diamond.
1.Q = 12.856 eV, P = -7.75 eV. 2.Q = 12.856 eV, P = -16.42 eV.
a.Before configuration interaction, b.After configuration interaction.

and is appreciably less stable than the $^3A_{2g}$ state in case 1, but in case 2 it shows a strong dependence on the value of P and is near the lowest levels of energy. The marked difference in the two cases occurs because the energies of the single-electron molecular orbitals of e_g and e_u symmetry, i.e. C and D, are more dependent upon the value of P than the orbitals belonging to the one-dimensional representations. The general effect of this dependence is that all the energy levels become more compressed and hence configuration-interaction effects even more significant as P decreases. This effect was also observed in the neutral vacancy calculation.

The energies of the allowed transitions from the $^3A_{2g}$ ground state and from the $^1A_{1g}$ level, which is within 0.3 eV of the ground state, are given below. If the $^1A_{1g}$ level is 0.3 eV above the lowest level the transition from $^1A_{1g} \rightarrow {}^1E_u$ would be very weak, if observable at all/at room temperature. However, it is possible that the $^1A_{1g}$ level is closer to the ground state than this in the actual crystal.

	Case 1 P = -7.75 eV	Case 2 P = -16.42 eV
$^3A_{2g} \rightarrow {}^3E_u$	1.23 eV	0.75 eV
$^3A_{2g} \rightarrow {}^3A_{1u}$	3.55 eV	3.05 eV
$^3A_{2g} \rightarrow {}^3A_{1u}$	(6.73 eV)	3.17 eV
$^1A_{1g} \rightarrow {}^1E_u$	4.12 eV	3.59 eV

There are other possible transitions from the $^3A_{2u}$ level, but these are even less likely, especially since the true value of P is probably closer to -7.75 eV than to -16.42 eV, such that case I more closely resembles the true situation using the present approximations.

It is noteworthy that for the neutral isolated divacancy the transition energy decreases with decreasing values of P, whereas, for the neutral isolated vacancy the reverse trend is observed. The explanation for this is that for the neutral isolated vacancy before configuration interaction the ^1E and $^1T_2$ levels involved in the transition arise from the v^2t^2 configuration and therefore contain equal admixtures of the one-electron molecular integrals. Even after configuration interaction the lowest levels arise predominantly from this configuration. However, for the neutral divacancy transitions must occur between levels of gerade and ungerade symmetry and these will, of course, arise from different configurations and so contain different admixtures of the one-electron molecular integrals A,B,C and D. The varying dependence of these integrals on P, is the basic cause of the decrease of transition energies as P decreases.

It is also interesting to note that if only the lowest group of states is considered it is easy to understand why the states of gerade symmetry are lowered much more in energy by configuration interaction than the ungerade symmetry states. The former arise from the configuration $a_{1g}^2a_{2u}^2e_u^2$ and interact strongly with the gerade states arising from the configuration $a_{1g}^2a_{2u}^2e_g^2$ which also belongs to the

'ground state group of configurations' and lie just above the lowest group of levels. However, to find suitable symmetry states to interact with the lowest ungerade states we must consider levels from higher configurations. These are, in general, of much higher energies and interact less with the lowest-lying states. The second-lowest $^3A_{1u}$ level arises from the configuration $a_{1g}^2 a_{2u} e_g e_u^2$ and shows a strong dependence on P for reasons discussed previously.

The present calculation predicts that since the lowest level is non-degenerate there would be no Jahn-Teller effect causing distortion of the nuclear framework in the ground state. However, there is always the possibility that Jahn-Teller effects could split the ^1E_g level and shift one of its components to a lower level, below the $^3A_{2g}$ level. But since the lowering would need to exceed ½ eV we are inclined to think that this is rather unlikely. It is also possible that symmetric relaxation terms may alter the relative ordering of the lowest levels.

Since the lowest level is a triplet we expect the defect to be paramagnetic and hence to exhibit resonance in an E.P.R. study. Many lines with spin S = 1 have been observed in E.P.R. studies and it is therefore possible that the origin of some of these lines lies in the electronic behaviour of the defect electrons of the divacancy in the neutral state.

It is interesting to note that a transition between the $^3A_{2g}$ and $^3A_{1u}$ levels is allowed only in the z direction. Therefore polarisation effects should be observed which would manifest themselves in optical dichroism studies. Also the low energy transition between $^3A_{2g}$ and ^3E_u is allowed only in the x and y directions.

4.8 Relation with Experiment

We are now ready to compare our purely theoretical values with the results of absorption experiments. In view of the various approximations inherent in our model we must not expect exact agreement, and in any case the interpretation of the experimental absorption curve of irradiated diamonds is itself uncertain. We may therefore expect that our theoretical predictions might be of help in assigning the different parts of the measured absorption spectrum.

The spectrum for irradiated type II diamonds obtained by Clark et al [27] showed a broad absorption band between 1.65 and 2.4 eV with an intense line at 1.673 eV known as the GR1 band and also a band in the ultra-violet region of the spectrum. This intense band commenced at about 2.8 eV and the absorption increased to a maximum near 4 eV after which it decreased only to be masked by the beginning of the region of continuous absorption. There are also sharp lines at 3.315 and 4,133 eV which have been used to measure the strength of the band [31,32]. There have been several studies, for example [34], which suggest that GR1 and u - v bands arise from transitions within the same centre or from associated defect centres.

It is also clear from many studies that the u - v band is very complex. However, on the basis of the present quantitative calculation, it is suggested that at least part of this absorption band may arise from electronic transitions involving the electrons immediately surrounding the isolated neutral divacancy as the result of the spin-

and orbitally-allowed $^3A_{2g} \rightarrow {}^3A_{1u}$ transition. There also exists the possibility of a transition between the $^1A_{1g}$ and ^1E_u levels. This calculation does not substantiate the possible association of the isolated neutral divacancy with the GR1 band (1.65-2.4 eV) or with the TH5 band (2.3-2.8 eV) [37], produced as a result of annealing the sample. It seems more likely that this latter band arises from some complex impurity defect being formed.

The association of at least part of the u - v band with a neutral isolated divacancy and the GR1 band with the isolated vacancy in some particular charge state would provide a consistent explanation as both these bands are produced by room temperature irradiation. The formation of divacancies should be possible at the energies of irradiation used in most investigations so far. Their formation involves the rupture of only seven bonds, whereas two single vacancies involve the breaking of eight bonds, and therefore they are quite likely to exist on energetic grounds. In silicon for example, they have been observed at temperatures as low as $20^{o}K$ as a primary event in irradiation.

The predicted low energy transition between the $^3A_{2g}$ and ^3E_u level is also of interest. However, there seems to be no published work available of any investigations in this region.

4.9 Conclusion

In this chapter we have discussed the application of the defect molecule method to a neutral isolated divacancy in the otherwise perfect diamond lattice. Using free atom non-orthogonal Slater functions for the 2s and 2p electrons on the atoms which are neighbouring the defect,

the modified molecular-orbital treatment predicts electronic transitions among the electrons surrounding an isolated neutral divacancy which correspond to transitions in the ultra-violet region of the spectrum. A spin- and orbitally-allowed $^3A_{2g} \rightarrow {}^3A_{1u}$ transition is predicted as well as a low energy transition between the $^3A_{2g}$ and ^3E_u level. A broad band would be expected, because of lattice vibrations within the crystal and the influence of other atoms not considered in this calculation. This centre should be paramagnetic and show optical dichroism.

CHAPTER 5

LATTICE DISTORTION AROUND SINGLE VACANCIES IN DIAMOND-TYPE CRYSTALS

The displacement of the atoms around a single vacancy in the diamond and silicon crystals to fifth neighbour have been determined using a dynamic relaxation program. The interaction between the atoms of the crystal are approximated by use of a valence force potential, while the rebonding of the vacancy electrons is assumed to be in pairs which may be described by a Morse-type potential function. The formation energy of the single vacancy has also been determined.

5.1 Introduction

One of the most important assumptions of the bond model approach, as it has been enunciated so far, has been to assume that the atoms in the crystal near where the defect has been created remain in their perfect lattice sites. In this chapter we examine this assumption and endeavour to obtain some estimate of the extent of distortion around a single vacancy in diamond and silicon crystals. As a by-product of the study it is possible to obtain an estimate of the formation energy of a single vacancy in these valence crystals.

The principle objective of previous relevant studies [54,55,70] has been the determination of the formation and migration energies of the isolated vacancy in diamond-type crystals. As a consequence, relaxation and distortion effects have been considered only in so far as they were thought to influence these energies. At the time of commencing this investigation no detailed work was available giving the configurations of the atoms nearest the defect. We were aware of some work by Seeger and Swanson, but were unable to obtain any

detailed information about the method used. Since our investigation their work on silicon and germanium, but not diamond, has been published [55] along with a related study by Hasiguti [69] on the isolated divacancy in silicon and germanium crystals. We propose to discuss in section 5.2 the general approach of previous studies which are relevant to the determination of the configuration of the atoms surrounding the single vacancy and its formation energy. In the following two sections (5.3 and 5.4) we discuss the model and the potential interaction between the atoms used in this investigation. The results obtained for the single vacancy in diamond are presented in section 5.5, while those for silicon are given in the next section. Our results are compared with previous calculations and experiment in section 5.7.

5.2 Previous Theoretical Models

Previous studies have been based on the assumption that the properties of the valence crystals and the response of the lattice to relaxation may be adequately approximated by pair-wise interactions between nearest neighbour atoms using a generalized Morse-type potential of the kind

$$U(r) = D\left[\frac{\alpha_2}{\alpha_1-\alpha_2}\exp\left\{-\alpha_1(r-r_o)\right\} - \frac{\alpha_1}{\alpha_1-\alpha_2}\exp\left\{-\alpha_2(r-r_o)\right\}\right] \qquad (5.1)$$

where D is the bond dissociation energy, r_o the equilibrium internuclear distance in the perfect crystal, and α_1 and α_2 parameters to be determined from the physical properties of the crystal. In

most studies [54,69,70] α_1 has been assumed to be equal to 2 α_2 and α_2 determined from the compressibility of the crystal. However, Seeger and Swanson [55] determined α_1 and α_2 from the known pressure dependence of the compressibility in silicon and germanium [71,72]. For germanium, the ratio of α_1 to α_2 was found to differ significantly from 2 ($\alpha_1/\alpha_2 \simeq 5.1$), while for silicon ($\alpha_1/\alpha_2 \simeq 1.76$). The use of the pair-wise potential interaction between nearest neighbour atoms only is grossly inadequate for diamond-type crystals. Such a potential gives unsatisfactory predictions for the second order elastic constants [73] and the phonon dispersion curves of these crystals [74].

The estimates of D, the bond dissociation energy, differ significantly depending upon whether the promotion energy for an electron from the s^2p^2 ground state of the isolated atom to the sp^3 valence state of that atom, E_p, is included. The studies by Swalin [54], Scholz and Seeger [70] and Hasiguti [69] have neglected this term and chosen $D = \frac{1}{2} E_s$, where E_s is the heat of sublimation at room temperature. Lidiard [75] has stated that such an estimate is too small, because the promotion energy cannot be ignored. One should therefore use the relation

$$D = \tfrac{1}{2} (E_s + E_p) \qquad (5.2)$$

where E_s and E_p are defined above. Seeger and Swanson [55] used this latter expression for D, but also used the estimated value of E_s at $0^\circ K$. The low temperature values of E_s are larger than the room temperature estimates.

The energy of formation estimated for the isolated vacancy using the model proposed by Swalin may be considered to involve three contributions.

a) The energy required to remove an atom from its lattice site and place it on the surface. This contribution to the energy is 2D.

b) The energy gained from rebonding of the four vacancy electrons on the atoms nearest the defect. It is assumed that the rebonding of the atoms is in pairs similar to that used in valence bond theory. However, only one particular bonding scheme is considered and interactions between the two bonded pairs of electrons within the defect are neglected. This model has some justification from the work of Watkins [10] and the calculation by Coulson and Kearsley [1]. However, it is rather extreme.

c) The third contribution comes from the increase in lattice energy within the vicinity of the defect due to the displacement of atoms from their perfect lattice sites.

The increase in energy due to the movement of atoms surrounding the vacancy was deduced in the Swalin study by prescribing a definite structure to the defect and then using a geometrical decrease in strain with increasing distance from the vacancy. Scholz and Seeger [70] have commented that such a law is not predicted by elasticity theory. They used the Born theory within the harmonic approximation with restricted relaxation to estimate the energy increase, but do not give any details of the assumption they have made or the magnitude of the displacements of the atoms surrounding the defect. Scholz (private

communication) has stated that the extent of distortion around the vacancy was not calculated in their study. Seeger and Swanson [55] used a less restrictive model than in the previous calculations; nevertheless, only very limited relaxation was permitted. The four atoms nearest the defect were allowed to move, but only one of their three nearest-neighbour atoms was permitted to relax. The remaining two nearest-neighbour atoms and the next-nearest neighbour atoms were held fixed on their perfect lattice sites.

All these studies used the same potential relationship to describe the rebonding of the vacancy electrons on the atoms nearest the defect as for the rest of the crystal. This approximation neglects local changes in force constants near the defect and also the fact that while a Morse curve may give a reasonable representation of bond energy and other properties near the equilibrium separation, at distances like those between atoms nearest the defect its validity is doubtful.

This whole approach neglects the changes in electronic energy within the crystal on defect formation. Benneman [4] used a first principle band theory method based upon the pseudo-potential approach and estimated the formation energy of a point defect as the difference in energy between that of the imperfect and the perfect lattice. Because of the complexity of the calculation he was unable to include relaxation terms. In our calculation we have used the classical approach and developed a model which overcomes the major deficiences of the previous studies. In the next two sections we discuss the basis of the model used and its application to the isolated single vacancy in diamond-type crystals.

5.3 Dynamic Model for the Defect Lattice

The method which we have used to determine the configuration of the atoms surrounding a point defect in the crystal is an adaptation of the computer simulated techniques developed by Bullough and Perrin [76] using a discrete atom model. They used such a model to study the nucleation and growth of interstitial loops in α-iron. Since the diamond-type lattice may be considered to be composed of two interpenetrating f.c.c. sublattices, it is convenient to establish within the computer an array which consists of a large parallelepiped of discrete interacting atoms which belong to one of the two sublattices. It is necessary to select a suitable potential relationship for the interaction between the atoms. Ideally, this potential should involve both central and non-central force terms. We will discuss this point at length in the next section. For the present we shall assume that a suitable potential is available. In the present investigation we have used a parallelepiped containing 686 'atoms' and placed the point defect, in our case a vacancy, at the centre of this array of atoms. It is a good approximation to hold the atoms near the boundary of this assembly fixed. These atoms are sufficiently far from the point defect such that this constraint does not influence the configuration of the atoms near the vacancy. We checked this point in one case by using an assembly with over 2000 atoms and found no differences in the relaxed configuration.

The energy of the assembly of atoms in the perfect crystal was evaluated using the prescribed potential relation. A defect was then introduced into the system. In general, one may either remove an atom or atoms so as to create a vacancy or assembly of vacancies, or alternatively introduce extra atoms into interstitial positions. The computer program was developed to handle all these possibilities, although, we have only considered the single vacancy so far. The total energy of the system including the defect may now be re-evaluated. In most systems the removal or addition of an extra atom causes the atoms in the vicinity of the disturbance to experience a net force and so they move to minimize the total energy of the system again. By integrating the classical equations of motion for the complete set of interacting atoms the new atomic configuration around the vacancy may be found. It is possible to write

$$\ddot{x}_\alpha^i(t) = m^{-1} F_\alpha^i(\underset{\sim}{x}^i(t), \underset{\sim}{x}^j(t), \ldots \underset{\sim}{x}^n(t)) \qquad (5.3)$$

where $x_\alpha^i(t)$ (α=1,2,3) are the cartesian components of the position vector $\underset{\sim}{x}^i(t)$ for atom i, at time t, relative to a fixed laboratory system of axes. F_α^i is the net force on atom i in the direction $\underset{\sim}{x}_\alpha$ and depends upon the position of the other atoms j...n, at a particular time t, which are interacting with atom i. For a system with central forces only this equation reduces to a sum of component terms which are each a function of the distance between atom i and one of the other atoms. However, when non-central terms are included such a decomposition is not so readily available. We may also write

$$F_\alpha^i(t) = -\frac{\partial \Phi}{\partial x_\alpha^i(t)} \qquad (5.4)$$

where Φ is the expression for the total potential energy of the system with n interacting particles. Now, we use the method of discretization to solve the set of differential equations according to the following scheme

$$\dot{x}_\alpha^i(t) = (\Delta t)^{-1} \left\{ V_\alpha^i(t + \Delta t/2) - V_\alpha^i(t - \Delta t/2) \right\}$$

$$= m^{-1} F_\alpha^i(\underset{\sim}{x}^i(t), \underset{\sim}{x}^j(t), \ldots, \underset{\sim}{x}^n(t))$$

and

$$V_\alpha^i(t + \Delta t/2) = (\Delta t)^{-1} \left\{ x_\alpha^i(t + \Delta t) - x_\alpha^i(t) \right\} .$$

Thus from the configuration and velocity distribution after time t (the latter strictly after time $(t - \Delta t/2)$ the co-ordinates and velocity of each atom at a subsequent time are

$$V_\alpha^i(t + \Delta t/2) = V_\alpha^i(t - \Delta t/2) + \Delta t(m^{-1}) F_\alpha^i(\underset{\sim}{x}^i(t), \ldots, \underset{\sim}{x}^n(t)) \qquad (5.5)$$

$$x_\alpha^i(t + \Delta t) = x_\alpha^i(t) + \Delta t \, V_\alpha^i(t + \Delta t/2) \quad . \qquad (5.6)$$

While holding the atoms near the boundary fixed, each atom in the assembly is considered in turn and the force on it due to neighbouring atoms evaluated. From the difference equations (5.5) and (5.6) the mean velocity and hence new position of each atom after the current time step is determined. After the velocity and position of each atom is updated a norm proportional to the kinetic energy of the lattice

is evaluated and the process considered for the next time step. Using a suitable choice of time step the kinetic energy passes through a maximum value after a few complete iterations. At this point the atoms are brought to rest and the iterations restarted. This dynamic procedure ensures very rapid convergence to the absolute minimum in total potential energy. This method also has the advantage that metastable configurations can usually be avoided and the true stable configuration found.

In view of the success of Bullough and Perrin in applying this technique to defects in metals, it is a useful dynamic method for our purposes which will overcome many of the inadequacies of previous approaches and therefore forms the basis for the present investigation.

5.4 Potential Interaction between Atoms in the Diamond-Type Lattice

For the investigation for the configuration around defects in metals Bullough and Perrin used a non-equilibrium central-force potential to act between first and second neighbour atoms. This potential was also made to vanish, with zero slope, at a point mid-way between second and third neighbours. While this simple radial function proves to be an adequate description of the interactions for a crystal with metallic bonding it is clearly inadequate for valence crystals. Such crystals have strongly directional covalent bonding between nearest neighbour atoms with much weaker interactions between an atom and its second neighbours. It is unsatisfactory to suppose that the same radial potential function could be used to describe both these interactions. Also from dynamical

matrix theory Smith [73] has shown that to predict the second order elastic constants for diamond-type crystals it is necessary to include first neighbour non-central forces as well as the central forces. Hence, it was necessary to use a function which included non-central as well as central terms. Fortunately, a potential relation for diamond which has many of the desired characteristics has been determined recently by McMurry et al.[77].

These workers have expressed the potential energy of the diamond-type crystal in terms of valence co-ordinates which involve changes in bond lengths and bond angles. A useful discussion of this internal co-ordinates system may be found in a book by Wilson et al. [78]. A valence force potential expression was derived which yields calculated phonon dispersion relations in extremely good agreement with experimental data obtained by Warren et al. [79,81] for diamond. The elastic stiffness constants c_{11},c_{12} and c_{44} calculated from the slopes of the curves at the origin agreed very well with the data obtained by McSkimin and Bond [80] using an ultrasonic method. Also, the Raman frequency obtained by Robertson et al. [17] was used as a fitting parameter. The use of a potential expressed in terms of valence co-ordinates to describe the properties of a diamond crystal had previously been investigated by Musgrave and Pople [82].

The expression for the total deformation energy, Φ, in terms of the valence force co-ordinates may be expressed as follows for a system of n interacting particles

$$\Phi = \sum_{i=1}^{n} \Phi_i$$

where Φ_i is the potential energy contribution associated with each atom in the array. Now

$$\Phi_i = \tfrac{1}{2} F_r \sum_{j=1}^{4} (\Delta r_{ij})^2 + \sum_{j=1}^{3} \sum_{k=j+1}^{4} \Big[r_o^2 F_\theta (\Delta\theta_{jik})^2 + f_{rr} \Delta r_{ij} \Delta r_{ik} + r_o f_{r\theta} \left(\Delta r_{ij} \Delta\theta_{jik} + \Delta r_{ik} \Delta\theta_{jik} \right) \Big] \qquad (5.7)$$

where the terms represent contributions to the potential energy arising from the various spring constants. Typical quantities r_{ij}, θ_{jik} are defined in fig. 5.1. The force constants are defined as follows:

F_r is a bond stretching constant for nearest neighbour atoms i and j

F_θ is an angular rigidity constant for the angle θ_{jik}

f_{rr} is an interaction constant for a bond pair, such that j and k are nearest neighbours to i

$f_{r\theta}$ is an interaction constant for the bond ij which forms an arm of the angle θ_{jik}.

The equilibrium internuclear distance between nearest neighbour atoms is r_o.

In the expression for Φ_i we have neglected the terms containing $f_{\theta\theta}$ and $f_{\theta\theta^*}$, because in general the energy contribution from these terms will be small. To include such terms leads to a complicated expression for the force on each atom. It is important to note that this function effectively gives us the deformation potential energy,

since for the perfect crystal Φ is zero. Now, the force acting on the atom i in the x_α direction ($\alpha = 1,2,3$) at time t is as given in equation (5.4). We may also write this equation as

$$F_\alpha^i(t) = - \frac{\partial \sum_{i=1}^{n} \Phi_i}{\partial x_\alpha^i(t)} \quad . \tag{5.8}$$

It should be noted that terms other than Φ_i are functions of $x_\alpha^i(t)$. The expression for the force on a particular atom involves the knowledge of the derivatives of $\Delta r_{ij}, \Delta\theta_{jik}$ and $\Delta\theta_{iji}$ (see fig. 5.1 for definitions) with respect to $x_\alpha^i(t)$.

For the radial term we have

$$\frac{\partial\ \Delta r_{ij}}{\partial x_\alpha^i} = \frac{x_\alpha^i - x_\alpha^j}{r_{ij}} \tag{5.9}$$

where the terms are as defined previously. Note that we have abbreviated the symbol $x_\alpha^i(t)$ to x_α^i for convenience. Using directional cosines we may express $\cos\theta_{jik}$ as

$$\cos\theta_{jik} = \sum_{\alpha=1}^{3} \frac{(x_\alpha^j - x_\alpha^i)\ (x_\alpha^k - x_\alpha^i)}{r_{ij}\ r_{ik}} \quad . \tag{5.10}$$

Now

$$\cos\theta_{jik} = \cos(\theta_{jik}^o + \Delta\theta_{jik})$$

$$= \cos\theta_{jik}^o \cos\Delta\theta_{jik} - \sin\theta_{jik}^o \sin\Delta\theta_{jik} \quad .$$

For the perfect diamond-type lattice at equilibrium

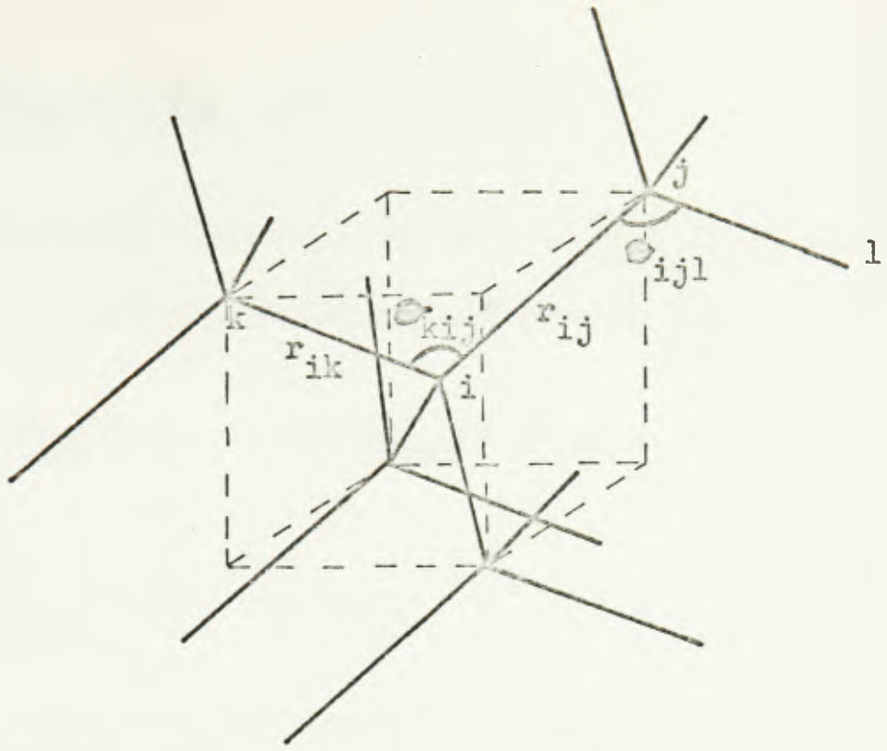


Fig.5.1 A section of the diamond-type lattice showing the terms for the valence-force coordinate potential.

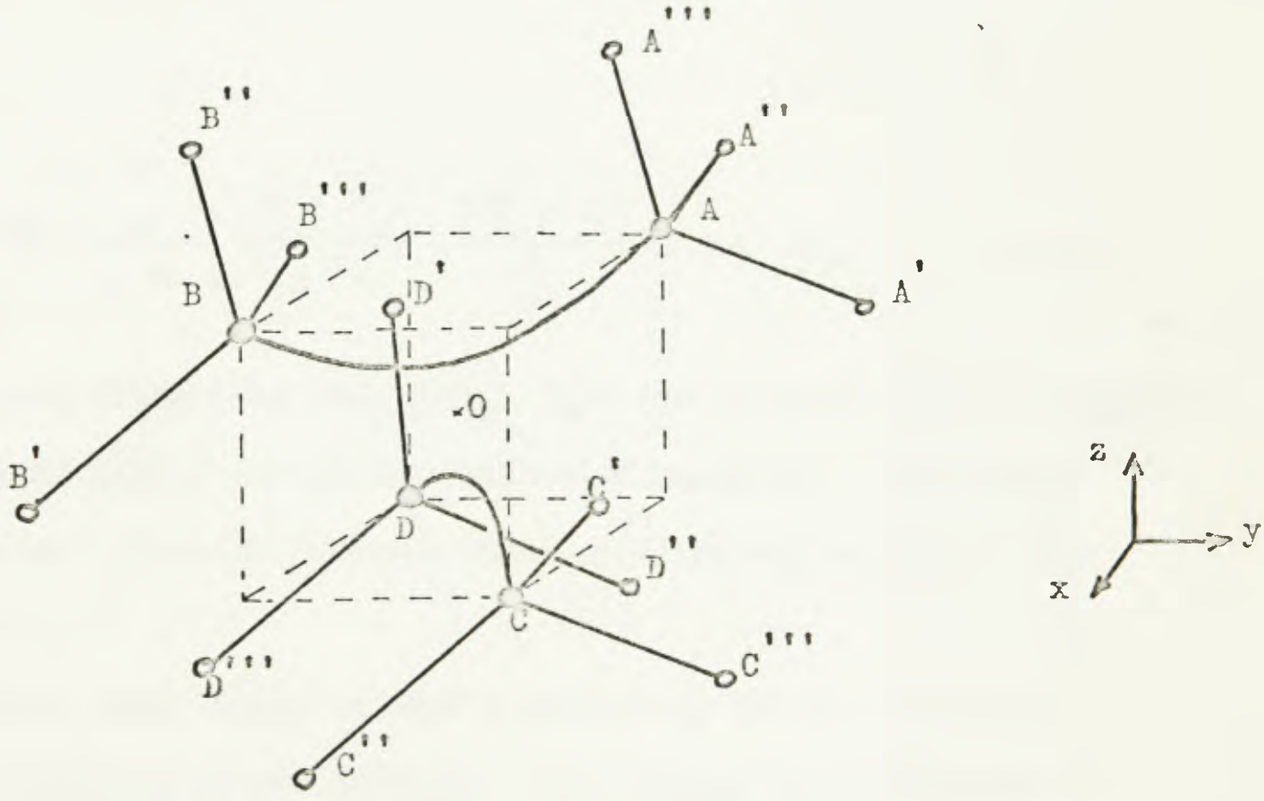


Fig.5.2 A single vacancy in the diamond-type lattice showing the rebonding scheme and the second neighbours to the vacancy.

$$\cos \theta^{o}_{jik} = -\frac{1}{3}, \quad \sin \theta^{o}_{jik} = 2\sqrt{2}/3 .$$

Now, the harmonic approximation assumes that $\Delta\theta_{jik}$ is small; therefore, neglecting anharmonic effects we may write

$$\cos \Delta\theta_{jik} \simeq 1, \qquad \sin \Delta\theta_{jik} \simeq \Delta\theta_{jik} .$$

Hence

$$\cos \theta_{jik} \sim -\frac{1}{3} - \frac{2\sqrt{2}}{3} \Delta\theta_{jik} . \tag{5.11}$$

By use of equations (5.10) and (5.11) we obtain

$$\frac{\partial \Delta\theta_{jik}}{\partial x^{i}_{\alpha}} = \frac{3}{2\sqrt{2}} \left\{ \left[\frac{(x^{i}_{\alpha} - x^{k}_{\alpha})}{r^{2}_{ik}} + \frac{(x^{i}_{\alpha} - x^{j}_{\alpha})}{r^{2}_{ij}} \right] \times \cos \theta_{jik} - \frac{(x^{i}_{\alpha} - x^{k}_{\alpha}) + (x^{i}_{\alpha} - x^{j}_{\alpha})}{r_{ij}\, r_{ik}} \right\} \tag{5.12}$$

and

$$\frac{\partial \Delta\theta_{ijl}}{\partial x^{i}_{\alpha}} = \frac{3}{2\sqrt{2}} \left[\frac{(x^{j}_{\alpha} - x^{l}_{\alpha})}{r_{ij}\, r_{jl}} - \frac{(x^{j}_{\alpha} - x^{i}_{\alpha})}{r^{2}_{ij}} \times \cos \theta_{ijl} \right] . \tag{5.13}$$

It is through terms like $\partial \Delta\theta_{ijl} / \partial x^{i}_{\alpha}$ that the force on atom i depends upon the position of its second nearest neighbours. Hence, this valence force potential function seems particularly useful for our purposes.

However, there still remains a difficulty in applying this potential function to our problem. The valence force function is essentially an equilibrium potential such that if we break a bond or remove an atom from the crystal no relaxation of the lattice

occurs. While at first sight this may seem surprising it is perhaps reasonable. In saturated hydrocarbons the average carbon-carbon single bond length is 1.537 ± 0.005 Å compared with 1.544 Å in the diamond crystal [83]. If we argue that the single bond in saturated hydrocarbons is fully relaxed, then the 'tension' in the C - C bond in diamond should be very small, since ΔR is 0.007 Å. Hence, it follows that the relaxation of surrounding atoms on breaking a bond should be small. This is, of course, a very simple-minded argument and ignores the effect of electron re-arrangement which may result in a change in the state of hybridisation of the atoms nearest the defect. However, the success of the valence-force function in predicting the physical properties of diamond suggests that it is a reasonable argument. Therefore, we may reason that any distortion of the lattice in the vicinity of the vacancy results from the rebonding of the vacancy electrons. As a consequence of this situation we must apply external forces between the four atoms nearest the defect which will correspond to the effect of rebonding of vacancy electrons. Unfortunately, this is not easy to accomplish in practice, because we have no direct knowledge of the magnitude of the rebonding forces or how they vary with distance. Reluctantly, we were forced to adopt an approach similar to that of previous workers and to assume that the atoms nearest the defect rebonded in pairs so as to give a tetragonal distortion to the vacancy. We assumed that the rebonding could be described by a Morse-type potential of the kind given in equation (5.1). Interactions between the two electron pairs were

neglected since it was not possible to give an estimate of this effect. The use of the Morse-potential is also inadequate, because bonding will not be along the line joining the atoms nearest the defect as this function assumes. It follows that the rebonding forces may be much weaker than suggested by this model.

The parameters α_1 and α_2 for the Morse-potential were determined for the diamond crystal from the compressibility, β, and the Grüneisen constant, γ. Fortunately, in diamond these quantities are essentially independent of temperature [36,84]; however, in silicon γ is strongly temperature dependent and cannot be used in the determination of the parameters. For the compressibility we have

$$\frac{1}{\beta} = -\frac{r_o}{3}\left(\frac{dp}{dr}\right)_o$$

$$= -\frac{2r_o}{9v}\left(\frac{d\phi}{dr}\right)_o + \frac{r_o^2}{9v}\left(\frac{d^2\phi}{dr^2}\right)_o \qquad (5.14)$$

where ϕ is the energy per cell and is equal to 4 U(r) where U(r) is the energy per bond, therefore using the form of the potential U(r) given in equation (5.1) we obtain for the diamond-type crystal

$$\frac{1}{\beta} = \frac{1}{3a} D\, \alpha_1 \alpha_2 \qquad (5.15)$$

where $a = \left(\frac{4r_o}{\sqrt{3}}\right)$ is the cell constant.

For the Grüneisen parameter, which is an anharmonic term, we have used the semi-empirical relation, known as the Dugdale-MacDonald relation [85], rather than the relation derived by Slater [86]. The former semi-empirical relation has been found by experience to give more reasonable agreement with experiment in many cases. We have

$$\gamma = -\frac{v}{2}\,\frac{\left(\frac{\partial^2(pv^{2/3})}{\partial^2 v}\right)_T}{\left(\frac{\partial(pv^{2/3})}{\partial v}\right)_T} - \frac{1}{3} \qquad (5.16)$$

$$= -\frac{1}{27\,v^{7/3}}\left[\frac{28v}{\beta} - 6r_o^2\left(\frac{\partial^2\phi}{\partial r^2}\right)_o + r_o^3\left(\frac{\partial^3\phi}{\partial r^3}\right)_o\right] .$$

For the generalised Morse function

$$\gamma = \frac{r_o}{6}(\alpha_1 + \alpha_2) . \qquad (5.17)$$

Using the Slater relationship one obtains the following expression for the Grüneisen parameter

$$\gamma = \frac{r_o}{6}(\alpha_1 + \alpha_2) + \frac{1}{3} . \qquad (5.18)$$

Hence from a knowledge of β, D and γ the parameters α_1 and α_2 may be calculated.

Using these parameters in the potential expression for the rebonding of the vacancy electrons and the valence-force potential function for the rest of the lattice in the program previously described, a dynamic relaxation leading to the configuration of minimum energy may be achieved for the isolated vacancy. In the next section we report the results for the diamond crystal while the displacement of atoms around a single vacancy in the silicon lattice is discussed in section 5.6.

5.5 Distortion around a Single Vacancy in the Diamond Crystal

The values of the valence force constants used in equation (5.7) are those obtained by McMurry et al.[77] and are listed below:

F_r = 3.890 millidyne/Å = 24.822 eV/Å^2

F_θ = 0.3582 " = 2.2360 "

f_{rr} = 0.1373 " = 0.8571 "

$f_{r\theta}$ = 0.2803 " = 1.7497 "

(1 millidyne/Å = 6.2422 eV/Å^2).

In order to calculate D, the bond dissociation energy, we have used equation (5.2). The heat of sublimation at room temperature, E_s, was taken as 7.22 eV/mole [54]. The promotion energy, E_p, of an electron from the s^2p^2 ground state of the isolated carbon atom to the sp^3 valence state of the atom, was estimated by Skinner and Pritchard [87] to be 8.14 eV on the basis of limited spectroscopic data. Lidiard (unpublished data) has calculated E_p for the carbon, silicon and germanium atom theoretically using

Hartree-Fock functions for the s and p orbitals on the isolated atom. He determined the energies of the single configuration states and then expressed the valence state energies in terms of these quantities. See, for example, Van Vleck [88] or Coulson [89] for a discussion of the valence state. The estimate of E_p for the carbon atom determined by Lidiard was 7.46 eV, which is in good agreement with the estimate of 7.545 eV deduced by Öpik (private communication to A.B. Lidiard) using the experimentally known energy values for the spectroscopic states as well as extrapolation from isoelectronic ions. There is no quantitative evidence available to support the hypothesis by Voge [90] that because of resonance with certain s^2p^2 configurations the promotion energy to the valence state will be lowered to near that for the ^5S spectroscopic state of the configuration $1s^2\ 2s^1\ 2p^3$. We cannot therefore agree with Bäuerlein [91] or Herman [92] that $E_p \simeq 4.16$ eV. In the present study we have used the value of E_p obtained by Lidiard. Using equation (5.2) we obtain a value of 7.34 eV for the bond dissociation energy, D, in the diamond crystal.

The Grüneisen parameter for diamond has been estimated by Berman and Thewlis [84] to be 1.3, while the bulk modulus $\left(= \frac{1}{\beta}\right)$ for diamond is quoted as 5.448×10^{12} dyne/cm^2 [36]. Substituting these values into equations (5.15) and (5.17) we obtain

$$a_1 = 3.720\ \text{Å}^{-1}, \qquad a_2 = 1.332\ \text{Å}^{-1}.$$

The ratio α_1/α_2 is 2.80 which is larger than that assumed in previous studies.

In table 5.1 we have given the co-ordinates of the nearest-neighbour and next-nearest neighbour atoms to the vacancy before and after rebonding. The vacancy is placed at the position (0,0,0) and we have bonded the atom A at $(\bar{1},1,1)$ with the atom B at $(1,\bar{1},1)$, while atom C$(1,1,\bar{1})$ is bonded with D$(\bar{1},\bar{1},\bar{1})$ as shown in fig. 5.2. These co-ordinates are in units of a/4, where a is the cell constant. At equilibrium the atoms A,B,C and D have been displaced 0.17Å from their perfect lattice sites, while the distances between these atoms are as follows:

$$A\,B = C\,D = 2.18\text{Å}$$

$$B\,C = B\,D = A\,C = A\,D = 2.33\text{Å}.$$

These distances should be compared with the undistorted crystal value of 2.52Å. The displacement of the second neighbour atoms to the vacancy A' ... D''' (also shown in fig. 5.2) depends upon their position relative to the atoms nearest the defect. Atoms A',B',C' and D' are displaced 0.08Å while the other second neighbour atoms are displaced 0.03Å. The maximum displacement of any third neighbour atom was 0.02Å. Fourth nearest neighbours are displaced approximately 0.01Å while the fifth neighbour atoms are displaced 0.01-0.04Å. The fact that some fifth neighbours to the vacancy are displaced more than third or fourth neighbour atoms is perhaps not surprising. Herman [74] has previously shown that

for the diamond-type lattice fifth neighbour interactions and above are more important in determining the vibrational spectrum than third or fourth neighbour interactions. This fact is manifest even more markedly in the silicon study reported in the next section.

The distance between the atoms nearest the defect is much greater than had been previously supposed by Swalin [54] or Scholz and Seeger [70]. That is, the displacement of the atoms A,B,C and D is much less. This is due to the inclusion of non-central force terms in the potential for the atoms surrounding the defect. As a consequence of this we expect the gain in energy from rebonding to be less than had been predicted in previous studies and the estimate of the formation energy to be higher.

As discussed in section 5.2 there are three main energy terms which contribute to E_f, the formation energy of a single vacancy in the crystal. The first is the energy required to remove an atom from its lattice site and place it on the surface. On average this energy is 2D. The second contribution is the energy gained from rebonding of the vacancy electrons in pairs within the defect. We denote this quantity E_B. The other main term is the increase in the energy of the rest of the lattice from distortion as a result of rebonding (denoted E_D). Therefore, we may write

$$E_f = 2D - E_B + E_D \qquad (5.19)$$

TABLE 5.1

Configuration of the atoms surrounding a single vacancy in the Diamond crystal

Atom	Before Rebonding	After Rebonding	Atom	Before Rebonding	After Rebonding
A	$(\bar{1},1,1)^*$	(-0.87,0.87,0.98)	B"	$(0,\bar{2},2)$	(-0.01,-1.97,2.00)
B	$(1,\bar{1},1)$	(0.87,-0.87,0.98)	B'''	(2,0,2)	(1.97,0.01,2.00)
C	$(1,1,\bar{1})$	(0.87,0.87,-0.98)	C'	(2,2,0)	(1.94,1.94,-0.02)
D	$(\bar{1},\bar{1},\bar{1})$	(-0.86,-0.86,-0.98)	C"	$(2,0,\bar{2})$	(1.97,-0.01,-2.00)
A'	$(\bar{2},2,0)$	(-1.94,1.94,0.02)	C'''	$(0,2,\bar{2})$	(-0.01,1.97,-2.00)
A"	(0,2,2)	(0.01,1.97,2.00)	D'	$(\bar{2},\bar{2},0)$	(-1.94,-1.94,-0.02)
A'''	$(\bar{2},0,2)$	(-1.97,-0.01,2.00)	D"	$(\bar{2},0,\bar{2})$	(-1.97,0.02,-2.00)
B'	$(2,\bar{2},0)$	(1.94,-1.94,0.02)	D'''	$(0,\bar{2},\bar{2})$	(0.02,-1.97,-2.00)

*In units of a/4

At the new energy minimum for the crystal containing a single vacancy we find that E_B = 9.02 eV and E_D = 1.96 eV. Hence,

$$E_f = 7.62 \text{ eV} .$$

This value is higher than the previous estimates by Swalin (E_f = 4.16 eV) or Scholz and Seeger (E_f = 5.79 eV). However, each of these workers used only central force terms and a value of D which was 3.73 eV lower than that used in this work.

5.6 Distortion around the Single Vacancy in the Silicon Crystal

Recently Solbrig (private communication from H.L. McMurry) has obtained a preliminary set of valence force constants for silicon using the valence force model proposed by McMurry et al. The fit to the phonon dispersion curves obtained by Dolling [93] and Palevsky et al. [94] is not as good as for diamond, but is still impressive and sufficiently accurate for our purposes. We have again assumed that there is no relaxation of the atoms surrounding the vacancy on removal of an atom; hence, all distortion results from rebonding of vacancy electrons. In crystalline silicon the Si-Si bond length is 2.35Å compared with 2.32 ± 0.02Å in such compounds as Si_2H_6 and Si_2Cl_6 [83]. It follows, therefore, that this assumption will provide a less accurate description than for the diamond crystal. The values for the valence force constants are as follows:

F_r = 1.485 millidyne/Å = 9.2697 eV/Å^2

F_θ = 0.02944 " = 0.1838 "

f_{rr} = 0.02697 " = 0.1684 "

$f_{r\theta}$ = 0.03997 " = 0.2495 "

Lidiard (private communication) determined theoretically the value of the tetrahedral valence state energy above the ground state in the silicon atom to be 6.063 eV. This compares favourably with the extrapolated value of 6.22 eV obtained by Skinner and Pritchard [87]. The crude estimate of 7.2 eV for E_p determined by Slater [95] is believed to be too high. Seeger and Swanson [55] have used this latter estimate. We have chosen the value 6.063 eV for E_p and 3.66 eV for E_s. It follows from eqn.(5.2) that the bond dissociation energy for silicon is 4.86 eV.

In the determination of the parameters α_1 and α_2 it was not possible to use both the values for the compressibility and the Grüneisen constant, because the latter shows a very strong temperature dependence. Equations (5.15) and (5.17) are derived by assuming that these quantities are independent of temperature. The room temperature value for γ of 0.45 is near the estimated value of 0.43 at 0°K; however, at intermediate temperatures γ passes through a minimum and is actually negative at temperatures near 30°K. [96]. This temperature dependence may be traced to the behaviour of the transverse acoustic modes. A similar situation has been observed in germanium [97]. We believe that

eqn.(5.17) is inadequate for silicon and so we have assumed that $\alpha_1 = 2\alpha_2$ and then used eqn.(5.15) with the value of 9.793×10^{11} dyne/cm^2 for the bulk modulus [98]. The parameters for the Morse potential function in silicon are given below:

$$D = 4.86 \text{ eV}, \quad \alpha_1 = 2.02 \text{Å}^{-1} .$$

This set of parameters is designated <u>case 1</u>. We have for comparison also used the Seeger and Swanson parameters, namely

$$D = 5.9 \text{ eV}, \quad \alpha_1 = 1.728 \text{Å}^{-1}, \quad \alpha_2 = 0.984 \text{ Å}^{-1} .$$

This combination of parameters is denoted <u>case 2</u>.

The configuration of the 1st and 2nd neighbour atoms surrounding the vacancy before and after rebonding for both sets of data are shown in table 5.2. For silicon, the final configuration is not as symmetrical as the the diamond crystal. This is because the relaxation is not quite complete. The presence of the vacancy in silicon causes much greater deformation of the lattice than for diamond, especially for 5th and 6th neighbour atoms. However, the differences from the equilibrium configuration are probably very small. There are only slight differences in the predicted equilibrium positions of the first and second neighbours to the defect in the two cases for the relaxed configuration despite the differences in parameters.

TABLE 5.2

Configuration of the atoms surrounding a single vacancy in the silicon crystal

Atom	Before Rebonding	After Rebonding case 1 $a_1 = 2a_2$	After Rebonding case 2 Seeger and Swanson Parameters
A	$(\bar{1},1,1)^*$	(-0.71,0.71,0.94)	(-0.70,0.70,0.94)
B	$(1,\bar{1},1)$	(0.71,-0.71,0.94)	(0.70,-0.70,0.94)
C	$(1,1,\bar{1})$	(0.71,0.71,-0.94)	(0.71,0.71,-0.94)
D	$(\bar{1},\bar{1},\bar{1})$	(-0.69,-0.69,-0.93)	(-0.69,-0.69,-0.93)
A'	$(\bar{2},2,0)$	(-1.83,1.83,0.11)	(-1.82,1.83,0.12)
A''	(0,2,2)	(0.00,1.93,1.97)	(0.00,1.93,1.96)
A'''	$(\bar{2},0,2)$	(-1.93,0.00,1.97)	(-1.93,0.00,1.97)
B'	$(2,\bar{2},0)$	(1.83,-1.83,0.11)	(1.83,-1.82,0.12)
B''	$(0,\bar{2},2)$	(0,00,-1.93,1.97)	(0.00,-1.93,1.97)
B'''	(2,0,2)	(1.93,0.00,1.97)	(1.93,0.00,1.96)
C'	(2,2,0)	(1.83,1.83,-0.11)	(1.83,1.83,-0.12)
C''	$(2,0,\bar{2})$	(1.94,0.00,-1.97)	(1.94,0.00,-1.96)
C'''	$(0,2,\bar{2})$	(0.00,1.93,-1.97)	(0.00,1.94,-1.96)
D'	$(\bar{2},\bar{2},0)$	(-1.81,-1.81,-0.09)	(-1.80,-1.80,-0.09)
D''	$(\bar{2},0,\bar{2})$	(-1.92,0.02,-1.95)	(-1.92,0.02,-1.95)
D'''	$(0,\bar{2},\bar{2})$	(0.02,-1.92,-1.95)	(0.02,-1.92,-1.95)

*In units of a/4

For case 1 ($a_1 = 2a_2$) with bonding between atoms A and B and between atoms C and D, these atoms have been displaced approximately 0.56Å from their lattice sites in the perfect crystal. The distances between the atoms are as follows:

$$A\,B = C\,D = 2.7\text{Å}$$

$$A\,C = B\,C = A\,D = B\,D = 3.2\text{Å}$$

These distances should be compared with the undistorted distance of 3.84Å. The second neighbour atoms, A',B',C' and D' are displaced on average 0.36Å while the remaining second neighbours are displaced 0.11Å from their positions in the perfect crystal. Displacements of third neighbours are in the range 0.04–0.11Å and those for fourth neighbours 0.02–0.05Å depending upon their position in the crystal relative to the atoms nearest the defect. A somewhat greater displacement of 0.06–0.16Å is experienced by fifth neighbours. This increased displacement compared with third and fourth neighbours is consistent with the diamond results and the previous work by Herman [74].

The results for case 2 using Seeger and Swanson parameters closely parallel these findings and are summarised below.

Neighbour to Vacancy	Displacement
1st	0.58Å
2nd	0.11 - 0.38Å
3rd	0.05 - 0.11Å
4th	0.02 - 0.05Å
5th	0.07 - 0.17Å

also

$$A\,B = C\,D = 2.7\text{Å}$$

$$A\,C = A\,D = B\,C = B\,D = 3.2\text{Å}$$

As in the previous section the formation energy is determined from eqn.(19). The results for the two cases are summarised in table 5.3. For the convenience of the discussion to follow, we have also given the values obtained by Seeger and Swanson [55]. All these results are discussed in the next section.

TABLE 5.3

Values of terms contributing to the formation energy of an isolated vacancy in Silicon

Term	Case 1 $a_1 = 2a_2$	Case 2 Seeger and Swanson Parameters	Seeger and Swanson study
D(eV)	4.86	5.9	5.9
E_B(eV)	8.86	10.90	11.25
E_D(eV)	2.80	2.82	1.80
E_f(eV)	3.66	3.72	2.35

5.7 Discussion of Results and Relation to Experiment

The results which we have obtained are based on the assumption that the vacancy electrons rebond in pairs so that a tetragonal distortion of the defect results. We have neglected any interaction between the pairs of electrons and assumed that the energy of re-bonding and hence the forces between the atoms may be represented by

a Morse-type potential function. It is possible that such a representation will cause a more extreme distortion than in the actual crystal, because rebonding will not be directly along the line joining the two atoms as is assumed in this model and electron-electron interactions should be important. However, using such a model the results show that the disturbance of the surrounding lattice due to the tetragonal distortion is very much greater for the silicon crystal than for diamond. What is also apparent, especially for silicon, is the non-local character of the deformation which causes significant displacement of atoms which are 5th neighbours to the vacancy. A model which endeavours to predict the electronic structure of the single vacancy such as that described in chapter 2 may have severe limitations when applied to a single vacancy in silicon. In the diamond crystal all displacements beyond first neighbours are less than 0.1Å, so the defect molecule model seems more realistic. The displacement of the atoms neighbouring the defect are fairly large and some correction should be made in the electronic calculation to incorporate this effect.

There are no previous theoretical studies on the isolated vacancy in diamond with which the present findings may be usefully compared. Also because the isolated vacancy in diamond has not yet been positively identified, there are no experimental estimates available for its formation energy. The value obtained in the present study (7.62 eV) is much larger than previous estimates, [54,70]. However, in the earlier estimates a much smaller value for D was

chosen. Until definite experimental results are available the uncertainities will remain.

It is interesting to compare the present findings for the silicon vacancy with previous results. This analysis suggests that the restricted relaxation model used by Seeger and Swanson is inadequate if one is interested in the configuration of the atoms surrounding the defect. These workers found that at equilibrium the distance between atoms A and B was 2.6$\mathring{A}$, which is only slightly less than in the present work. However, the results differ significantly for the displacement of second neighbours which is hardly surprising. No other study on the single vacancy has tried to realistically estimate the extent of distortion.

The present estimate of the formation energy is higher than those obtained in previous studies [54,55,70]. The two factors which contribute to this are firstly the higher estimate of D, except for ref.[55], and secondly the larger value for E_D the distortion energy, coupled with a lower value for E_B. The higher distortion energy results because of the choice of a valence force potential for the rest of the lattice. This function contains non-central force terms which cause the lattice to be more rigid against displacements which change the bond angles. This point is demonstrated clearly by comparing the two values for E_f in table 5.3 obtained using the Seeger and Swanson parameters for re-bonding with and without non-central forces for the rest of the lattice. The calculations also show that the use of parameters derived from the compressibility alone give good agreement with the

generalised Morse-potential relation. There is still some confusion as to the experimental value for the formation energy of the isolated vacancy in silicon. Several studies on intrinsic material using radiotracer investigations suggest that the self-diffusion energy is in the range 4.7 to 5.2 eV (99-102). However, Watkins [48] using impurity diffusion measurements has deduced that the self-diffusion energy in silicon is probably 'around 3.5-4.0 eV'. He also estimates that the migration energy for the single vacancy is 0.33 eV, although earlier studies favoured higher values. The present estimate of E_f is in good agreement with the result obtained by Watkins. It is interesting to note that even though there is 1 eV difference between the estimates of D used in case 1 and case 2 the two estimates of E_f differ by only 0.06 eV. This is partly compensated for by the different values of α_1 and α_2 in the two cases, but there is a rough independence of E_f on the value of D. This was noted also in a previous study [55].

5.8 Summary and Conclusion

The distortion around a single vacancy in a diamond-type crystal has been investigated using a dynamic relaxation method based upon the equations of motion. The interactions between the atoms of the crystal are approximated by use of a valence force potential, while the rebonding of the vacancy electrons is assumed to be in pairs which may be described by a Morse-type potential function. The re-bonding causes the vacancy to undergo a tetragonal distortion. Examination of displacements to fifth neighbours from the defect reveal that the deformation of the lattice is much more significant

for silicon than for diamond. The neglect of distortion in the defect molecule approximation for electronic calculations is thought to be less serious in the diamond lattice than for silicon. The formation energies of the single vacancy have also been determined in this study.

CHAPTER 6

INVESTIGATION OF THE JAHN-TELLER EFFECTS AND THE SYMMETRIC TERM FOR THE ELECTRONIC LEVELS OF THE SINGLE VACANCY IN DIAMOND

The theory of the static Jahn-Teller effect is developed and applied to the lowest electronic levels of the single isolated vacancy in its various charge states. The extent of symmetric relaxation associated with the lowest levels is also estimated. The results suggest that the GR1 band in irradiated diamonds is unlikely to be associated with the neutral charge state of the vacancy.

6.1 Introduction

In chapter 3 we found that for the various charge states of the single vacancy the ground and low-lying excited electronic levels were in some cases orbitally degenerate. Jahn and Teller [103] have shown that with the exception of linear molecules a geometrical configuration in which the electronic state is orbitally degenerate cannot be the stable state of the system. Jahn [104] has shown that the theorem is also applicable to spin degeneracy with the exception of systems which contain an odd number of electrons and have a special twofold degeneracy known as Kramers degeneracy [105], which cannot be removed by changes in the electrostatic environment. With these two exceptions the electronic degeneracy is removed because there is a nuclear configuration of lower symmetry in which the system has a lower energy. It is the removal of orbital degeneracy which is the more important of the two effects. In general, the additional instability caused by spin

degeneracy is very small and is usually neglected. Van Vleck [106] was the first to develop a quantitative basis for the Jahn-Teller effect as applied to the degenerate states of the octahedral group. Öpik and Pryce [107] have developed the theory further, mainly for the octahedral case, but they have also considered cases for which spin-orbital coupling is important. The minimization of the total electronic energy of the system with respect to the distortions of the nuclear framework is known as the static Jahn-Teller effect. However, there are always at least two geometrically equivalent configurations of the nuclear framework for which the electronic state has its degeneracy lifted such that the system will resonate between them. A discussion of this effect, known as the dynamical Jahn-Teller effect, has been given by Longuet-Higgins et al.[108].

Lannoo [109] has applied the theory of the static Jahn-Teller effect to the various charge states of the vacancy in diamond and examined the distortion of some of the low-lying degenerate electronic states. This calculation was based upon a perturbation theory approach to the problem. Lidiard and Stoneham [110] have suggested that the model proposed is inadequate, because of its failure to move the atomic orbitals which make up the l.c.a.o. function with the nucleus and core electrons of the atoms involved. Failure to move these atomic orbitals leads to large changes in the one centre part of the expectation value of the potential energy, whereas, a 'rigid atom model' which moves the atomic orbitals with the nucleus and core electrons would predict that there was no

change in this term to a first approximation. Lannoo et al. [14] have repeated the calculation using the rigid atom model. However, we believe that there are still some serious limitations inherent in the calculation if one is concerned with predicting the lowest electronic levels for the various charge states of the single vacancy. These workers have assumed that the variation of the overlap integral with internuclear distance may be neglected (Lannoo private communication) and that the overlap term in the normalisation constant for the single electron molecular orbital wave functions may also be neglected. It is also assumed that the eigenvectors for the configurations contributing to an electronic level of a particular symmetry may be obtained from a calculation using the unmodified a.s.m.o. theory [109]. We believe that these assumptions are not justified and therefore reduce the validity of the calculation.

The energies of all electronic levels will be dependent upon the extent of coupling with the symmetric mode, Qa. This symmetric term has not been adequately investigated. Lannoo et al. [14] have shown that the lowering in energy due to the symmetric mode is large relative to the Jahn-Teller distortion energies. It has tacitly been assumed by previous workers that the contribution of the symmetric term to all the lowest levels within a particular charge state of a vacancy will be constant. However, this has not been quantitatively demonstrated. In this chapter we re-examine the Jahn-Teller effect and also the effect of a

symmetric distortion on the lowest electronic levels of the single vacancy in its various charge states. Section 6.2 discusses the theory of the static Jahn-Teller effect as it has been applied to the single vacancy in diamond. The determination of the effective frequencies of the lattice for the various modes is outlined in section 6.3, while in section 6.4 the results of the Jahn-Teller calculation are presented. In the following section these are discussed and related to previous calculations. The influence of the symmetric term on the energy levels is discussed in section 6.6 and the relationship of all the results to experiment is given in the final section.

6.2 The Static Jahn-Teller Effect for the Vacancy in Diamond

In the model to be discussed we have neglected spin and spin-orbit coupling effects entirely. Also it has been assumed that the electronic levels are sufficiently separated from one another such that interlevel coupling effects may be ignored. These effects have been recently discussed in general terms [111]. All dynamical effects have been neglected even though some experimental stress splitting data [111,112] suggests that such effects may be important, especially at higher temperatures. We again assume that only the nearest neighbours to the vacancy contribute to its interaction with the lattice distortions.

Since there are four nearest neighbours to the vacancy, A,B,C and D, with cartesian coordinates $(\bar{1},1,1)$, $(1,\bar{1},1)$, $(1,1,\bar{1})$ and $(\bar{1},\bar{1},\bar{1})$ in the undistorted crystal, displacements of these atoms may be

described in terms of 12 normal co-ordinates which may easily be obtained using group theoretical methods (see, for example, ref. 113). Three of the co-ordinates represent translations of T_2 symmetry and three rotations of T_1 symmetry which are of no interest to us in the present problem. The remaining six vibrational normal co-ordinates are given in Appendix C.1 in terms of the small displacements $X_\alpha, Y_\alpha, Z_\alpha$ (α = A,B,C,D) of the atoms. These co-ordinates are also given in ref.[15] and their significance is shown in fig. 4 of ref.[14]. We have followed the lead of Lannoo and Stoneham [15] and used the fairly standard notation of Griffiths [114] rather than that used by previous workers. The Q_a mode is the 'breathing' or symmetrical mode of symmetry A_1. The normal co-ordinates Q_ε and Q_θ are E modes while the Q_ξ, Q_η and Q_ζ modes belong to the T_2 representation of the T_d group.

Now, for a given degenerate electronic state the energy of a particular vibronic level $E(q,Q)$ may be expressed as

$$E(q,Q) = \frac{\langle \Psi | \mathcal{H} | \Psi \rangle}{\langle \Psi | \Psi \rangle} \qquad (6.1)$$

where Ψ is the vibronic wave-function and $\mathcal{H}$ the vibronic Hamiltonian for the system. Q represents a set of normal co-ordinates describing distortions of the vacancy environment while q represents the defect electron co-ordinates. The Hamiltonian for the system may be written as:

$$\mathcal{H} = H_{elec.}(q,Q) + H_{nucl.}(Q) \qquad (6.2)$$

where $H_{elec.}$ is the electronic Hamiltonian. If we choose the minimum value of the nuclear potential energy, i.e. when the nuclei are in their perfect lattice sites, to be the zero of the nuclear potential energy scale, then within the harmonic approximation we may write for $H_{nucl.}$, the nuclear Hamiltonian

$$H_{nucl.} = -\frac{\hbar^2}{2M} \sum_{\alpha} \frac{\partial^2}{\partial Q_\alpha^2} + \frac{1}{2} M \sum_{\alpha} \omega_\alpha^2 Q_\alpha^2 \qquad (6.3)$$

where the first term is the kinetic energy of the nuclei and the second is known as the quasi-elastic potential energy. This latter term represents the change in potential energy of the system when the nuclei are displaced from their equilibrium position in the perfect lattice, in such a way that a finite vibration corresponding to the normal co-ordinate Q_α results. M is the mass of the carbon atom and ω_α is the effective or response frequency of the lattice for the α mode. Strictly speaking we should use a distribution of frequencies instead of a few discrete frequencies. This is an important limitation on our formulation of the problem.

In general for a degenerate level it is not possible to use the method of Born and Oppenheimer and apply the adiabatic approximation to factorize the vibronic wave-function. For an electronic level of degeneracy d in a system with N normal

co-ordinates the vibronic functions $\Psi(q,Q)$ are usually well described by dN terms each of the form $\chi(Q)\ \phi(q,Q)$ where $\chi(Q)$ is the vibrational part and $\phi(q,Q)$ the electronic part of the wave-function. However, near the minimum energy configurations we may use an approximate form of the adiabatic approximation such that the vibronic wave-function is separable into an electronic and vibrational part [15]. Now, for the electronic part, $\phi'(q,Q)$, we can write

$$\phi'(q,Q) = \sum_{i=1}^{d} a_i \psi_i \qquad (6.4)$$

where ψ_i are the electronic wave-functions for the states comprising the degenerate level for zero distortions. The linear terms in the distortion Q_a of the Hamiltonian for the Jahn-Teller effect involve matrix elements of the form

$$\langle \psi_i | H_{elec.} | \psi_j \rangle \ .$$

Using the rigid atom model proposed by Lidiard and Stoneham [110] and developed by Lannoo et al.[14] it is assumed that the atomic orbitals on the atoms nearest to the vacancy follow the atomic displacements rigidly. Therefore, a hybrid orbital 'a^o' on the atom nearest the defect in its perfect lattice site will be transformed to an equivalent orbital 'a' centred on the new position of the atom. For small displacements of the nuclei we may expand the orbitals on the atom and the electronic Hamiltonian for the system in terms of a Taylor series in the normal

co-ordinates. To first order we may write

$$a = a^0 + \sum_\alpha \left(\frac{\partial a}{\partial Q_\alpha}\right)_0 Q_\alpha \qquad (6.5)$$

and

$$H_{elec.} = H^0_{elec.} + \sum_\alpha \left(\frac{\partial H_{elec.}}{\partial Q_\alpha}\right)_0 Q_\alpha \,. \qquad (6.6)$$

Therefore

$$\psi_i = \psi_i^0 + \sum_\alpha \left(\frac{\partial \psi_i}{\partial Q_\alpha}\right)_0 Q_\alpha \,. \qquad (6.7)$$

By substituting for ψ_i and $H_{elec.}$ in $\langle\psi_i|H_{elec.}|\psi_j\rangle$ from eqns. (6.6) and (6.7) and retaining only first order terms in Q_α we obtain the expression

$$\langle\psi_i|H_{elec.}|\psi_j\rangle = \langle\psi_i^0|H^0_{elec.}|\psi_j^0\rangle + \sum_\alpha \left(\frac{\partial}{\partial Q_\alpha}\langle\psi_i|H_{elec.}|\psi_j\rangle\right)_0 Q_\alpha \,. \qquad (6.8)$$

The first term in the present problem is diagonal and gives the electronic energy for zero Q_α. The nuclear term in eqn.(6.3) is not subject to a Jahn-Teller effect, hence it is also diagonal. We now solve the secular equation whose elements are given by the terms linear in Q_α in eqn.(6.8). The form of the matrix may be determined using group theoretical techniques [114]. This

yields eigenvalues which correspond to a new electronic energy $E_n(Q_\alpha)$ for each particular level. These energies are a function of the normal co-ordinates of the system. By minimizing the total energy of the system (electronic + nuclear) with respect to the various normal co-ordinates and solving the resulting set of simultaneous equations the new equilibrium configurations of the previously degenerate levels may be determined.

For the octahedral group, and in particular the single vacancy, we have to consider the two- and three-fold degenerate levels of the system. Non-degenerate levels cannot give rise to distortion modes. However, it is possible that all levels may be lowered in energy, without distortion, because of interaction with the symmetric mode Q_a. In our calculations to first order, there is no coupling between the various modes since all terms of the form $Q_\alpha Q_\beta$ give second order contributions and are therefore ignored. At this stage therefore we may ignore the symmetric contribution and just consider the distortion modes, but we will return to the symmetric term in section 6.6.

The two-fold degenerate E level comprises two states $|\theta\rangle$ and $|\varepsilon\rangle$, which transform like $2x^2 - y^2 - z^2$ and $y^2 - z^2$ respectively and are degenerate in the undistorted environment with electronic energy E^o. It is easily shown group theoretically that the only possible distortion for E states will result from coupling with the E modes to give a tetragonal distortion. The Jahn-Teller equation for the E manifold may be written as

$$W = \left[E^0 + \sum_\alpha \left\{ -\frac{\hbar^2}{2M} \frac{\partial^2}{\partial Q_\alpha^2} + \frac{1}{2} M\omega_\alpha Q_\alpha^2 \right\} \right] \begin{pmatrix} 1 & 0 \\ 0 & 1 \end{pmatrix}$$

$$+ I_{EE}\, Q_\theta \begin{pmatrix} -1 & 0 \\ 0 & 1 \end{pmatrix} + I_{EE}\, Q_\varepsilon \begin{pmatrix} 0 & 1 \\ 1 & 0 \end{pmatrix} \qquad (6.9)$$

where the first term is as defined previously. The latter terms which depend on I_{EE} give rise to the Jahn-Teller effect. Within the rigid atom approximation

$$I_{EE} = \left(\frac{\partial}{\partial Q_\varepsilon} \langle \theta | H_{\text{elec.}} | \varepsilon \rangle \right)_0 . \qquad (6.10)$$

For discussion it is convenient to define polar co-ordinates ρ and ϕ in the space of the co-ordinates Q_ε and Q_θ

$$Q_\theta = \rho \cos\phi, \qquad Q_\varepsilon = \rho \sin\phi$$

then we have

$$E_n(\rho) = \text{const} \pm I_{EE}\, \rho + \tfrac{1}{2} M \omega_E^2 \rho^2 \qquad (6.11)$$

such that the minimum in the Jahn-Teller energy occurs at

$$\rho = |I_{EE}| \,/\, M\omega_E^2 \qquad (6.12)$$

and its value is $\Delta E_{EE} = -\dfrac{I_{EE}^2}{2M\,\omega_E^2}$ (6.13)

This value of ΔE_{EE} is independent of ϕ to first order. Hence the locus of minimum energy is a circle in the $(Q_\varepsilon, Q_\theta)$ plane such that there are an infinite number of distortions of lowest energy.

However, Öpik and Pryce [107] have shown that in the real physical system if the quasi-elastic term is modified to include third order terms, a term in cos 3ϕ appears in the minimum energy expression. Hence, there are three possible tetragonal distortions which will represent an energy minimum for the system. Corresponding to these minima the tetragonal configurations will have symmetry axes along the <100>, <010> and <001> directions. It is not possible, however, without an explicit calculation including the higher order terms to decide whether the system will be compressed or elongated along the tetragonal symmetry axis. One complete set of co-ordinates for the energy minima is

$$\begin{aligned} Q_\theta &= \rho & Q_\varepsilon &= 0 \\ Q_\theta &= -\tfrac{1}{2}\rho & Q_\varepsilon &= \frac{\sqrt{3}}{2}\rho \\ Q_\theta &= -\tfrac{1}{2}\rho & Q_\varepsilon &= -\frac{\sqrt{3}}{2}\rho \end{aligned} \qquad (6.14)$$

corresponding to $\phi = 0$, $\frac{2\pi}{3}$ and $\frac{4\pi}{3}$ respectively. There is also a similar set of configurations corresponding to $\phi = \frac{\pi}{3}$, π and $\frac{5\pi}{3}$.

For the threefold degenerate state the results are formally the same irrespective of whether we are considering the T_1 or the T_2 irreducible representation. When all the modes are zero, i.e. $Q_\alpha = 0$, the three electronic states $|\xi\rangle$, $|\eta\rangle$ and $|\zeta\rangle$ belonging to a T representation are degenerate. These states transform like x,y,z or yz,zx,xy. The vibronic Hamiltonian for such a level is more complicated than previously, because there are terms linear in $Q_\varepsilon, Q_\theta, Q_\xi, Q_\eta$ and Q_ζ. We may write the Jahn-Teller equation for

the T manifold as follows

$$W = \left[E^0 + \sum_\alpha \left\{ \frac{\hbar^2}{2M} \frac{\partial^2}{\partial Q_\alpha^2} + \frac{1}{2} M\omega_\alpha^2 Q_\alpha^2 \right\} \right] \begin{pmatrix} 1 & 0 & 0 \\ 0 & 1 & 0 \\ 0 & 0 & 1 \end{pmatrix}$$

$$+ \frac{I_{TE}}{6} \begin{pmatrix} 2Q_\theta & \cdot & \cdot \\ \cdot & -Q_\theta + \sqrt{3}\, Q_\varepsilon & \cdot \\ \cdot & \cdot & -Q_\theta - \sqrt{3} Q_\varepsilon \end{pmatrix} + I_{TT} \begin{pmatrix} \cdot & Q_\zeta & Q_\eta \\ Q_\zeta & \cdot & Q_\xi \\ Q_\eta & Q_\xi & \cdot \end{pmatrix} . \qquad (6.15)$$

The values of I_{TE} and I_{TT} may be written as

$$I_{TE} = \sqrt{3} \left[\frac{\partial}{\partial Q_\varepsilon} \left(\langle \eta | H_{elec.} | \eta \rangle - \langle \zeta | H_{elec.} | \zeta \rangle \right) \right]_0 \qquad (6.16)$$

$$I_{TT} = \left(\frac{\partial}{\partial Q_\xi} \langle \eta | H_{elec.} | \zeta \rangle \right)_0 \qquad (6.17)$$

from group theory [114]. The method of solution of the secular equation has been outlined by Öpik and Pryce [107]. No attempt was made to solve the equation generally, but only the stationary states for the energy were determined. There are stationary points of three types of symmetry: tetragonal, trigonal and one of a lower symmetry, termed intermediate, because the corresponding energy for this configuration lies between those of the trigonal and tetragonal stationary points. There is more than one stationary point for each of the three symmetry types. Lannoo [109] has repeated the calculation for the vacancy system and has confirmed the results of the previous workers. The configurations and energy lowering corresponding to the various stationary points are shown

in Table 6.1. There are four equivalent trigonal distortions with symmetry axes along the $\langle\bar{1},\bar{1},\bar{1}\rangle$, $\langle 1,1,\bar{1}\rangle$, $\langle 1,\bar{1},1\rangle$ and $\langle\bar{1},1,1\rangle$ directions and three of the tetragonal symmetry as previously discussed.

If the stable configuration is tetragonally distorted then the energy reduction is given by

$$\Delta E_{TE} = \frac{1}{9} \frac{I_{TE}^2}{2M\omega_E^2} \quad . \tag{6.18}$$

For a trigonal distortion the lowering ΔE_{TT} is

$$\Delta E_{TT} = \frac{4}{3} \frac{I_{TT}^2}{2M\omega_T^2} \quad . \tag{6.19}$$

Hence

$$\Delta E_{TE} > \Delta E_{TT} \quad \text{if} \quad \frac{I_{TE}^2}{\omega_E^2} > \frac{12\ I_{TT}^2}{\omega_T^2} \ .$$

The values of I_{TE} and I_{TT} may be determined from eqns.(6.16) and (6.17) respectively. However, before we can determine the energy lowerings for the electronic states, we must have reliable estimates of the effective frequencies ω_E and ω_T. The technique we have applied to determine these quantities is outlined in the next section. Using the expression given above for ΔE_{TE} and ΔE_{TT} and the values determined for I_{TE}, I_{TT}, ω_E and ω_T it is now possible to determine the magnitude of the Jahn-Teller effect for the threefold degenerate levels.

TABLE 6.1

Stationary points of the octahedral group for a T_1 or T_2 electronic state

Symmetry	Tetragonal			Intermediate						Trigonal			
$\begin{vmatrix} a_1 \\ a_2 \\ a_3 \end{vmatrix}$	$\begin{vmatrix} 0 \\ 0 \\ 1 \end{vmatrix}$	$\begin{vmatrix} 0 \\ 1 \\ 0 \end{vmatrix}$	$\begin{vmatrix} 1 \\ 0 \\ 0 \end{vmatrix}$	$\frac{1}{\sqrt{2}}\begin{vmatrix} 1 \\ 1 \\ 0 \end{vmatrix}$	$\frac{1}{\sqrt{2}}\begin{vmatrix} 1 \\ -1 \\ 0 \end{vmatrix}$	$\frac{1}{\sqrt{2}}\begin{vmatrix} 1 \\ 0 \\ 1 \end{vmatrix}$	$\frac{1}{\sqrt{2}}\begin{vmatrix} 1 \\ 0 \\ -1 \end{vmatrix}$	$\frac{1}{\sqrt{2}}\begin{vmatrix} 0 \\ 1 \\ 1 \end{vmatrix}$	$\frac{1}{\sqrt{2}}\begin{vmatrix} 0 \\ 1 \\ -1 \end{vmatrix}$	$\frac{1}{\sqrt{3}}\begin{vmatrix} 1 \\ 1 \\ 1 \end{vmatrix}$	$\frac{1}{\sqrt{3}}\begin{vmatrix} -1 \\ -1 \\ -1 \end{vmatrix}$	$\frac{1}{\sqrt{3}}\begin{vmatrix} 1 \\ 1 \\ -1 \end{vmatrix}$	$\frac{1}{\sqrt{3}}\begin{vmatrix} 1 \\ -1 \\ 1 \end{vmatrix}$	$\frac{1}{\sqrt{3}}\begin{vmatrix} -1 \\ 1 \\ 1 \end{vmatrix}$
Q_0	$2q_1^*$	$2q_1$	$-4q_1$	$-q_1$	$-q_1$	$-q_1$	$-q_1$	$+2q_1$	$+2q_1$	0	0	0	0
Q_ε	$2\sqrt{3}q$	$-2\sqrt{3}q_1$	0	$-\sqrt{3}q_1$	$-\sqrt{3}q_1$	$\sqrt{3}q_1$	$\sqrt{3}q_1$	0	0	0	0	0	0
Q_ξ	0	0	0	0	0	0	0	$-\frac{3}{2}q_3^*$	$\frac{3}{2}q_3$	q_3^*	q_3	q_3	$-q_3$
Q_η	0	0	0	0	0	$-\frac{3}{2}q_3$	$\frac{3}{2}q_3$	0	0	q_3	q_3	$-q_3$	q_3
Q_ζ	0	0	0	$-\frac{3}{2}q_3$	$\frac{3}{2}q_3$	0	0	0	0	q_3	$-q_3$	q_3	q_3
Energy lowering	$\frac{1}{9}\frac{I_{TE}^2}{2M\omega_E^2}$			$\frac{I_{EE}^2}{72M\omega_E^2} + \frac{I_{TT}^2}{2M\omega_T^2}$						$\frac{4}{3}\frac{I_{TT}^2}{2M\omega_T^2}$			

$$^*q_1 = \frac{I_{TE}}{12M\omega_E^2}, \qquad q_3 = \frac{2}{3}\frac{I_{TT}}{M\omega_T^2}$$

6.3 The Effective Frequencies for the Lattice

The elastic energy of the crystal associated with distortions of the environment of the vacancy was introduced through terms involving the effective frequencies ω_E and ω_T. The values given to these terms is critical, since along with the I terms they determine the magnitude of the Jahn-Teller distortions. One of the major assumptions of this whole approach is that a small number of discrete frequencies can be used to describe the response of the lattice to distortion, instead of a distribution of frequencies. Using a simple model in which only the four atoms nearest the defect are allowed to move Lidiard and Stoneham [110] have shown that

$$\omega_E = \sqrt{2}\ \omega_T \ . \qquad (6.20)$$

They have used a rather simplified approach, but it is at least qualitatively consistent with the assumption that only these nearest neighbours contribute to the electron-phonon interactions. Lannoo et al. [14] noted that the density of vibrational states in diamond is peaked near the Raman frequency, ω_R, and rather arbitrarily assumed that ω_E was equal to ω_R ($= 2.5 \times 10^{14}$ rad/sec). This in fact is an upper bound to the phonon energies in the perfect crystal. From the force constants used by Swalin [54], Lidiard and Stoneham deduced that $\omega_E = 2.24 \times 10^{14}$ rad/sec.

Dr. Stoneham has brought to the author's attention the possibility of using the dynamic relaxation program discussed in chapter 5 to determine the effective frequencies ω_E, ω_T and ω_a

independently of one another. It is possible to apply unit forces to each of the atoms nearest the vacancy in the discrete atom model such that the overall force has the same symmetry as the normal mode. Then using the valence force potential function for the rest of the interactions in the crystal all the atoms may be relaxed, as previously, until the new equilibrium position is reached. Hence, we may explicitly determine Q_α. By assuming that the energy change is just linearly dependent upon the applied force, F_α, we may write

$$E(Q_\alpha) = -F_\alpha Q_\alpha + \tfrac{1}{2}M\omega_\alpha^2 Q_\alpha^2 \quad . \qquad (6.21)$$

Now, at equilibrium

$$\frac{\partial E}{\partial Q_\alpha} = -F_\alpha + M\omega^2 Q_\alpha = 0 \ .$$

Hence

$$\omega_\alpha = \sqrt{\frac{F_\alpha}{MQ_\alpha}} \qquad (6.22)$$

where M is the atomic mass. Since we know F_α, the applied force, and we can determine Q_α from the displacements of the atoms A,B,C,D under the applied forces, then we can evaluate ω_α. This approach is, in spirit, similar to that used in the Kansaki method [115], however, here we have actually removed the vacancy atom from the system. In table 6.2 we have given the co-ordinates of the atoms A,B,C and D before and after relaxation for applied forces corresponding to the distortions of Q_ε, Q_ξ and Q_a symmetry. These co-ordinates

are in units of a/4, where a is the cell constant. The relaxation program also gives us the displacement of atoms further from the defect due to these applied forces. If we had actual estimates of the electronic forces applied to the atoms nearest the defect, it would be possible to determine the position of the atoms in the surrounding lattice. It is here that the I terms from the Jahn-Teller equation become important.

For the applied forces of appropriate symmetry we find that at equilibrium

$$Q_\varepsilon = 0.0555\text{Å}$$
$$Q_\xi = 0.07313\text{Å}$$
$$Q_a = 0.07721\text{Å}$$

such that

$$\omega_E = 2.41 \times 10^{14} \text{ rad/sec}$$
$$\omega_T = 2.10 \times 10^{14} \text{ rad/sec}$$

and

$$\omega_a = 2.07 \times 10^{14} \text{ rad/sec} .$$

The value of ω_E is very close to that used by previous workers [110,14]. However, ω_T is larger than previous estimates. From this work we have the ratio $\omega_E:\omega_T$ equal to 1.15 compared with 1.41 from the simple model. No other estimate of ω_a was available before this determination. Lannoo et al.[14] chose to use the value 2.5×10^{14} rad/sec. Using the effective frequencies given above it is now possible to determine the magnitude of the Jahn-Teller distortions.

TABLE 6.2

Position of the atoms adjacent to the vacancy after relaxation for applied forces of appropriate symmetry

Atom	Initial Configuration	Relaxed Configuration		
		E symmetry	T_ξ symmetry	A_1 symmetry
A	$(\bar{1},1,1)$	(-1.0,1.022,0.978)*	(-1.007,1.029,1.029)	(-1.025,1.025,1.025)
B	$(1,\bar{1},1)$	(1.0,-1.022,0.978)	(0.993,-0.972,0.972)	(1.025,-1.025,1.025)
C	$(1,1,\bar{1})$	(1.0,1.022,-0.978)	(0.993,0.973,-0.972)	(1.025,1.025,-1.025)
D	$(\bar{1},\bar{1},\bar{1})$	(-1.0,-1.022,-0.978)	(-1.008,-1.030,-1.030)	(-1.025,-1.025,-1.025)

*All co-ordinates in units of a/4

6.4 Magnitude of the Jahn-Teller effects for the Electronic Levels

In chapter 3 we determined the lowest electronic levels for the various charge states of the single vacancy. On the basis of those calculations we have determined the possible Jahn-Teller splittings for the following lowest degenerate levels.

$$
\begin{aligned}
V^{+} &: \quad {}^{2}T_{2} \\
V^{o} &: \quad {}^{1}E,\ {}^{3}T_{1},\ {}^{1}T_{2} \\
V^{-} &: \quad {}^{2}T_{1},\ {}^{2}T_{2},\ {}^{2}E \\
V^{=} &: \quad {}^{1}E,\ {}^{3}T_{1},\ {}^{1}T_{2}
\end{aligned}
$$

In the Jahn-Teller calculations for a two-fold degenerate level we must determine the value of I_{EE}, while for a three-fold degenerate level it is necessary to know the magnitude of I_{TE} and I_{TT}. These quantities have been defined in eqn.(6.10), (6.16) and (6.17) respectively. As an illustration of how they may be determined we proposed to discuss in detail the determination of I_{TE} and I_{TT} for the lowest ${}^{3}T_{1}$ level of the isolated neutral vacancy.

The degenerate electronic states in the undistorted vacancy which transform like y and z may be expressed as follows:

$$
\begin{aligned}
|y\rangle &= c_1(\bar{v}\bar{v}zx) + \frac{c_2}{\sqrt{2}}\left[(vz\bar{z}y) - (vx\bar{x}y)\right] + c_3(y\bar{y}zx) \\
|z\rangle &= c_1(\bar{v}\bar{v}xy) + \frac{c_2}{\sqrt{2}}\left[(vx\bar{x}z) - (vy\bar{y}z)\right] + c_3(z\bar{z}xy)
\end{aligned}
\qquad (6.23)
$$

where c_1, c_2 and c_3 are eigenvectors corresponding to the relative contribution of the ${}^{3}T_{1}$ levels from the $v^2t_2^2$, vt_2^3 and t_2^4 configurations to the lowest ${}^{3}T_{1}$ level. Similar expressions

for all the other degenerate levels may be deduced from the determinantal wave-functions given in Appendix A.1. We are following the customary convention of using $|x\rangle$, $|y\rangle$ and $|z\rangle$ for the states belonging to the T_1 irreducible representation and $|\xi\rangle$, $|\eta\rangle$ and $|\zeta\rangle$ for the states of the T_2 representation.

Using the results from chapter 3 we have four possible sets of values for c_1,c_2 and c_3. These arise from the approximations case 1 and case 2 using single Slater functions for the 2s and 2p orbitals, and for similar cases using Clementi functions as the basis functions. The expressions for $|y\rangle$ and $|z\rangle$ may be substituted into eqn.(6.16) and (6.17) and then expanded such that I_{TE} and I_{TT} are reduced to a sum of derivatives of one and two electron molecular integrals. Hence

$$I_{TE} = -2\sqrt{3}\Big[\,DYHY(A-F) + 2A \times DVVYY + DVYVY\,(-A-2C-0.5D) + DXXYY(A-D-F) - DXYXY(A+0.5D) - \sqrt{2}\,DVYXZ(B-E) + DYYYY(0.5D-F)\Big] \qquad (6.24)$$

where

$$DYHY = \left(\frac{\partial}{\partial Q_\varepsilon}\langle y|H^0_{elec.}|y\rangle\right)_0$$

$$DVVYY = \left(\frac{\partial}{\partial Q_\varepsilon}\langle vy|\frac{1}{r_{12}}|vy\rangle\right)_0$$

and so on. Also

$A = c_1^2$, $B = c_1c_2$, $C = c_1c_3$, $D = c_2^2$, $E = c_2c_3$ and $F = c_3^2$

$$I_{TT} = DYHZ(-A+F)-2A \times DVVYZ + DVYVZ(A+0.5D+2C) + DXZXY(A-0.5D) + DXXYZ(-A-D+F) + \sqrt{2}\, DVHX(B+E) + DYYYZ(2F+D) - \sqrt{2}\, DVYXY(B+E) + 2\, DVXYY(B+3E) + \sqrt{2}\, B(DVVVX + DVXXX) \tag{6.25}$$

where A....F are as defined previously. Now we have

$$DYHZ = \left(\frac{\partial}{\partial Q_\xi} \langle y|H^o_{elec.}|z\rangle\right)_o$$

$$DVVYZ = \left(\frac{\partial}{\partial Q_\xi} \langle vy|\frac{1}{r_{12}}|vz\rangle\right)_o$$

and similarly for the other terms. The appropriate expressions for the other electronic levels of the vacancy in its various charge states are given in the Appendix C.2.

Now, we may write

$$\frac{\partial}{\partial Q_\alpha} = \sum_k \left(\frac{\partial}{\partial X_k}\frac{\partial X_k}{\partial Q_\alpha} + \frac{\partial}{\partial Y_k}\frac{\partial Y_k}{\partial Q_\alpha} + \frac{\partial}{\partial Z_k}\frac{\partial Z_k}{\partial Q_\alpha}\right) \tag{6.26}$$

where k = A,B,C,D and because of the unitary character of the transformation from the small cartesian displacements X_k, Y_k, Z_k to the normal co-ordinates we have

$$\frac{\partial X_k}{\partial Q_\alpha} = \frac{\partial Q_\alpha}{\partial X_k} \quad . \tag{6.27}$$

If we denote by R^o_{uv} the distance between atoms u and v in their perfect lattice position, then

$$R^{o}_{uv} = \left[(X^{o}_{v}-X^{o}_{u})^2 + (Y^{o}_{v}-Y^{o}_{u})^2 + (Z^{o}_{v}-Z^{o}_{u})^2 \right]^{\frac{1}{2}} \qquad (6.28)$$

$$= R \ .$$

Substituting the appropriate form for the normal co-ordinate given in Appendix C.1 we obtain

$$\frac{\partial}{\partial Q_{\varepsilon}} = \tfrac{1}{2} \left[\frac{d}{dR_{AB}} + \frac{d}{dR_{CD}} - \frac{d}{dR_{AC}} - \frac{d}{dR_{BD}} \right] \qquad (6.29)$$

$$\frac{\partial}{\partial Q_{\xi}} = \left[\frac{d}{dR_{AD}} - \frac{d}{dR_{BC}} \right] . \qquad (6.30)$$

Hence, we may now expand the derivatives of the one- and two-electron molecular integrals into a series of derivatives involving the atomic hybrids a,b,c,d by substituting for v,x,y,z and $H^{o}_{elec.}$ (from eqn. (2.3) and (2.4). In this way, using Mulliken's approximation for all three- and four-centre integrals, the problem is reduced to a series of terms involving the derivatives of the atomic integrals shown in table 6.3. The expressions for the derivatives of the molecular integrals in terms of these derivatives are given in Appendix C.3. It is important to note that the omission of terms involving $\frac{dS_{ab}}{dR_{AB}}$ by previous workers [14] is serious. Such terms in the expression for the tetragonal distortion arise from the derivative of the normalization factor and are multiplied by the values of the integral which, especially for the one-electron terms may be quite large, as shown in table 3.1.

For the single Slater functions it is possible to write the derivatives of the atomic integrals in analytic form as outlined

by Lannoo et al.[14]. However, for the Clementi functions this procedure is much more complicated. Therefore, in this calculation we have used the following numerical method of evaluating the derivatives of all the integrals. We have evaluated the required integrals at R_o, R_o+h and R_o-h where $R_o=2.52\text{Å}$ and $h=0.10\text{Å}$. Then the central difference formula tell us that if we know $f(R_o)$, $f(R_o+h)$ and $f(R_o-h)$ then the best approximation to $f'(R_o)$ is

$$f'(R_o) = \frac{f(R_o+h) - f(R_o-h)}{2h} . \qquad (6.31)$$

This is surprisingly accurate since the first non-vanishing correction is of order $h^2f'''(R_o)$. This formula is in fact equivalent to fitting a parabola through the three points $f(R_o)$, $f(R_o+h)$ and $f(R_o-h)$ and then determining the slope of the tangent at the point corresponding to $f(R_o)$. Using this technique and the Midiat program we obtain the values for the derivatives of the integrals shown in table 6.3. From these terms we may now determine the values of the derivatives of the molecular integrals for the two cases using Slater or Clementi functions. These are given in Appendix C4. It should be noted that the value of the one electron integral involved in the tetragonal calculation i.e. $\left(\frac{\partial}{\partial Q_\varepsilon} \langle y|H^o|y\rangle\right)_o$ depends upon the value of the self-penetration integral P. This dependence arises through the inclusion of a term involving the derivative of the normalization factor mentioned earlier. The importance of the dependence in the present calculation is clearly shown by the magnitude of the terms in Appendix C.4.

TABLE 6.3

Values of the derivatives of the atomic integrals used in the Jahn-Teller calculations

$\frac{d}{dR_{AB}}$ (Integral)	Slater Functions	Clementi Functions
$\langle a \mid b \rangle$	-0.2628	-0.2682
$\langle a \mid T \mid b \rangle$	-1.3518*	-1.8745
$\langle a \mid V_A \mid b \rangle$	5.7243	5.9728
$\langle a \mid V_B \mid a \rangle$	4.4407	4.7239
$\langle ab \mid \frac{1}{r_{12}} \mid ab \rangle$	-4.1224	-4.0085
$\langle ab \mid \frac{1}{r_{12}} \mid ba \rangle$	-1.4382	-2.0413
$\langle aa \mid \frac{1}{r_{12}} \mid ab \rangle$	-4.0991	-4.2215

*All derivatives in eV/Å

It is now possible to determine the values of I_{TE} and I_{TT} for the $^3T_1$ level. Then by using the values of ω_E and ω_T given in the previous section with the appropriate formulae from section 6.2, the lowering in energy and the extent of distortion may be calculated. A similar procedure may now be used to determine these quantities for the lowest degenerate levels of the V^+,V^o,V^- and $V^=$ systems. These results are given in tables 6.4 to 6.7. The discussion of all these results is given in the next section.

6.5 Discussion of Jahn-Teller Calculations

Several general features emerge from this study which underlie all the calculations. It is apparent that the magnitude of the Jahn-Teller effect is not very sensitive to whether we choose the Slater or Clementi functions to represent the wave-functions of the 2s and 2p orbitals on the carbon atom. This important finding is contrary to what had previously been conjected [15]. In fact, the uncertainty in these calculations as represented by the values for case 1 and case 2 with a particular basis set is much greater than the differences due to an alternative choice of functions. It is also clear that the magnitude of the effect depends upon the extent of configuration interaction. This is most easily seen from the variation of the trigonal terms, because here the values of the derivatives of the molecular integrals are the same in both cases (see Appendix C.4). Hence, the changes in energy lowerings are due solely to variations in the values of the eigenvectors.

TABLE 6.4

Values of the Jahn-Teller terms for the lowest $^2T_2$ level of the positive vacancy for Slater and Clementi functions

Function	Eigenvectors	I_{TE} eV/Å	ΔE_{TE} eV	q_1 Å	I_{TT} eV/Å	ΔE_{TT} eV	q_3 Å
Slater: Case 1	$c_1^1 = 0.9729$ $c_2^1 = -0.1858$ $c_3^2 = -0.1379$	-23.28	0.42	-0.027	-11.50	1.61	-0.138
Slater: Case 2	$c_1^1 = 0.9193$ $c_2^1 = -0.3097$ $c_3^2 = -0.2428$	-10.45	0.08	-0.012	-12.25	1.82	-0.147
Clementi: Case 1	$c_1^1 = 0.9778$ $c_2^1 = -0.1646$ $c_3^2 = -0.1300$	-26.37	0.53	-0.030	-11.52	1.61	-0.138
Clementi: Case 2	$c_1^1 = 0.8842$ $c_2^1 = -0.3570$ $c_3^2 = -0.3013$	- 8.43	0.05	-0.010	-12.43	1.88	-0.150

TABLE 6.5

Values of the Jahn-Teller terms for the lowest $^3T_1$, $^1T_2$ and ^1E levels of the neutral vacancy for Slater and Clementi functions

Function	Eigenvectors	I_{TE} eV/A	ΔE_{TE} eV	q_1 Å	I_{TT} eV/Å	ΔE_{TT} eV	q_3 Å
1. $^3T_1$ Level							
Slater: Case 1	$c_1 = 0.9638$ $c_2 = -0.2378$ $c_3 = -0.1206$	21.58	0.36	0.025	8.64	0.91	0.105
Slater: Case 2	$c_1 = 0.8587$ $c_2 = -0.4515$ $c_3 = -0.2426$	8.42	0.05	0.010	6.86	0.57	0.083
Clementi: Case 1	$c_1 = 0.9740$ $c_2 = -0.1980$ $c_3 = -0.1105$	24.67	0.47	0.028	8.37	0.85	0.102
Clementi: Case 2	$c_1 = 0.8054$ $c_2 = -0.5038$ $c_3 = -0.3122$	6.26	0.03	0.007	5.29	0.34	0.063

TABLE 6.5 (continued)

2. $^1T_2$ Level							
Slater: Case 1	$c_1 = 0.9865$ $c_2^2 = 0.1390$ $c_3^2 = -0.0871$	21.44	0.35	0.025	-5.18	0.33	-0.062
Slater: Case 2	$c_1 = 0.9671$ $c_2^2 = 0.2000$ $c_3^2 = -0.1570$	8.91	0.06	0.010	-4.20	0.21	-0.050
Clementi: Case 1	$c_1 = 0.9893$ $c_2^2 = 0.1183$ $c_3^2 = -0.0860$	24.00	0.44	0.028	-5.03	0.31	-0.061
Clementi: Case 2	$c_1 = 0.9556$ $c_2^2 = 0.1872$ $c_3^2 = -0.2276$	6.83	0.04	0.008	-3.39	0.14	-0.040

TABLE 6.5 (continued)

Function	Eigenvector	I_{EE} eV/Å	ΔE_{EE} eV	ρ Å
3. ^1E Level				
Slater: Case 1	$c_1 = 0.9549$ $c_2 = 0.2630$ $c_3 = -0.1377$	6.96	0.34	0.096
Slater: Case 2	$c_1 = 0.8786$ $c_2 = 0.3914$ $c_3 = -0.2738$	2.82	0.05	0.020
Clementi: Case 1	$c_1 = 0.9614$ $c_2 = 0.2449$ $c_3 = -0.1257$	7.92	0.43	0.110
Clementi: Case 2	$c_1 = 0.8231$ $c_2 = 0.4480$ $c_3 = -0.3490$	2.09	0.03	0.028

TABLE 6.6

Values of the Jahn-Teller terms for the lowest $^2T_2$, $^2T_1$ and ^2E levels of the negative vacancy for Slater and Clementi functions

Function	Eigenvector	I_{TE} eV/Å	ΔE_{TE} eV	q_1 Å	I_{TT} eV/Å	ΔE_{TT} eV	q_3 Å
1. $^2T_2$ Level							
Slater: Case 1	$c_1 = 0.9684$ $c_2 = -0.1803$ $c_3 = -0.1726$	-0.89	0.6×10^{-3}	-0.001	-3.09	0.12	-0.037
Slater: Case 2	$c_1 = 0.3641$ $c_2 = -0.3586$ $c_3 = -0.3533$	-1.91	3×10^{-3}	-0.002	-2.06	0.05	-0.024
Clementi: Case 1	$c_1 = 0.9743$ $c_2 = -0.1581$ $c_3 = -0.1606$	-1.19	1×10^{-3}	-0.001	-3.12	0.12	-0.037
Clementi: Case 2	$c_1 = 0.7786$ $c_2 = -0.4313$ $c_3 = -0.4559$	-2.27	4×10^{-3}	-0.003	-1.47	0.026	-0.018

TABLE 6.6 (continued)

2. $^2T_1$ Level							
Slater: Case 1	$c_1 = 0.9834$ $c_2 = 0.1813$	-1.01	7.9×10^{-4}	-0.001	-0.24	7.2×10^{-4}	-0.003
Slater: Case 2	$c_1 = 0.9602$ $c_2 = 0.2792$	-0.65	3×10^{-4}	-0.001	-1.03	0.013	-0.012
Clementi: Case 1	$c_1 = 0.9869$ $c_2 = 0.1619$	-0.90	6×10^{-4}	-0.001	-0.26	8×10^{-4}	-0.003
Clementi: Case 2	$c_1 = 0.9488$ $c_2 = 0.3158$	-0.40	1×10^{-4}	-4×10^{-4}	-1.55	0.029	-0.019

TABLE 6.6 (continued)

Function	Eigenvector	I_{EE} eV/Å	ΔE_{EE} eV	ρ Å
3. ^2E Level				
Slater: Case 1	$c_1 = 0.9630$ $c_2 = 0.2695$	0.91	0.006	0.012
Slater: Case 2	$c_1 = 0.8703$ $c_2 = 0.4924$	1.19	0.01	0.016
Clementi: Case 1	$c_1 = 0.9768$ $c_2 = 0.2144$	0.62	0.002	0.008
Clementi: Case 2	$c_1 = 0.8584$ $c_2 = 0.5129$	0.95	0.006	0.013

TABLE 6.7

Values of the Jahn-Teller terms for the lowest $^3T_1$, $^1T_2$ and ^1E levels for the double negative vacancy for Slater and Clementi functions

Function	Eigenvector	I_{TE} eV/Å	ΔE_{TE} eV	q_1 Å	I_{TT} eV/Å	ΔE_{TT} eV/Å	q_3 Å
1. $^3T_1$ Level							
Slater: Case 1	c = 1.0	-18.68	0.27	-0.022	-0.74	6.6×10^{-3}	-0.008
Slater: Case 2	c = 1.0	- 7.69	0.05	-0.009	-0.74	6.6×10^{-3}	-0.008
Clementi: Case 1	c = 1.0	-20.34	0.32	-0.023	0.48	2.8×10^{-3}	0.006
Clementi: Case 2	c = 1.0	- 5.32	0.02	0.006	0.48	2.8×10^{-3}	0.006
2. $^1T_2$ Level							
Slater: Case 1	c_1 = 0.9695 c_2 = 0.2450	-12.97	0.13	-0.015	1.22	0.018	0.014
Slater: Case 2	c_1 = 0.9186 c_2 = 0.3953	- 0.89	6×10^{-4}	-0.001	0.40	1.9×10^{-3}	0.005
Clementi: Case 1	c_1 = 0.9880 c_2 = 0.2096	-16.21	0.20	-0.018	0.30	0.001	0.004
Clementi: Case 2	c_1 = 0.9031 c_2 = 0.4294	0.30	7×10^{-5}	4×10^{-4}	-0.78	7×10^{-3}	-0.01

TABLE 6.7 (continued)

Function	Eigenvector	I_{EE} eV/Å	ΔE_{EE} eV	ρ Å
Slater: Case 1	c = 1.0	-6.49	0.29	0.09
Slater: Case 2	c = 1.0	-2.81	0.05	0.04
Clementi: Case 1	c = 1.0	-7.05	0.34	0.10
Clementi: Case 2	c = 1.0	-2.05	0.03	0.03

For the tetragonal cases the variations from case 1 to case 2 are much more significant. This is due partly to the changes in the values of the eigenvectors, but more importantly, to changes in the value of the one-electron term, for reasons outlined in the previous section. We have shown in chapter 3 that delocalization of electronic charge away from the vacancy does not cause changes in the relative ordering of the electronic energy levels. However, this effect does result in a change in the extent of configurational mixing which will effect the values obtained for the Jahn-Teller splittings, especially for the trigonal case. This effect remains to be fully investigated once some of the centres have been positively identified.

With the exception of the $^2T_2$ electronic level of V^+ and the $^3T_1$ level of V^o all the predicted distortions are fairly small. When discussing the extent of distortion for each degenerate electronic level it is most convenient to consider just one of the equivalent configurations which is lowest in energy. For a tetragonal distortion we choose the configuration with symmetry axis along the <100> direction. In this case Q_ε vanishes and the stable configuration may be represented as in fig. 6.1a). It is sufficient to know the distances ΔR_{AB} and ΔR_{AD} to define this configuration. Of the four possible equivalent configurations of lowest energy corresponding to a trigonal distortion the one for which $Q_\xi = Q_\eta = Q_\zeta$ has been considered here. In this case the three atoms A,B,C form an equilateral triangle and D is on the <111> symmetry axis as shown in fig. 6.1b. Again to define the

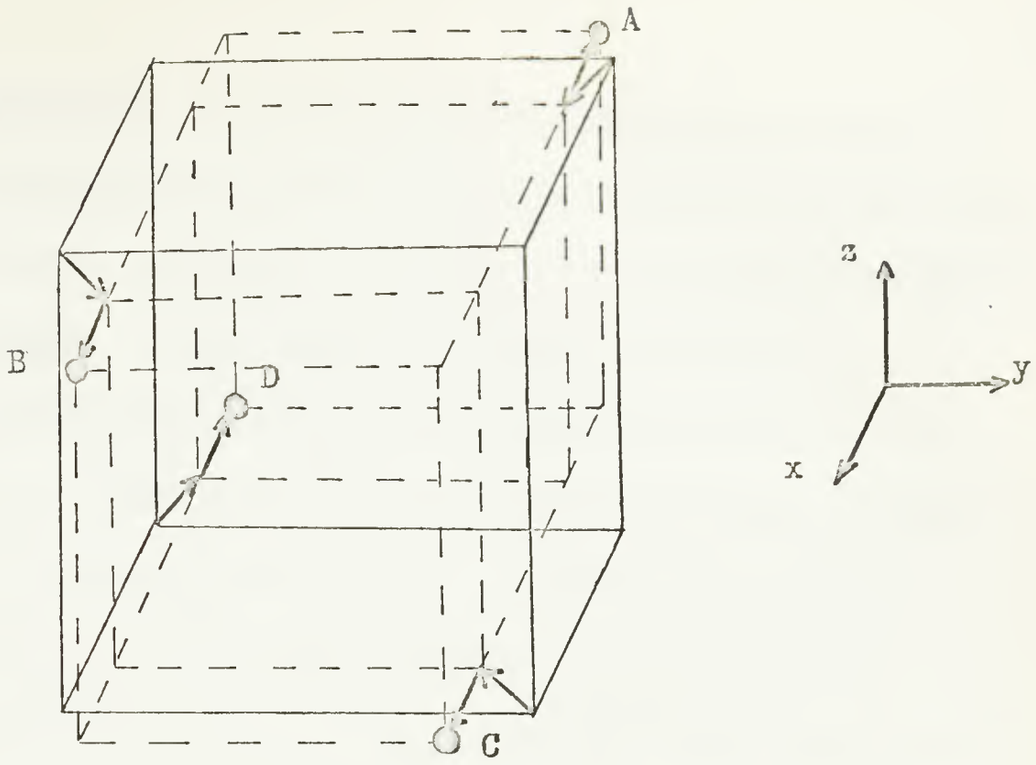


Fig.6.1a Model showing a tetragonal distortion of the single vacancy system in the <100> direction.

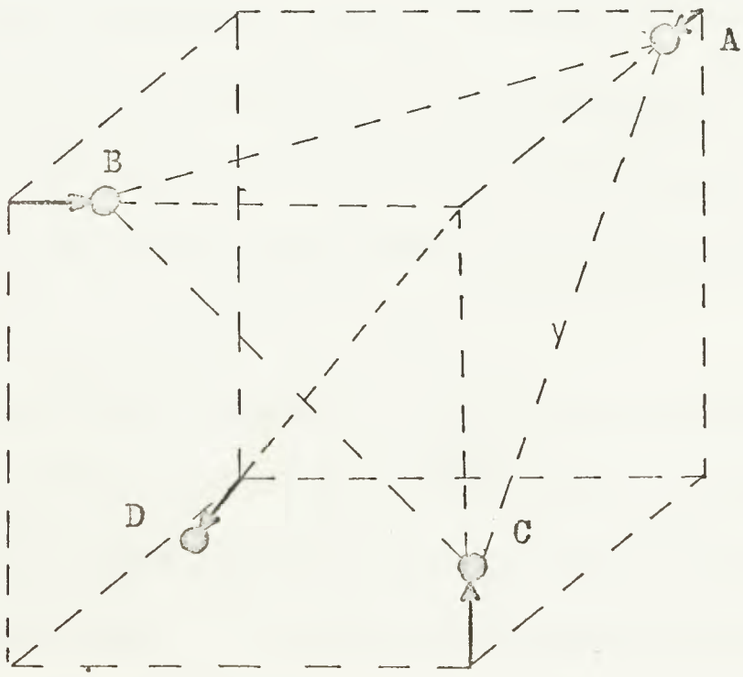


Fig.6.1b Model showing a trigonal distortion of the single vacancy system in the <111> direction.

new configuration it is sufficient to specify ΔR_{AD} and ΔR_{AB}. Instead of treating each level separately we have chosen a range of typical values for q_3, q_1 and ρ and determined the magnitude of the distortions. These results are shown in table 6.8.

It is difficult to make a valid comparison with the work of Lannoo et al. [14] because of the basic differences referred to earlier. However, some reference to this work is made in the discussion relating to each centre. Unfortunately, no experimental results are yet available for the magnitude of the Jahn-Teller effect for electronic levels of the single vacancy in the diamond crystal. To extrapolate from the work of Watkins on the silicon vacancy is rather dubious, because of the different characteristics of the two lattices. In chapter 5 it has been clearly demonstrated that the diamond lattice is much more rigid against possible distortion than the lattice of the silicon crystal. Therefore, we have not attempted such comparisons. We now propose to discuss the results for each centre separately and to relate them to the energy level scheme calculated in chapter 3.

i) V^+ centre

For the positively charged vacancy we have considered only the lowest $^2\Gamma_2$ level, because the undistorted calculation of chapter 3 predicts that this level is much lower in energy than any other electronic level. The results presented in table 6.4 show that there is very good agreement between the values obtained using Slater and Clementi functions. These results favour a trigonal distortion of the lattice in order to remove the orbital

TABLE 6.8

Extent of trigonal and tetragonal distortion for some typical values of q_3, q_1 and ρ*

q_3 Å	Trigonal displacements[x] Å	q_1 Å	Tetragonal displacements[x] Å	ρ Å	Tetragonal displacements Å
0.10[+]	$\Delta R_{AB} = -0.10$ $\Delta R_{AD} = 0.10$	0.03	$\Delta R_{AB} = -0.04$ $\Delta R_{AD} = 0.10$	0.10	$\Delta R_{AB} = 0.05$ $\Delta R_{AD} = -0.09$
0.05	$\Delta R_{AB} = -0.05$ $\Delta R_{AD} = 0.05$	0.02	$\Delta R_{AB} = -0.03$ $\Delta R_{AD} = 0.07$	0.05	$\Delta R_{AB} = 0.02$ $\Delta R_{AD} = -0.04$
0.02	$\Delta R_{AB} = -0.02$ $\Delta R_{AD} = 0.02$	0.01	$\Delta R_{AB} = -0.02$ $\Delta R_{AD} = 0.04$	0.02	$\Delta R_{AB} = 0.01$ $\Delta R_{AD} = -0.02$
0.01	$\Delta R_{AB} = -0.01$ $\Delta R_{AD} = 0.01$	0.005	$\Delta R_{AB} = -0.005$ $\Delta R_{AD} = 0.02$	0.01	$\Delta R_{AB} = 0.005$ $\Delta R_{AD} = -0.01$

*For definition of q_3, q_1 and ρ and relation to the normal co-ordinates see text

[x]Displacements refer to fig. 6.1

[+]For negative values of q_3, q_1 or ρ the displacements are of opposite sign.

degeneracy of the $^2T_2$ level. However, the predicted magnitude of this effect would appear to be much too large. It has not been possible to isolate the reason for this result; however, the possible inadequacy of the simple defect model for charged states of the vacancy and the limitation of the static Jahn-Teller calculations which includes only first order terms are certainly contributory factors. The very large difference between the present results and that of Lannoo et al.[14] may partly be explained by the fact thet the sign of the eigen-vector c_2 in the latter study is opposite to that used in the present work. We believe that this difference may arise from a numerical error in the previous work. If we were to take c_2 to be positive in our expressions we obtain values for ΔE_{TT} in the range 0.55 to 0.20 eV. However, we cannot justify such an alteration of sign.

ii) V^o centre

For the neutral vacancy we have evaluated the Jahn-Teller terms for the lowest $^3T_1$, ^1E and $^1T_2$ levels. These results are shown in table 6.5. For the $^3T_1$ level all the calculations predict that $\Delta E_{TT} > \Delta E_{TE}$. This study shows very clearly the general features common to most of the evaluations which were discussed earlier in this section. The magnitude of the trigonal distortion and the energy lowering are fairly large, but perhaps not unreasonably so. They also show a marked dependence on the extent of configuration interaction. The values of ΔR_{AB} and ΔR_{AD} for the trigonal equilibrium configuration using Slater functions are -0.10Å and 0.11Å (case 1) and -0.08Å and 0.09Å (case 2) respectively.

The results obtained by Lannoo are of the same order of magnitude as those determined in this investigation.

For the ^1E level the lowering in energy as a result of the tetragonal distortion is predicted to be less than the splitting of $^3T_1$ level. The change in ΔE_{EE} from case 1 to case 2 is very large. This reflects the uncertainty of the calculation. If the lowest ^1E and $^3T_1$ levels of V^0 shown in fig. 3.2 are corrected by the Jahn-Teller splittings given in table 6.5 we find that the $^3T_1$ level is predicted to be the ground state level in <u>all</u> four studies. This striking result is contrary to previous predictions. Before we go further and draw any firm conclusions about the ground state of the neutral vacancy it is necessary to consider the effect of the symmetric relaxation term on all the lowest levels. This aspect of the work is discussed further in section 6.6.

For the $^1T_2$ level it is interesting to note that for the approximation denoted case 1, a tetragonal distortion is favoured as the equilibrium configuration using both Slater and Clementi-type functions. However, because of the sensitivity of the tetragonal calculations to the value of the self-penetration integral, in the alternative approximation, case 2, a trigonal distortion is favoured. It is not possible to resolve these conflicting results without a more accurate knowledge of the parameters involved. The magnitude of the predicted splitting seem feasible. We return to a further discussion of these levels in a later section.

iii) V^- centre

The Jahn-Teller splittings for the $^2T_2$, $^2T_1$ and ^2E electronic levels of the negatively charged vacancy are all predicted to be small with the possible exception of the results for case 1 of the $^2T_2$ level. If the Jahn-Teller corrections shown in table 6.6 are made to the energy levels given in fig. 3.3 no changes in the relative ordering of these levels is observed. A trigonally distorted equilibrium configuration is predicted for the $^2T_2$ level, but for the $^2T_1$ level the situation is more uncertain although a trigonal distortion is favoured in the majority of the calculations. For both these levels the trigonal distortion is represented by a decrease in ΔR_{AD} and an increase in ΔR_{AB}.

iv) V^{2-} centre

A tetragonal equilibrium configuration is predicted for the ground state $^3T_1$ level as the result of the Jahn-Teller effect. Since there is no configuration interaction effect the magnitude of the trigonal distortion is the same in both approximations. The dependence of the tetragonal terms on the terms involving the derivative of the overlap integral is therefore very clearly demonstrated. For the $^1T_2$ level the studies denoted case 1 predict that the equilibrium configuration of this level will be tetragonally distorted, however, at the other limit a very small trigonal distortion is favoured. A wide range of uncertainty is also shown for the value of the tetragonal distortion associated with the ^1E level. The ordering of the energy levels shown in

fig. 3.4 for the doubly negatively charged vacancy are not altered as a result of the Jahn-Teller splittings.

Before we can relate any of the foregoing results to the meagre experimental evidence it is necessary to have an accurate knowledge of the relative ordering of the lowest electronic levels for each charge state of the vacancy. Up to now we have ignored the effects resulting from the symmetric relaxation of the nearest neighbour atoms surrounding the vacancy. We now propose to examine this effect in more detail before proceeding with further discussion of the results.

6.6 The Symmetric Relaxation Mode for the Single Vacancy

In the preceding calculations to first order it has been assumed that there is no coupling between the different normal modes. Hence, in order to calculate the distortion associated with a particular electronic level it was not necessary to evaluate the energy lowering due to the symmetric mode. However, to determine the relative ordering of the lowest levels, again to first order, it is necessary to evaluate the symmetric term for each electronic level. Previous studies have tacitly assumed that within a particular centre this term is the same for each level. However, this has not been quantitatively investigated. Lannoo et al.[14] have shown that this term may be large relative to the Jahn-Teller splittings. Therefore, we have chosen to investigate this symmetric term in more detail, because we are concerned with evaluating the relative ordering of the energy levels.

For an n-degenerate manifold the energy dependence on Q_a, the symmetric mode, to first order may be expressed as follows:

$$E(Q_a) = \left[E_o + I_a Q_a - \frac{\hbar^2}{2M} \frac{\partial^2}{\partial Q_a^2} + \tfrac{1}{2} M \omega_a^2 Q_a^2 \right] \begin{pmatrix} 1 & & \\ & 1 & \\ & & \ddots \\ & & & 1 \end{pmatrix} \tag{6.32}$$

where these terms with the exception of I_a have the same general meaning as previously. I_a will be defined shortly. All off-diagonal elements are zero. It follows, therefore, that when $\frac{\partial E(Q_a)}{\partial Q_a} = 0$

$$Q_a = - \frac{I_a}{M\omega_a^2} \quad . \tag{6.33}$$

Hence, the energy lowering, ΔE_a is given by:

$$\Delta E_a = - \frac{I_a^2}{2M \omega_a^2} \quad . \tag{6.34}$$

Now, in the definition of I_a, to first order, we differ from the work of Lannoo et al.[14].* In their study they have reasoned as follows: using eqn.(6.26) it is easily shown that:

---

*I am indebted to Dr. A.B. Lidiard for a very helpful discussion on this point.

$$\frac{\partial}{\partial Q_a} = \frac{1}{\sqrt{6}} \left[\frac{d}{dR_{AB}} + \frac{d}{dR_{AC}} + \frac{d}{dR_{AD}} + \frac{d}{dR_{BC}} + \frac{d}{dR_{BD}} + \frac{d}{dR_{CD}} \right]. \quad (6.35)$$

Therefore, in the expression for I_a one must include terms that represent the repulsion between the four atoms nearest the defect, as well as the electronic terms. This additional term will vanish by symmetry for a tetragonal or trigonal distortion as should be apparent from eqns. (6.29) and (6.30). Hence

$$I_a = \left(\frac{\partial}{\partial Q_a} \langle \psi_k | H_{elec.} | \psi_k \rangle \right)_o + \left(\frac{\partial}{\partial Q_a} \sum_{\gamma \neq \beta} I_{\gamma\beta} \right)_o \quad (6.36)$$

where the first term is the electronic contribution from the four vacancy electrons and $I_{\gamma\beta}$ ($\gamma \neq \beta$ = A,B,C,D) represents the interaction between atoms γ and β. However, we believe that the terms involving the repulsion between the nuclei neighbouring the vacancy are already included in the quasi-elastic term, because of the way we have determined ω_a in section 6.3 using the dynamical relaxation technique. Therefore, we have defined I_a to include only the electronic contribution, namely

$$I_a = \left(\frac{\partial}{\partial Q_a} \langle \psi_k | H_{elec.} | \psi_k \rangle \right)_o . \quad (6.37)$$

An alternative way of approach this problem would be through the Kansaki method [115]. If we use this approach then we may very easily show that the defect Hamiltonian will not include terms involving repulsion between the atoms nearest the defect. To a first approximation therefore we use the definition of I_a given by eqn.(6.37).

In order to determine the detailed expressions for I_a we substitute in (6.37) for the electronic state wave-function ψ_k from the wave-functions, ϕ_j, for the various configurations given in Appendix A.1 with suitable eigenvectors c_j, i.e.

$$\psi_k = \sum_{j=1}^{n} c_j \phi_j \ .$$

Therefore

$$I_a = \left(\frac{\partial}{\partial Q_a} \left(\sum_{i,j} c_i c_j a_{ij} \right) \right)_o$$

where

$$a_{ij} = \langle \phi_i | H_{elec.} | \phi_j \rangle \ .$$

On expansion of a_{ij} the expression for I_a reduces to a sum of terms involving the derivatives of the one- and two-electron molecular integrals shown in table 6.9 and terms involving the derivatives of the eigenvectors c_1,c_2 and c_3. These latter first-order terms which have been included in this study are usually very small and result in corrections of about one per cent, but in one or two isolated cases they amount to around five per cent of the total value. The form of the expressions for I_a for each electronic state may easily be deduced using the information given in Appendix A.2. The derivatives of the molecular integrals may be expressed in terms of the derivatives of the atomic integrals given in table 6.3 and are given in Appendix C.4. The values of the derivatives of the molecular integrals for both Slater and

TABLE 6.9

Values of the derivatives of the molecular integrals used in the calculation of the symmetric relaxation terms

$\frac{d}{dQ_a}$ (Integral)	Slater Function	Clementi Function
$\langle v\|H^o\|v\rangle$	8.3089*x 7.0976+	7.9303* 6.9067+
$\langle x\|H^o\|x\rangle$	2.4168* 3.7150+	2.4466* 4.2166+
$\langle vv\|\frac{1}{r_{12}}\|vv\rangle$	-1.6522	-1.4866
$\langle xx\|\frac{1}{r_{12}}\|xx\rangle$	-0.9796	-1.0528
$\langle vx\|\frac{1}{r_{12}}\|vx\rangle$	-1.4949	-1.4189
$\langle xy\|\frac{1}{r_{12}}\|xy\rangle$	-0.3154	-0.0201
$\langle vz\|\frac{1}{r_{12}}\|zv\rangle$	-0.0558	-0.0710
$\langle xy\|\frac{1}{r_{12}}\|yx\rangle$	1.0355	1.1000
$\langle vx\|\frac{1}{r_{12}}\|yz\rangle$	-0.4866	-0.5072

*Case 1 +Case 2 xAll derivatives in eV/Å

Clementi-type functions required for the present calculation are given in table 6.9. The change in the value of the one-electron integrals from case 1 to case 2 is the result of including terms involving the derivative of the overlap integral.

Using these values we may determine the numerical value of I_a for each electronic level. Then by substituting for I_a and ω_a in (6.33) and (6.34) we may determine the magnitude of the relaxation and the resulting lowering in energy to first order for each electronic level. It is of course necessary to determine the relaxation for the non-degenerate levels as well as for the degenerate levels. We have evaluated the symmetric term associated with the following electronic levels for the various charge states of the vacancy:

$$
\begin{aligned}
V^{+} &: {}^{2}T_2 \\
V^{o} &: {}^{3}T_1,\ {}^{1}E,\ {}^{1}T_2,\ {}^{5}A_2 \\
V^{-} &: {}^{2}T_2,\ {}^{2}T_1,\ {}^{2}E,\ {}^{4}A_2 \\
V^{=} &: {}^{3}T_1,\ {}^{1}E,\ {}^{1}T_2,\ {}^{1}A_1 .
\end{aligned}
$$

The values of I_a, Q_a and ΔE_a for each electronic level are given in tables 6.10 to 6.13 for the various charge states. For most levels the lowering in energy as the result of relaxation is of the order of 1 to 2 eV. In using eqn.(6.32) we assume that the energy change due to the symmetric relaxation was linear in terms involving I_a. However, it is more exact to include second order terms and to write

$$I'_a = I_a + \beta\, Q_a \qquad (6.38)$$

where

$$\beta = \left(\frac{\partial I_a}{\partial Q_a}\right)_o = \left(\frac{\partial^2}{\partial Q_a^2}\left(\sum_{i,j} c_i\, c_j\, a_{ij}\right)\right)_o .$$

Now, the predominant term in β is the term involving the derivative of the eigen-vectors by the derivative of the integrals a_{ij}. Therefore, we have defined β as

$$\beta = 2\sum_{i,j}\left(c_i \frac{\partial c_j}{\partial Q_a}\frac{\partial a_{ij}}{\partial Q_a} + c_j \frac{\partial c_i}{\partial Q_a}\frac{\partial a_{ij}}{\partial Q_a}\right) . \qquad (6.39)$$

Now, we replace I_a by I'_a in (6.32) and set $\frac{\partial E}{\partial Q_a} = 0$, hence we obtain

$$q'_a = -\frac{I_a}{(M\omega_a^2 + 2\beta)} \qquad (6.40)$$

and

$$\Delta E'_a = \tfrac{1}{2}\frac{I_a^2}{(M\omega_a^2 + 2\beta)} . \qquad (6.41)$$

Hence, $\Delta E'_a$ will be less than ΔE_a if β is positive. However, for most of the energy we have considered β is negative.

In tables 6.10 to 6.13 the values of I'_a, $\Delta E'_a$ and Q'_a are given for the various levels. For most levels the second order correction results in a very small change of the order of 0.1 eV in the energy lowering. However, the exception seems to be the ^2E level of the V^- centre where the correction is near 0.4–0.6 eV.

TABLE 6.10

Value of the symmetric terms for the $^2T_2$ level of the positive vacancy

Function	First Order Terms			Including Second Order Terms		
	I_a eV/Å	ΔE_a eV	Q_a Å	I'_a eV/Å	$\Delta E'_a$ eV	Q'_a Å
Slater: Case 1	13.95	1.83	-0.262	14.53	1.98	-0.284
Slater: Case 2	12.51	1.47	-0.235	12.91	1.56	-0.250
Clementi: Case 1	13.63	1.74	-0.256	14.01	1.84	-0.270
Clementi: Case 2	12.99	1.58	-0.244	13.21	1.64	-0.252

TABLE 6.11

Value of the symmetric term for the $^3T_1$, $^1T_2$, ^1E and $^5A_2$ levels of the neutral vacancy

Function	First Order Terms			Including Second Order Terms		
	I_a eV/Å	ΔE_a eV	Q_a Å	I'_a eV/Å	$\Delta E'_a$ eV	Q'_a Å
1. $^3T_1$ Level						
Slater: case 1	12.13	1.38	-0.228	13.26	1.64	-0.270
Slater: case 2	10.88	1.11	-0.204	11.99	1.34	-0.246
Clementi: case 1	12.17	1.39	-0.229	12.87	1.55	-0.254
Clementi: case 2	11.97	1.34	-0.225	12.74	1.52	-0.254
2. ^1E Level						
Slater: case 1	11.01	1.14	-0.207	11.65	1.27	-0.231
Slater: case 2	10.95	1.13	-0.206	11.35	1.21	-0.220
Clementi: case 1	10.97	1.09	-0.203	11.18	1.17	-0.217
Clementi: case 2	12.13	1.38	-0.228	12.27	1.41	-0.233
3. $^1T_2$ Level						
Slater: case 1	14.34	1.93	-0.269	14.70	2.03	-0.283
Slater: case 2	14.39	1.94	-0.270	14.71	2.03	-0.283
Clementi: case 1	14.55	1.99	-0.273	14.81	2.06	-0.283
Clementi: case 2	13.78	1.78	-0.259	13.90	1.81	-0.263
4. $^5A_2$ Level						
Slater: case 1	7.19	0.49	-0.135	7.19	0.49	-0.135
Slater: case 2	9.87	0.91	-0.185	9.87	0.91	-0.185
Clementi: case 1	7.87	0.58	-0.148	7.87	0.59	-0.148
Clementi: case 2	12.15	1.39	-0.228	12.15	1.39	-0.228

TABLE 6.12

Value of the symmetric term for the $^2T_2$, $^2T_1$, ^2E and $^4A_2$ levels of the negatively charged vacancy

Function	First Order Terms			Including Second Order Terms		
	I_a eV/Å	ΔE_a eV	Q_a Å	I'_a eV/Å	$\Delta E'_a$ eV	Q'_a Å
1. $^2T_2$ Level						
Slater: case 1	11.43	1.23	-0.215	12.04	1.36	-0.237
Slater: case 2	12.48	1.46	-0.234	13.08	1.60	-0.257
Clementi: case 1	11.98	1.35	-0.225	12.32	1.42	-0.237
Clementi: case 2	15.04	2.12	-0.282	15.20	2.17	-0.288
2. $^2T_1$ Level						
Slater: case 1	9.32	0.82	-0.175	9.56	0.86	-0.184
Slater: case 2	10.63	1.06	-0.200	10.81	1.10	-0.206
Clementi: case 1	9.76	0.89	-0.183	9.94	0.93	-0.190
Clementi: case 2	12.84	1.55	-0.241	13.00	1.58	-0.245
3. ^2E Level						
Slater: case 1	12.00	1.35	-0.225	13.73	1.74	-0.290
Slater: case 2	11.29	1.20	-0.212	13.53	1.67	-0.296
Clementi: case 1	12.88	1.56	-0.242	13.97	1.82	-0.283
Clementi: case 2	13.54	1.72	-0.254	15.96	2.34	-0.345
4. $^4A_2$ Level						
Slater: case 1	9.36	0.82	-0.176	9.36	0.82	-0.176
Slater: case 2	10.83	1.10	-0.203	10.83	1.10	-0.203
Clementi: case 1	10.05	0.95	-0.189	10.05	0.95	-0.189
Clementi: case 2	13.32	1.66	-0.250	13.32	1.66	-0.250

TABLE 6.13

Value of the symmetric term for the $^3T_1$, ^1E, $^1T_2$ and $^1A_1$ levels of the doubly negatively charged vacancy

Function	First Order Terms			Including Second Order Terms		
	I_a	ΔE_a	Q_a	I'_a	$\Delta E'_a$	Q'_a
1. $^3T_1$ Level						
Slater: case 1	7.23	0.490	-0.136	7.23	0.49	-0.136
Slater: case 2	10.00	0.94	-0.188	10.00	0.94	-0.188
Clementi: case 1	8.64	0.70	-0.162	8.64	0.70	-0.162
Clementi: case 2	13.67	1.75	-0.257	13.67	1.75	-0.257
2. $^1T_2$ Level						
Slater: case 1	8.60	0.69	-0.161	9.18	0.79	-0.183
Slater: case 2	10.75	1.09	-0.202	11.38	1.21	-0.225
Clementi: case 1	10.25	0.99	-0.192	10.72	1.08	-0.210
Clementi: case 2	14.57	1.99	-0.274	15.14	2.15	-0.295
3. ^1E Level						
Slater: case 1	6.57	0.41	-0.123	6.57	0.41	-0.123
Slater: case 2	9.34	0.82	-0.175	9.34	0.82	-0.175
Clementi: case 1	7.61	0.54	-0.143	7.61	0.54	-0.143
Clementi: case 2	12.64	1.50	-0.237	12.64	1.50	-0.237
4. $^1A_1$ Level						
Slater: case 1	9.44	0.84	-0.177	9.70	0.88	-0.187
Slater: case 2	12.26	1.41	-0.230	12.63	1.50	-0.244
Clementi: case 1	10.74	1.08	-0.202	10.86	1.11	-0.206
Clementi: case 2	15.95	2.39	-0.300	15.99	2.40	-0.301

TABLE 6.14

Displacement of, and distance between, the nearest neighbour atoms to the vacancy for various values of the symmetric mode

Q_a Å	$X_A = -\frac{Q_A}{\sqrt{12}}$ Å	$\Delta R_A = \sqrt{3}\ X_A$ Å	$R_{AB} = \sqrt{8}\ (\frac{a}{4} - X_A)$ Å
0.0	0.0	0.0	2.52
-0.10	0.029	0.050	2.44
-0.15	0.043	0.075	2.40
-0.20	0.058	0.100	2.36
-0.25	0.072	0.125	2.32
-0.30	0.087	0.150	2.28
-0.35	0.101	0.175	2.24

X_A represents the displacements of atom A in the x direction

ΔR_A represents the total inward displacement of atom A

R_{AB} is the distance between the atoms A and B after symmetric relaxation, Q_a

a cell constant.

We propose now to discuss these results in detail, and to relate the findings to the energy level schemes determined in chapter 3. We will concentrate on the values obtained when the second order corrections are involved.

6.7 Discussion of the Results for the Symmetric Relaxation and Comparison of the Calculated Electronic Structure with Experiment

From the results obtained it is apparent that for a particular charge state of the vacancy the lowering in energy for each of the lowest electronic levels is not constant. For example, the variation in $\Delta E'_a$, for the neutral vacancy is clearly shown in table 6.11. Because of these differences it becomes important to consider the effect of the symmetric term when determining the relative ordering of the energy levels. For the V^+ and V^o centres the results obtained using Clementi-type functions for the 2s and 2p orbitals are in reasonable agreement with the values determined using Slater-type functions. However, for V^- and $V^=$, particularly with the case 2 approximations, the agreement is much poorer. No general pattern emerges for the relationship between the results obtained with the two limiting approximations, case 1 and case 2, for a given set of analytic wave-functions. For all levels Q_a is negative such that the symmetric relaxation is predicted to be inwards. This was also found to be the case in the study by Lannoo et al.[14]. We observe that there are no marked variations in Q_a from one charged state of the vacancy to another. It is not surprising that the relaxation is inwards since by requiring the atoms nearest the

defect to be sp^3 hybridised the system is constrained against outwards relaxation.

The displacement of the atoms corresponding to each value of Q_a for the various levels of the vacancy in all its possible charge states are not given; however, in table 6.14 we show a range of values of Q_a which span the values of Q_a given in tables 6.10 to 6.13, and the corresponding displacement of the atoms nearest the defect. The symmetric relaxation term, Q_a, for most of the electronic levels fall within the range 0.20 to 0.30Å which corresponds to a displacement of 0.10 to 0.15Å for the atoms nearest the defect. Hence, the distance between nearest neighbour atoms to the defect is now in the range 2.36 to 2.28Å compared with the perfect lattice next-nearest neighbour of 2.52Å. These are fairly large displacements which cannot be ignored when undertaking any electronic calculation. It also raises the question that it may not be sufficient to include such effects as a perturbation on the undistorted vacancy calculations. At this stage we cannot be certain of this point. However, an alternative approach which included the symmetric term, and possibly the Jahn-Teller terms, as an integral part of the calculation would be useful. We now relate these findings to the electronic energy level schemes which were determined for the undistorted vacancy systems in chapter 3. Then the corrected energy level schemes are compared with the experimental information which is presently available.

i) V^+ centre

For this centre we have considered only the lowest $^2T_2$ level. We have found the symmetric and Jahn-Teller terms to be large. It seems unlikely that any other electronic level would be the ground state of this centre from examination of fig. 3.1 and the current findings. On the basis of this calculation we predict that the V^+ centre will be paramagnetic ($S = \frac{1}{2}$) with a symmetry axis along the <111> direction. It is possible that this centre is responsible for the 'a' system of lines observed by Baldwin [40] and others.

ii) V^0 centre

In fig. 6.2 we have corrected the lowest electronic energy levels for the equilibrium values of the symmetric term and the Jahn-Teller terms for the V^0 centre. Of course, when observing optical transition the Franck-Condon principle is assumed to be obeyed such that the excited states will have the same nuclear configuration as the ground state of the system. However, our concern is first to determine the ground state of the system, therefore it is necessary to examine the equilibrium configurations. The most interesting finding is that after corrections have been made to the electronic states obtained in the undistorted vacancy calculation the $^3T_1$ level is always lowest using both Slater- and Clementi-type functions. Our calculation predicts that this level is between 0.6 to 0.9 eV below the ^1E level. If this corrected electronic structure represents the true situation for a neutral vacancy in diamond then we can say that this centre

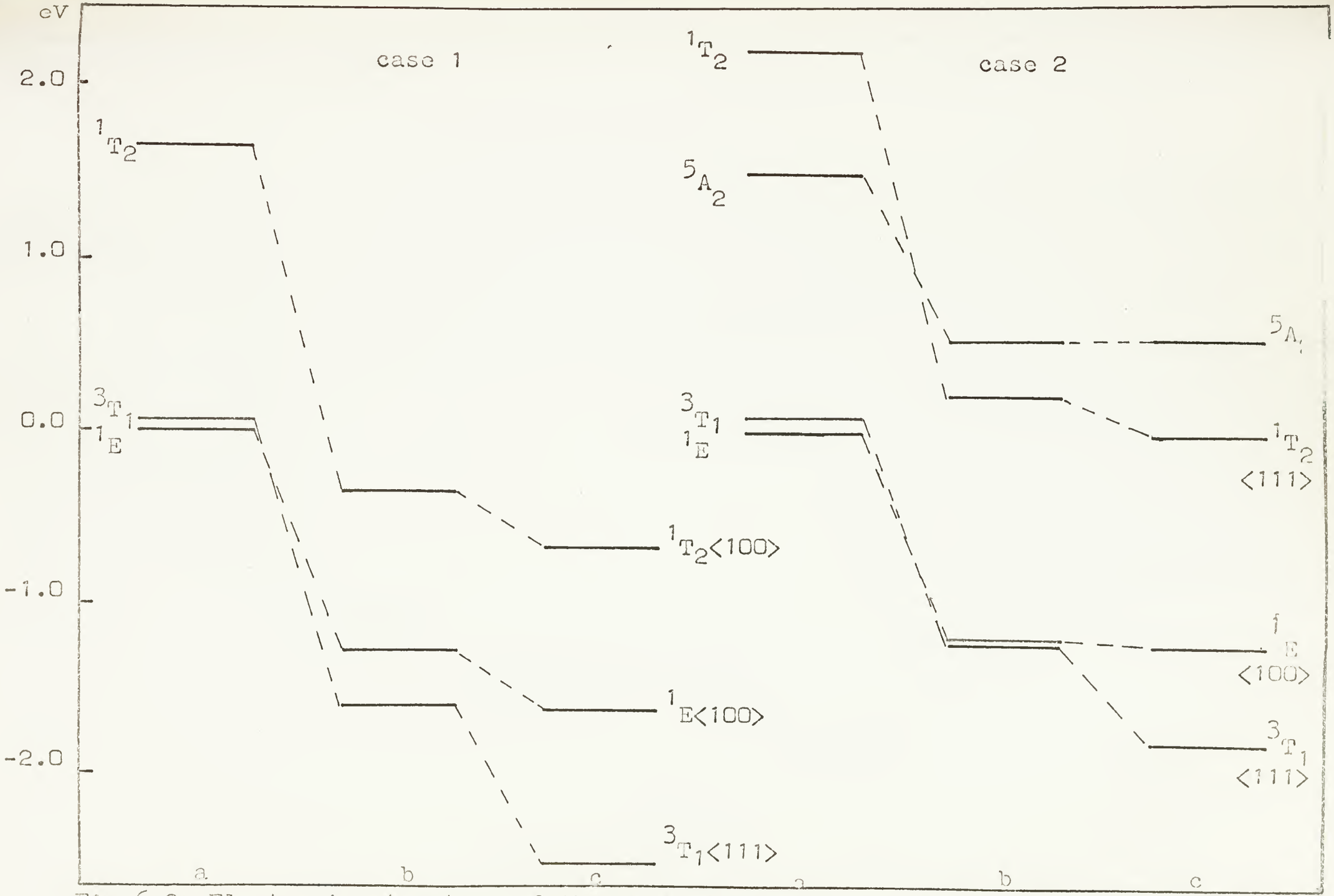


Fig.6.2a Electronic structure of the neutral vacancy in diamond using Slater functions. a,undistorted calculation after c.i. b,levels from a.corrected for symmetric relaxation effects.c, levels from b.corrected for Jahn-Teller distortion terms.

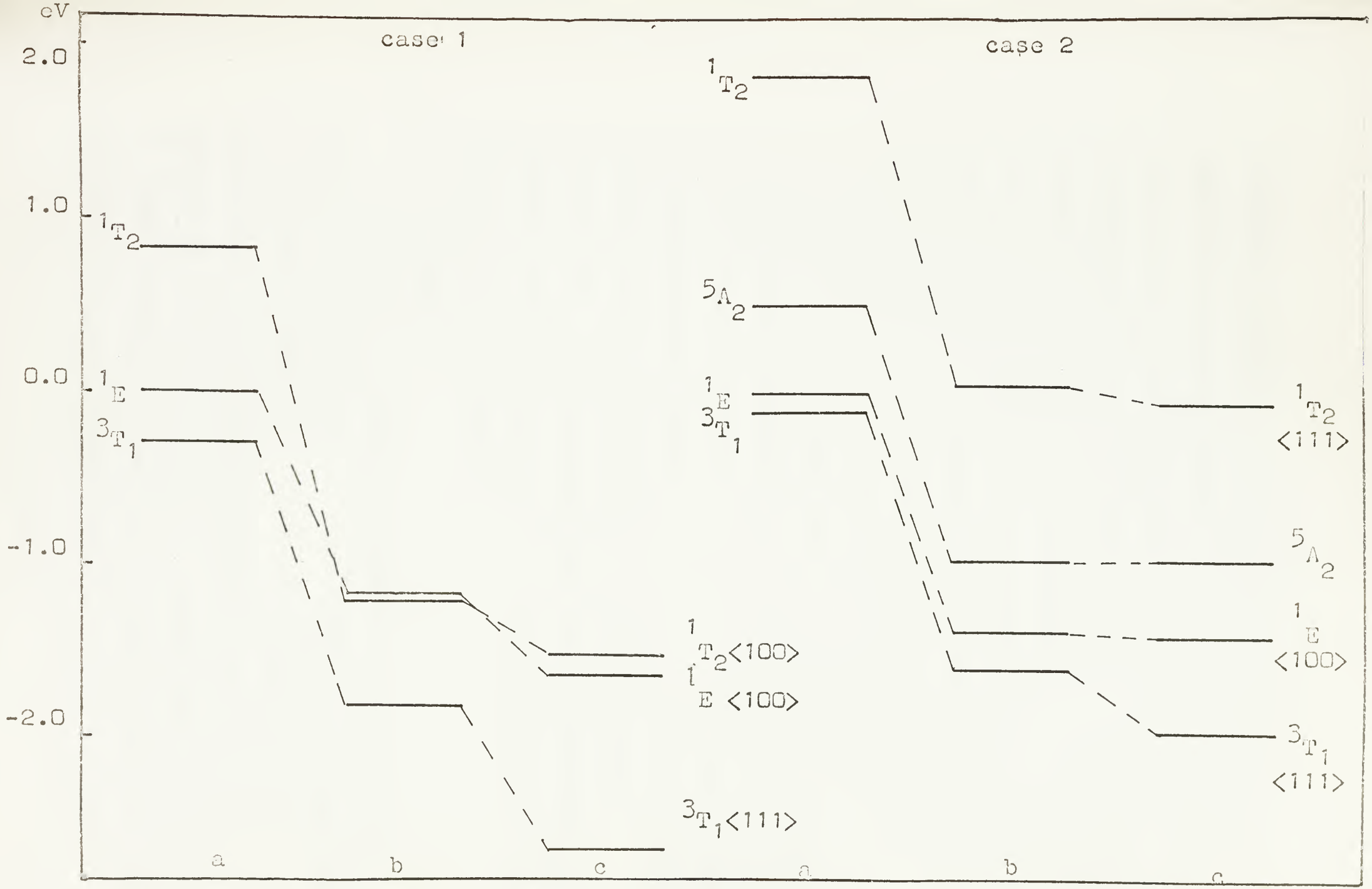


Fig.6.2b Electronic structure of the neutral vacancy in diamond using Clementi functions. a, undistorted calculation after c.i. b,levels from a. corrected for symmetric relaxation effects.c,levels from b.corrected for Jahn-Teller distortion terms.

is not responsible for the GR1 optical absorption band which is observed in irradiated diamonds. This finding, if correct, would negate the work of Lannoo and Stoneham [15] on the calculation of the Huang-Rhys factor and the band moments of the GR1 band as their calculation was based upon the assumption that this band could be associated with the neutral vacancy. Their calculation also assumes that the equilibrium value of the breathing mode, Q_a, is the same for the ^1E and $^1T_2$ state. This assumption has also been found to be incorrect.

We predict that if the isolated single vacancy does exist it should exhibit paramagnetism with a total spin, S, equal to 1 and symmetry axis in the <111> direction. It is possible that this centre may be responsible for the b,d or e system of lines observed by Lomer and Wild [43] which we have discussed elsewhere [8]. However, these can be but tentative proposals because of the uncertainty of many of the experimental results for reasons discussed in chapter 1.

iii) V^- centre

The corrected electronic structure for this centre using Slater-type functions which is shown in fig. 6.3a predicts that the $^4A_2$ level is still most likely to be the lowest level. However, for the calculations using Clementi-type functions (fig. 6.3b) this is not the case. At one extreme (case 1) the $^4A_2$ level is lowest, but there is a ^2E level only 0.09 eV above this level while at the other limit (case 2) the $^2T_2$ level is

predicted to be the ground state level 0.11 eV below the ^2E level and 0.63 eV below the $^4A_2$ level. On the basis of our present calculations we would predict that electronic transitions between the defect electrons of the negatively charged vacancy are unlikely to be associated with the GR1 band. However, if any isolated vacancy/centre is to be associated with this band the negatively charged state would appear to be the most likely for the following reasons. Firstly, the defect molecule approach is almost certainly less satisfactory for the charge states of the vacancy than for the neutral state, because no attempt has been made to modify the wave-functions obtained from the neutral carbon atom for the 2s and 2p orbitals to account for the extra electronic charge. Secondly, the lowest electronic levels are fairly close together in the V^- centre such that inter-level coupling effects of the kind recently discussed [111] may well be important. In particular the stress splitting data for the GR1 band is consistent with a centre having mixed tetragonal and trigonal distortions. This would be possible between the ^2E and $^2T_2$ levels shown in case 2 of the Clementi study. By contrast the levels of the neutral vacancy are well separated such that large interlevel coupling effects are unlikely. As shown in table 2.2 allowed transitions may occur between the $^2T_2$ or ^2E levels and the $^2T_1$ level of the V^- centre. We are unable to associate our findings with any of the observed E.S.R. spectra for the irradiated diamond system. Without further investigation our conclusions about this centre must remain tentative.

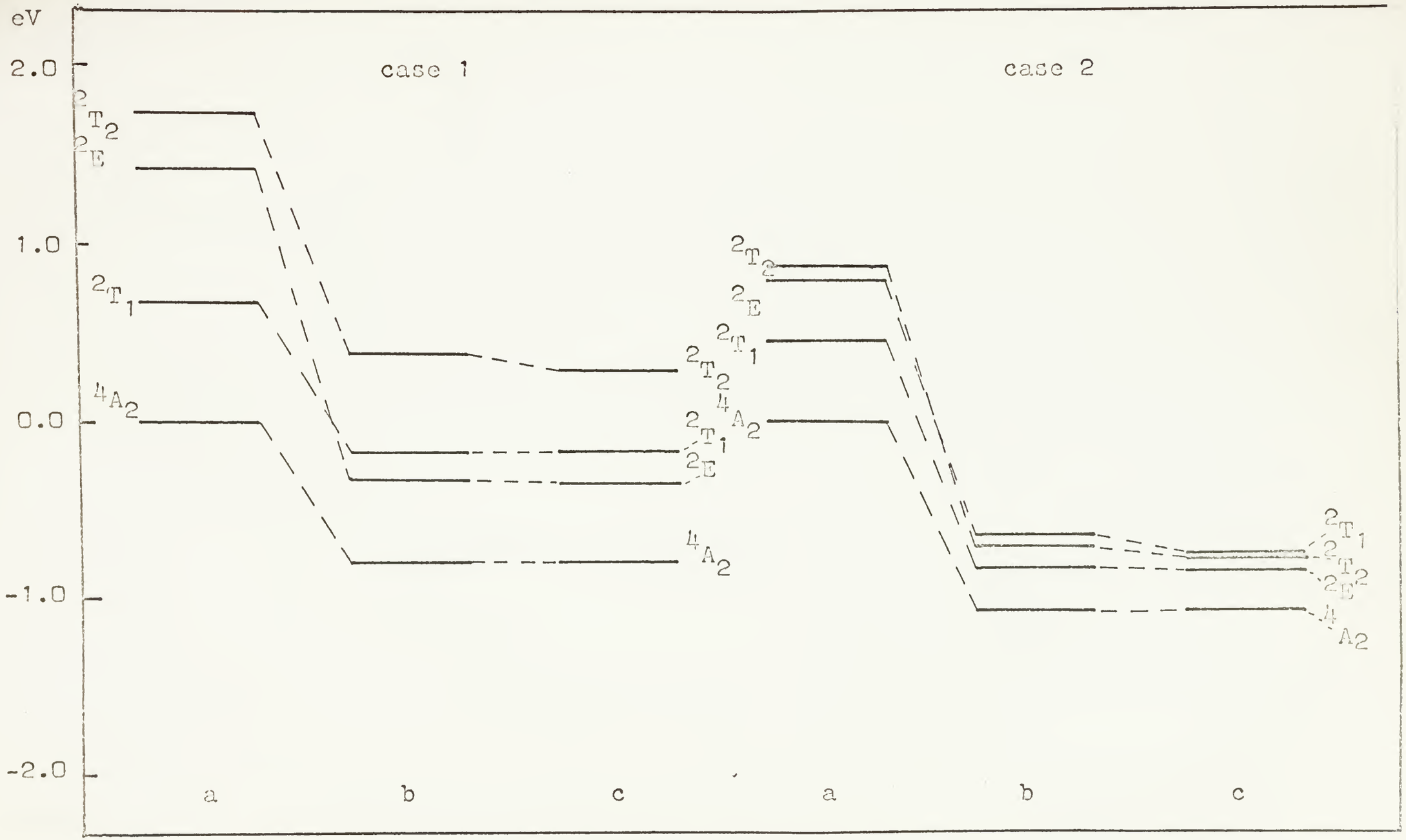


Fig.6.3a Electronic structure of the negatively charged vacancy in diamond using Slater functions.a,undistorted calculation after c.i. b,levels from a. corrected for symmetric relaxation effects.c,levels from b. corrected for Jahn-Teller distortion terms.

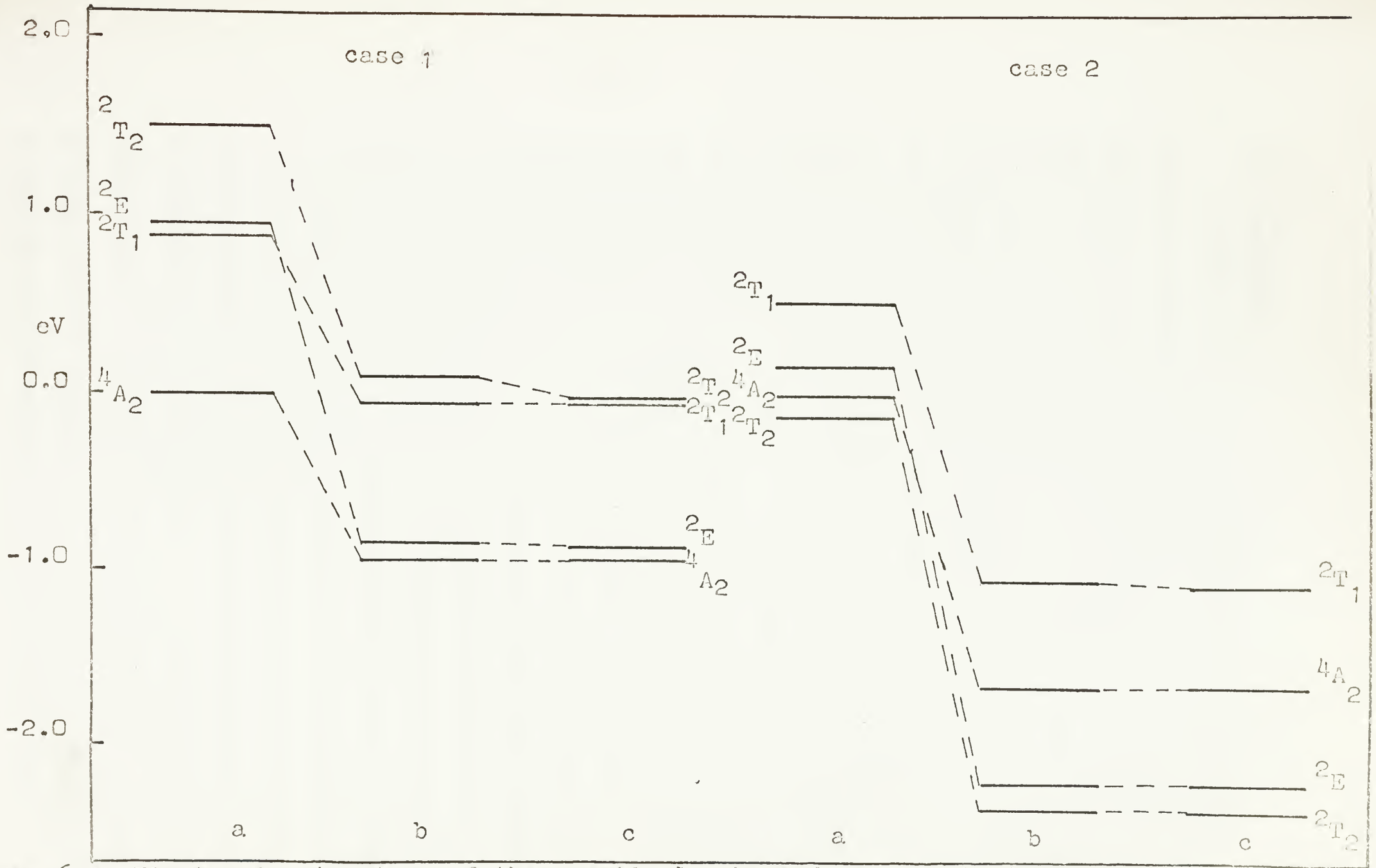


Fig.6.3b Electronic structure of the negatively charged vacancy in diamond using Clementi functions. a,undistorted calculation after c.i. b,corrected levels from a.including symmetric relaxation effects.c,levels from b.corrected for J.-T. TERMS.

iv) V^{2-} centre

For this centre the $^3T_1$ level is predicted to be lowest after the corrections have been made with the exception of the calculation denoted case 2 using Clementi-type functions. In this case the $^1A_1$ level is lowest. If this centre exists then it should have a symmetry axis in the <100> direction and exhibit paramagnetic resonance. However, we must remember that the model as presented is probably least valid for this centre.

Based on the findings from the present calculation it seems unlikely that the GR1 band can be associated with the isolated vacancy system. However, it is possible that an impurity - defect pair system or a multiple defect such as an aggregate of vacancies is responsible for the observed optical absorption. The former seems to be a definite possibility because all diamonds are known to contain at least traces of nitrogen and non-gaseous impurities. It does seem surprising that annealing experiments show that the GR1 band is still observable at temperatures greater than 900°K if this band is associated with the isolated vacancy, when the single vacancy in silicon is thought to be mobile at around 60°K [10]. For this reason we are also inclined to eliminate the isolated interstitial atom as a possible source of this absorption band despite the calculation of Yamaguchi [13] to the contrary. We have been unable to correlate any of the centres investigated with the 'c' system of lines which are known to be associated with a centre which is in some way related to the origin of the GR1 band [42].

Further calculations which take explicit account of relaxation and distortion terms from the beginning of the calculation would be useful. Also since the values of these terms is sensitive to the magnitude of the eigen-vectors from the configuration interaction matrix, the role of delocalization of the electronic wave-function from the vacancy should perhaps be more extensively studied. The assumptions involving the neglect of exchange and polarization effects also require further investigation. Unfortunately all these modifications destroy the major advantage of the model, namely its simplicity.

6.8 Conclusion

The Jahn-Teller splittings and the symmetric relaxation energies associated with the lowest electronic levels of the charge states of the vacancy have been calculated. The electronic structures for the various centres evaluated in chapter 3 have been corrected for these effects. On the basis of the present calculations we conclude that the GR1 band in irradiated diamonds is not associated with the isolated neutral vacancy and is unlikely to be associated with the negatively charged state of this defect.

CHAPTER 7

ELECTRONIC STRUCTURE OF THE ISOLATED VACANCY IN SILICON

The electronic structure of the isolated vacancy in its various charged states in the silicon lattice has been calculated using the defect molecule approach. Atomic Hartree-Fock functions determined by Clementi are used to approximate the 3s and 3p orbitals on the silicon atom in the crystal. Perturbation corrections to allow for symmetric relaxation and Jahn-Teller distortions of the lattice have also been made. The spin multiplicities of the ground state for the various charged centres determined using a modified theory agree with the experimental results obtained by Watkins.

7.1 Introduction

The experimental work of Watkins and others has established, with reasonable certainty, that the isolated vacancy in silicon exists in at least three charge states, V^+, V^o and V^- and possibly also in the double negatively charged state under suitable conditions. Watkins has had considerable success in explaining his observations qualitatively in terms of a one-electron model. Clearly, however, this is a very oversimplified approach and is inadequate for quantitative work as has been demonstrated by Stoneham and Lannoo [111]. From the alternative viewpoint, within the framework of the pseudo-potential band theory method Callaway and Hughes have had only limited success with their first principles calculation. Besides the computational difficulties the approach is not easily adaptable to handle charged centres or to incorporate relaxation effects which may be large

in silicon. The defect molecule approach also has its limitations, which are certainly more serious in silicon than in diamond; nevertheless, it is worthwhile examining the results obtained using this model and assessing its worth by comparing the theoretical results with the known experimental findings. This method has the advantage of giving us some information about the extent of symmetric relaxation and Jahn-Teller distortion effects associated with the lowest states of these defects.

The modifications made to the defect molecule method compared with the diamond calculations are discussed in section 7.2, while the Hamiltonian for the system is given in section 7.3. The form of the wave-functions and the method for determining the energy levels is outlined in the next section. The results obtained using the undistorted model with Clementi-type functions for the 3s and 3p orbitals are given in section 7.5 for both a modified and an unmodified study. Section 7.6 contains a discussion of the determination of the effective frequencies of the silicon lattice, while the magnitude of the symmetric terms and the Jahn-Teller corrections to the electronic levels are calculated in sections 7.7 and 7.8 respectively and then compared with experiment. Some further general comments on the method and all the results including their relationship with experiment are given in section 7.9.

7.2 Model for the Isolated Vacancy in Silicon

The approach to the current problem closely resembles the diamond work reported in previous chapters, and is based on the method developed in chapter 2. We assume that the electronic properties of the defect centre are determined primarily by the n vacancy electrons which are considered to be localized within the defect and do not diffuse out into the rest of the crystal. From the resonance work of Watkins we know this is far from true for some impurity-vacancy pairs and for the isolated vacancy there is probably considerable delocalization of the electronic wave-function. However, we may argue from the preliminary study in diamond (section 3.5) that provided the delocalisation is not too great we may expect this model to predict the same relative ordering of the lowest electronic states as one incorporating delocalisation. The effect of neglecting this effect on the magnitude of the John-Teller and symmetric relaxation terms is more difficult to estimate.

Although, there will be some relaxation of the atoms surrounding the defect, which may not necessarily be small if the results of chapter 5 are a true indication, we have initially chosen to neglect this effect and to use the undistorted lattice parameters to specify the model. However, we will include this effect as a perturbation on the calculation in section 7.7. The internuclear separation between the nearest neighbour atoms to the defect is therefore 7.2566 a.u. The problem now to be solved is the determination of the distribution of the vacancy electrons

in the electric field of the neighbouring atoms and the much weaker tetrahedral field of the rest of the crystal. We assume that the atoms of the perfect silicon crystal are in a tetrahedral sp^3 state and the possible role of d orbitals in bonding is not considered within the approximation used in this investigation. Hence, on removal of an atom from the crystal the four valence electrons on the atoms nearest the defect - termed vacancy electrons - which were covalently bonded to this atom are initially considered to be in sp^3 hybrid orbitals as shown in fig. 2.1. The effects of polarisation by other electron clouds on the electronic properties of the vacancy electron system are neglected; however, we have included the exchange term in the Hamiltonian between the vacancy electrons and other valence electrons on the atoms nearest the defect. This model does provide a useful starting point as there have been no previous calculations using this approach.

7.3 The Hamiltonian for the System

The spin-independent Hamiltonian for the system may be written in the following form:

$$H = H^{\circ} + H^{1}$$

where

$$H^{\circ} = \sum_{i=1}^{n} (T_i + V_i) \qquad (7.1)$$

and

$$H^1 = \sum_{i>j} \frac{1}{r_{ij}} \qquad (7.2)$$

for $i,j = 1,2,\ldots n$ where n is the number of vacancy electrons.

T_i = kinetic energy operator for the i^{th} electron

$V_i = \sum_K V_{Ki}$

where $K = A,B,C,D$ and V_{Ki} is the potential energy of interaction of the i^{th} vacancy electron with atom K which is neighbouring the defect. V_{Ki} may be expressed explicitly as the interaction of the i^{th} vacancy electron with the nucleus of nuclear charge 14, with the K and L shell electrons surrounding the nucleus and with the bonded valence electrons of the atom. We have not been able to evaluate all these contributions explicitly because of the computational time required to determine the values of the integrals for a full compliment of s and p electrons. However, we may write:

$$V_{Ki} = -\frac{Z_{eff}}{r_{Ki}} + \begin{array}{l}\text{repulsion from}\\ \text{the tetrahedral}\\ \text{hybrids around K}\end{array} - \begin{array}{l}\text{exchange interaction}\\ \text{between the vacancy}\\ \text{electron i and bonded valence}\\ \text{electrons on K}\end{array} \qquad (7.3)$$

where Z_{eff} is the effective nuclear charge as seen by the valence electrons. If the nucleus was totally screened by its K and L shell electrons then $Z_{eff} = 4.0$. When dealing with interatomic potential terms such as $\langle b|V_A|b\rangle$ and $\langle a|V_A|b\rangle$ we have used this

value for Z_{eff}. However, for the intra-atomic potential term, $\langle a|V_A|a\rangle$, this is a rather extreme approximation. Slater's rules for an isolated atom predict that for an electron in the valence shell the effective nuclear charge experienced by this electron as a result of screening from the inner shell electrons in the K and L shell would be 5.2. There is reason to believe however that these rules are less accurate for predicting screening constants for the higher shells and therefore, we have preferred to use the estimate obtained by Clementi and Raimondi [116] of $Z_{eff} = 4.88$. This is based upon an analysis to determine the best set of single Slater-type functions to approximate the properties predicted by his atomic Hartree-Fock functions. It is important to note that in this study we have evaluated eqn. (7.3) explicitly instead of using the Goeppert-Mayer and Sklar approximation (eqn.2.9).

7.4 Determination of Wave-functions and Energy Level Scheme

We now proceed as outlined in chapter 2 to determine the energy expressions for the various levels of each centre. The one-electron molecular orbitals v, t_x, t_y and t_z are expressed in terms of the tetrahedral hybrid orbitals a,b,c and d. Then the n-electron determinantal wave-functions for each symmetry state belonging to a particular configuration are determined. These are given in Appendix A.1, while in Appendix A.2 the expressions for the energies of the various symmetry levels before configuration interaction are listed in terms of the molecular

integrals A-K defined in chapter 2. The molecular integrals may be expressed in terms of integrals involving the hybrid orbitals a,b,c and d. These integrals then reduce to a series of one- and two-electron integrals of Coulomb, hybrid, exchange and ionic type which may be evaluated using the Diatomic Molecular Integral Program referred to earlier. The three- and four-centre integrals are evaluated using the Mulliken approximation. Before we can evaluate these integrals it is necessary to make some choice as to the form of the 3s and 3p wave-functions for these orbitals on the silicon atoms nearest the defect. We have once again chosen to use the ortho-normal set of self-consistent atomic Hartree-Fock functions determined by Clementi [60] for the ^3P ground state of the silicon atom as a suitable approximation for these orbitals. These functions are given in table 7.1. In table 7.2 the values of the basic one- and two-electron integrals required for the vacancy calculation are listed.

The value for the one-centre Coulomb integral, Q, was calculated analytically to be 11.45 eV compared with the semi-empirical value of 8.10 eV obtained using the procedure described in Appendix A.3. This suggests that it may be valuable to consider the case where this integral is modified. It should be stressed, however, that this estimate of Q is subject to reasonable uncertainty, because of the lack of information about the parameters from which it is deduced. It will nevertheless give us some information about the sensitivity of the ordering

TABLE 7.1

Hartree-Fock functions for the isolated silicon atom

Basis	Orbital Exponent	3s	Basis	Orbital Exponent	3p
1s	14.00000	0.06602	2p	7.00000	-0.12080
3s	15.98210	0.00170	4p	15.84610	-0.00151
3s	10.59690	-0.04004	4p	10.51460	-0.00300
3s	7.77150	-0.08885	4p	6.83460	-0.07161
3s	5.23940	-0.20265	4p	4.72810	0.01063
3s	2.90000	-0.04761	4p	2.30100	0.48091
3s	2.08920	0.61435	4p	1.30130	0.57523
3s	1.29450	0.52025	4p	0.77340	0.04276

TABLE 7.2

Values of one- and two-electron integrals for silicon vacancy calculation: Clementi functions

Integral	Value	Integral	Value
$\langle a\|T\|a\rangle$	28.6204*	$\langle a\|b\rangle$	0.2045
$\langle a\|T\|b\rangle$	0.0781	$\langle aa\|\frac{1}{r_{12}}\|aa\rangle$	11.4494
$\langle a\|V_A\|a\rangle$	-42.5759	$\langle ab\|\frac{1}{r_{12}}\|ab\rangle$	5.2054
$\langle a\|V_A\|b\rangle$	-2.3400	$\langle ab\|\frac{1}{r_{12}}\|ba\rangle$	0.4132
$\langle b\|V_A\|b\rangle$	-5.3716	$\langle aa\|\frac{1}{r_{12}}\|ab\rangle$	1.7379

*All energies are in electron volts

of the lowest levels to variations in Q. Using the form for the potential discussed in section 7.3 the intra-atomic integral $\langle a|V_A|a\rangle$ is independent of Q. It is now possible to determine the energy of the various symmetry states for a particular configuration and then to allow configurational mixing between symmetry states from different configurations to obtain the lowest levels for each centre.

7.5 Results for the Isolated Vacancy

In this section we present the results obtained for V^+, V^o, V^- and $V^=$ using both the modified and unmodified values for Q. Table 7.3 contains the values of the one- and two-electron molecular integrals, A-K, which are required to determine the electronic levels before configuration interaction. As was the case for the diamond problem there are considerable changes in the values of the two-electron integrals as Q decreases. These differences again have a significant effect on the energy level which results. The difference between the one-electron integrals A and B is now only 2.02 eV compared with a difference of nearly 12 eV in the diamond calculation. As a consequence of this we expect configurational mixing between the various configurations from states of the same symmetry and spin multiplicity to be even more important than in the diamond vacancy system in determining the ordering of the lowest levels. It should also be noted that the energy difference, A-B, is the separation between the levels of a_1 and t_2 symmetry in the one-electron model used in the qualitative discussion by Watkins to describe his results.

TABLE 7.3

Molecular integrals required for the silicon vacancy calculations: Clementi functions

Integral	Unmodified Case Q = 11.45 eV	Modified Case Q = 8.10 eV
A^+	-31.2772*	-31.2772
B	-29.2541	-29.2541
C	6.8430	6.4416
D	6.8653	5.6528
E	6.7682	6.1704
F	6.6601	5.2262
G	1.8168	1.1645
J	1.5573	0.2341
K	-1.6236	-0.6945

+Integrals defined as in chapter 2

*All energies are in electron volts

The delocalisation investigation on the diamond vacancy in section 3.5 suggests that this separation will decrease further with increasing delocalisation of the electronic wave-function from the vacancy.

In figs. 7.1 to 7.4 the predicted energy level schemes for the V^+,V^0,V^- and $V^=$ centres before and after configuration interaction are shown for the undistorted vacancy model using both values of Q. From the diagrams it is apparent that in the calculation with Q = 8.10 eV the energy level schemes are much more compact than in the calculation with the analytical value of 11.45 eV for Q. There are cases for Q = 8.10 eV where symmetry states from 'higher' configurations are almost degenerate with similar symmetry states from 'lower' configurations before configuration interaction. For example, in the calculation for the neutral vacancy the $^3T_1$ level from the $v^2t_2^2$ configuration is only 0.06 eV below the $^3T_1$ level from the vt_2^3 configuration. Also in the V^- calculation only 0.30 eV separates the $^2T_2$ levels from the $v^2t_2^3$,vt_2^4 and t_2^5 configurations before configuration mixing. If we were to use the simple one-electron model proposed by Watkins in which all electron-electron interactions terms are neglected symmetry states from different configurations should be separated from one another by 2.02 eV. Also in the one-electron model, we expect all the symmetry states belonging to a particular configuration to be degenerate. In fact, this is far from true in some cases. For example, the $^1A_1$, ^1E, $^1T_2$ and $^3T_1$ symmetry states from the $v^2t_2^2$ configuration span 4.9 eV with Q = 11.45 eV and 1.2 eV with Q = 8.10 eV. Even in this latter case the levels

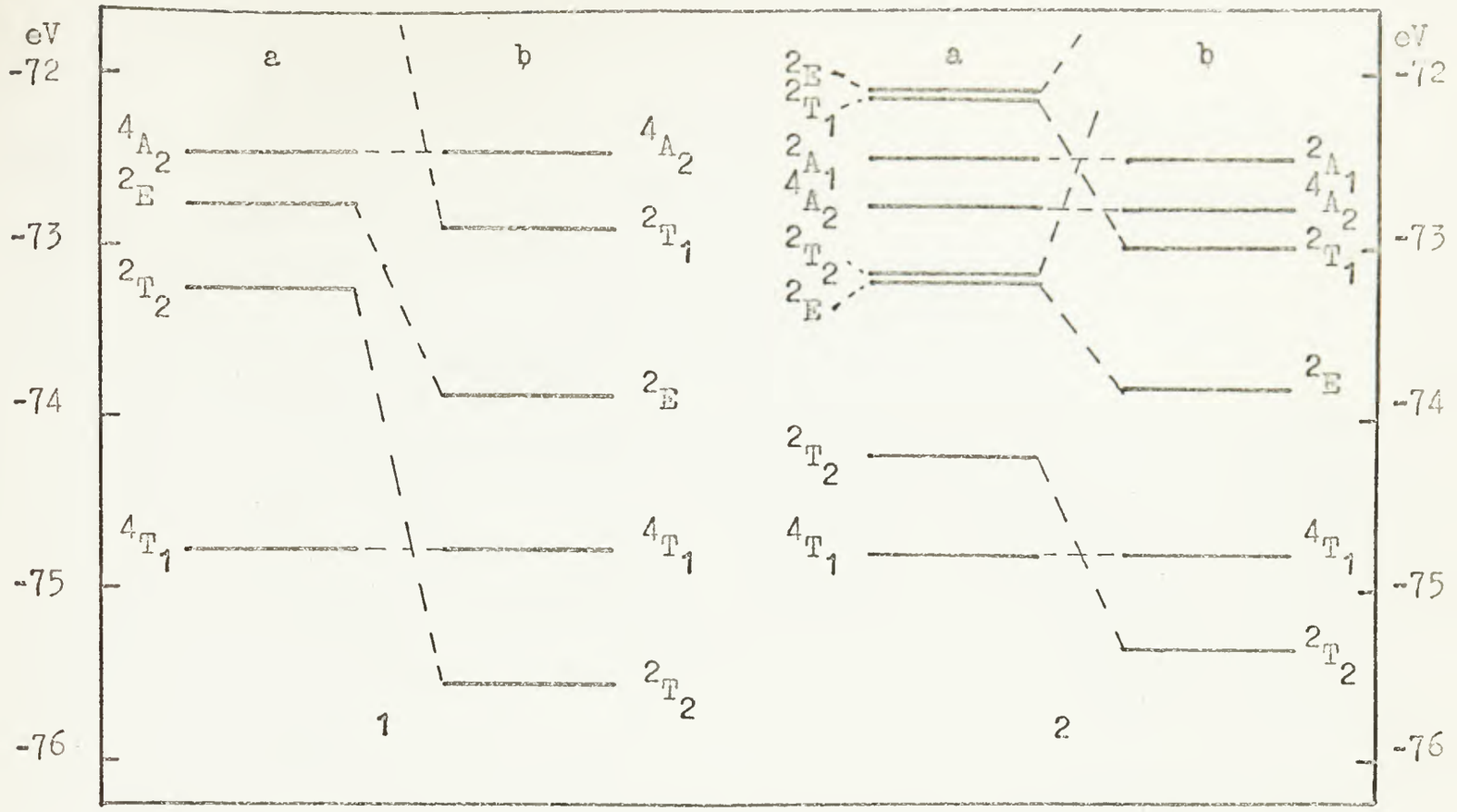


Fig.7.1 Electronic structure of the positively charged vacancy in the silicon crystal. a. before configuration interaction, b. after configuration interaction. 1. Q = 11.45 eV 2. Q = 8.10 eV.

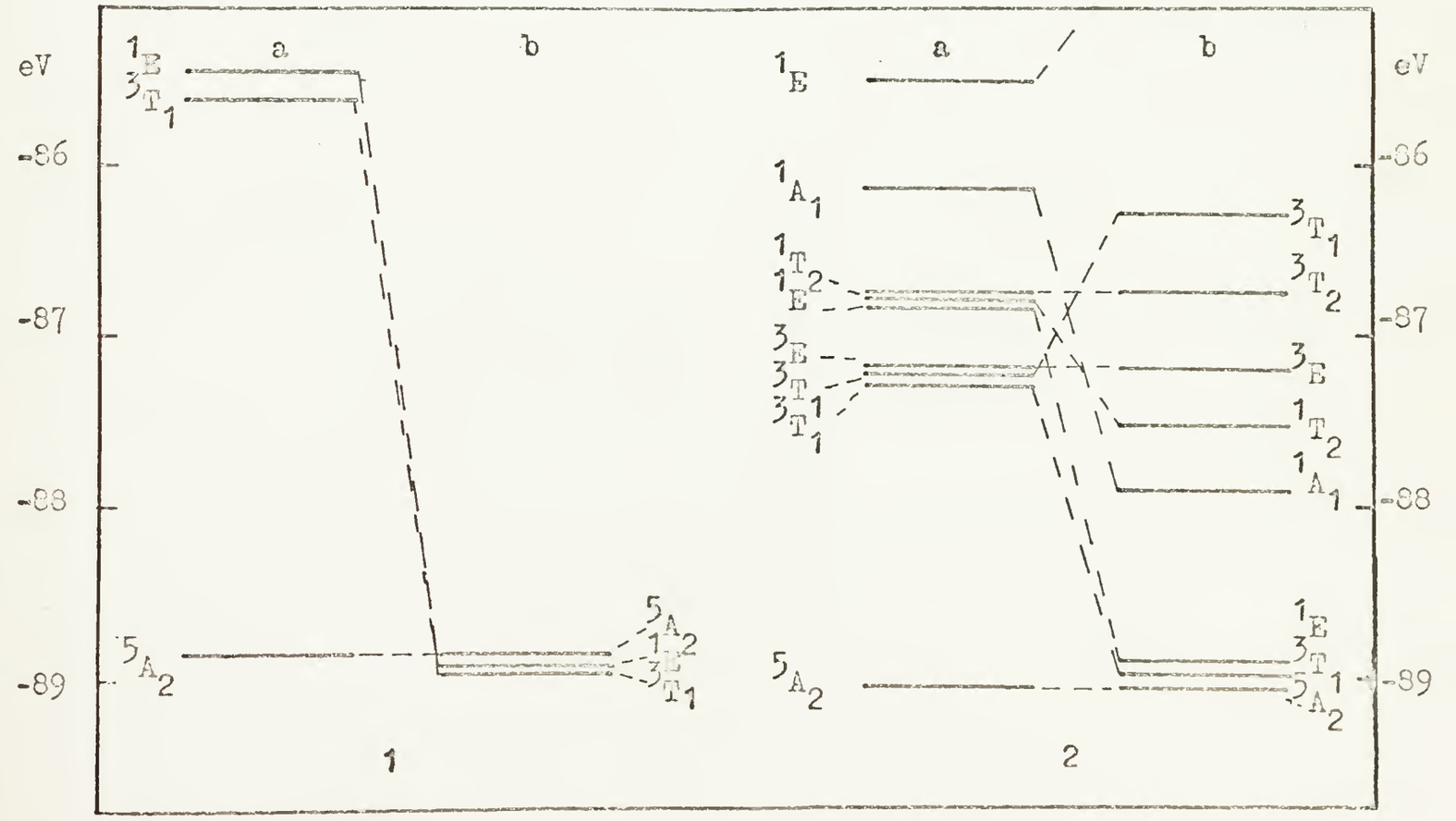


Fig.7.2 Electronic structure of the neutral vacancy in the silicon crystal. a. before configuration interaction, b. after configuration interaction. 1. Q = 11.45 eV 2. Q = 8.10 eV.

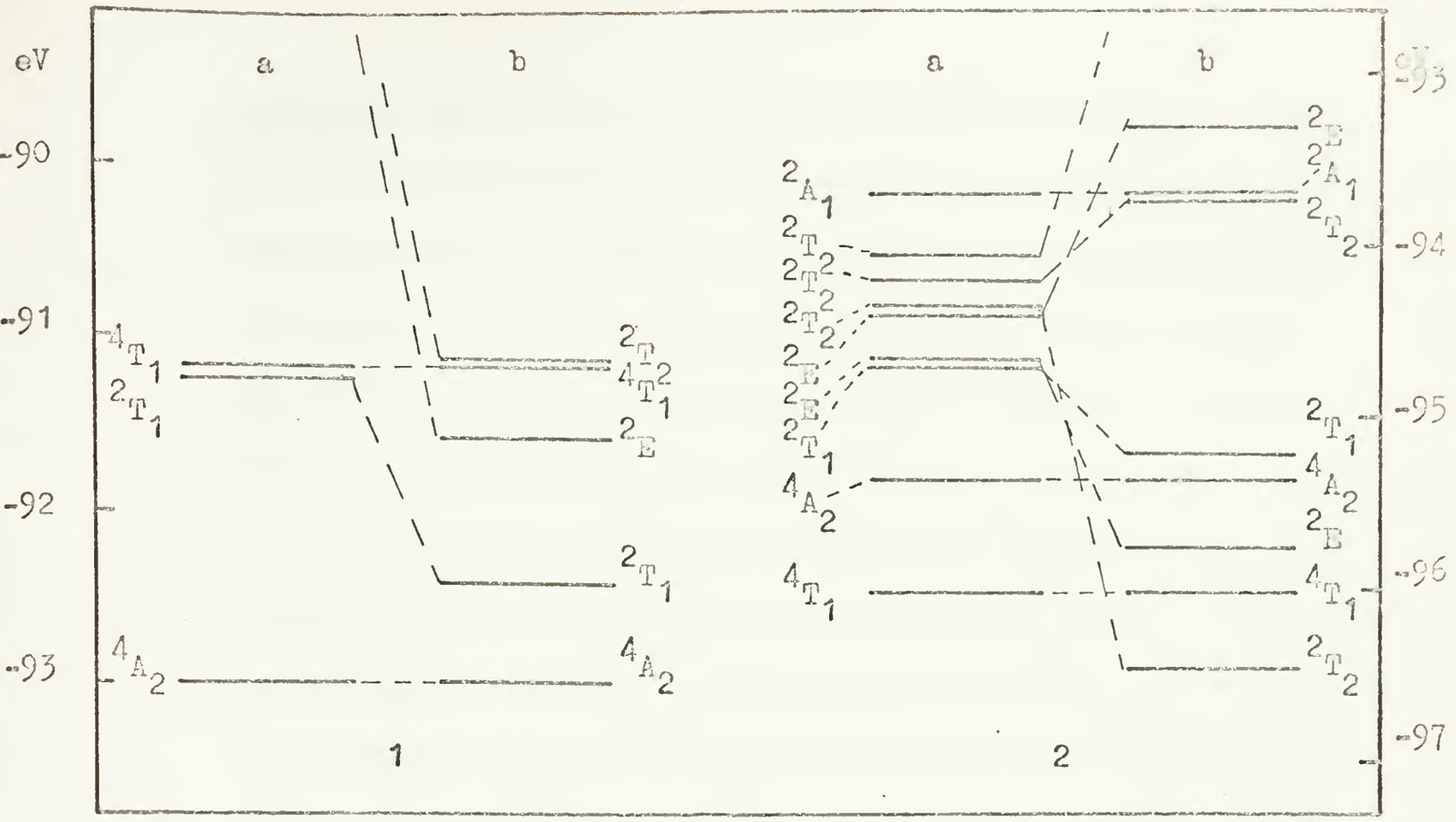


Fig.7.3 Electronic structure of the single negatively charged vacancy in the silicon crystal. a. before configuration interaction, b. after configuration interaction. 1. Q = 11.45 eV 2. Q = 8.10 eV.

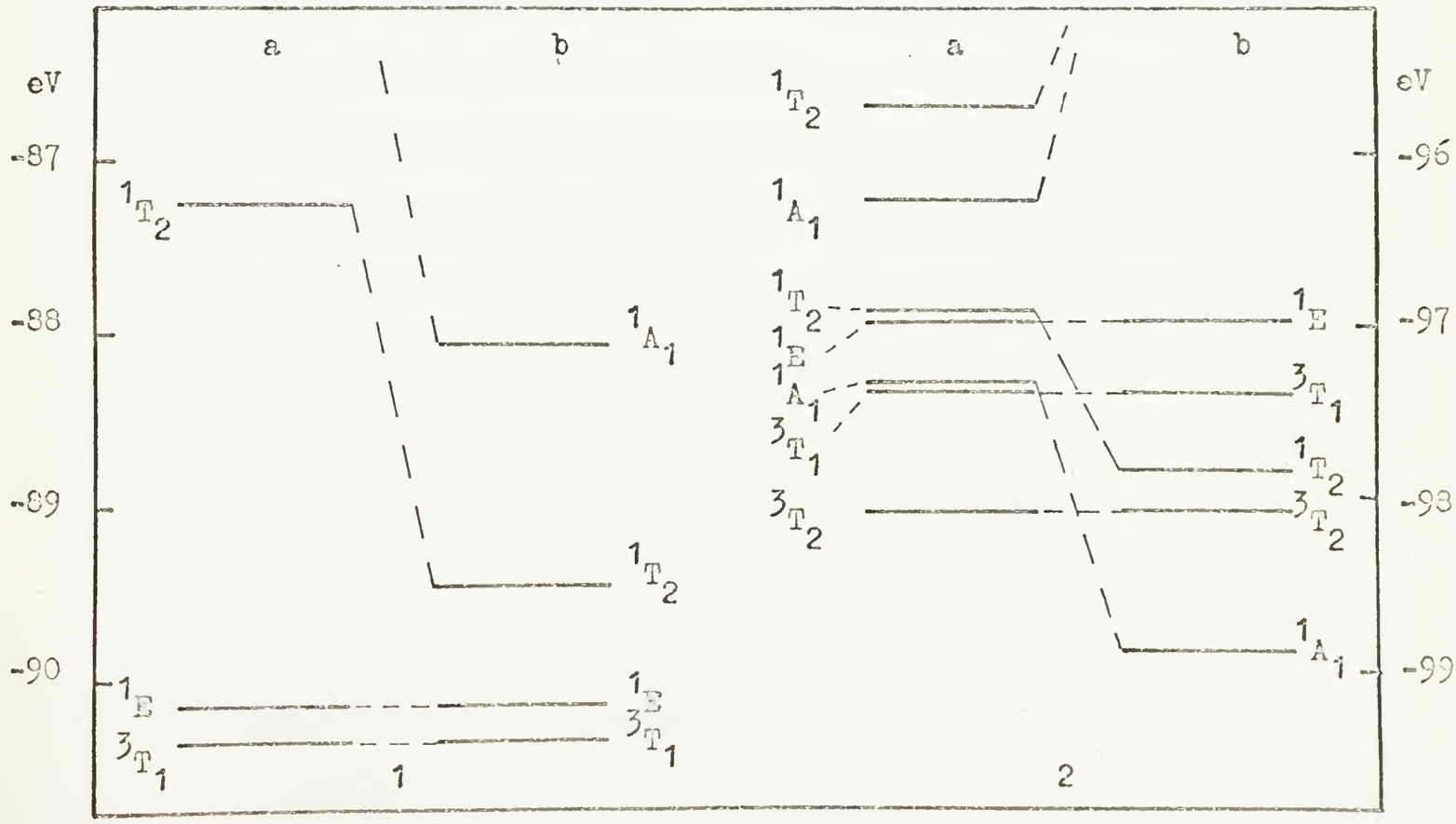


Fig.7.4 Electronic structure of the double negatively charged vacancy in the silicon crystal. a. before configuration interaction, b. after configuration interaction. 1. Q = 11.45 eV 2. Q = 8.10 eV.

can hardly be regarded as nearly degenerate. From the energy level schemes it is apparent that in almost all the calculations configuration interaction has a major role in determining the relative ordering of the energy levels and often causes very significant changes in the energies of the levels. We now look in more detail at the calculation for each centre.

For the positively charged vacancy, the calculation shown in fig. 7.1 predicts that for both estimates of the one-centre coulomb integral the $^2T_2$ level is lowest in energy after configuration interaction has been included. Before the mixing of the symmetry states from the various configurations the $^4T_1$ level is lowest in energy. This differs from the calculation for the diamond vacancy where the $^2T_2$ level is always lowest in energy. The prediction of a doublet level as the ground state of this centre is in agreement with the experimental findings of Watkins [10]. The predicted ordering of the lowest levels is the same for both calculations. Electronic transitions from the $^2T_2$ to the ^2E and $^2T_1$ levels are allowed, but are unlikely to be observed because these levels would not be bound states in the band gap of the semi-conductor. However, they may give rise to resonance states in the conduction band.

The $^5A_2$, $^3T_1$ and ^1E electronic levels of the V^o centre are predicted to be very close together after configuration interaction in both calculations given in fig. 7.2. The position of the ^1E and $^3T_1$ levels is very dependent upon the extent of

configurational mixing. In the calculation with Q = 8.10 eV marked changes in the ordering of the energy levels result due to mixing of like symmetry states from different configurations. For Q = 11.45 eV the $^3T_1$ level is lowest only 0.02 eV below the ^1E level and 0.05 eV below the $^5A_2$ level, while for Q = 8.10 eV the $^5A_2$ level is lowest 0.06 eV below the $^3T_1$ level and 0.15 eV below the ^1E level. These levels are so close together that such factors as the Jahn-Teller distortion effects, symmetric relaxation terms and possibly interlevel coupling effects will be important in determining the ground state for this centre. The position of the $^1A_1$ and $^1T_2$ levels is very sensitive to the value given to Q as also was the case in the diamond vacancy calculation. Watkins' study would suggest that this centre should be diamagnetic. We defer further discussion of this centre until section 7.7.

The unmodified study for the negatively charged vacancy, given in fig. 7.3, predicts that the $^4A_2$ level is lowest; however, the $^2T_2$ and $^4T_2$ levels are very sensitive to the value of Q and for Q = 8.10 the $^2T_2$ level is predicted to be the ground state of this centre. As mentioned earlier the $^2T_2$ symmetry states from the three possible configurations are separated by only 0.3 eV for Q = 8.10 eV and configuration interaction is sufficient to cause the $^2T_2$ level to become the ground state for the V^- centre. For Q = 11.45 eV configuration interaction effects are also large for the ^2E and $^2T_2$ levels but the lowest symmetry states from the $v^2t_2^3$ configuration are initially about 5 eV above

the $^4A_2$ level. Watkins [10] predicts that the lowest level in this centre is a doublet such that the modified results seem to be in better agreement with experiment.

Figure 7.4 shows the results of a calculation for the double negatively charged centre. Again the ordering of the levels is very sensitive to the value chosen for Q. In particular the energy of the $^1A_1$ and $^3T_2$ levels alters significantly relative to that for the ^1E and $^3T_2$ levels. In the unmodified case the $^3T_1$ level is lowest 0.20 eV below the ^1E level, whereas in the modified case the $^1A_1$ level is lowest 0.80 eV below the $^3T_2$ level. For Q = 8.10 eV the $^1A_1$ symmetry state from the configuration t_2^6 is predicted to be 1.05 eV lower in energy than the same symmetry state from the $v^2t_2^4$ configuration. This is contrary to what would be predicted with the simple one-electron model and reflects the importance of the electron-electron interaction terms in this calculation. Watkins predicts that the ground state of this centre is diamagnetic. Hence, it would seem that the modified case again gives the better agreement with experiment. However, it must be remembered that the model is least applicable to this centre.

The calculations using the defect molecule method with an undistorted model for the vacancy predict ground states of the correct multiplicity for the V^+, V^- and $V^=$ centres when we choose a semi-empirical value of 8.10 eV for Q. For the V^o centre the calculation is ambiguous. Electron-electron interaction terms and configuration interaction effects are shown to be very important

in determining the relative ordering of the lowest levels. Before we can draw any firm conclusions as to the ground states of these centres we must consider the energy corrections due to the symmetric relaxation terms and the Jahn-Teller distortion effects.

7.6 The Effective Frequencies for the Silicon Lattice

Before we can proceed with the calculation of the symmetric relaxation terms and the Jahn-Teller energies it is necessary to determine suitable values for the response frequencies of the lattice, ω_a,ω_E and ω_T to various distortions. We have again made use of the dynamic relaxation program described in chapter 5 and the method outlined in section 6.3. For the system containing the vacancy forces which were $1/\sqrt{5}$ times the unit force were applied to the four atoms nearest the defect instead of unit forces because of the longer time to reach the relaxed equilibrium state for this lattice as a consequence of larger displacements of atoms than for the diamond crystal. This does not effect the relation 6.21 as we have assumed that the energy change is linearly dependent upon the applied force. The displacements of the atoms nearest the defect at equilibrium under the applied forces are given in table 7.4. Using these equilibrium values the following values for the effective frequencies are calculated

TABLE 7.4

Position of the atoms adjacent to the vacancy in silicon after relaxation for applied forces of appropriate symmetry

Atom	Initial Co-ordinates	Relaxed Co-ordinates		
		E symmetry	T_ξ symmetry	A_1 symmetry
A	$(\bar{1},1,1)$*	(-1.0,1.054,0.947)	(-1.032,1.087,1.087)	(-1.085,1.085,1.085)
B	$(1,\bar{1},1)$	(1.0,-1.055,0.946)	(0.977,-0.924,0.924)	(1.085,-1.085,1.085)
C	$(1,1,\bar{1})$	(1.0,1.055,0.945)	(0.977,0.924,-0.924)	(1.085,1.085,-1.085)
D	$(\bar{1},\bar{1},\bar{1})$	(-1.0,-1.055,-0.945)	(-1.034,-1.089,-1.089)	(-1.088,-1.088,-1.088)

*All co-ordinates in units of a/4

$$\omega_E = 0.54 \times 10^{14} \text{ rad/sec}$$
$$\omega_T = 0.44 \times 10^{14} \text{ rad/sec}$$
$$\omega_a = 0.39 \times 10^{14} \text{ rad/sec.}$$

Elkin and Watkins [117] have calculated that ω_E is equal to 0.63×10^{14} rad/sec using the Swalin force constants [54] while the value for the Raman frequency is 0.985×10^{14} rad/sec. We note that the effective frequencies are a much smaller proportion of the Raman frequency for the silicon crystal than in the diamond case. Because of the larger displacements of the atoms nearest the silicon vacancy the assumption embodied in eqn.(6.21) will be less accurate in the present problem. However, at present we have no better means of calculating these frequencies.

7.7 The Symmetric Relaxation Term for the Isolated Vacancy

In the previous chapter the theory for the change in energy of the electronic levels as a function of the magnitude of the symmetric mode, Q_a, was developed. The equilibrium configuration and the lowering in energy for each level to first order is calculated using eqns. (6.33) and (6.34). When second order terms are included the appropriate relationships are given by eqns. (6.40) and (6.41). We have calculated by this method the lowering in energy and the equilibrium configuration for the following levels due to a symmetric relaxation.

V^+ : $^2T_2$, $^4T_1$

V^o : $^3T_1$, ^1E, $^5A_2$, $^1T_2$, $^1A_1$

V^- : $^4A_1$, $^2T_1$, ^2E, $^2T_2$, $^4T_1$

$V^=$: $^3T_1$, ^1E, $^1T_2$, $^3T_2$, $^1A_1$

To determine I_a, the electron-lattice coupling term, for each level it is necessary to know the derivatives of the atomic integrals. The formula given in eqn.(6.31) was used to calculate their values and these are given in table 7.5. Using these values for the derivatives and formulae based upon the information given in Appendices A.2 and C.2. the values of I_a for each level has been calculated. In tables 7.6 to 7.9 the values for the lowering in energy and the extent of relaxation, including first and second order terms, are given for the lowest levels of the V^+, V^o,V^- and $V^=$ centres. The results for the V^o,V^- and $V^=$ systems are shown in figs. 7.5, 7.6 and 7.7 respectively using a value of 0.39×10^{14} rad/sec for ω_a. From the tables it is apparent that this calculation predicts a very large lowering in energy for all levels. Comparison of the predicted distortions Q_a' with tables 7.10 reveals that these are unreasonably large values. For most levels Q_a' has a value between -1.75 and -2.25Å. To obtain such a large distortion it is necessary for each atom nearest the defect to be displaced about 1Å inwards which is most unlikely.

TABLE 7.5

Values of the derivatives of the atomic integrals for the silicon vacancy calculation

$\frac{d}{dR_{AB}}$ (Integral)	Clementi Functions	$\frac{d}{dR_{AB}}$ (Integral)	Clementi Functions
$\langle a \mid b \rangle$	-0.1845*	$\langle ab \mid \frac{1}{r_{12}} \mid ab \rangle$	-2.1329
$\langle a \mid T \mid b \rangle$	-0.5307	$\langle ab \mid \frac{1}{r_{12}} \mid ba \rangle$	-0.8105
$\langle a \mid V_A \mid b \rangle$	2.7116	$\langle aa \mid \frac{1}{r_{12}} \mid ab \rangle$	-1.8829
$\langle a \mid V_B \mid a \rangle$	2.6797		

*All derivatives in eV/Å

TABLE 7.6

Values of the symmetric term for the lowest $^2T_2$ and $^4T_1$ levels of the positive vacancy

Value of Q eV	ω_a=0.39x10^{14} rad/sec			ω_a=0.54x10^{14} rad/sec		
	Ia' eV/Å	ΔEa' eV	Qa' Å	Ia' eV/Å	ΔEa' eV	Qa' Å
1. $^2T_2$ Level						
11.45	8.20	7.54	-2.01	7.83	3.60	-0.96
8.10	7.65	6.58	-1.77	7.55	3.35	-0.90
2. $^4T_1$ Level						
11.45	7.12	5.60	-1.61	7.12	2.81	-0.84
8.10	7.14	5.72	-1.62	7.14	2.83	-0.84

TABLE 7.7

Value of the symmetric terms for the lowest $^3T_1$, $^1T_2$, ^1E $^1A_1$ and $^5A_2$ levels of the neutral vacancy

Value of Q eV	ω_a=0.39x10^{14} rad/sec			ω_a=0.54x10^{14} rad/sec		
	Ia' eV/Å	ΔEa' eV	Qa' Å	Ia' eV/Å	ΔEa' eV	Qa' Å
1. $^3T_1$ Level						
11.45	8.88	8.71	-2.30	8.15	3.90	-1.03
8.10	8.30	7.69	-2.08	7.81	3.59	-0.97
2. ^1E Level						
11.45	8.78	8.55	-2.25	8.14	3.89	-1.02
8.10	7.71	6.71	-1.77	7.64	3.44	-0.91
3. $^1T_2$ Level						
11.45	9.44	10.03	-2.25	9.16	4.94	-1.11
8.10	10.22	11.76	-2.42	9.96	5.84	-1.20
4. $^5A_2$ Level						
11.45	7.68	6.66	-1.74	7.68	3.48	-0.91
8.10	7.87	7.00	-1.78	7.87	3.65	-0.93
5. $^1A_1$ Level						
8.10	9.55	10.33	-2.16	9.54	5.38	-1.13

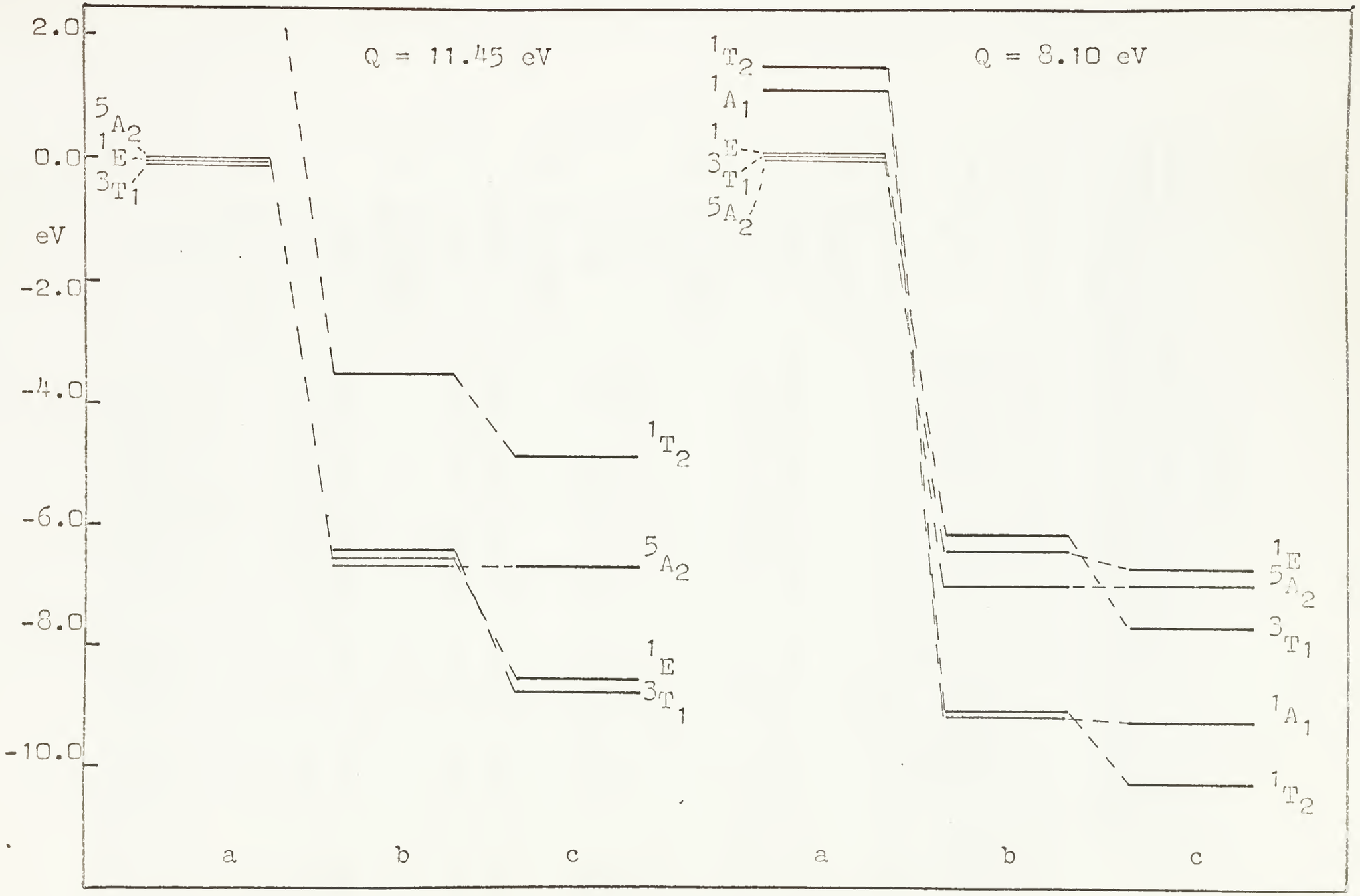


Fig.7.5 Electronic structure of the neutral vacancy in silicon with $\omega_a = 0.39 \times 10^{14}$ rad/sec. a, $Q_a = 0$. b, Q_a includes first-order terms only. c, Q_a includes first- and second-order terms.

TABLE 7.8

Value of the symmetric terms for the lowest $^2T_2$, $^2T_1$, ^2E, $^4T_1$ and $^4A_2$ levels of the negatively charged vacancy

Value of Q eV	ω_a=0.39x10^{14} rad/sec			ω_a=0.54x10^{14} rad/sec		
	Ia' eV/Å	ΔEa' eV	Qa' Å	Ia' eV/Å	ΔEa' eV	Qa' Å
1. $^2T_2$ Level						
11.45	10.18	11.26	-2.75	9.03	4.76	-1.16
8.10	9.34	9.86	-2.11	9.34	5.14	-1.10
2. $^2T_1$ Level						
11.45	8.70	8.50	-2.04	8.51	4.27	-1.02
8.10	8.45	8.06	-1.93	8.40	4.16	-1.00
3. ^2E Level						
11.45	9.58	10.06	-2.53	8.66	4.39	-1.10
8.10	8.99	9.13	-2.03	8.99	4.76	-1.06
4. $^4T_1$ Level						
11.45	8.08	7.36	-1.82	8.08	3.83	-0.95
8.10	9.06	9.23	-2.05	9.06	4.80	-1.10
5. $^4A_2$ Level						
11.45	8.34	8.44	-1.95	8.64	4.40	-1.02
8.10	8.58	8.32	-1.94	8.58	4.34	-1.01

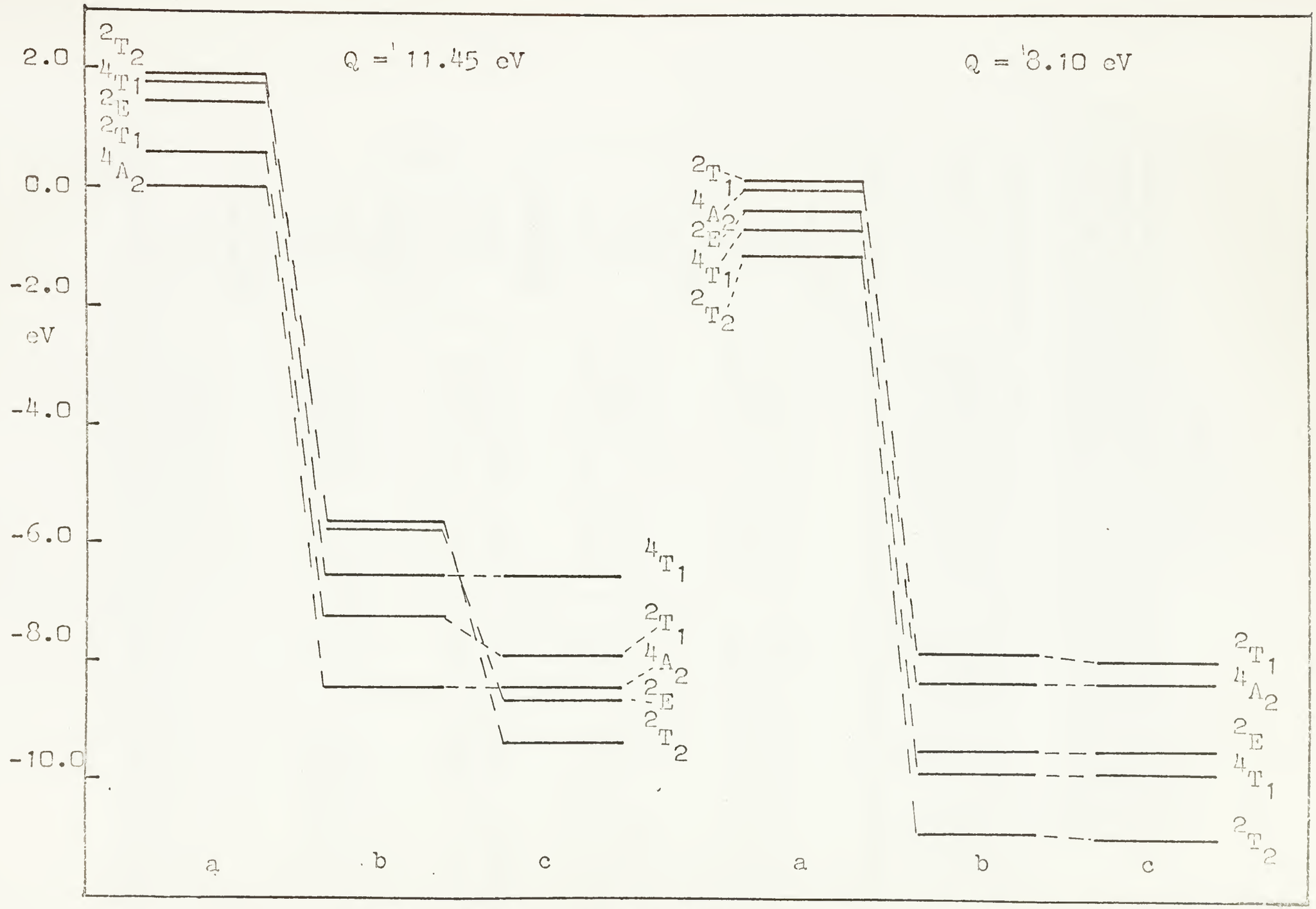


Fig.7.6 Electronic structure of the negatively charged vacancy on silicon with $\omega_a = 0.39 \times 10^{14}$ rad/sec. a, $Q_a = 0$ b, Q_a includes first-order terms only. c, Q_a includes first- and second-order terms.

TABLE 7.9

Value of the symmetric term for the lowest $^3T_1$, ^1E, $^1T_2$ $^3T_2$ and $^1A_1$ levels of the double negatively charged vacancy

Value of Q eV	ω_a=0.39x10^{14} rad/sec			ω_a=0.54x10^{14} rad/sec		
	Ia' eV/Å	ΔEa' eV	Qa' Å	Ia' eV/Å	ΔEa' eV	Qa' Å
1. $^3T_1$ Level						
11.45	8.33	7.83	-1.88	8.33	4.08	-0.98
8.10	9.01	9.18	-2.04	9.01	4.79	-1.06
2. $^1T_2$ Level						
11.45	9.03	9.11	-2.26	8.51	4.25	-1.06
8.10	10.01	11.22	-2.46	9.54	5.35	-1.17
3. ^1E Level						
11.45	8.11	7.43	-1.83	8.11	3.88	-0.96
8.10	8.59	8.34	-1.94	8.59	4.35	-1.01
4. $^3T_2$ Level						
11.45	7.72	6.73	-1.74	7.72	3.53	-0.92
8.10	9.59	10.38	-2.16	9.59	5.40	-1.13
5. $^1A_1$ Level						
11.45	11.34	13.23	-3.32	9.21	4.91	-1.23
8.10	10.21	11.77	-2.31	10.20	6.12	-1.20

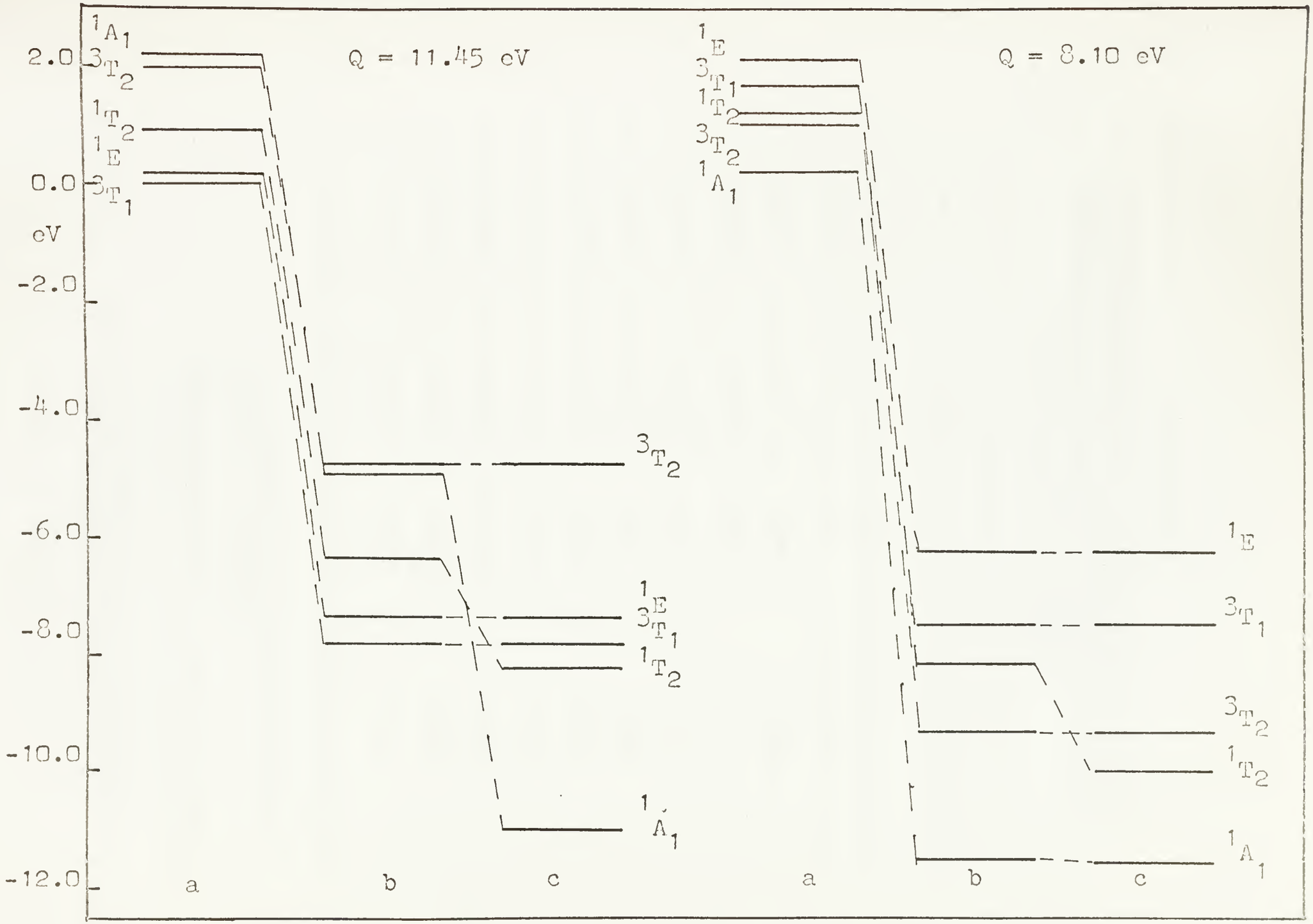


Fig.7.7 Electronic structure of the double negatively charged vacancy in silicon with $\omega_a = 0.39\times10^{14}$ rad/sec. a, $Q_a = 0$ b, Q_a includes first-order terms only. c, Q_a includes first- and second-order terms.

TABLE 7.10

Displacement of, and distance between, the nearest neighbour atoms of the silicon vacancy for various values of the symmetric mode

Q_a Å	$X_A = -\frac{Q_a}{\sqrt{12}}$ Å	$\Delta R_A = \sqrt{3}\, X_A$ Å	$R_{AB} = \sqrt{8}\,(\frac{a}{4} - X_A)$ Å
0.0	0.0	0.0	3.84
-0.80	0.231	0.40	3.19
-0.90	0.260	0.45	3.11
-1.00	0.289	0.50	3.02
-1.10	0.318	0.55	2.94
-1.75	0.505	0.875	2.41
-2.00	0.578	1.000	2.21
-2.25	0.650	1.125	2.00
-2.50	0.722	1.250	1.80
-2.75	0.794	1.375	1.62

X_A represents the displacement of atom A in the x direction

ΔR_A represents the total inward displacement of atom A

R_{AB} is the distance between atoms A and B after a symmetric relaxation Q_a

a is the cell constant

There are at least two possible reasons for the inadequacy of this calculation. It may be that the estimate of the electronic term I_a using such a simple model is too large. Delocalisation of the electronic wave-function from the defect may cause a decrease in the magnitude of this term. However, the value of this term is already significantly reduced relative to the calculated value for the diamond vacancy problem. Therefore, we are inclined to think that this is not the principal factor causing the unsatisfactory estimate. The results would also be in error if an incorrect value was chosen for the response frequency, ω_a, of the breathing mode. Our estimate of this factor was based upon the assumption that there was a linear dependence of the energy change on the applied force. This is probably reasonable for small displacements of the atoms in the lattice, but is an oversimplification in the present problem. Higher order terms involving the applied force may also be important. For example, if we included second order terms then eqn. (6.21) becomes

$$E(Q_a) = - (F_a^o + f_a Q_a) Q_a + \tfrac{1}{2} M(\omega_a')^2 Q_a^2 \qquad (7.4)$$

where

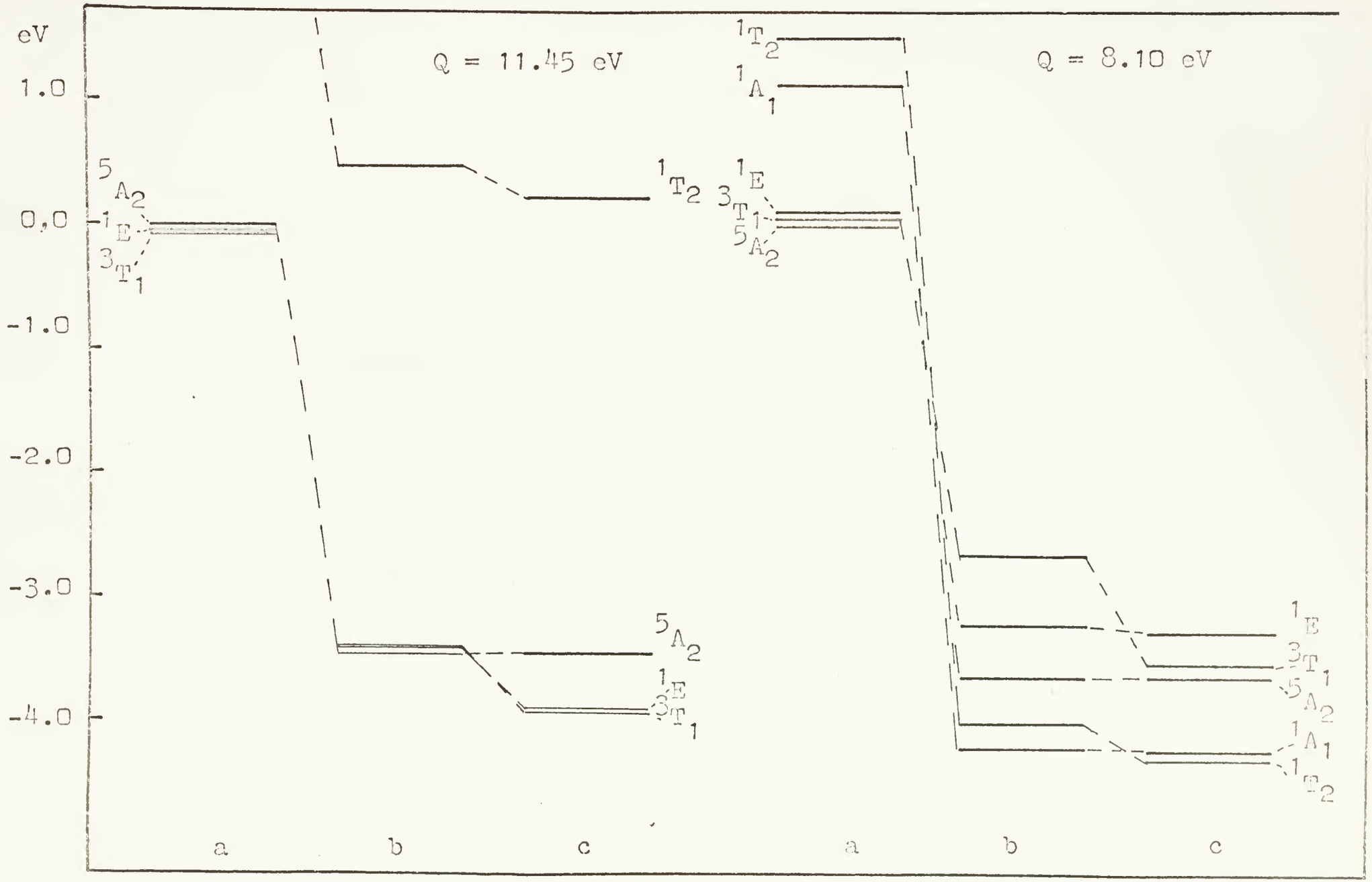
$$f_a = \left(\frac{\partial F_a}{\partial Q_a}\right)_o$$

and F_a^o is the applied force. Now at equilibrium $\dfrac{\partial E(Q_a)}{\partial Q_a} = 0$ such that

$$\omega_a' = \omega_a \sqrt{\left(1 + \frac{2f_a Q_a}{F_a}\right)} \qquad (7.5)$$

where ω_a is the effective frequency when f_a is zero and ω_a' is the frequency including second order terms. For our problem it is necessary to postulate that $\frac{f_a Q_a}{F_a}$ is positive such that $\omega_a' > \omega_a$ in order to reduce the magnitude of the symmetric relaxation. To examine the influence of a change in the value of ω_a on the energy lowerings and the ordering of the lowest levels we rather arbitrarily choose $\omega_a = 0.54 \times 10^{14}$ rad/sec., the value calculated for ω_E. In tables 7.6 to 7.9 the values for I_a', $\Delta E_a'$ and Q_a' are given using the above value for ω_a. The results for V^o,V^- and $V^=$ showing first and second order terms are presented in fig. 7.8,7.9 and 7.10 respectively. Comparison of the results in the tables reveal that the energy lowerings and extent of relaxation are reduced to about half their previous values when ω_a is increased from 0.39 to 0.54×10^{14} rad/sec. Q_a is now in the range 0.90 to 1.10 for most levels which corresponds to a displacement of about 0.5Å inwards for the atoms nearest the defect. These are still quite large displacements but at least more reasonable. The experimental work of Watkins also predicts that the relaxation of the atoms nearest the defect will be inwards.

It is significant that while the magnitude of the distortions are sensitive to the value chosen for ω_a, for the case where Q = 8.10 eV at least, the ordering of the lowest level remains largely unchanged. This is evident from a comparison of figs.7.5 and 7.8, figs. 7.6 and 7.9 and figs. 7.7 with fig. 7.10. With



Fig,7.8 Electronic structure of the neutral vacancy in silicon with $\omega_a = 0.54\times10^{14}$ rad/sec. a, $Q_a = 0$ b, Q_a includes first-order terms only. c, Q_a includes first- and second-order terms.

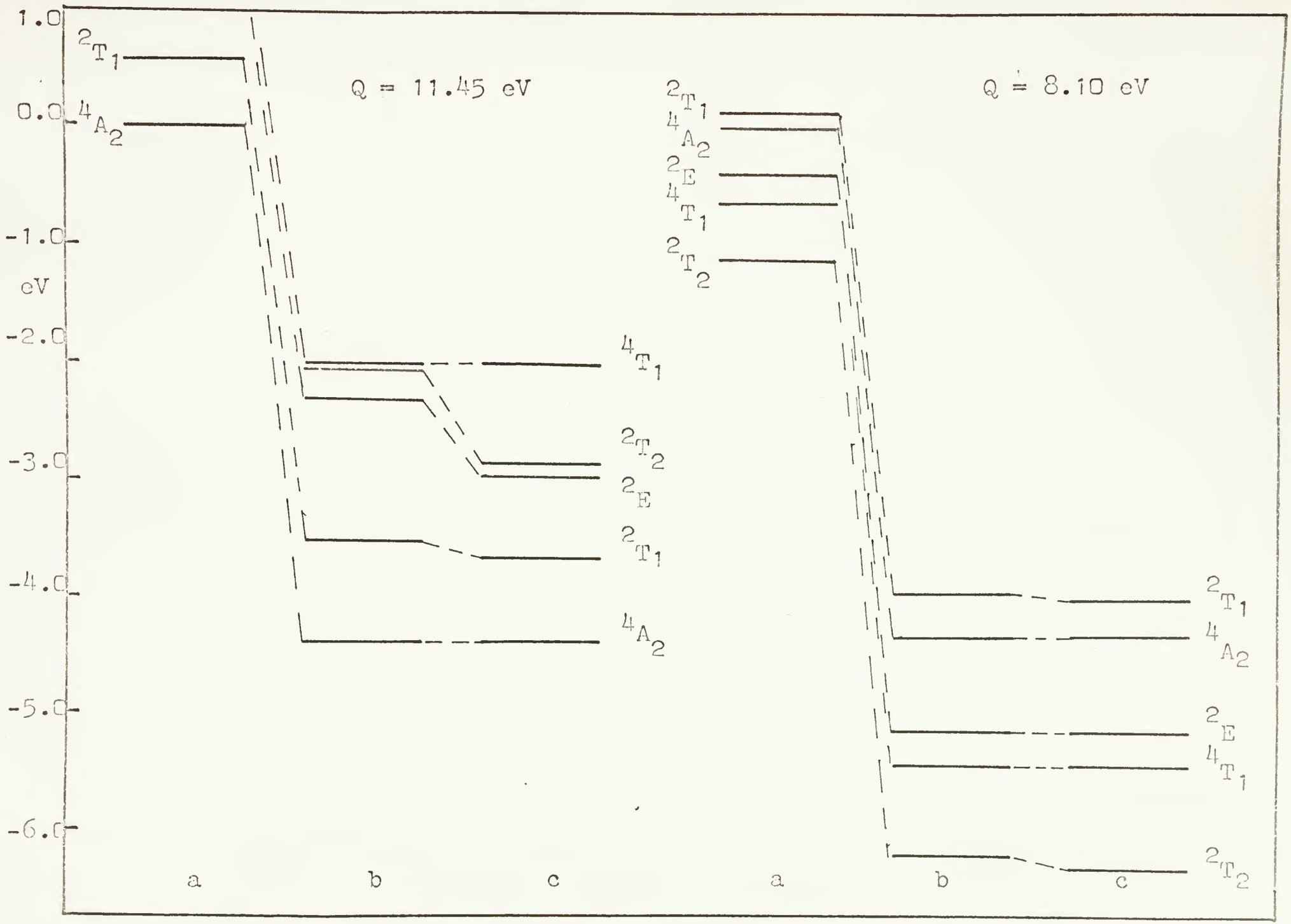


Fig.7.9 Electronic structure of the negatively charged vacancy in silicon with $\omega_a = 0.54 \times 10^{14}$ rad/sec. a, $Q_a = 0$ b, Q_a includes first-order terms only. c, Q_a includes first- and second-order terms.

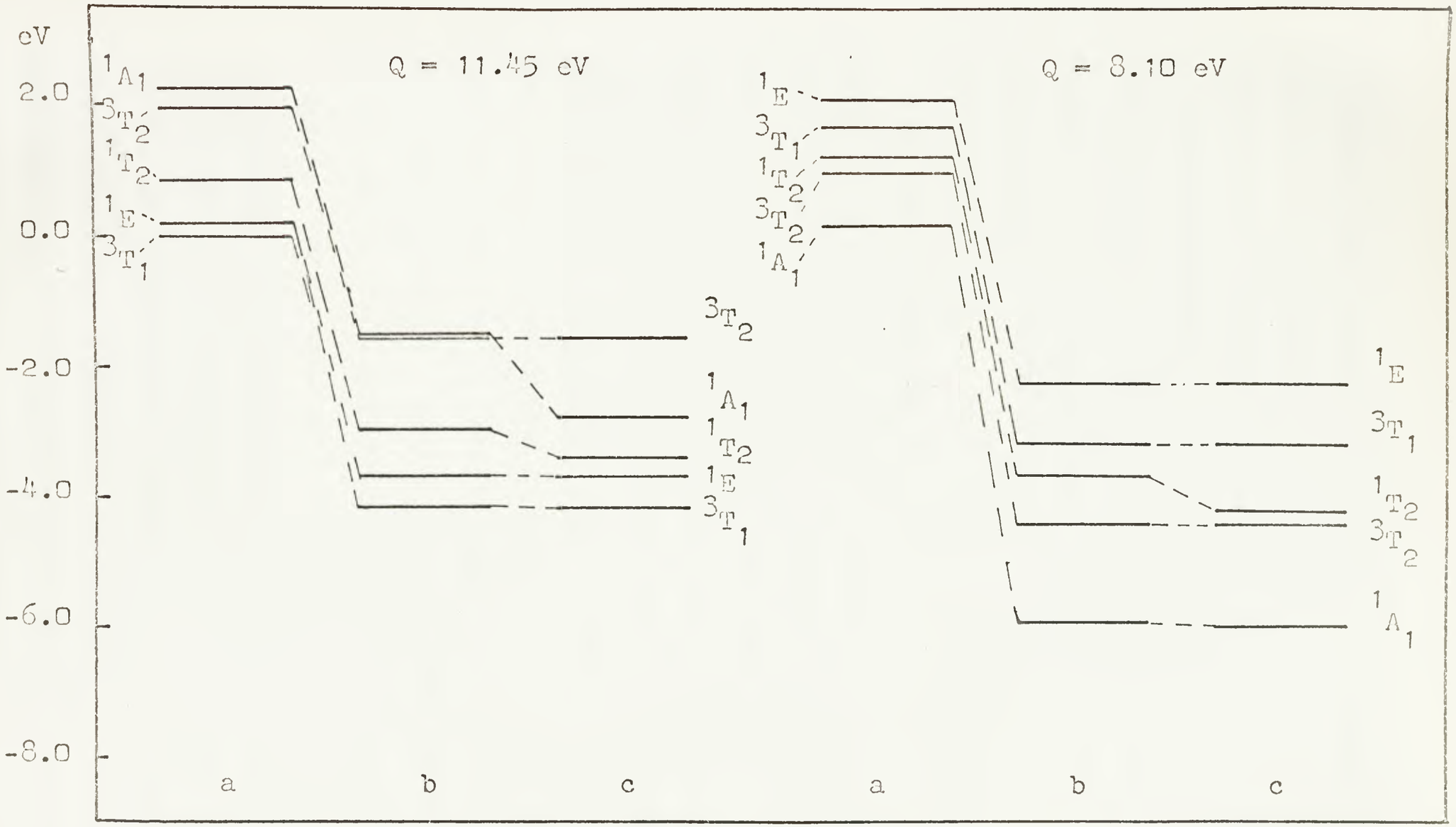


Fig.7.10 Electronic structure of the double negatively charged vacancy in silicon with $\omega_a = 0.54\times10^{14}$ rad/sec. a, $Q_a = 0$ b, Q_a includes first-order terms only. c, Q_a includes first- and second-order terms.

Q = 11.45 eV this is not so for the V^- and $V^=$ calculation because with $\omega_a = 0.39 \times 10^{14}$ rad/sec second order terms are very important in determining the lowest levels. However, as ω_a increases the importance of second order terms is diminished such that large changes in the relative ordering of the lowest levels does not occur when this correction is applied. With Q = 8.10 eV second order terms fulfil a much less important role in determining the lowest energy levels of a particular centre.

For the V^+ centre the $^2T_2$ level is still predicted to be lowest in all cases even further below the $^4T_1$ level than in the previous study. Hence, we can have reasonable confidence that this level is the ground state for this particular centre. For the V^o centre we now have conflicting results for different values of Q, although for a given value of Q the ordering of the energy levels is very similar as ω_a is varied. For Q = 11.45 eV, first order terms result in small changes in the relative energies of the lowest levels such that the $^5A_2$ level is predicted to be lowest just below the ^1E and $^3T_1$ levels. However, when the second order correction is made the $^3T_1$ level again becomes lowest in energy just below the ^1E level. Using a value of 8.10 eV for Q very different results are obtained. As observed in the undistorted calculation the $^1T_2$ and $^1A_1$ levels are very sensitive to the value chosen for Q and in this case they become the lowest levels. While there is an uncertainty about the magnitude of the relaxation due to an inadequate knowledge of ω_a, it is significant that the $^1T_2$ level is lowest in both studies. For $\omega_a = 0.39 \times 10^{14}$ rad/sec the $^1T_2 - {}^1A_1$ separation

is 1.06 eV while for $\omega_a = 0.54 \times 10^{14}$ rad/sec the separation is only 0.09 eV. For the T_d system the $^1T_2 \rightarrow {}^1A_1$ is a spin- and orbitally-allowed transition. Since the ground state of the neutral vacancy is believed to be near the valence band edge this transition may be observable in the near infra-red if our model with this approximation for Q is reasonable. Of course here we have quoted the difference in energy between the equilibrium configurations of these two levels, rather than the Franck-Condon transition energy.

For the V^- centre, three of the four calculations shown in figs. 7.6 and 7.9 predict that the $^2T_2$ level is lowest in energy. As discussed earlier, for Q = 11.45 eV the second order terms cause large changes in the ordering of the lowest energy levels. However, for the alternative choice of Q, no changes in the order of the lowest levels results from second order corrections. With Q = 8.10 eV the $^2T_2$ level is 1.09 eV below the $^4T_1$ level and 1.45 eV below the ^2E level for $\omega_a = 0.39 \times 10^{14}$ rad/sec. while for $\omega_a = 0.54 \times 10^{14}$ rad/sec the $^2T_2$ level is 0.80 eV below the $^4T_1$ level and 1.10 eV below the ^2E level. The transition for the $^2T_2$ level to the ^2E level is allowed, but is unlikely to be observed unless the ^2E level corresponds to a resonance state in the conduction band.

The $^1A_1$ level of the V^{2-} centre is lowest in energy in three of the four calculations shown in figs. 7.7 and 7.10. For Q = 11.45 eV this level shows a strong dependence on the second order terms, and are responsible for this level being lowest when $\omega_a = 0.39 \times 10^{14}$ rad/sec.

However, for Q = 8.10 eV second order terms have a negligible effect on the energy of this level. If the $^1A_1$ level is the ground state of this centre then it will be diamagnetic as suggested by Watkins.

As with the previous calculations using the undistorted model, the approximation with Q = 8.10 eV appears to be in better agreement with experiment. For such a choice of Q the calculation predicts ground state levels for each of the vacancy centres which have the correct spin-multiplicity and suggest possible allowed electronic transitions for the V^o and V^- centres which may be observable. We now propose to examine the Jahn-Teller distortion terms for the lowest degenerate levels in each centre.

7.8 Jahn-Teller Calculations for the Isolated Vacancy in Silicon

The calculations for the Jahn-Teller splittings are based upon the theory already outlined in the previous chapter. The approximations of this first order theory will be at least as serious as for the diamond vacancy. We have calculated the splittings of the following levels using the simple model

V^+ : $^2T_2$, $^4T_1$

V^o : ^1E, $^3T_1$, $^1T_2$

V^- : ^2E, $^2T_2$, $^1T_2$, $^4T_1$

$V^=$: $^1T_2$, ^1E, $^3T_1$, $^3T_2$

In order to determine the values of the I terms for each level we have made use of the formulae given in Appendices C.2 and C.3 and the derivatives of the integrals shown in table 7.5. Using the values for the I terms so obtained and the appropriate values for the

effective frequencies ω_E and ω_T given in section 7.6 the Jahn-Teller energy splittings and the extent of distortion for each level was evaluated. In Tables 7.11,7.12,7.13 and 7.14 the results for the lowest levels of the V^+,V^0,V^- and $V^=$ centres are given respectively. The displacement of the atoms nearest the defect may be determined by comparing the values for the normal co-ordinates with table 6.8.

With the exception of the splittings for the $^2T_2$ level of V^+ the energy lowerings for all the levels as a result of Jahn-Teller distortions are predicted to be small. In fact the calculated splitting of a given level, is in general smaller for the silicon vacancy than for the same level in the diamond vacancy calculation. This is easily seen by comparing the present results with those of the previous chapter. This is a surprising result as we might have expected the distortions in the silicon vacancy to be greater in accordance with what was calculated for the symmetric relaxation problem. However, the calculation predicts that the symmetric term is mainly responsible for a larger displacement of the silicon atoms nearest the vacancy and not the Jahn-Teller terms. It is possible that the inclusion of higher order terms in the calculation would reverse the findings of the present Jahn-Teller calculations. If the values of ω_E and ω_T are underestimated using the dynamic relaxation programe for the same reasons as postulated for the symmetric response frequency ω_a then the predicted Jahn-Teller distortions will be even smaller than those shown in the tables.

TABLE 7.11

Values of the Jahn-Teller terms for the lowest $^2T_2$ and $^4T_1$ level of the positive vacancy in silicon.

Value of Q (eV)	Eigenvectors	I_{TE} eV/	ΔE_{TE} eV	q_1	I_{TT} eV/	ΔE_{TT} eV	q_3
1. $^2T_2$ Level							
11.45	$c_1 = 0.8278$ $c_2 = -0.4343$ $c_3 = -0.3551$	-1.73	0.02	-0.017	-5.65	3.76	-0.67
8.10	$c_1 = 0.7979$ $c_2 = -0.4386$ $c_3 = -0.4125$	-1.80	0.02	-0.018	-5.36	3.40	-0.63
2. $^4T_1$ Level							
11.45	$c_1 = 1.0$	-3.78	0.00	-0.04	4.72	0.25	0.05
8.10	$c_1 = 1.0$	-3.90	0.10	-0.04	4.86	0.25	0.05

TABLE 7.12

Values of the John-Teller terms for the lowest ^1E, $^3T_1$ and $^1T_2$ levels of the neutral vacancy in silicon

Value of Q eV	Eigenvectors	I_{TE} eV/Å	ΔE_{TE} eV	q_1 Å	I_{TT} eV/Å	ΔE_{TT} eV	q_3 Å
1. $^3T_1$ Level							
11.45	c_1 = 0.6047 c_2 =−0.6517 c_3 =−0.3852	0.85	0.005	0.009	1.56	0.29	0.18
8.10	c_1 = 0.6540 c_2 =−0.6111 c_3 =−0.4460	0.81	0.004	0.008	0.95	0.11	0.11
2. $^1T_2$ Level							
11.45	c_1 = 0.9266 c_2 = 0.3545 c_3 =−0.1720	2.04	0.057	0.03	-0.74	0.065	-0.09
8.10	c_1 = 0.8899 c_2 = 0.1443 c_3 =−0.4328	1.27	0.01	0.012	-0.44	0.03	-0.05

TABLE 7.12

/... continued

Value of Q eV	Eigenvectors	I_{EE} eV/Å	ΔE_{EE} eV	ρ Å
3. ^1E Level				
11.45	$c_1 = 0.7705$ $c_2 = 0.4702$ $c_3 = -0.4304$	0.36	0.007	0.04
8.10	$c_1 = 0.7050$ $c_2 = 0.5059$ $c_3 = -0.4970$	0.30	0.005	0.04

TABLE 7.13

Values of the Jahn-Teller terms for the lowest ^2E, $^2T_1$, $^2T_2$ and $^4T_1$ levels of the negatively charged vacancy

Value of Q eV	Eigenvectors	I_{TE} eV/Å	ΔE_{TE} eV	q_1 Å	I_{TT} eV/Å	ΔE_{TT} eV	q_3 Å
1. $^2T_2$ Level							
11.45	$c_1 = 0.7072$ $c_2 = -0.4803$ $c_3 = -0.5188$	0.25	4×10^{-4}	0.003	-0.13	2×10^{-3}	-0.015
8.10	$c_1 = 0.6087$ $c_2 = -0.4934$ $c_3 = -0.6213$	-0.67	3×10^{-3}	-0.007	0.31	0.01	0.036
2. $^2T_1$ Level							
11.45	$c_1 = 0.9220$ $c_2 = 0.3872$	-0.78	4×10^{-3}	-0.008	-1.26	0.19	-0.15
8.10	$c_1 = 0.9141$ $c_2 = 0.4054$	-0.03	6×10^{-6}	-3×10^{-4}	-1.43	0.24	-0.17

TABLE 7.13 (continued)

Value of Q eV	Eigenvectors	I_{TE} eV/Å	ΔE_{TE} eV	q_1 Å	I_{TT} eV/Å	ΔE_{TT} eV	q_3 Å
3. $^4T_1$ Level							
11.45	$c_1 = 1.0$	-4.83	0.15	-0.05	-0.59	0.004	-0.007
8.10	$c_1 = 1.0$	-1.07	0.007	-0.001	-0.544	0.003	-0.006
Value of Q eV	Eigenvectors	I_{EE} eV/Å	E_{EE} eV	ρ Å			
4. ^2E Level							
11.45	$c_1 = 0.6540$ $c_2 = 0.7565$	1.21	0.09	0.14			
8.10	$c_1 = 0.7407$ $c_2 = 0.6719$	0.46	0.01	0.05			

TABLE 7.14

Values of the Jahn-Teller terms for the lowest ^1E, $^3T_1$, $^1T_2$ and $^3T_2$ levels of the doubly-negatively charged vacancy

Value of Q eV	Eigenvectors	I_{TE} eV/Å	ΔE_{TE} eV	q_1 Å	I_{TT} eV/Å	ΔE_{TT} eV	q_3 Å
1. $^3T_1$ Level							
11.45	$c_1 = 1.0$	-4.56	0.14	-0.05	-0.29	0.01	-0.033
8.10	$c_1 = 1.0$	-1.02	7×10^{-3}	-0.01	-0.28	0.01	-0.033
2. $^3T_2$ Level							
11.45	$c_1 = 1.0$	1.343	0.012	0.014	0.35	0.013	0.039
8.10	$c_1 = 1.0$	2.24	0.033	0.022	0.19	4×10^{-3}	0.02
3. $^1T_2$ Level							
11.45	$c_1 = 0.8244$ $c_2 = 0.5661$	2.29	0.034	0.02	0.36	0.016	0.043
8.10	$c_1 = 0.8350$ $c_2 = 0.5502$	2.37	0.037	0.02	0.30	0.010	0.035

TABLE 7.14 (continued)

Value of Q eV	Eigenvectors	I_{EE} eV/Å	ΔE_{EE} eV	ρ Å
4. ^{1}E Level				
11.45	$c_1 = 1.0$	-1.60	0.15	0.19
8.10	$c_1 = 1.0$	-0.47	0.01	0.05

The predicted values for the Jahn-Teller splittings are in general slightly larger for the case with Q = 11.45 eV, but there are some exceptions. However, for both values of Q the predicted distortions are at least of the same order of magnitude.

We have been unable to account for the unsatisfactory value obtained for the extent of trigonal distortion of the lowest $^2T_2$ level of the positive vacancy. The wave-functions and formulae leading to the expression for I_{TT} given in Appendix C.2 have been extensively checked, but no error in the formal relationship can be found. As for the diamond calculation the large value arises because of the negative eigenvector c_2, however examination of the configuration interaction matrix suggests that this is correct. For a positive value of c_2 a trigonal distortion corresponding to an energy lowering of about 0.15 eV would result, but what is important is that this distortion is then still two orders of magnitude greater than the predicted value for a tetragonal distortion. Watkins has suggested that the ground state of a V^+ centre is tetragonally distorted. Therefore, it would seem that a first order perturbation-type Jahn-Teller calculation is unsatisfactory for this system.

For the neutral vacancy both calculations predict that the $^3T_1$ level will undergo a trigonal distortion. For the $^1T_2$ level a trigonal distortion is again favoured, but the energy difference between a trigonal and tetragonal equilibrium configuration is only 0.01 eV in both studies. For the ^1E level the predicted splitting

is extremely small. No change in the ordering of the lowest electronic levels shown in figs. 7.5 and 7.8 result from including the Jahn-Teller corrections. For Q = 11.45 eV the $^3T_1$ level is still predicted to be lowest slightly below the ^1E level while for Q = 8.10 eV the $^1T_2$ level remains lowest in energy.

No change in the relative ordering of the energy levels for the V^- centre result from including the Jahn-Teller correction terms given in table 7.13 as a perturbation on the calculation. The $^2T_2$ level which seems most likely to be the ground state of this system undergoes a very small Jahn-Teller distortion, despite the large symmetric relaxation associated with this level. A trigonal distortion is favoured, but there is less than 0.01 eV between the energies of the equilibrium tetragonal and trigonal configurations. The $^2T_1$ level also favours a trigonal distortion while the $^4T_1$ level is predicted to have a tetragonal equilibrium configuration.

The experimental results of Watkins suggests that the ground state of the V^- centre with total spin S = ½ undergoes a mixed tetragonal and trigonal distortion. On application of the static Jahn-Teller theorem with only intralevel coupling a mixed distortion is never predicted as the equilibrium configuration. However, Stoneham and Lannoo [111] have shown that a mixed distortion of the correct symmetry results from the interlevel coupling of $(E+T_2)$ or (T_1+T_2). If we ignore coupling between levels of different spin multiplicity then the present calculation suggests that the coupling is more likely to be between the $^2T_2$ and ^2E levels. However, a separation of 1 to 1.5 eV between these levels is rather too large

if this interlevel coupling is to be important.

The results of the calculations for the $^3T_1$, $^3T_2$ and $^1T_2$ levels of the V^{2-} centres given in table 7.14 predicts that a tetragonal equilibrium configuration is favoured for these levels in most cases, although the energy difference between the tetragonal and trigonal configurations is very small. Again no change in the ordering of the energy levels shown in figs. 7.7 to 7.10 result from including the Jahn-Teller corrections. Hence from our calculations it seems most probable that the ground state of this centre is the $^1A_1$ level.

7.9 Comments on Results

The limitations of the calculation for the isolated single vacancy in silicon using a defect molecule approach will certainly be as least as serious as for the diamond vacancy. However, the model does successfully predict the ground state levels of the correct spin-multiplicities for the various charge states. We have shown using this model that electron-electron interaction effects and configuration interaction terms are very important in determining the relative ordering of the lowest levels. There is an uncertainty as to the true value for the one-centre coulomb integral, but it almost certainly has a value in the range 8.10 to 11.45 eV. The perturbation calculations using a rigid atom model for the symmetric relaxation and Jahn-Teller effects suggests that the former is more important in determining the ordering of the lowest levels. Therefore, it would be important to include such terms from the beginning of the calculation in a more sophisticated model. We have calculated that the symmetric relaxation of the nearest

neighbour atoms is inwards. However, we have constrained the system by requiring that the atoms nearest the defect remain in a state of sp^3 hybridisation such that this result was probably inevitable.

To first order the Jahn-Teller distortions with the exception of the $^2T_2$ level of the V^+ centre are predicted to be very small which is contrary to what has been suggested by Watkins. However, in view of the large magnitude of the symmetric mode Q_a, second order coupling terms of the kind $Q_a Q_\alpha$ where $\alpha = \varepsilon, \theta, \xi, \eta, \zeta$ may be very important in determining the magnitude of the Jahn-Teller effect. While it is unlikely that delocalisation of the electronic wave-function from the vacancy will effect the relative ordering of the lowest levels, the magnitude of the Jahn-Teller terms may be sensitive to this effect. The role of interlevel coupling terms based on the theory discussed by Stoneham and Lannoo [111] and dynamic Jahn-Teller effects remain to be investigated. From this fairly simple model we have been able to obtain some interesting results for the vacancy system which would not be accessible using a band theory approach. The calculation for the V^0 centre does also suggest that Callaway and Hughes might have been more successful if they had tried to find a bound states for this centre of T_2 symmetry.

7.10 Conclusion and Summary

The electronic structure of the isolated vacancy in its various charged states has been calculated using a defect molecule approach. Corrections to allow for symmetric relaxation and Jahn-Teller distortions of the lattice have also been made. The calculations using a semi-empirical value of the one-centre coulomb integral give better agreement with experiment. The predicted ground states of the various centres are:

V^+: $^2T_2$; V^0: $^1T_2$; V^-: $^2T_2$; $V^=$: $^1A_1$.

GENERAL DISCUSSION OF THESIS

In each chapter of this thesis we have presented a detailed discussion of the relevant results. However, it is useful to take an overall look at the whole thesis and, with a fear of too much repetition in mind, highlight the most important findings and their significance towards further research in this area.

The defect molecule approach was chosen as the best method available for calculating the electronic structure of an isolated vacancy or divacancy in a diamond-type crystal because, despite its limitations, it was computationally feasible and capable of yielding information which at the present time is not attainable using a band theory approach. Using this method we have calculated the electronic structure of the undistorted single vacancy in its various charge states in the diamond and silicon crystal. By using a perturbation type approach and the rigid atom approximation proposed by Lidiard and Stoneham the lowest electronic levels for each centre have been corrected for symmetric relaxation and Jahn-Teller distortion terms. We have also applied the method to the undistorted isolated divacancy in the diamond crystal.

The relative ordering of the energy levels for the various charge states of the undistorted vacancy in diamond was, in some cases, sensitive to the choice of function used to

represent the 2s and 2p orbitals on the atom in the crystal. The most notable case was the V^0 centre for which the ^1E electronic level was predicted to be the ground state with the $^3T_1$ excited state just above this level when simple Slater-type functions were used. However, the ordering of these two levels was inverted when atomic Hartree-Fock functions were used in the evaluation. Using a very simple model the influence of delocalizing the electronic wave-function of the defect electrons on the relative ordering of the electronic energy levels was investigated. For the neutral charged state of the vacancy no change in the ordering of the lowest levels resulted for reasonable amounts of delocalization, although there were reasonably large changes in the relative separation of some of the levels. When the lowest levels of the V^0 centre were corrected for the symmetric relaxation and Jahn-Teller effects (chapter 6) the $^3T_1$ level was found to be lowest in all studies independent of the choice of functions for the orbitals. It was predicted that this centre would have a trigonally distorted equilibrium configuration as a result of the Jahn-Teller effect. On the basis of these results it is predicted that the GR1 band is not associated with electronic transitions involving defect electrons from the neutral vacancy.

All studies predicted that the $^2T_2$ level is the ground state level for the positive vacancy. It is interesting to note that the modified a.s.m.o. calculations for the case 1

approximation do not predict that the V^+ centre is necessarily any less stable than the V^0 or V^- centres (see table 3.2). This is important since it has been argued, on the basis of the unmodified calculation by Coulson and Kearsley, that this centre was very much less stable than the V^0 or V^- centres. Our calculation favours a trigonal equilibrium configuration as a result of the Jahn-Teller distortion of the $^2T_2$ level. The calculation supports the hypothesis of Baldwin that this centre is responsible for the 'a' system of lines observed in the electronic spin resonance experiments. Using Slater functions the modified calculation for the V^- centre suggests that the $^4A_2$ level is the ground state of this centre. A similar finding is also obtained for the approximation case 1 with Clementi functions. However, in the other limit, the $^2T_2$ level is lowest. Delocalisation studies also tend to support the finding that the $^4A_2$ level is lowest in energy. For reasons outlined in section 6.7 we cannot definitely eliminate the possibility that the GR1 band may be associated with the electronic properties of the V^- centre, however, it does seem unlikely in view of the present results.

For the V^{2-} centre the calculation using Slater functions suggests that the $^3T_1$ level is always the ground state of the system. A tetragonal distortion of the system is favoured as the equilibrium configuration. Case 2 of the study involving Clementi functions does suggest that the $^1A_1$ electronic level

is the ground state of this system. The model is not sufficiently reliable for this charge state to resolve the conflict. In all the studies for the single vacancy in diamond the energy correction term resulting from the symmetric relaxation of the atoms nearest the defect for most levels had a magnitude in the range 1 to 2 eV. The importance of this term in determining the ordering of the lowest levels suggests that in a more detailed calculation it would be necessary to include this effect as a fundamental part of the problem rather than as a perturbation correction.

The electronic calculations related to the single isolated vacancy in silicon were reported in chapter 7. Atomic Hartree-Fock functions obtained by Clementi were used to approximate the 3s and 3p orbitals on the silicon atoms in the crystal. Using a modified a.s.m.o. theory the ground states of the centres V^+, V^0, V^- and $V^=$ were predicted to have the same total spin as those observed by Watkins. Electron-electron interaction and configurational mixing terms were very important in determining the lowest levels for the various centres using this model. With the exception of the lowest $^2T_2$ level of the V^+ centre first order Jahn-Teller splittings were predicted to be smaller than those for similar levels in the diamond vacancy calculation. However, the symmetric relaxation terms were shown to be very much larger, although we were unable to obtain reliable estimates of these terms. From a theoretical viewpoint, the defect molecule approach is less

satisfactory for the silicon vacancy calculation than for the diamond study; nevertheless, the results obtained are encouraging. A more detailed calculation should include the symmetric relaxation effect as an integral part of the problem. In view of the results of chapter 5, long range effects involving displacement of atoms which are at least fifth neighbours from the defect may be important in determining the electronic properties of a particular centre. Improved Jahn-Teller energies may be obtained by including higher order terms and by allowing for interlevel coupling effects. Watkins has suggested that the magnitude of the Jahn-Teller effect is such that it should be included as an integral part of the calculation. However, such refinements to the model will destroy the overall simplicity of the method.

The undistorted calculation for the neutral divacancy in diamond using Slater-type functions for the 2s and 2p orbitals on the carbon atoms in the crystal suggest that this centre may be responsible for a part of the u-v band observed in the spectra of irradiated diamonds. This centre should be paramagnetic and exhibit optical dichroism. However, in view of the more detailed calculations on the isolated vacancy which have been reported these results must be treated very cautiously. Symmetric relaxation terms in particular may cause changes in the relative ordering and separation of the lowest levels. It would be of interest to have the results of a more detailed calculation which either incorporated such terms as an

intimate part of the problem or at least as a first order correction. The use of atomic Hartree-Fock functions and the extension to charge states and even to the silicon problem where the experimental results are more certain may prove to be rewarding. The complication with the silicon divacancy problem is the possible increased relaxation of the atoms surrounding the defect relative to the vacancy problem and the possibility of very large Jahn-Teller effects if the observations reported by Watkins are correct.

The dynamic relaxation program described in chapter 5 represents a significant improvement on the relatively simple methods which have been used in previous investigations to estimate the displacement of atoms around point defects and their formation energy in valence crystals. We have been able to demonstrate that the displacement of atoms in the vicinity of a single vacancy in the silicon crystal are much greater than for the diamond crystal due to the rebonding of the vacancy electrons in pairs such that a tetragonal distortion of the vacancy results. When a valence force potential which includes non-central forces is used to represent the interaction between atoms in the crystal it is found that the displacements of some fifth neighbour atoms to the defect are much greater than the displacements of third and fourth neighbours. Higher formation energies for the single vacancy than have been previously predicted theoretically are obtained. The major limitation of the method is that some estimate of the

forces associated with the rebonding of the defect electrons has to be made. At present these estimates are very crude. The usefulness of the method will increase as more information about these forces becomes available from electronic calculations. The method is potentially applicable to germanium and to the III-V and II-VI compounds with the zinc-blende structure. The program may also be used to estimate the displacement of atoms around divacancies and interstitial atoms in valence-type crystals.

References

1. C.A. Coulson and M.J. Kearsley, Proc. Roy. Soc. A241, 433 (1957).

2. T. Yamaguchi, J. Phys. Soc. Japan 17, 1359 (1962).

3. W. Kohn, Solid State Physics 5, 258 (1957), Ed. F. Seitz and D. Turnbull, Academic Press, N.Y.

4. K.H. Bennemann, Phys. Rev. 137 A1497 (1965).

5. J. Callaway and A.J. Hughes, Phys. Rev. 156, 860 (1967).

6. A.M. Stoneham, Proc. Phys. Soc. 88, 135 (1966).

7. B.S. Gourary and A.E. Fein, J. Appl. Physics, Suppl. 33, 331 (1962).

8. F.P. Larkins, Dissertation Dip. Advanced Maths. Oxford (1967).

9. J. Callaway and A.J. Hughes, Phys. Rev. 164, 1043 (1967).

10. G.D. Watkins, Proceedings Symposium on Radiation Damage in Semiconductors, p.97 (1965), Dunod, Paris.

11. A.B. Lidiard, Proceedings Sante Fe Conference on Radiation Effects in Semiconductors, 1967, p.85. Ed. F.L. Vook, Plenum Press, N.Y. (1968).

12. M.H. Cohen and V. Heine, Phys. Rev. 122, 1821 (1961).

13. T. Yamaguchi, J. Phys. Soc. Japan, 18, 368 (1963).

14. J. Friedel, M. Lannoo and G. Leman, Phys. Rev. 164, 1056 (1967).

15. M. Lannoo and A.M. Stoneham, J. Phys. Chem. Solids, 29, 1987 (1968).

16. R. Berman, (Ed.) Physical Properties of Diamond, (1965) O.U.P. London.

17. R. Robertson, J.J. Fox and A.E. Martin, Phil. Trans. Roy. Soc. A232, 463 (1934).

18. G.B. Sutherland, E.D. Blackwell and W.G. Simeral, Nature 174, 901 (1954).

19. W. Kaiser and W.L. Bond, Phys. Rev. 115, 857 (1959).

20. R.J. Elliot, Proc. Phys. Soc. 76, 787 (1960).

21. J.F.H. Custers, Physica 18, 489 (1952).

22. J.F.H. Custers, Nature 176, 173 (1955).

23. I.G. Austin and R. Wolfe, Proc. Phys. Soc. B69, 325(1956).

24. H.B. Dyer, F.A. Raal, L. DuPreez and J.H.N. Loubser, Phil. Mag. 11, 763 (1965).

25. F.A. Raal, Am. Mineralogist, 42, 354 (1967).

26. E.C. Lightowlers, Science and Technology of Industrial Diamonds, 1, 27 (1967). Industrial Diamond Information Bureau, London.

27. C.D. Clark, R.W. Ditchburn and H.B. Dyer, Proc. Roy. Soc. A234, 363 (1956).

28. E.D. Trifinov, Dokl Akad Nauk, SSSR, 147, 826 (1962).

29. C.D. Clark and C. Norris, Diamond Conference (1965), unpublished.

30. E.W.J. Mitchell, Science and Technology of Industrial Diamonds, 1, 17 (1967). Industrial Diamond Information Bureau, London.

31. C.D. Clark, P.J. Kemmey and E.W.J. Mitchell, Dis. Faraday Soc. 31, 96 (1961).

32. I. Duncan, Ph.D Thesis, Reading University (1963).

33. H.B. Dyer and P. Ferdinando, Brit. J. Appl. Phys. 17, 419 (1966).

34. H.B. Dyer and L. DuPreez, J. Chem. Phys. 42, 1898 (1965).

35. C.D. Clark and D.W. Palmer, Proc. Fourth Symposium on Reactivity of Solids, p.436 (1960). Elsevier, Amsterdam.

36. E.W.J. Mitchell, Physical Properties of Diamond p.394 (1965). Ed. R. Berman, O.U.P. London.

37. C.D. Clark, R.W. Ditchburn and H.B. Dyer, Proc. Roy. Soc. A237, 75 (1956).

38. J. Owen, Physical Properties of Diamond, p.274 (1965). Ed. R. Berman, O.U.P. London.

39. E.A. Faulkner and J.N. Lomer, Phil. Mag. 7, 1995 (1962).

40. J.A. Baldwin, Phys. Rev. Letters, 10, 220 (1963).

41. L. DuPreez, Diamond Conference (1967), unpublished.

42. I. Duncan, Proc. 7th Int. Conf. on Physics of Semiconductors, Vol. 3, Radiation Damage in Semiconductors, p.135 (1964). (Paris-Rayaumont).

43. J.N. Lomer and A.M.A. Wild, Diamond Conference (1968). Unpublished.

44. E.A. Harris, J. Owen and C. Windsor, Bull. Amer. Phys. Soc. 8, 252 (1963).

45. C.D. Clark, I. Duncan, J.N. Lomer and P.W. Whippey, Proc. Brit. Ceramic Soc. 1, 85 (1964).

46. G.D. Watkins, Clarendon Laboratory Report, Oxford (1967).

47. J.W. Corbett, Electron Radiation Damage in Semiconductors and Metals, 1966, Academic Press, N.Y.

48. G.D. Watkins, Proceedings of International Conference on Crystal Lattice Defects, 1962, J. Phys. Soc. Japan, Suppl. II, 18, 22 (1963).

49. G.D. Watkins (private communication).

50. G.D. Watkins and J.W. Corbett, Phys. Rev. 138, A543, A555 (1965).

51. H.Y. Fan and A.K. Ramdas, J. Appl. Physics, 30, 1127 (1959).

52. L.J. Cheng, J.C. Corelli, J.W. Corbett and G.D. Watkins, Phys. Rev. 152, 761 (1966).

53. G.D. Watkins and J.W. Corbett, Disc. Faraday Soc. 31, 86 (1961).

54. R.A. Swalin, J. Phys. Chem. Solids, 18, 290 (1961).

55. A. Seeger and M.L. Swanson, Int. Symp. on Lattice Defects in Semiconductors, Tokyo, Sept. 1966, p.93 (1968). Ed. R.R. Hasiguti, Uni. Tokyo Press.

56. R.S. Mulliken, Phys. Rev. 43, 279 (1933).

57. M. Goeppert-Mayer and A.L. Sklar, J. Chem. Phys. 6, 645 (1938).

58. J.C. Slater, Phys. Rev. 36, 57 (1930).

59. S. Flodmark, Tables of Molecular A and B Functions (1957) Institute of Theoretical Physics, Stockholm.

60. E. Clementi, Supplement to IBM J. Res. and Dev. 9, 2 (1965).

61. M.J. Kearsley, D. Phil. Thesis, Oxford (1956).

62. F.J. Corbato and A.C. Switendick, Methods of Computational Physics, Vol. 2, Ed. Adler, Fernbach and Rotemberg, Academic Press (1963).

63. F.R.A. Hopgood, Midiat on Atlas Atlas Computing Laboratory, August 1966.

64. R.S. Mulliken, J. Chim. Phys. 46, 500 (1949).

65. W. Moffitt, Proc. Roy. Soc. A210, 224, 245 (1951).

66. R.G. Parr and R. Pariser, J. Chem. Phys. 21, 466, 767 (1953).

67. R. Pariser, J. Chem. Phys. 21, 568 (1953).

68. E.U. Condon and G.H. Shortley, The Theory of Atomic Spectra (1967) C.U.P.

69. R.R. Hasiguti, Int. Symp. on Lattice Defects in Semiconductors, Tokyo, Sept. 1966, p.131 (1968). Ed. R.R. Hasiguti. Uni. Tokyo Press.

70. A. Scholz and A. Seeger, in Radiation Damage in Semiconductors (Paris - Rayaumont, 1964), p.315, Dunod, Paris (1965).

71. P.W. Bridgman, Physics of High Bressures, Bell, London (1949), C.A. Swenson, Solid State Physics 11, 41 (1960). Ed. F. Seitz and D. Turnbull, Academic Press, N.Y.

72. H.J. McSkimin and P. Andreatch, Jr., J. Appl. Phys. 34, 651 (1963).

73. H.M. Smith, Phil. Trans. Roy. Soc. A241, 105 (1948).

74. F. Herman, J. Phys. Chem. Solids, 8, 405 (1959).

75. A.B. Lidiard, in Radiation Damage in Semiconductors (Paris-Rayaumont, 1964), p.336, Dunod, Paris (1965).

76. R. Bullough and R.C. Perrin, Proc. Roy. Soc. A305, 541 (1968).

77. H.L. McMurry, A.W. Solbrig, Jr., J.K. Boyter and C. Noble, J. Phys. Chem. Solids, 28, 2359 (1967).

78. E.B. Wilson, Jr., J.C. Decius and P.C. Cross, Molecular Vibrations, McGraw Hill (1955).

79. J.L. Warren, R.G. Wenzel and J.L. Yarnell, Proc. Symp. Inelastic Scattering, Bombay 1964, 1, 361 (1965), IAEA, Vienna.

80. H.J. McSkimin and W.L. Bond, Phys. Rev. 105, 116 (1957).

81. J.L. Warren, J.L. Yarnell, G. Dolling and R.A. Cowley, Phys. Rev. 158, 805 (1967).

82. M.J.P. Musgrave and J.A. Pople, Proc. Roy. Soc. A268, 474 (1962).

83. L.E. Sutton. Ed. Interatomic Distances, Suppl. Chem. Soc. Special Publication No. 18 (1965).

84. R. Berman and J. Thewlis, Nature 176, 834 (1955).

85. M.H. Rice, R.G. McQueen and J.W. Walsh, Solid State Physics 6, 44 (1958). Ed. F. Seitz and D. Turnbull, Academic Press, N.Y.

86. J.C. Slater, Introduction to Chemical Physics, p.450, McGraw Hill, N.Y. (1939).

87. H.A. Skinner and H.D. Pritchard, Trans. Faraday Soc. 49, 1255 (1953).

88. J.H. Van Vleck, J. Chem. Phys. 1, 177, 219 (1933).

89. C.A. Coulson, Valence, p.207, O.U.P. (1961).

90. H.H. Voge, J. Chem. Phys. 4, 581 (1936), 16, 984 (1948).

91. R. Bäuerlein, Proc. Int. School of Physics, Enrico Fermi Course XVIII, Radiation Damage in Solids, p.358, Academic Press, (1962).

92. F. Herman, Proceedings Sante Fe Conference on Radiation Effects in Semiconductors, p.86, Ed. F.L. Vook, Plenum Press, N.Y. (1968).

93. G. Dolling, in Inelastic Scattering of Neutrons in Solids and Liquids, Vol. II, p.37 (1963), IAEA Vienna.

94. H. Palevsky, D.J. Hughes, W. Kley and E. Tunkelo, Phys. Rev. Letters, 2, 258 (1959).

95. J.C. Slater, Phys. Rev. 98, 1039 (1955).

96. D.F. Gibbins, Phys. Rev. 112, 136 (1958), P.W. Sparks and C.A. Swenson, Phys. Rev. 163, 779 (1967).

97. A. Bienenstock, Phil. Mag. 9, 755 (1964).

98. H.J. McSkimin, J. Appl. Physics, 24, 988 (1953).

99. B.N. Oshchesin, Phys. Status Solidi, 3, K61 (1963).

100. W.R. Wilcox and T.T. La Chapelle, J. Appl. Physics, 35, 240 (1964).

101. B.J. Masters and J.M. Fairfield, Appl. Physics Letters, 8, 280 (1966).

102. R.N. Ghoshtagore, Phys. Rev. Letters, 16, 890 (1966).

103. H.A. Jahn and E. Teller, Proc. Roy. Soc. A161, 220 (1937).

104. H.A. Jahn, Proc. Roy. Soc. A164, 117 (1938).

105. H.A. Kramers, Proc. Acad. Sci. Amst. 33, 959 (1930).

106. J.H. Van Vleck, J. Chem. Phys. 7, 72 (1939).

107. U. Öpik and M.H.L. Pryce, Proc. Roy. Soc. A238, 425 (1957).

108. H.C. Longuet-Higgins, U. Öpik, M.H.L. Pryce and R.A. Sack, Proc. Roy. Soc. A244, 1 (1958).

109. M. Lannoo, Theses de Troisieme Cycle, Orsay (1966).

110. A.B. Lidiard and A.M. Stoneham, Science and Technology of Industrial Diamonds, 1, 1 (1967). Industrial Diamond Information Bureau, London.

111. A.M. Stoneham and M. Lannoo, J. Phys. Chem. Solids (to be published).

112. W.A. Runciman, Proc. Phys. Soc. 86, 629 (1965).

113. D. Schonland, Molecular Symmetry, Van Nostrand, London (1965).

114. J.S. Griffiths, The Theory of Transition-Metal Ions, C.U.P. (1964).

115. H. Kanzaki, J. Phys. Chem. Solids, 2, 24 (1957).

116. E. Clementi and D.L. Raimondi, J. Chem. Phys. 38, 2686 (1963).

117. E.L. Elkin and G.D. Watkins, Phys. Rev. 174, 881 (1968).

APPENDIX A1

Un-normalized Configurational Wave-functions for the Single Isolated Vacancy ($S_z = S$)

1. Positively Charged State (V^+)

configuration v^2t_2

$(v\bar{v}x)$	
$(v\bar{v}y)$	$^2T_2$
$(v\bar{v}z)$	

configuration vt_2^2

$(vx\bar{x}) + (vy\bar{y}) + (vz\bar{z})$	$^2A_1$
$(vx\bar{x}) - (vy\bar{y})$	^2E
$(vz\bar{z}) - (vy\bar{y})$	
(vyz)	
(vzx)	$^4T_1$
(vxy)	
$(vy\bar{z}) - (v\bar{y}z)$	
$(vz\bar{x}) - (v\bar{z}x)$	$^2T_2$
$(vx\bar{y}) - (v\bar{x}y)$	
$2(\bar{v}yz) - (vy\bar{z}) - (v\bar{y}z)$	
$2(\bar{v}zx) - (vz\bar{x}) - (v\bar{z}x)$	$^2T_1$
$2(\bar{v}xy) - (vx\bar{y}) - (v\bar{x}y)$	

configuration t_2^3

(xyz)	$^4A_2$
$(\bar{x}yz) - (xy\bar{z})$	^2E
$(\bar{x}yz) - (x\bar{y}z)$	
$(y\bar{y}x) + (z\bar{z}x)$	$^2T_2$
$(x\bar{x}y) + (z\bar{z}y)$	
$(x\bar{x}z) + (y\bar{y}z)$	

$$(\bar{z}\bar{z}x) - (y\bar{y}x)$$
$$(x\bar{x}y) - (z\bar{z}y) \qquad {}^2T_1$$
$$(y\bar{y}z) - (x\bar{x}z)$$

2. Neutral Vacancy (V^0)

configuration $v^2t_2^2$

$$(v\bar{v}x\bar{x}) + (v\bar{v}y\bar{y}) + (v\bar{v}z\bar{z}) \qquad {}^1A_1$$

$$(v\bar{v}z\bar{z}) - v\bar{v}x\bar{x}) \qquad {}^1E$$
$$2(v\bar{v}x\bar{x}) - (v\bar{v}y\bar{y}) - (v\bar{v}z\bar{z})$$

$$(v\bar{v}y\bar{z}) - (v\bar{v}\bar{y}z) \qquad {}^1T_2$$
$$(v\bar{v}z\bar{x}) - (v\bar{v}\bar{z}x)$$
$$(v\bar{v}x\bar{y}) - (v\bar{v}\bar{x}y)$$

$$(v\bar{v}yz)$$
$$(v\bar{v}zx) \qquad {}^3T_1$$
$$(v\bar{v}xy)$$

configuration vt_2^3

$$(vxyz) \qquad {}^5A_2$$
$$(vxy\bar{z}) + (v\bar{x}yz) + (vx\bar{y}z) - 3(\bar{v}xyz) \qquad {}^3A_2$$

$$(vxy\bar{z}) - (v\bar{x}yz) \qquad {}^3E$$
$$(v\bar{x}yz) - (vx\bar{y}z)$$
$$(vx\bar{y}\bar{z}) + (vz\bar{x}\bar{y}) + (\bar{v}z\bar{x}y) + (\bar{v}xyz) - 2(vy\bar{z}\bar{x}) - 2(\bar{v}y\bar{z}x) \qquad {}^1E$$

$$(vx\bar{y}\bar{z}) - (\bar{v}\bar{z}xy) + (\bar{v}\bar{x}yz) - (vz\bar{x}\bar{y})$$

$$(vy\bar{y}x) - (vz\bar{z}x) \qquad {}^3T_1$$
$$(vz\bar{z}y) - (vx\bar{x}y)$$
$$(vx\bar{x}z) - (vy\bar{y}z)$$

$$(v\bar{y}\bar{y}x) + (v\bar{z}\bar{z}x)$$
$$(v\bar{x}\bar{x}y) + (v\bar{z}\bar{z}y) \qquad {}^3T_2$$
$$(v\bar{x}\bar{x}z) + (v\bar{y}\bar{y}z)$$

$$(v\bar{y}\bar{y}x) - (v\bar{z}\bar{z}x) - (\bar{v}\bar{y}\bar{y}x) + (\bar{v}\bar{z}\bar{z}x)$$
$$(v\bar{x}\bar{x}y) - (v\bar{z}\bar{z}y) - (\bar{v}\bar{x}\bar{x}y) + (\bar{v}\bar{z}\bar{z}y) \qquad {}^1T_1$$
$$(v\bar{x}\bar{x}z) - (v\bar{y}\bar{y}z) - (\bar{v}\bar{x}\bar{x}z) + (\bar{v}\bar{y}\bar{y}z)$$

$$(v\bar{z}\bar{z}x) + (v\bar{y}\bar{y}x) - (\bar{v}\bar{z}\bar{z}x) - (\bar{v}\bar{y}\bar{y}x)$$
$$(v\bar{z}\bar{z}y) + (v\bar{x}\bar{x}y) - (\bar{v}\bar{z}\bar{z}y) - (\bar{v}\bar{x}\bar{x}y) \qquad {}^1T_2$$
$$(v\bar{x}\bar{x}z) + (v\bar{y}\bar{y}z) - (\bar{v}\bar{x}\bar{x}z) - (\bar{v}\bar{y}\bar{y}z)$$

configuration t_2^4

$$(x\bar{x}z\bar{z}) + (y\bar{y}z\bar{z}) + (x\bar{x}y\bar{y}) \qquad {}^1A_1$$

$$(z\bar{y}z\bar{y}) - (x\bar{y}x\bar{y}) \qquad {}^1E$$
$$2(z\bar{x}z\bar{x}) - (x\bar{y}x\bar{y}) - (z\bar{y}z\bar{y})$$

$$(x\bar{x}y\bar{z}) - (x\bar{x}\bar{y}z)$$
$$(y\bar{y}z\bar{x}) - (y\bar{y}\bar{z}x) \qquad {}^1T_2$$
$$(z\bar{z}x\bar{y}) - (z\bar{z}\bar{x}y)$$

$$(x\bar{x}yz)$$
$$(y\bar{y}zx) \qquad {}^3T_1$$
$$(z\bar{z}xy)$$

3. Single Negatively-Charged State (V^-)

configuration $v^2t_2^3$

$$(v\bar{v}xyz) \qquad {}^4A_2$$
$$(v\bar{v}xyz) - (v\bar{v}x\bar{y}z) \qquad {}^2E$$
$$(v\bar{v}x\bar{y}z) + (v\bar{v}\bar{x}yz) - 2(v\bar{v}xy\bar{z})$$

$(v\bar{v}y\bar{y}x) - (v\bar{v}z\bar{z}x)$ $(v\bar{v}z\bar{z}y) - (v\bar{v}x\bar{x}y)$ $(v\bar{v}x\bar{x}z) - (v\bar{v}y\bar{y}z)$	$^2T_1$
$(v\bar{v}y\bar{y}x) + (v\bar{v}z\bar{z}x)$ $(v\bar{v}z\bar{z}y) + (v\bar{v}x\bar{x}y)$ $(v\bar{v}x\bar{x}z) + (v\bar{v}y\bar{y}z)$	$^2T_2$

configuration vt_2^4

$(vx\bar{x}y\bar{y}) + (vy\bar{y}z\bar{z}) + (vx\bar{x}z\bar{z})$	$^2A_1$
$2(vy\bar{y}z\bar{z}) - (vx\bar{x}z\bar{z}) - (vy\bar{y}x\bar{x})$ $(vx\bar{x}z\bar{z}) - (vy\bar{y}x\bar{x})$	^2E
$(vx\bar{x}y\bar{z}) - (vx\bar{x}y\bar{z})$ $(vy\bar{y}z\bar{x}) - (vy\bar{y}z\bar{x})$ $(vz\bar{z}x\bar{y}) - (vz\bar{z}x\bar{y})$	$^2T_2$
$(vx\bar{x}y\bar{z}) + (vx\bar{x}y\bar{z}) - 2(v\bar{x}x\bar{y}z)$ $(vy\bar{y}z\bar{x}) + (vy\bar{y}z\bar{x}) - 2(v\bar{y}y\bar{z}x)$ $(vz\bar{z}x\bar{y}) + (vz\bar{z}x\bar{y}) - 2(v\bar{z}z\bar{x}y)$	$^2T_1$
$(vx\bar{x}yz)$ $(vy\bar{y}zx)$ $(vz\bar{z}xy)$	$^4T_1$

configuration t_2^5

$(y\bar{y}z\bar{z}x)$ $(x\bar{x}z\bar{z}y)$ $(x\bar{x}y\bar{y}z)$	$^2T_2$

4. Double Negatively-Charged State ($V^{=}$)

configuration $v^2t_2^4$

$(\bar{v}\bar{v}\bar{x}\bar{x}\bar{y}\bar{y}) + (\bar{v}\bar{v}\bar{y}\bar{y}\bar{z}\bar{z}) + (\bar{v}\bar{v}\bar{x}\bar{x}\bar{z}\bar{z})$	$^1A_1$
$(\bar{v}\bar{v}\bar{x}\bar{x}\bar{z}\bar{z}) - (\bar{v}\bar{v}\bar{x}\bar{x}\bar{y}\bar{y})$	^1E
$2(\bar{v}\bar{v}\bar{y}\bar{y}\bar{z}\bar{z}) - (\bar{v}\bar{v}\bar{x}\bar{x}\bar{z}\bar{z}) - (\bar{v}\bar{v}\bar{x}\bar{x}\bar{y}\bar{y})$	
$(\bar{v}\bar{v}\bar{x}\bar{x}yz)$	
$(\bar{v}\bar{v}\bar{y}\bar{y}zx)$	$^3T_1$
$(\bar{v}\bar{v}\bar{z}\bar{z}xy)$	
$(\bar{v}\bar{v}\bar{x}\bar{x}\bar{y}\bar{z}) - (\bar{v}\bar{v}\bar{x}\bar{x}yz)$	
$(\bar{v}\bar{v}\bar{y}\bar{y}\bar{z}\bar{x}) - (\bar{v}\bar{v}\bar{y}\bar{y}zx)$	$^1T_2$
$(\bar{v}\bar{v}\bar{z}\bar{z}\bar{x}\bar{y}) - (\bar{v}\bar{v}\bar{z}\bar{z}xy)$	

configuration vt_2^5

$(v\bar{z}\bar{z}\bar{y}\bar{y}\bar{x}) - (\bar{v}z\bar{z}\bar{y}\bar{y}x)$	
$(v\bar{x}\bar{x}\bar{z}\bar{z}\bar{y}) - (\bar{v}x\bar{x}\bar{z}\bar{z}y)$	$^1T_2$
$(v\bar{x}\bar{x}\bar{y}\bar{y}\bar{z}) - (\bar{v}x\bar{x}\bar{y}\bar{y}z)$	
$(vz\bar{z}\bar{y}\bar{y}x)$	
$(vx\bar{x}\bar{z}\bar{z}y)$	$^3T_2$
$(vx\bar{x}\bar{y}\bar{y}z)$	

configuration t_2^6

$(x\bar{x}\bar{y}\bar{y}\bar{z}\bar{z})$	$^1A_1$

APPENDIX A2

Matrix Elements of the Hamiltonian, H, coupling the Electronic Wave-Functions from each configuration for the vacancy in a particular charge state

Vacancy	Sym. Level	Matrix Element	A	B	C	D	E	F	G	J	K
V^+	$^2T_2$	[1|1]*	2	1	1		2		-1		
(n=3)		[2|2]	1	2			2	1	-1	1	
		[3|3]		3		1		2			
		[1|2]									$-\sqrt{2}$
		[1|3]							$\sqrt{2}$		
		[2|3]									1
	$^2A_1$	[2|2]	1	2		1	2		-1	2	
	^2E	[2|2]	1	2		1	2		-1	-1	
		[3|3]		3				3			
		[2|3]									1.5
	$^2T_1$	[2|2]	1	2			2	1	1	-1	
		[3|3]		3		1		2		-2	
		[2|3]									$\sqrt{3}$
	$^4T_1$	[2|2]	1	2			2	1	-2	-1	
	$^4A_2$	[3|3]		3				3		-3	
V^o	$^1A_1$	[1|1]	2	2	1	1	4		-2	2	
(n=4)		[3|3]		4		2		4			
		[1|3]							2		

* $[1|1] \equiv \frac{\langle \Psi_1 | H | \Psi_1 \rangle}{\langle \Psi_1 | \Psi_1 \rangle}$ where Ψ_1 is the wave function for the particular symmetry state from the configuration $v^2 t_2^{n-2}$. Similarly [2|2] refers to configuration $v t_2^{n-1}$, and [3|3] to configuration t_2^n.

Appendix A2 (continued)

Vacancy	Sym. Level	Matrix Element	A	B	C	D	E	F	G	J	K
V^o	^1E	[1|1]	2	2	1	1	4		-2	-1	
		[2|2]	1	3			3	3			
		[3|3]		4		2		4		-3	
		[1|2]									$\sqrt{6}$
		[1|3]							1		
		[2|3]									$-\sqrt{6}$
	$^1T_1$	[2|2]	1	3		1	3	2		-2	
	$^1T_2$	[1|1]	2	2	1		4	1	-2	1	
		[2|2]	1	3		1	3	2			
		[3|3]		4		1		5		-1	
		[1|2]									$\sqrt{2}$
		[1|3]						1			
		[2|3]									$\sqrt{2}$
	$^3A_2$	[2|2]	1	3			3	3	1	-3	
	^3E	[2|2]	1	3			3	3	-2		
	$^3T_1$	[1|1]	2	2	1		4	1	-2	-1	
		[2|2]	1	3		1	3	2	-2	-2	
		[3|3]		4		1		5		-3	
		[1|2]									$-\sqrt{2}$
		[1|3]							1		
		[2|3]									$\sqrt{2}$
	$^3T_2$	[2|2]	1	3		1	3	2	-2		
	$^5A_2$	[2|2]	1	3			3	+3	-3	-3	

Appendix A2 (continued)

Vacancy	Sym. Level	Matrix Element	A	B	C	D	E	F	G	J	K
V^-	$^2A_1$	[2|2]	1	4		2	4	4	-2		
(n=5)	^2E	[1|1]	2	3	1		6	3	-3		
		[2|2]	1	4		2	4	4	-2	-3	
		[1|2]									$\sqrt{3}$
V^-	$^2T_1$	[1|1]	2	3	1	1	6	2	-3	-2	
		[2|2]	1	4		1	4	5		-3	
		[1|2]									$\sqrt{3}$
	$^2T_2$	[1|1]	2	3	1	1	6	2	-3		
		[2|2]	1	4		1	4	5	-2	-1	
		[3|3]		5		2		8		-4	
		[1|2]									-1
		[1|3]							$\sqrt{2}$		
		[2|3]									$\sqrt{2}$
	$^4A_2$	[1|1]	2	3	1		6	3	-3	-3	
	$^4T_1$	[2|2]	1	4		1	4	5	-3	-3	
$V^=$	$^1A_1$	[1|1]	2	4	1	2	8	4	-4		
(n=6)		[3|3]		6		3		12		-6	
		[1|3]							$\sqrt{3}$		
	^1E	[1|1]	2	4	1	2	8	4	-4	-3	
	$^1T_2$	[1|1]	2	4	1	1	8	5	-4	-1	
		[2|2]	1	5		2	5	8	-1	-4	
		[1|2]									2
	$^3T_1$	[1|1]	2	4	1	1	8	5	-4	-3	
	$^3T_2$	[2|2]	1	5		2	5	8	-3	-4	

APPENDIX A3

The Semi-empirical value for Q in the Diamond and Silicon Calculations

We wish to obtain a semi-empirical value for

$$Q = \int a^*(1)\, a^*(2)\, \frac{1}{r_{12}}\, a(1)\, a(2)\, d\tau_1\, d\tau_2$$

where

$$a = \tfrac{1}{2}\left\{ \psi\ (ns:A) + \sqrt{3}\ \psi(np\sigma:A) \right\}$$

and where n = 2 for carbon and n = 3 for silicon.

It is possible to express the available data including Q in terms of the Slater F,G and I functions using the information provided by Condon and Shortley [68]. The terms of F_K and G_K

$$Q = \frac{1}{16}\left\{ F_0(ss) + 6\, F_0(sp) + 9\, F_0(pp) + 12\, G_1(sp) + 36\, F_2(pp) \right\}.$$

The Carbon Atom

The spectroscopic states for an isolated carbon atom in the valence state sp^3 are known to be ^5S, ^3D, ^3P and ^3S with energies 33735.2 cm^{-1}, 64088.56 cm^{-1}, 75256.3 cm^{-1} and 105800.5 cm^{-1} above the ground state ^3P of the normal carbon atom in its s^2p^2 state. These term energies may also be expressed in terms of F, G and I as outlined in the paper by Coulson and Kearsley [1]. We have

Appendix A3 (continued)

$$W(^5S) = C - 3\,G_1(sp) - 15\,F_2(pp)$$
$$W(^3D) = C - 2\,G_1(sp) - 6\,F_2(pp)$$
$$W(^3P) = C - 2\,G_1(sp)$$
$$W(^3S) = C + G_1(sp) - 15\,F_2(pp)$$

where

$$C = I(2p) - I(2s) + 2\,F_o(pp) - F_o(ss) - F_o(sp) + 5\,F_2(pp) + 2\,G_1(sp).$$

It is not possible to solve these equations for a unique choice of C, F_2 and G_1. However, Skinner and Pritchard [87] solved for all possible triplets from these equations and averaged over the results. They obtained

$$C = 13.5243 \text{ eV}$$
$$G_1(sp) = 2.1426 \text{ eV}$$
$$F_2(pp) = 0.2064 \text{ eV}.$$

Now, it is possible to show, Kearsley [61], that for a pure 2S state for the sp^3 quadrivalent state, the ionisation potential $\varepsilon(2s)$ is given by

$$\varepsilon(2s) = - I(2s) - 3\,J(sp) + {}^3/_2\,K(sp)$$

which gives

Appendix A3 (continued)

$$\varepsilon(2s) = - I(2s) - 3\, F_0(sp) + {}^3/2\, G_1(sp).$$

Similarly, we may approximate the electron affinity A(2s) for the same valence state by

$$\begin{aligned} A(2s) &= \varepsilon(2s) - J(ss) \\ &= - I(2s) - 3\, F_0(sp) + {}^3/2\, G_1(sp) - F_0(ss) \ . \end{aligned}$$

For a 2p electron in the sp^3: V_4 state

$$\varepsilon(2p) = - I(2p) - F_0(sp) - 2\, F_0(pp) + 7\, F_2(pp) + \tfrac{1}{2}\, G_1(sp)$$

$$A(2p) = - I(2p) - F_0(sp) - 3\, F_0(pp) + 3\, F_2(pp) + \tfrac{1}{2}\, G_1(sp) \ .$$

Skinner and Pritchard [87] estimated $\varepsilon(2s)$, $A(2s)$, $\varepsilon(2p)$ and $A(2p)$ to have the following values

$$\varepsilon(2s) = 21.34 \text{ eV}, \qquad A(2s) = 9.11 \text{ eV}$$

$$\varepsilon(2p) = 11.54 \text{ eV}, \qquad A(2p) = 0.46 \text{ eV} \ .$$

From this data we may now determine the F's and G's required to evaluate Q

$$F_0(ss) = 12.23 \text{ eV} \qquad F_2(pp) = 0.206 \text{ eV}$$

$$F_0(sp) = 11.34 \text{ eV} \qquad I(2s) = - 52.14 \text{ eV}$$

$$F_0(pp) = 10.26 \text{ eV} \qquad I(2p) = - 40.88 \text{ eV}$$

$$G_1(sp) = 2.143 \text{ eV}.$$

These values differ slightly from those quoted by Coulson and Kearsley because a more accurate value have been used in converting from cm^{-1} to eV. For the tetrahedral hybrid states these values lead to the result

$$Q = 12.856 \text{ eV}$$

$$\varepsilon(a) = 16.42 \text{ eV} .$$

The value of Q is different to that found by Coulson and Kearsley (Q = 13.293 eV) because, we believe a numerical error was made in the previous work.

The Silicon atom

For the silicon atom it is more difficult to obtain a reliable estimate of Q because only the energy of the ^3D spectroscopic state for the isolated silicon atom in the valence state sp^3 is known. However, Skinner and Pritchard have estimated that the terms C, G_1 and F_2 have the following values

$$C = 70644 \text{ cm}^{-1} = 8.7174 \text{ eV}$$

$$G_1(sp) \simeq 9000 \text{ cm}^{-1} = 1.1106 \text{ eV}$$

$$F_2(pp) \simeq 660 \text{ cm}^{-1} = 0.0814 \text{ eV}.$$

The values for $\varepsilon(3s)$, $A(3s)$, $\varepsilon(3p)$ and $A(3p)$ are estimated to be

$$\varepsilon(3s) = 17.93 \text{ eV} \qquad \varepsilon(3p) = 8.99 \text{ eV}$$

$$A(3s) = 7.93 \text{ eV} \qquad A(3p) = 3.42 \text{ eV} .$$

Using these values and the formulae given earlier we obtain the following values for the F and G terms

$F_0(ss) = 10.00$ eV $F_2(pp) = 0.0814$ eV

$F_0(sp) = 7.690$ eV $I(3s) = -39.33$ eV

$F_0(pp) = 6.355$ eV $I(3p) = -28.26$ eV

$G_1(sp) = 1.1106$ eV .

These values predicted that

$$Q = 8.10 \text{ eV}$$

and

$$\varepsilon(a) = 12.55 \text{ eV}.$$

APPENDIX A4

1. Values of the One-Electron Integrals used in the vacancy and divacancy calculations for diamond

Integral*	Clementi Functions	Slater Functions
$\langle a \mid p \rangle$	0.1426	0.1130
$\langle a \mid b \rangle$	0.2421	0.1654
$\langle a \mid e \rangle$	0.0941	0.0499
$\langle a \mid d \rangle$	0.0499	0.0152
$\langle a \mid T \mid a \rangle$	36.0505	28.8426
$\langle a \mid T \mid p \rangle$	0.2384	-0.6024
$\langle a \mid T \mid b \rangle$	0.4610	-0.1446
$\langle a \mid T \mid e \rangle$	-0.0747	-0.2581
$\langle a \mid T \mid d \rangle$	-0.1379	-0.1551
$\langle a \mid V_A \mid a \rangle$	-43.185+	-36.835× -36.59⊥
$\langle a \mid V_A \mid p \rangle$	-4.0502	-4.7823
$\langle a \mid V_A \mid b \rangle$	-4.0171	-2.8290
$\langle a \mid V_A \mid e \rangle$	-1.3719	-0.6960
$\langle a \mid V_A \mid d \rangle$	-0.5195	-0.1650
$\langle p \mid V_A \mid p \rangle$	-15.4312	12.047
$\langle b \mid V_A \mid b \rangle$	-8.1505	-7.9250
$\langle e \mid V_A \mid e \rangle$	-5.7675	-5.7130
$\langle d \mid V_A \mid d \rangle$	-4.7140	-4.6270

---

*Definitions as for the divacancy

+For modified Q = 12.856 eV

×Computed

⊥From incomplete gamma functions

APPENDIX A4

2. **Values of the Two-Electron Integrals used in the vacancy and divacancy calculations for diamond**

Integral*	Clementi Functions	Slater Functions
$\langle aa\left\|\frac{1}{r_{12}}\right\|aa\rangle$	17.8067+×	19.0664×
$\langle ap\left\|\frac{1}{r_{12}}\right\|ap\rangle$	10.0692	10.2736
$\langle ab\left\|\frac{1}{r_{12}}\right\|ab\rangle$	7.9185	7.8502
$\langle ae\left\|\frac{1}{r_{12}}\right\|ae\rangle$	5.7315	5.7059
$\langle ad\left\|\frac{1}{r_{12}}\right\|ad\rangle$	4.6882	4.6272
$\langle aa\left\|\frac{1}{r_{12}}\right\|ap\rangle$	2.7918	2.3709
$\langle aa\left\|\frac{1}{r_{12}}\right\|ab\rangle$	3.0584	2.1809
$\langle aa\left\|\frac{1}{r_{12}}\right\|ae\rangle$	1.0090	0.5552
$\langle aa\left\|\frac{1}{r_{12}}\right\|ad\rangle$	0.4654	0.1439
$\langle ap\left\|\frac{1}{r_{12}}\right\|pa\rangle$	0.7370	0.5672
$\langle ab\left\|\frac{1}{r_{12}}\right\|ba\rangle$	0.8229	0.4189
$\langle ae\left\|\frac{1}{r_{12}}\right\|ea\rangle$	0.1082	0.0347
$\langle ad\left\|\frac{1}{r_{12}}\right\|da\rangle$	0.0265	0.0028

*Definifiton as for the divacancy
× Calculated values
+All integrals in electron volts

APPENDIX B1

Configurations Wave-functions for a Neutral Divacancy

configuration $a_{1g}^2 a_{2u}^2 e_g^2$

$(\bar{v}\bar{v}uu\bar{x}\bar{x}) + (\bar{v}\bar{v}uu\bar{y}\bar{y})$	$^1A_{1g}$
$(\bar{v}\bar{v}uu\bar{x}\bar{y})$	$^3A_{2g}$
$(\bar{v}\bar{v}uu\bar{x}\bar{x}) - (\bar{v}\bar{v}uu\bar{y}\bar{y})$ $(\bar{v}\bar{v}uu\bar{x}\bar{y}) + (\bar{v}\bar{v}uu\bar{y}\bar{x})$	^1E_g

configuration $a_{1g}^2 a_{2u}^2 e_u^2$

$(\bar{v}\bar{v}uu\bar{z}\bar{z}) + (\bar{v}\bar{v}uu\bar{t}\bar{t})$	$^1A_{1g}$
$(\bar{v}\bar{v}uu\bar{z}\bar{t})$	$^3A_{2g}$
$(\bar{v}\bar{v}uu\bar{z}\bar{z}) - (\bar{v}\bar{v}uu\bar{t}\bar{t})$ $(\bar{v}\bar{v}uu\bar{z}\bar{t}) + (\bar{v}\bar{v}uu\bar{t}\bar{z})$	^1E_g

configuration $a_{1g}^2 a_{2u}^2 e_g e_u$

$(\bar{v}\bar{v}uu\bar{x}t) - (\bar{v}\bar{v}uu\bar{y}z)$	$^3A_{1u}$
$(\bar{v}\bar{v}uu\bar{x}\bar{t}) - (\bar{v}\bar{v}uu\bar{x}\bar{t}) + (\bar{v}\bar{v}uu\bar{y}z) - (\bar{v}\bar{v}uu\bar{y}\bar{z})$	$^1A_{1u}$
$(\bar{v}\bar{v}uu\bar{x}z) + (\bar{v}\bar{v}uu\bar{y}t)$	$^3A_{2u}$
$(\bar{v}\bar{v}uu\bar{x}\bar{z}) + (\bar{v}\bar{v}uu\bar{y}\bar{t}) - (\bar{v}\bar{v}uu\bar{x}z) - (\bar{v}\bar{v}uu\bar{y}t)$	$^1A_{2u}$
$(\bar{v}\bar{v}uu\bar{x}z) - (\bar{v}\bar{v}uu\bar{y}t)$ $(\bar{v}\bar{v}uu\bar{x}t) + (\bar{v}\bar{v}uu\bar{y}z)$	^3E_u
$(\bar{v}\bar{v}uu\bar{x}z) - (\bar{v}\bar{v}uu\bar{x}z) + (\bar{v}\bar{v}uu\bar{y}\bar{t}) - (\bar{v}\bar{v}uu\bar{y}t)$ $(\bar{v}\bar{v}uu\bar{x}t) - (\bar{v}\bar{v}uu\bar{x}\bar{t}) + (\bar{v}\bar{v}uu\bar{y}z) - (\bar{v}\bar{v}uu\bar{y}\bar{z})$	^1E_u

Appendix B1 (continued)

configuration $a_{1g}a_{2u}^2e_g^3$

$(vu\bar{u}x\bar{x}y)$ $(vu\bar{u}y\bar{y}x)$	^3E_g
$(vu\bar{u}i\bar{x}\bar{x}\bar{y}) - (\bar{v}u\bar{u}x\bar{x}y)$ $(vu\bar{u}y\bar{y}\bar{x}) - (\bar{v}u\bar{u}y\bar{y}x)$	^1E_g

configuration $a_{1g}a_{2u}^2e_g^2e_u$

$(vu\bar{u}xyz)$ $(vu\bar{u}xyt)$	^5E_u
$(vu\bar{u}x\bar{x}t) - (vu\bar{u}y\bar{y}t) - (vu\bar{u}\bar{x}yz) + (vu\bar{u}x\bar{y}z)$	$^3A_{1u}$
$(vu\bar{u}x\bar{x}z) - (vu\bar{u}y\bar{y}z) + (vu\bar{u}\bar{x}yt) - (vu\bar{u}x\bar{y}t)$	$^3A_{2u}$
$(vu\bar{u}x\bar{x}\bar{z}) - (\bar{v}u\bar{u}x\bar{x}z) - (vu\bar{u}y\bar{y}\bar{z}) + (\bar{v}u\bar{u}y\bar{y}z) +$ $(vu\bar{u}\bar{x}y\bar{t}) - (\bar{v}u\bar{u}\bar{x}yt) - (vu\bar{u}\bar{x}yt) + (\bar{v}u\bar{u}x\bar{y}t)$	$^1A_{2u}$
$(vu\bar{u}x\bar{x}\bar{t}) - (\bar{v}u\bar{u}x\bar{x}t) - (vu\bar{u}y\bar{y}\bar{t}) + (\bar{v}u\bar{u}y\bar{y}t) -$ $(vu\bar{u}\bar{x}y\bar{z}) + (\bar{v}u\bar{u}\bar{x}yz) + (vu\bar{u}x\bar{y}\bar{z}) - (\bar{v}u\bar{u}x\bar{y}z)$	$^1A_{1u}$
$(vu\bar{u}x\bar{y}\bar{z}) - (\bar{v}u\bar{u}x\bar{y}z)$ $(vu\bar{u}x\bar{y}\bar{t}) - (\bar{v}u\bar{u}x\bar{y}t)$	^3E_u (i)
$(vu\bar{u}x\bar{x}z) + (vu\bar{u}y\bar{y}z)$ $(vu\bar{u}x\bar{x}t) + (vu\bar{u}y\bar{y}t)$	^3E_u (ii)
$(vu\bar{u}x\bar{x}z) - (vu\bar{u}y\bar{y}z) - (vu\bar{u}\bar{x}yt) + (vu\bar{u}x\bar{y}t)$ $(vu\bar{u}x\bar{x}t) - (vu\bar{u}y\bar{y}t) + (vu\bar{u}\bar{x}yz) - (vu\bar{u}x\bar{y}z)$	^3E_u (iii)
$(vu\bar{u}x\bar{y}z) + (vu\bar{u}\bar{x}yz) - 2(\bar{v}u\bar{u}xyz)$ $(vu\bar{u}x\bar{y}t) + (vu\bar{u}\bar{x}yt) - 2(\bar{v}u\bar{u}xyt)$	^3E_u (iv)

$$(v\bar{u}u\bar{x}x\bar{z}) - (\bar{v}u\bar{u}x\bar{x}z) + (vu\bar{u}y\bar{y}z) - (\bar{v}u\bar{u}y\bar{y}z) \qquad {}^1E_u \quad \text{(i)}$$
$$(v\bar{u}u\bar{x}x\bar{t}) - (\bar{v}u\bar{u}x\bar{x}t) + (vu\bar{u}y\bar{y}t) - (\bar{v}u\bar{u}y\bar{y}t)$$

$$(v\bar{u}u\bar{x}x\bar{z}) - (\bar{v}u\bar{u}x\bar{x}z) - (vu\bar{u}y\bar{y}z) + (\bar{v}u\bar{u}y\bar{y}z) - \qquad {}^1E_u \quad \text{(ii)}$$
$$(v\bar{u}u\bar{x}y\bar{t}) + (\bar{v}u\bar{u}xyt) + (vu\bar{u}x\bar{y}t) - (\bar{v}u\bar{u}xy\bar{t})$$
$$(v\bar{u}u\bar{x}x\bar{t}) - (\bar{v}u\bar{u}x\bar{x}t) - (vu\bar{u}y\bar{y}t) + (\bar{v}u\bar{u}y\bar{y}t) +$$
$$(v\bar{u}u\bar{x}y\bar{z}) - (\bar{v}u\bar{u}xyz) - (vu\bar{u}x\bar{y}z) + (\bar{v}u\bar{u}xy\bar{z})$$
$$(\bar{v}u\bar{u}x\bar{y}z) + (\bar{v}u\bar{u}xy\bar{z}) + (vu\bar{u}xyz) + (vu\bar{u}x\bar{y}\bar{z})$$
$$-2(\bar{v}u\bar{u}xy\bar{z}) - 2(vu\bar{u}xyz)$$
$$(\bar{v}u\bar{u}x\bar{y}t) + (\bar{v}u\bar{u}xyt) + (vu\bar{u}x\bar{y}\bar{t}) + (vu\bar{u}xy\bar{t}) \qquad {}^1E_u \quad \text{(iii)}$$
$$-2(\bar{v}u\bar{u}xy\bar{t}) - 2(vu\bar{u}xyt)$$

configuration $a_{1g}a_{2u}^2e_ge_u^2$

As for configuration $a_{1g}a_{2u}^2e_g^2e_u$ but with 'x' replaced by 'z', 'y' by 't' and vice versa. Also $u \to g$ and $A_{1u} \to A_{2g}$ and $A_{2u} \to A_{1g}$

configuration $a_{1g}a_{2u}^2e_u^3$

As for configuration $a_{1g}a_{2u}^2e_g^3$ but with 'x' replaced by 'z' and 'y' by 't'. Also $g \to u$

configuration $a_{1g}^2a_{2u}e_g^3$

As for configuration $a_{1g}a_{2u}^2e_g^3$ but with 'v' replaced by 'u' and vice versa. Also $g \to u$.

configuration $a_{1g}^2a_{2u}e_ge_u^2$

As for configuration $a_{1g}a_{2u}^2e_g^2e_u$ but with 'v' replaced by 'u' and vice versa. Also $u \to g$ and $A_{1u} \to A_{2g}$ and $A_{2u} \to A_{1g}$.

configuration $a_{1g}^2 a_{2u} e_g e_u^2$

As for configuration $a_{1g} a_{2u}^2 e_g^2 e_u$ but with 'v' replaced by 'u', 'x' by 'z', 'y' by 't' and vice versa.

configuration $a_{1g}^2 a_{2u} e_u^3$

As for configuration $a_{1g} a_{2u}^2 e_g^3$ but with 'v' replaced by 'u', 'x' by 'z', 'y' by 't' and 'u' by 'v'.

APPENDIX B2

Energies for the various configurations of the Neutral Isolated Divacancy

Configuration $a_{1g}^2 a_{2u}^2 e_g^2$

$$A_1 \equiv 2A + 2B + 2C + E + F + 4G + 4P + 4T - 2J - 2Q - 2U$$

$^1A_{1g}$ $\quad A_1 + 1 + K$

$^3A_{2g}$ $\quad A_1 + L - 1$

^1E_g $\quad A_1 + K - 1$

Configuration $a_{1g}^2 a_{2u}^2 e_g e_u$

$$A_2 \equiv 2A + 2B + C + D + E + F + 4G - 2J + 2P - Q + 2T - U + 2R-S + 2V - W$$

$^3A_{1u}$ $\quad A_2 - \Gamma + \Lambda - Z + x$

$^1A_{1u}$ $\quad A_2 - \Gamma - \Lambda + Z + x$

$^3A_{2u}$ $\quad A_2 - Y + \Gamma - r + X$

$^1A_{2u}$ $\quad A_2 + Y + \Gamma + r + X$

^3E_u $\quad A_2 + X - Y - \Gamma + r$

^1E_u $\quad A_2 + \frac{1}{2}(x+X) + \frac{1}{2}(Y+Z) + \frac{1}{2}(\Lambda-r)$

Configuration $a_{1g}^2 a_{2u}^2 e_u^2$

$$A_3 \equiv 2A + 2B + 2D + E + F + 4G - 2J + 4R - 2S + 4V - 2W$$

$^3A_{2g}$ $\qquad A_3 + N - n$

$^1A_{1g}$ $\qquad A_3 + n + M$

^1E_g $\qquad A_3 + M - n$

Configuration $a_{1g} a_{2u}^2 e_g^3$

$$A_4 = A + 2B + 3C + 2G - J + 3P - Q + 6T - 3u + F + K + 2L - l$$

^3E_g $\qquad A_4 - Q$

^1E_g $\qquad A_4 + Q$

Configuration $a_{1g} a_{2u}^2 e_g^2 e_u$

$$A_5 = A + 2B + 2C + D + F + 2G - J + 4T - 2U + 2V - W + 2P - Q + R - \tfrac{1}{2}(Z+Y) + X + x$$

$^3A_{1u}$ $\qquad A_5 - S + \tfrac{1}{2}[r-\Lambda] + \tfrac{1}{2}(K+L)$

^5E_u $\qquad A_5 - Q - S - \tfrac{1}{2}(Z+Y) + L - l$

$^3A_{2u}$ $\qquad A_5 - S + \tfrac{1}{2}(r-\Lambda) + \tfrac{1}{2}(K+L)$

$^1A_{2u}$ $\quad A_5 + S + \frac{1}{2}(r-\Lambda) + \frac{1}{2}(K+L)$

$^1A_{1u}$ $\quad A_5 + S + \frac{1}{2}(r-\Lambda) + \frac{1}{2}(K+L)$

^3E_u (i) $\quad A_5 + S + L - 1$

(ii) $\quad A_5 - S + K + 1$

(iii) $\quad A_5 - S + \frac{1}{2}(K+L) + \frac{1}{2}(\Lambda-r)$

(iv) $\quad A_5 + 2Q + L - \frac{1}{3}(Y+Z+S) - 1$

^1E_u (i) $\quad A_5 + K + S + 1$

(ii) $\quad A_5 + \frac{1}{2}(K+L) + S + \frac{1}{2}(\Lambda-r)$

(iii) $\quad A_5 + L + Y + Z - S - 1 + 2Q$

Configuration $a_{1g}a_{2u}^2e_ge_u^2$

$$A_6 \equiv A + 2B + C + 2D + F + 2G - J + 4V - 2W + 2T - U + 2R - S + P - \tfrac{1}{2}(Z+Y) + x + X$$

$^3A_{2g}$ $\quad A_6 - Q + \frac{1}{2}(r-\Lambda) + \frac{1}{2}(M+N)$

$^3A_{1g}$ $\quad A_6 - Q + \frac{1}{2}(r-\Lambda) + \frac{1}{2}(M+N)$

^5E_g $\quad A_6 - S - Q - \frac{1}{2}(Z+Y) + N - n$

$^1A_{1g}$ $\quad A_6 + Q + \frac{1}{2}(r-\Lambda) + \frac{1}{2}(M+N)$

$^1A_{2g}$ $\quad A_6 + Q + \frac{1}{2}(r-\Lambda) + \frac{1}{2}(M+N)$

Appendix B2 (continued)

^3E_g

(i) $A_6 + Q + N - n$

(ii) $A_6 - Q + M + n$

(iii) $A_6 - Q + \frac{1}{2}(M+N) + \frac{1}{2}(\Lambda - r)$

(iv) $A_6 + 2S + N - \frac{1}{3}(Y+Z+Q) - n$

^1E_g

(i) $A_6 + M + Q + n$

(ii) $A_6 + \frac{1}{2}(M+N) + Q + \frac{1}{2}(\Lambda - r)$

(iii) $A_6 + N + (Y+Z) - Q + 2S - n$

Configuration $a_{1g} a_{2u}^2 e_u^3$

$A_7 = A + 2B + 3D + 2G - J + 3R - S + F + 6V - 3N + M + 2N - n$

^3E_u $A_7 - S$

^1E_u $A_7 + S$

Configuration $a_{1g}^2 a_{2u} e_g^3$

$$A_8 \equiv 2A + B + 3C + 2G - J + 3T - U + E + 6P - 3Q + K + 2L - 1$$

^3E_u	$A_8 - u$
^1E_u	$A_8 + u$

Configuration $a_{1g}^2 a_{2u} e_u^3$

$$A_{11} \equiv 2A + B + 3D + 2G - J + E + 3V - W + 6R - 3S + M + 2N - n$$

^3E_g	$A_{11} - W$
^1E_g	$A_{11} + W$

Configuration $a_{1g}^2 a_{2u} e_g^2 e_u$

$$A_9 = 2A + B + 2C + D + E + 2G - J + 4P - 2Q + 2R - S + 2T - U + V - \tfrac{1}{2}(Y+Z) + X + x$$

$^3A_{2g}$	$A_9 - W + \tfrac{1}{2}(r-\Lambda) + \tfrac{1}{2}(K+L)$
^5E_g	$A_9 - W - U - \tfrac{1}{2}(Y+Z) + L - 1$
$^3A_{1g}$	$A_9 - W + \tfrac{1}{2}(r-\Lambda) + \tfrac{1}{2}(K+L)$
$^1A_{1g}$	$A_9 + W + \tfrac{1}{2}(r-\Lambda) + \tfrac{1}{2}(K+L)$
$^1A_{2g}$	$A_9 + W + \tfrac{1}{2}(r-\Lambda) + \tfrac{1}{2}(K+L)$

^3E_g	(i)	$A_9 + W + L - 1$
	(ii)	$A_9 - W + K + 1$
	(iii)	$A_9 - W + \frac{1}{2}(K+L) + \frac{1}{2}(\Lambda-r)$
	(iv)	$A_9 + 2U + L - \frac{1}{3}(W+Z+Y) - 1$
^1E_g	(i)	$A_9 + K + W + C$
	(ii)	$A_9 + \frac{1}{2}(K+L) + W + \frac{1}{2}(\Lambda-r)$
	(iii)	$A_9 + L + (Y+Z) - W - 1 + 2U$

Configuration $a_{1g}^2 a_{2u} e_g e_u^2$

$$A_{10} \equiv 2A + B + C + 2D + E + 2G - J + 4R - 2S + 2P - Q + 2V - W + T - \tfrac{1}{2}(Z+Y) + x + X$$

$^3A_{1u}$	$A_{10} - U + \frac{1}{2}(r-\Lambda) + \frac{1}{2}(M+N)$
^5E_u	$A_{10} - U - W - \frac{1}{2}(Z+Y) + N - n$
$^3A_{2u}$	$A_{10} - U + \frac{1}{2}(r-\Lambda) + \frac{1}{2}(M+N)$
$^1A_{2u}$	$A_{10} + U + \frac{1}{2}(r-\Lambda) + \frac{1}{2}(M+N)$
$^1A_{1u}$	$A_{10} + U + \frac{1}{2}(r-\Lambda) + \frac{1}{2}(M+N)$

^3E_u (i) $A_{10} + U + N - n$

(ii) $A_{10} - U + M + n$

(iii) $A_{10} - U + \frac{1}{2}(M+N) + \frac{1}{2}(\Lambda-r)$

(iv) $A_{10} + 2W + N - \frac{1}{2}(U+Y+Z) - n$

^1E_u (i) $A_{10} + M + U + n$

(ii) $A_{10} + \frac{1}{2}(M+N) + U + \frac{1}{2}(\Lambda-r)$

(iii) $A_{10} + N + 2W - U + (Y+Z) - n$

Configuration $a_{1g}a_{2u}e_g^2e_u^2$

$^7A_{2u}$ $A + B + 2C + 2D + G - J + 2P - 2Q + 2R - 2S + 2T - 2U + 2V - 2W + L - 1 + 2X + 2x - 2Z - 2Y + N - n$

APPENDIX C1

The Normal co-ordinates for the vibrational modes of the Tetrahedral Group

The neighbours to the vacancy A,B,C,D have co-ordinates $(\bar{1},1,1)$ $(1,\bar{1},1)$, $(1,1,\bar{1})$ and $(\bar{1},\bar{1},\bar{1})$ respectively. Writing the x displacement of A as X_A, and so on, the Q_α are given below.

$$Q_a = \frac{1}{\sqrt{12}}\left[\left\{-X_A + X_B + X_C - X_D\right\} + \left\{Y_A - Y_B + Y_C - Y_O\right\} + \left\{Z_A + Z_B - Z_C - Z_D\right\}\right] \subset A_1$$

$$Q_\theta = \frac{1}{\sqrt{24}}\left[2\left\{-X_A + X_B + X_C - X_D\right\} - \left\{Y_A - Y_B + Y_C - Y_D\right\} - \left\{Z_A + Z_B - Z_C - Z_D\right\}\right]$$

$$Q_\varepsilon = \frac{1}{\sqrt{8}}\left[\left\{Y_A - Y_B + Y_C - Y_D\right\} - \left\{Z_A + Z_B - Z_C - Z_D\right\}\right] \subset E$$

$$Q_\xi = \frac{1}{\sqrt{8}}\left[\left\{Y_A + Y_B - Y_C - Y_D\right\} + \left\{Z_A - Z_B + Z_C - Z_D\right\}\right]$$

$$Q_\eta = \frac{1}{\sqrt{8}}\left[\left\{X_A + X_B - X_C - X_D\right\} + \left\{-Z_A + Z_B + Z_C - Z_D\right\}\right] \subset T_2$$

$$Q_\zeta = \frac{1}{\sqrt{8}}\left[\left\{X_A - X_B + X_C - X_D\right\} + \left\{-Y_A + Y_B + Y_C - Y_D\right\}\right]$$

APPENDIX C2

Jahn-Teller terms for the lowest electronic levels of the Vacancy in its various charge states

Let c_1, c_2, c_3 be the eigenvectors for the single configuration wave functions contributing to the lowest electronic state wave function of a particular symmetry and spin multiplicity. Then we define

$$A = c_1^2, \quad B = c_1 c_2, \quad C = c_1 c_3$$
$$D = c_2^2, \quad E = c_2 c_3, \quad F = c_3^2 \ .$$

The I_{TE} or I_{EE} expressions which result in a tetragonal distortion involve terms such as DYHY, DVVYY, which are defined as follows:

$$DYHY \equiv \left(\frac{\partial}{\partial Q_\varepsilon} \langle y | H^o | y \rangle \right)_o$$

$$DVVYY \equiv \left(\frac{\partial}{\partial Q_\varepsilon} \langle vy | \frac{1}{r_{12}} | vy \rangle \right)_o$$

and so on. For the calculation of the extent of trigonal distortion, the I_{TT} expressions contain terms such as DYHZ, DVVYZ, etc. which are defined as:

$$DYHZ = \left(\frac{\partial}{\partial Q_\xi} \langle y | H^o | z \rangle \right)_o$$

$$DVVYZ = \left(\frac{\partial}{\partial Q_\xi} \langle vy | \frac{1}{r_{12}} | vz \rangle \right)_o$$

1. Positive Vacancy

a) $^2T_2$ level

$$I_{TE} = 2\sqrt{3}\Big[\text{DYHY}(A-D) + \text{DVVYY}(2A-D) + \text{DVYVY}(-A + 0.5D - \sqrt{2}\,C) + \text{DXXYY}(-D+F) + \text{DXYXY}(-D-1.5F) - \text{DYYYY}(0.5F) + \text{DVYXZ}(\sqrt{2}\,B+5E)\Big]$$

$$I_{TT} = \text{DYHZ}(A+D) - \text{DVHX}(E + \sqrt{2}\,B) + \text{DVYVZ}(-A - \sqrt{2}\,C - 0.5D) + \text{DVVYZ}(2A+D) + \text{DVYXY}(E - \sqrt{2}\,B) - \text{DVXYY}(\sqrt{2}\,B+E) + \text{DXXYZ}(D+F) - \text{DVVVX}(\sqrt{2}\,B) + \text{DXZXY}(D - 1.5F) - E(\text{DVXXX}) - F(\text{DYYYZ})\ .$$

b) $^4T_1$ level

$$I_{TT} = -\text{DYHZ} - \text{DVVYZ} - \text{DXXYZ} + \text{DVYVZ} + \text{DXYXZ}$$

$$I_{TE} = -2\sqrt{3}\Big[\text{DYHY} + \text{DVVYY} + \text{DXXYY} - \text{DVYVY} - \text{DXYXY}\Big]\ .$$

2. Neutral Vacancy

a) $^3T_1$ level

$$I_{TE} = -2\sqrt{3}\Big[\text{DYHY}(A-F) + \text{DVVYY}(2A) + \text{DVYVY}(-A-2C + 0.5D) + \text{DXXYY}(A-D-F) + \text{DXYXY}(-A - 0.5D) - \sqrt{2}\,\text{DVYXZ}(B-E) + \text{DYYYY}(0.5D-F)\Big]$$

$$I_{TT} = \text{DYHZ}(-A+F) - \text{DVVYZ}(2A) + \text{DVYVZ}(A+0.5D + 2C) + \text{DXZXY}(A-0.5D) + \text{DXXYZ}(-A-D+F) + \text{DVHX}(\sqrt{2}\,B + \sqrt{2}\,E) + \text{DYYYZ}(2F+D) - \text{DVYXY}(\sqrt{2}\,B + \sqrt{2}\,E) + \text{DVXYY}(\sqrt{2}\,B + 3\sqrt{2}\,E) + \sqrt{2}\,B(\text{DVVVX} + \text{DVXXX})\ .$$

b) ^1E level

$$I_{EE} = 2/\sqrt{3}\Big[\text{DYHY}(-A+F) - \text{DVVYY}(2A) + \text{DVYVY}\,(A+2C-1.5D)$$
$$+ \text{DYYYY}(-0.5A+0.5F) + \text{DXYXY}(A+1.5D)$$
$$\text{D DVYXZ}(-\sqrt{6}\,B + \sqrt{6}\,E) + \text{DXXYY}(2F)\Big] .$$

c) $^1T_2$ level

$$I_{TE} = 2\sqrt{3}\Big[\text{DYHY}(-A+F) - \text{DVVYY}(2A) + \text{DVYVY}(A+1.5D+2C)$$
$$+ \text{DXXYY}(-A+F+D) - \text{DXYXY}\,(A+1.5D+2F) +$$
$$+ \text{DYYYY}(-0.5D+F) + \text{DVYXZ}(5\sqrt{2}\,B + 5\sqrt{2}\,E)\Big]$$

$$I_{TT} = \text{DYHZ}(A-F) + \sqrt{2}\,\text{DVHX}(-B+E) + \text{DVVYZ}(2A)$$
$$+ \text{DXZXY}(A-1.5D+2F) + \text{DYYYZ}(-D-2F)$$
$$+ \text{DXXYZ}(A+D-F) + \text{DVYVZ}(-A+1.5D-2C)$$
$$- \sqrt{2}\,B(\text{DVVVX} + \text{DVXXX}) + \text{DVYXY}(\sqrt{2}\,B - \sqrt{2}\,E)$$
$$+ \text{DXVYY}(-\sqrt{2} + 3\sqrt{2}\,E) .$$

3. <u>Negative Vacancy</u>

a) $^2T_2$ level

$$I_{TT} = \text{DYHZ}(-D-F) + \text{DXXYZ}(A-D-2F) + \text{DYYYZ}\,(-A-2D-2F)$$
$$+ \text{DXZXY}(-1.5A+2D+F) - \text{DVVYZ}(D)$$
$$+ \text{DVYVZ}(0.5D - \sqrt{2}\,C) - \text{DVHX}(\sqrt{2}\,E+B) - \text{DVXXX}(\sqrt{2}\,E)$$
$$+ B * \text{DVVVX} - \text{DVXYY}(3\sqrt{2}\,E+3B) + \text{DVYXY}\,(B + 3\sqrt{2}\,E) .$$

$$I_{TE} = -2\sqrt{3}\Big[\text{DYHY}(-D+F) + \text{DXXYY}(-A-D+2F) + \text{DYYYY}(0.5A-D+F) + \text{DXYXY}(1.5A+2D-F) - \text{DVVYY}(D) + \text{DVYVY}(0.5D + \sqrt{2}\,C) + \text{DVYXZ}(\sqrt{2}\,E + 5B)\Big].$$

b) ^2E level

$$I_{EE} = -1/\sqrt{12}\Big[\text{DXYXY}(3A) + 2D(2\,\text{DYHY} + 2\text{DVVYY} - \text{DVYVY} + 4\,\text{DXXYY} + \text{DYYYY}) + \sqrt{12}\,B\times\text{DVYXZ}\Big].$$

c) $^2T_1$ level

$$I_{TE} = 2\sqrt{3}\Big[\text{DYHY}(D) + \text{DXYXY}(0.5A) + \text{DXXYY}(A+D) + \text{DYYYY}(-0.5A+D) + D(\text{DVVYY} - 1.5\,\text{DVYVY}) - \sqrt{3}\,B\times\text{DVYXZ}\Big]$$

$$I_{TT} = \text{DYHZ}(D) + \sqrt{3}\,B(\text{DVHX} + \text{DVVVX} + 3\,\text{DVXYY} - \text{DVYXY}) + \text{DYYYZ}(A+2D) + \text{DXXYZ}(-A+D) - \text{DXYXZ}(0.5A) + D(\text{DVVYZ} - 1.5\,\text{DVYVZ}).$$

d) $^4T_1$ level

$$I_{TE} = 2\sqrt{3}\Big[\text{DYHY} + \text{DVVYY} + \text{DYYYY} + \text{DXXYY}\Big]$$

$$I_{TT} = \text{DYHZ} + \text{DVVYZ} + 2\,\text{DYYYZ} + \text{DXXYZ}\,.$$

4. <u>Double Negatively Charged Vacancy</u>

a) ^1E level

$$I_{EE} = 1/\sqrt{12}\Big[\text{DYHY} + 2\,\text{DVVYY} - \text{DVYVY} + 2\,\text{DXXYY} + 0.5\,\text{DYYYY}\Big].$$

b) $^3T_1$ level

$$I_{TE} = 2\sqrt{3}\left[\text{DYHY} + 2\,\text{DVVYY} - \text{DVYVY} + \text{DYYYY} + \text{DXXYY}\right]$$

$$I_{TT} = \text{DYHZ} + 2\,\text{DVVYZ} - \text{DVYVZ} + 2\,\text{DYYYZ} + \text{DXXYZ}.$$

c) $^1T_2$ level

$$\begin{aligned} I_{TE} = 2\sqrt{3}\Big[&\text{DYHY}(A-D) + \text{DVVYY}(2A-D) \\ &+ \text{DVYVY}(-A+2D) + \text{DYYYY}(A-D) \\ &+ \text{DXXYY}(A-2D) + \text{DXYXY}(-2A+D) - 2B \times \text{DVYXZ}\Big] \end{aligned}$$

$$\begin{aligned} I_{TT} = &\text{DYHZ}(-A-D) + \text{DVVYZ}(-2A-D) \\ &+ \text{DVYVZ}(A+2D) - \text{DYYYZ}(2A+2D) \\ &- \text{DXXYZ}(A+2D) + \text{DXZXY}(2A+D) - 2B\,(\text{DVHX} + \text{DVVVX} + \text{DVXXX} \\ &+ 3\,\text{DVXYY} - 3\,\text{DVYXY}). \end{aligned}$$

d) $^3T_2$ level

$$I_{TE} = -2\sqrt{3}\left[\text{DYHY} + \text{DVVYY} + 2\,\text{DXXYY} - \text{DXYXY} + \text{DYYYY}\right]$$

$$I_{TT} = -\,\text{DYHZ} - \text{DVVYZ} - 2\,\text{DXXYZ} - 2\,\text{DYYYZ} + \text{DXYXZ}\ .$$

APPENDIX C3

Derivatives of Molecular Integrals in terms of the derivatives of the Atomic Integrals

We have used the following notation to abbreviate the atomic integrals

$$SAB \equiv \langle a | b \rangle$$

$$AVBA \equiv \langle a | V_B | a \rangle$$

$$AABB \equiv \langle a(1)\ b(2) | \frac{1}{r_{12}} | a(1)\ b(2) \rangle$$

$$ABAB \equiv \langle a(1)\ b(2) | \frac{1}{r_{12}} | b(1)\ a(2) \rangle$$

and so on. The derivatives of these integrals with respect to R_{AB}, the distance between atoms A and B, are written as, DSAB, DAVBA, DAABB, DABAB ... . Also we have used the notation

$$N_1 = 0.5(1 + 3\ SAB)^{-\frac{1}{2}}$$

$$N_2 = 0.5(1 - S_{AB})^{-\frac{1}{2}} .$$

1. Derivatives with respect to Q_ξ

$$DYHZ = N_2^2 \left[4\ DAVBA - 4\ DATB - 8\ DAVAB - 8\ DSAB \times AVBA \right]$$

$$DVHX = N_1 N_2 \left[- 4\ DAVBA - 4\ DATB - 8\ DAVAB - 8\ DSAB \times AVBA \right]$$

$$DVYVZ = N_1^2 N_2^2 \left[- 4\ DAABB - 8\ SAB \times DAABB - 4\ (SAB)^2 \times DAABB \right]$$

$$DVYXY = N_1 N_2^3 \left[4\ DAABB - 4(SAB)^2 \times DAABB \right]$$

$$DVVVX = N_1^3 N_2 \left[-4\ DAABB - 16\ DAAAB - 8\ SAB \times DAABB - 8\ DABAB - 32\ DABAD \right]$$

$$DVXYY = N_1 N_2^3 \left[-4\ DAABB - 16\ DSAB \times AABB + 8\ DABAB \right]$$

$$DXXYZ = N_2^4 \left[4\ DAABB - 16\ DSAB \times AABB - 8\ SAB \times DAABB - 8\ DABAB + 32\ DABAD \right]$$

$$DXZXY = N_2^4 \left[-4\ DAABB + 8\ SAB \times DAABB - 4(SAB)^2 \times DAABB \right]$$

$$DVXXX = N_1 N_2^3 \left[-4\ DAABB - 16\ DAAAB + 8\ SAB \times DAABB - 8\ DABAB + 32\ DABAD \right]$$

$$DYYYZ = N_2^4 \left[4\ DAABB - 16\ DAAAB + 8\ DABAB \right]$$

$$DVVYZ = N_1^2 N_2^2 \left[4\ DAABB + 8\ SAB \times DAABB - 16\ DSAB \times AABB - 8\ DABAB - 32\ DABAD \right] .$$

2. Derivatives with respect to Q_ε

$$DYHY = 4\,N_2^2 \times DSAB \times YHY + 0.5\,N_2^2 \left[-8\,DATB - 16\,DAVAB - 16\,DSAB \times AVBA + 8\,SAB \times DAVBA \right]$$

$$DVVYY = N_1^2 N_2^2 \left[-8\,DAAAB - 8\,DABAB - 8\,DSAB \times AABB + 4\,SAB \times DAABB - 16\,SAB \times DSAB \times AABB + 4(SAB)^2 \times DAABB - 16\,DABAD \right] + 4\,N_2^2 \times DSAB \times VVYY$$

$$DVYVY = 4N_2^2\,DSAB \times VYVY + N_1^2 N_2^2 \left[-4\,DAABB - 8\,DAAAB - 4\,DABAB + 8\,SAB \times DSAB \times AABB - 2(SAB)^2 \times DAABB + 8\,DSAB \times AABB - 4\,SAB \times DAABB \right]$$

$$DVYXZ = N_1 N_2^3 \left[4\,DAABB - 4\,DABAB + 8\,SAB \times DSAB \times AABB - 2(SAB)^2 \times DAABB \right]$$

$$DXXYY = 4\,N_2^2 \times DSAB \times XXYY + N_2^4 \left[-8\,DAAAB - 8\,DSAB \times AABB + 4\,SAB \times DAABB + 8\,DABAB + 16\,SAB \times DSAB \times AABB - 4(SAB)^2 \times DAABB - 16\,DABAD \right]$$

$$DYYYY = 8\,N_2^2 \times DSAB \times YYYY + N_2^4 \left[-16\,DAAAD + 8\,SAB \times DAABB - 16\,DSAB \times AAAB + 32\,DABAD \right]$$

$$DXZXZ = -4\,N_2^2 \times DSAB \times XZXZ + N_2^4 \Big[-4\,DAABB + 8\,DAAAB - 4\,DABAB - 8\,DSAB \times AABB + 4\,SAB \times DAABB + 8\,SAB \times DSAB \times AABB - 2(SAB)^2 \times DAABB \Big] .$$

3. **Derivatives with respect to Q_a** (symmetric relaxation)

$$DVHV = 2\sqrt{6}\,N_1^2 \Big[-DSAB \times VHV + DATB + 2\,DAVAB + DAVBA + 2\,DAVBC \Big]$$

$$DXHX = 4\,N_2^2/\sqrt{6} \Big[DSAB \times YHY + 3\,DAVBA - DATB - 2\,DAVAB - 2\,DAVBC \Big]$$

$$DVVVV = 2\sqrt{6}\,N_1^4 \Big[-2\,DSAB \times VVVV \times N_1^{-2} + DAABB + 4\,DAAAB + 2\,DABAB + 4\,DABCC + 8\,DABAC + 2\,DABCD \Big]$$

$$DXXXX = N_2^4/\sqrt{6} \Big[8\,DSAB \times YYYY \times N_2^{-2} + 12\,DAABB - 16\,DAAAB - 16\,DABCC + 24\,DABAB - 32\,DABAC + 24\,DABCD \Big]$$

$$DXXYY = 8N_2^4/\sqrt{6} \Big[DSAB \times XXYY \times N_2^{-2} + 1.5\,DAABB - 2\,DAAAB - 2\,DABCC - DABAB - DABCD + 4\,DABAC \Big]$$

$$DXYXY = 4N_2^4/\sqrt{6} \Big[2\,DSAB \times XZXZ \times N_2^{-2} - DAABB - 4\,DAAAB + 2\,DABAB + 4\,DABCC - 2\,DABCD \Big]$$

$$DVZVZ = 4/\sqrt{6}\left[\left(N_2^2 - 3N_1^2\right) \times DSAB \times VZVZ + N_1^2N_2^2\ (-\ DAABB + 2\ DABAB + 4\ DAAAB - 4\ DABCC - 2\ DABCD)\right]$$

$$DVXYZ = \sqrt{6}\left[\left(N_2^2 - N_1^2\right) \times DSAB \times VXYZ + 2/3\ N_1N_2^3\ (DAABB + 2\ DABAB - 2\ DABCD)\right]$$

$$DVVXX = 4/\sqrt{6}\left[\left(N_2^2 - 3N_1^2\right) \times DSAB \times VVYY + N_1^2N_2^2\ (3\ DAABB + 4\ DAAAB - 2\ DABAB + 4\ DABCC - 2\ DABCD - 8\ DABAC)\right] .$$

APPENDIX C4

Values of the derivatives of the molecular integrals used in the Jahn-Teller calculations for the single vacancy in Diamond

$\frac{d}{dQ_\xi}$ (integral)	Clementi Functions	Slater Functions
$\langle y \lvert H^o \rvert z \rangle$	-12,8235*	-11.7702
$\langle v \lvert H^o \rvert x \rangle$	-16.7565	-16.7369
$\langle vv \lvert \frac{1}{r_{12}} \rvert yz \rangle$	1.1817	1.1210
$\langle vx \lvert \frac{1}{r_{12}} \rvert yy \rangle$	-1.0882	-1.0749
$\langle vv \lvert \frac{1}{r_{12}} \rvert vx \rangle$	4.0695	4.2085
$\langle vy \lvert \frac{1}{r_{12}} \rvert xy \rangle$	2.4284	2.5462
$\langle xy \lvert \frac{1}{r_{12}} \rvert xz \rangle$	2.3005	1.7870
$\langle vx \lvert \frac{1}{r_{12}} \rvert xx \rangle$	5.1366	4.9964
$\langle yy \lvert \frac{1}{r_{12}} \rvert yz \rangle$	3.8278	3.3737
$\langle vy \lvert \frac{1}{r_{12}} \rvert vz \rangle$	2.2648	1.8086
$\langle xx \lvert \frac{1}{r_{12}} \rvert yz \rangle$	1.0021	1.0306

*All derivatives in eV/A

Appendix C4 (continued)

$\frac{d}{dQ_\epsilon}$ (integral)	Clementi Functions	Slater Functions
$\langle y \lvert H^o \rvert y \rangle$	-8.1787[+] -3.8432[*]	-7.4022 -4.2221
$\langle vy \lvert \frac{1}{r_{12}} \rvert vy \rangle$	0.4648	0.5070
$\langle vv \lvert \frac{1}{r_{12}} \rvert yy \rangle$	1.2779	1.3758
$\langle vx \lvert \frac{1}{r_{12}} \rvert yz \rangle$	-0.8300	-0.8875
$\langle xy \lvert \frac{1}{r_{12}} \rvert xy \rangle$	0.7279	0.6415
$\langle yy \lvert \frac{1}{r_{12}} \rvert yy \rangle$	1.9287	1.7287
$\langle xx \lvert \frac{1}{r_{12}} \rvert yy \rangle$	-0.1560	-0.2777

[+]Case 1

[*]Case 2